

**STUDIES ON THE PERFORMANCE,  
COMBUSTION & EMISSION  
CHARACTERISTICS OF A MULTI-  
CYLINDER SI ENGINE FUELED WITH LPG  
ALONG WITH VARYING STEAM  
INDUCTION RATES**

Thesis

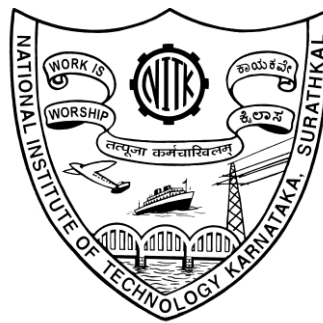
Submitted in partial fulfillment of the requirements for the

Degree of

**DOCTOR OF PHILOSOPHY**

by

**SHANKAR K. S**



**DEPARTMENT OF MECHANICAL ENGINEERING**

**NATIONAL INSTITUTE OF TECHNOLOGY**

**KARNATAKA**

**SURATHKAL, MANGALORE - 575025**

**AUGUST, 2013**



## **D E C L A R A T I O N**

I hereby *declare* that the Research Thesis entitled **STUDIES ON THE PERFORMANCE, COMBUSTION & EMISSION CHARACTERISTICS OF A MULTI-CYLINDER SI ENGINE FUELED WITH LPG ALONG WITH VARYING STEAM INDUCTION RATES** which is being submitted to the **National Institute of Technology Karnataka, Surathkal** for the award of the Degree of **Doctor of Philosophy in Mechanical Engineering** is a *bonafide report of the research work carried out by me*. The material contained in this Research Thesis has not been submitted to any University or Institution for the award of any Degree.

**SHANKAR K. S**

(Register No. 050602ME05P07)

Department of Mechanical Engineering

Place: NITK, SURATHKAL

Date: 26.08.2013



# C E R T I F I C A T E

This is to *certify* that the Research Thesis entitled **STUDIES ON THE PERFORMANCE, COMBUSTION & EMISSION CHARACTERISTICS OF A MULTI-CYLINDER SI ENGINE FUELED WITH LPG ALONG WITH VARYING STEAM INDUCTION RATES** submitted by **SHANKAR K. S** (Register No. 050602ME05P07) as the record of the work carried out by him, is *accepted as the Research Thesis submission* in partial fulfillment of the requirements for the award of Degree of **Doctor of Philosophy.**

**Dr. P. MOHANAN**

Research Guide

**Chairman - DRPC**



## **ACKNOWLEDGEMENTS**

I had a wonderful time during my Ph.D course in the Department of Mechanical Engineering, National Institute of Technology Karnataka, Surathkal. I wish to express my sincere appreciation to those who have contributed to this thesis and supported me in one way or the other during this amazing journey.

First and foremost, it is my privilege to express my deep sense of gratitude and respect to my research guide Dr. P. Mohanan, Professor and former Head, Department of Mechanical Engineering for his excellent guidance and constant motivation throughout my work. With his enthusiasm and inspiration throughout my course of study he provided encouragement, sound advice, good company, excellent teaching and lots of good ideas. Being my M. Tech. guide I have known Dr. P. Mohanan since 2002 as a dedicated and truthful person. I cannot imagine this work without his technical input right from the beginning. Because of his practical approach and helping nature, it was pleasure for me to work under him. Besides being a guide, he is also a mentor to me.

I am thankful to Dr. Prasad Krishna, Professor and Head, Department of Mechanical Engineering for his help and wholehearted support. I would also like to thank the former heads of Mechanical Engineering Department Dr. G. C Mohan Kumar & Dr. T. P Ashok Babu, for their support and encouragement.

I am thankful to Dr. D. V. R Murthy, Professor, Department of Chemical Engineering, and Dr. A. V Adhikari, Professor, Department of Chemistry, for being the members of the Research Progress Assessment Committee and offering their useful comments and suggestions during this work.

I am very much thankful to the Management and Principal of P. A. College of engineering, Mangalore and my colleagues of the Department of Mechanical Engineering for their wholehearted support.

I wish to remember the help extended to me by Sri. Nagesh, Sri. Jayantha, Sri. Yathisha and Sri. Raviraj of fuels and IC engines lab during the experimental work.

I wish to place on record my sincere appreciation to Sri. Jaganath, Mondovi Motors, Surathkal for his technical support.

I would like to express my hearty thanks to my friend Vighnesha Nayak, research scholar, who was always available for any help I needed during the experimental work. Thanks are also due to Dinesha P, Vishal A. S, Haridas Rathode and George Varghese, for their friendship and the support they have given to me throughout the research work.

I would like to express my deepest gratitude to my parents, sisters and family for always being there with me to provide the best opportunities in my life.

Finally, I would like to thank all those who have helped me directly or indirectly in completing this research work.

NITK Surathkal

August, 2013

**Shankar K. S**



## ABSTRACT

Vehicle and fuel technologies have undergone important developments in the last 30 years. The volatility of oil prices and increasing concerns about the environment has influenced researchers to look in to possible alternatives to petroleum based fuels. Efforts are on to improve the combustion efficiency of the engines operating with conventional fuels. The various alternative fuels for spark ignition (SI) engines on which research is going on at present includes alcohols, liquefied petroleum gas (LPG), natural gas etc. Ethanol enriched gasoline blends are increasingly being used in SI engines due to the renewable nature of ethanol as well as increased governmental regulatory mandates. Ethanol can be produced from natural products or waste materials, compared with gasoline which is produced from non-renewable natural sources. In addition, ethanol shows good antiknock characteristics.

Gaseous fuels are promising alternative fuels due to their economical costs, high octane numbers, higher heating values and lower polluting exhaust emissions. From the point of view of reduction of exhaust emissions such as unburnt hydrocarbon (HC) and carbon monoxide (CO), liquefied petroleum gas (LPG) is a useful alternative fuel for SI engines. Due to its higher octane value, LPG fuel can be used under the higher compression ratios. Combustion of LPG results in greater emissions of the oxides of nitrogen ( $\text{NO}_x$ ) than that for gasoline, the values reaching more than double at some operating conditions. Injection of water into the intake manifold has been found to be an effective way to reduce  $\text{NO}_x$  emission in SI, CI and LPG engines.

The present study deals with experimental investigations on the effect of steam induction with the intake air while using LPG as fuel on engine performance, combustion and emissions in a modified multi-cylinder SI engine. The engine operating parameters of speed, throttle opening positions and static ignition timings are varied. To compare the results of the above experiments, an ethanol enriched gasoline blend is optimized as a baseline fuel based on engine performance, combustion and emissions. The experimental setup consists of a stationary, four-stroke, four cylinder, multipoint port fuel injection (MPFI) engine of 44 kW capacity at 6000 rpm, which is connected to an eddy current dynamometer for loading. A piezo-electric pressure transducer is used for recording the cylinder pressure. The set

up has a stand-alone panel box consisting of air box, fuel tank, manometer, fuel measuring unit, differential pressure transmitters for air and fuel flow measurements, process indicator and engine indicator. An AVL Digas 444 five gas Exhaust gas analyzer is used to measure the NO<sub>x</sub> (ppm), CO (%vol.), CO<sub>2</sub> (%vol.) and HC (ppm) emissions in the exhaust.

Initially experiments are conducted to study the performance, combustion and emission characteristics of the test engine fueled with ethanol enriched gasoline blends viz: E5, E10, E15 and E20 (on volume basis, and E5 means 5% ethanol and 95% gasoline) to optimize a baseline fuel. In the next part tests are conducted on the engine modified to run with injection of LPG as fuel and the combustion, performance and emission characteristics are evaluated. Separate four gas injectors are installed in the inlet manifold near the inlet port of each cylinder for injecting LPG. The gas injectors are operated by solenoid valves driven by 12V DC power supply. A separate gas ECU has been used for driving the solenoid valves. Experiments are conducted at wide open throttle (WOT) and part throttle conditions with varying loads in the engine speed range of 2000 rpm to 4500 rpm. Tests with ethanol enriched gasoline are conducted at the pre-set static ignition timing of 5 degree before top dead center (bTDC). The LPG performance and emissions are evaluated at various static ignition timings of 3, 4, 5 and 6 deg. bDTC. In the last part of the investigations, the engine tests are conducted with LPG along with steam induction. The waste heat from the exhaust gas has been used to generate steam from deionized water. Steam to LPG flow rates of 10, 15, 20 and 25% (on mass basis) are used. The steam is mixed with the intake air in the intake manifold of the engine.

Results of the experiments have shown that among the various ethanol enriched blends, the blend of 20% ethanol was the most suitable one from the engine performance and CO & HC emissions points of view. At WOT operations the effect of ethanol blending on coefficient of variation of IMEP is to reduce it by an average of 2% with E15 fuel blend when compared to gasoline fuel operation over the entire speed range. All the ethanol-gasoline blends exhibit better cyclic variation pattern compared to gasoline at WOT operation. The engine performance has improved with the addition of ethanol, increasing the thermal efficiency and reducing the brake

specific energy consumption. A significant reduction in the HC emission was observed as a result of leaning effect and additional fuel oxygen caused by the ethanol addition. CO emission is reduced by addition of ethanol to gasoline. All engine exhaust emissions were lower at 3500-4000 rpm at various throttle valve opening condition except  $\text{NO}_x$  which has shown an increasing trend with ethanol blended fuel. Hence it can be concluded that blending ethanol up to 20% to gasoline will reduce the cycle-by-cycle combustion variations and emissions though a marginal increase in  $\text{NO}_x$  emissions results.

The findings of the experiments with LPG suggest that higher thermal efficiency and therefore improved fuel economy can be obtained from SI engines running on LPG as against gasoline at the pre-set static ignition timing of 5 deg. bTDC. Also the exhaust emissions of CO, HC have reduced considerably. But the emissions of  $\text{NO}_x$  have increased significantly at higher engine speeds. The CO emission has reduced from an average value of 5 % to about 1.3 % and corresponding change in HC noticed was from 350 ppm to 22 ppm when LPG was used instead of gasoline at pre-set static ignition timing. The  $\text{NO}_x$  emission with LPG was almost double when compared to that with gasoline at higher engine speeds. When engine runs with LPG, better performance has been observed when static ignition timing is advanced to 6 deg. bTDC. Advancing the static ignition timing has also resulted in reduced CO and HC emissions. But the advanced ignition timing shows a further increase in  $\text{NO}_x$  emissions. Retarding the ignition timing achieves lesser  $\text{NO}_x$  emissions at higher engine speeds.

Steam induction is one of the methods to reduce  $\text{NO}_x$  emissions. Steam induction will reduce the peak temperature of the engine cylinder so that  $\text{NO}_x$  formation will be reduced. The experimental results showed that steam induction worked as a cooling means for the fuel-air charge and slowing the burning rates, resulting in reduction of the peak combustion temperature. It is found that  $\text{NO}_x$  emissions have reduced significantly by 20 - 45% over the entire operating range when compared to LPG operation. No considerable changes in CO and HC emissions are observed. Hence use of LPG with advanced ignition timing of 6deg. bTDC with steam induction up to 25% steam to fuel mass ratio at higher engine speeds and up to 10% steam to fuel mass

ratio at lower engine speeds can be used from the point of view of improved engine performance and reduced exhaust emissions.

When comparing the performance and emissions of ethanol enriched gasoline and LPG with steam induction, it is noted that, comparatively E20 blends performs better than LPG alone. With steam induction the performance with LPG deteriorates. The brake thermal efficiency of 15% steam with LPG at wide open throttle condition and 3500 rpm is lower by 3.5% when compared to E20. CO reduces with LPG when compared to E20. But a slight increment is noted when steam is inducted. NO<sub>x</sub> emissions are higher for both E20 and LPG when compared to gasoline. However, with the induction of steam along with LPG, the NO<sub>x</sub> can be substantially brought down. At 3500 rpm and wide open throttle condition, the NO<sub>x</sub> emissions of E20 and 15% steam with LPG are similar. But at 4500 rpm, NO<sub>x</sub> emission is higher by 580 ppm.

From the experimental investigations it can be concluded that use of ethanol enriched blends in unmodified engine is an alternative for the use of gasoline as a sole fuel. However with the current option of LPG as alternative fuel to SI engines, it can be used along with steam induction as a means to considerably reduce NO<sub>x</sub> emissions, with marginal reduction in engine performance.

**Key words:** Multi-cylinder engine, S. I Engine, LPG, Ethanol enriched gasoline, Performance, Combustion, Emissions, Oxides of nitrogen, Steam induction.

# CONTENTS

TITLE	Page No.
ACKNOWLEDGEMENTS	
ABSTRACT	
CONTENTS	i-v
LIST OF FIGURES	v-x
LIST OF PLATES	xi
LIST OF TABLES	xii
NOMENCLATURE	xiii-xv
<b>CHAPTER 1. INTRODUCTION</b>	<b>1-12</b>
1.1 ALTERNATIVE FUELS FOR ENGINES	3
1.1.1 Ethanol enriched gasoline in SI engines	4
1.1.2 LPG as fuel in SI Engine	7
1.2 CYCLE-BY-CYCLE VARIATIONS OF SI ENGINE	8
1.3 NO <sub>x</sub> REDUCTION TECHNIQUES	9
1.4 PRESENT WORK	11
1.5 ORGANIZATION OF THE THESIS	12
<b>CHAPTER 2. LITERATURE REVIEW</b>	<b>13-46</b>
2.1 USE OF ETHANOL IN SI ENGINES	13
2.2 USE OF LPG IN SI ENGINES	19
2.3 CYCLE-BY-CYCLE COMBUSTION VARIATION	27
2.4 NO <sub>x</sub> REDUCTION METHODS	31
2.5 HEAT RELEASE RATE ANALYSIS	38
2.6 RESEARCH GAPS	44
2.7 OBJECTIVES OF THE RESEARCH	44
2.8 SCOPE	46
<b>CHAPTER 3. EXPERIMENTAL TEST RIG AND                   INSTRUMENTATION</b>	<b>47-58</b>
3.1 TEST ENGINE DESCRIPTION	47
3.2 MODIFICATION OF THE ENGINE SETUP FOR OPERATION WITH LPG	49

<b>Table of contents (contd.)</b>	<b>Page No.</b>
3.2.1    LPG engine control unit (Gas ECU)	51
3.2.2    Safety measures and flame arrestor	51
3.3    STEAM INDUCTION SYSTEM DEVELOPMENT	52
3.4    MEASUREMENT SYSTEM	54
3.4.1    Cylinder pressure measurement	55
3.4.2    Air and fuel flow measurements	55
3.4.3    Engine speed measurement	56
3.4.4    Load measurement	56
3.4.5    Temperature measurement	57
3.4.6    Static ignition timing measurement	57
3.4.7    Exhaust emission measurement	57
3.4.8    Calibration of instruments	58
<b>CHAPTER 4.    EXPERIMENTAL METHODOLOGY</b>	<b>59-74</b>
4.1    SCHEME OF ENGINE EXPERIMENTAL STUDIES	59
4.2    DETERMINATION OF IMEP AND $COV_{IMEP}$	62
4.3    HEAT RELEASE RATE	64
4.3.1    Thermodynamics of heat release	65
4.4    ERROR AND UNCERTAINTY ANALYSIS	70
4.4.1    Sample Calculations	72
<b>CHAPTER 5.    RESULTS AND DISCUSSION</b>	<b>75-154</b>
5.1    PERFORMANCE, COMBUSTION AND EMISSION	75
STUDIES WITH ETHANOL ENRICHED GASOLINE BLENDS	
5.1.1    Torque	75
5.1.2    Brake power	77
5.1.3    Brake thermal efficiency(BTE)	78
5.1.4    Brake specific energy consumption (BSEC)	80
5.1.5    Equivalence ratio ( $\Phi$ )	82
5.1.6    Pressure-crank angle diagrams	83
5.1.7    Variation of peak pressure and IMEP	85
5.1.8    COV of IMEP and COV of $P_{max}$	89
5.1.9    Heat release rate analysis	92

<b>Table of contents (contd.)</b>	<b>Page No.</b>
5.1.10 Carbon monoxide (CO)	95
5.1.11 Hydrocarbon (HC)	97
5.1.12 Oxides of Nitrogen (NO <sub>x</sub> )	99
5.1.13 Carbon Dioxide (CO <sub>2</sub> )	101
5.2 PERFORMANCE, COMBUSTION AND EMISSION STUDIES OF LPG AT STATIC IGNITION TIMING OF 5 deg. bTDC	103
5.2.1 Torque	103
5.2.2 Brake power	103
5.2.3 Brake thermal efficiency (BTE)	104
5.2.4 Brake specific energy consumption (BSEC)	105
5.2.5 Indicated Mean Effective Pressure(IMEP)	106
5.2.6 Heat release rate analysis	108
5.2.7 Carbon monoxide (CO)	110
5.2.8 Hydrocarbon (HC)	111
5.2.9 Oxides of Nitrogen (NO <sub>x</sub> )	113
5.3 LPG PERFORMANCE, COMBUSTION AND EMISSIONS AT VARIOUS STATIC IGNITION TIMINGS	115
5.3.1 Torque	115
5.3.2 Brake thermal efficiency (BTE)	116
5.3.3 Brake specific energy consumption (BSEC)	116
5.3.4 Indicated Mean Effective Pressure (IMEP)	117
5.3.5 Equivalence ratio	119
5.3.6 Heat release analysis	120
5.3.7 Carbon monoxide (CO)	121
5.3.8 Hydrocarbon (HC)	122
5.3.9 Oxides of Nitrogen (NO <sub>x</sub> )	123
5.3.10 Carbon dioxide(CO <sub>2</sub> )	123
5.4 PERFORMANCE, COMBUSTION AND EMISSION STUDIES OF LPG WITH STEAM INDUCTION	125
5.4.1 Torque	126

<b>Table of contents (contd.)</b>	<b>Page No.</b>
5.4.2 Brake thermal efficiency (BTE)	127
5.4.3 Brake specific energy consumption (BSEC)	128
5.4.4 Indicated mean effective pressure (IMEP)	129
5.4.5 Pressure-crank angle diagrams	130
5.4.6 COV of IMEP	132
5.4.7 COV of Heat release	134
5.4.8 Carbon monoxide (CO)	136
5.4.9 Hydrocarbon (HC)	137
5.4.10 Oxides of nitrogen (NO <sub>x</sub> )	139
5.4.11 Exhaust gas temperature (EGT)	142
5.4.12 Carbon dioxide (CO <sub>2</sub> )	143
<b>5.5 COMPARATIVE STUDIES WITH LPG-STEAM AND ETHANOL ENRICHED GASOLINE</b>	<b>145</b>
5.5.1 Brake thermal efficiency (BTE)	145
5.5.2 COV of IMEP	146
5.5.3 COV of heat release	148
5.5.4 Carbon monoxide (CO)	148
5.5.5 Hydrocarbon (HC)	149
5.5.6 Oxides of nitrogen (NO <sub>x</sub> )	150
<b>5.6 CONCLUSIONS</b>	<b>154</b>
<b>CHAPTER 6. CONCLUSIONS AND SCOPE FOR FUTURE WORK</b>	<b>155-160</b>
6.1 CONCLUSIONS	155
6.2 SCOPE FOR FUTURE WORK	160
<b>REFERENCES</b>	<b>161-172</b>
Appendix I: Specifications of the experimental setup	173
Appendix II: Specifications of gas ECU	175
Appendix III: Specifications of the exhaust gas analyzer	176
List of Publications based on Ph.D Research Work	177
Bio-data	179



## LIST OF FIGURES

<b>Figure No.</b>	<b>Title</b>	<b>Page No.</b>
3.1	Schematic of the experimental setup	48
3.2	Block diagram of LPG injection system	50
3.3	Block diagram of steam induction system	53
4.1	Scheme of experiments with ethanol enriched gasoline blends	59
4.2	Scheme of experiments with LPG at different static ignition timings	60
4.3	Scheme of experiments at different static ignition timings with LPG and steam	61
4.4	Flow chart to find IMEP and COV of IMEP	63
4.5	Flow chart to find heat release rate and COV of heat release per cycle	69
5.1	Torque with engine speed for ethanol blends at (a) WOT and (b) 50% WOT	76
5.2	Torque with ethanol blends at (a) 3500 rpm and (b) 4500 rpm	76
5.3	Brake power with engine speed for ethanol blends at (a) WOT and (b) 50%WOT	78
5.4	Brake thermal efficiency (BTE) with engine speed for ethanol blends at (a) WOT and (b) 50%WOT	79
5.5	Brake thermal efficiency with ethanol blends at (a) 3500 rpm and (b) 4500 rpm	79
5.6	Influence of ethanol blends on brake thermal efficiency at 3500 rpm	80
5.7	BSEC with engine speed for ethanol blends at (a) WOT and (b) 50%WOT	81
5.8	BSEC with ethanol blends at (a) 3500 rpm and (b) 4500 rpm	81
5.9	Influence of ethanol blends on BSEC at 3500 rpm	81
5.10	Equivalence ratio with engine speed for ethanol blends at (a) WOT and (b) 50%WOT	83
5.11	Cylinder pressure of 25 combustion cycles vs crank angle for gasoline at 3500 rpm, (a) WOT and (b) 50% WOT	84
5.12	(a) $P_{max}$ and (b) IMEP for 25 consecutive cycles for gasoline at WOT & 3500rpm	84
5.13	Pressure vs crank angle for ethanol blends at WOT, (a) 3500 rpm & (b) 4500 rpm	85

<b>Figure No.</b>	<b>Title</b>	<b>Page No.</b>
5.14	Pressure vs crank angle for ethanol blends at 50% WOT, (a) 3500 rpm & (b) 4500 rpm	85
5.15	$P_{\max}$ of 25 cycles for ethanol blends at 3500 rpm, (a) WOT & (b) 50% WOT	86
5.16	IMEP of 25 cycles for ethanol blends at 3500 rpm, (a) WOT & (b) 50% WOT	86
5.17	Time return map of IMEP of 25 cycles for ethanol blends at 3500 rpm, (a) WOT & (b) 50% WOT	87
5.18	Time return map of IMEP of 25 cycles for ethanol blends at WOT, (a)2500 rpm, (b) 3500 rpm & (c) 4500 rpm	88
5.19	Time return map of (a) $P_{\max}$ and (b) crank angle of $P_{\max}$ of 25 cycles for ethanol blends at 3500 rpm	89
5.20	IMEP with engine speed for ethanol blends at (a) WOT and (b) 50% WOT	90
5.21	$COV_{(IMEP)}$ with engine speed for ethanol blends at (a) WOT and (b) 50% WOT	90
5.22	Variation of COV of IMEP at 3500 rpm for ethanol blends	91
5.23	Variation of COV of $P_{\max}$ with engine speed for ethanol blends at (a) WOT and (b) 50% WOT	92
5.24	Gross heat release rate for ethanol blends at WOT, (a) 2500, (b) 3500 & (c) 4500 rpm	93
5.25	Gross heat release rate for ethanol blends at 50% WOT, (a) 2500, (b) 3500 & (c) 4500 rpm	93
5.26	COV of heat release per cycle for ethanol blends at (a) WOT and (b) 50% WOT	94
5.27	COV of heat release per cycle at 3500 rpm for ethanol blends	94
5.28	Time return map of heat release per cycle for ethanol blends at 3500 rpm, (a) WOT & (b) 50% WOT	95
5.29	CO with engine speed for ethanol blends at (a) WOT and (b) 50% WOT	96
5.30	CO with ethanol blends at (a) 3500 rpm and (b) 4500 rpm	96
5.31	Influence of ethanol blends on CO at 3500 rpm	97
5.32	HC with engine speed for ethanol blends at (a) WOT and (b) 50% WOT	98
5.33	HC with ethanol blends at (a) 3500 rpm and (b) 4500 rpm	98

<b>Figure No.</b>	<b>Title</b>	<b>Page No.</b>
5.34	Influence of ethanol blends on HC at 3500 rpm	99
5.35	NO <sub>x</sub> with engine speed for ethanol blends at (a) WOT and (b) 50% WOT	99
5.36	EGT with engine speed for ethanol blends at (a) WOT and (b) 50% WOT	100
5.37	NO <sub>x</sub> with ethanol blends at (a) 3500 rpm and (b) 4500 rpm	100
5.38	Influence of ethanol blends on NO <sub>x</sub> at 3500 rpm	101
5.39	CO <sub>2</sub> with engine speed for ethanol blends at (a) WOT and (b) 50% WOT	102
5.40	Torque with engine speed for LPG at (a) WOT & (b) 50% WOT	103
5.41	Brake power with engine speed for LPG at (a) WOT & (b) 50% WOT	104
5.42	BTE with engine speed for LPG at (a) WOT & (b) 50% WOT	105
5.43	BSEC with engine speed for LPG at (a) WOT & (b) 50% WOT	106
5.44	IMEP with engine speed for LPG at (a) WOT & (b) 50% WOT	106
5.45	Time return map of IMEP for LPG at 3500 rpm at (a) WOT & (b) 50% WOT	107
5.46	COV of IMEP for LPG at (a) WOT & (b) 50% WOT	108
5.47	COV of IMEP for LPG at 3500 rpm and different throttle valve openings	108
5.48	Time return map of heat release per cycle for LPG at 3500 rpm at (a) WOT & (b) 50% WOT	109
5.49	COV of heat release per cycle for LPG at (a) WOT & (b) 50% WOT	109
5.50	COV of heat release per cycle for LPG at 3500 rpm and different throttle valve openings	110
5.51	CO with engine speed for LPG at (a) WOT & (b) 50% WOT	111
5.52	CO at different throttle valve openings for LPG at 3500 rpm	111
5.53	HC with engine speed for LPG at (a) WOT & (b) 50% WOT	112
5.54	HC at different throttle valve openings for LPG at 3500 rpm	112

<b>Figure No.</b>	<b>Title</b>	<b>Page No.</b>
5.55	NO <sub>x</sub> with engine speed for LPG at (a) WOT & (b) 50% WOT	113
5.56	NO <sub>x</sub> with throttle openings for LPG at 3500 rpm	114
5.57	Torque with engine speed for LPG at 5, 6, 4 & 3 deg. bTDC, (a) WOT & (b) 50% WOT	115
5.58	BTE with engine speed for LPG at 5, 6, 4 & 3 deg. bTDC, (a) WOT & (b) 50% WOT	116
5.59	BSEC with engine speed for LPG at 5, 6, 4 & 3 deg. bTDC, (a) WOT & (b) 50% WOT	117
5.60	IMEP with engine speed for LPG at 5, 6, 4 & 3 deg. bTDC, (a) WOT & (b) 50% WOT	117
5.61	Time return map of IMEP for LPG at 5, 6, 4 & 3 deg. bTDC, 3500 rpm, (a) WOT & (b) 50% WOT	118
5.62	COV of IMEP for LPG at 5, 6, 4 & 3 deg. bTDC, (a) WOT & (b) 50% WOT	118
5.63	Equivalence ratio for LPG at 5, 6, 4 & 3 deg. bTDC, (a) WOT & (b) 50% WOT	119
5.64	Time return map of heat release per cycle for LPG at 5, 6, 4 & 3 deg. bTDC, 3500 rpm, (a) WOT & (b) 50% WOT	120
5.65	COV of heat release per cycle for LPG at 5, 6, 4 & 3 deg. bTDC, (a) WOT & (b) 50% WOT	120
5.66	CO for LPG at 5, 6, 4 & 3 deg. bTDC, (a) WOT & (b) 50% WOT	121
5.67	HC for LPG at 5, 6, 4 & 3 deg. bTDC, (a) WOT & (b) 50% WOT	122
5.68	NO <sub>x</sub> for LPG at 5, 6, 4 & 3 deg. bTDC, (a) WOT & (b) 50% WOT	123
5.69	CO <sub>2</sub> for LPG at 5, 6, 4 & 3 deg. bTDC, (a) WOT & (b) 50% WOT	124
5.70	Torque with speed for LPG along with steam at 5 deg. bTDC, (a) WOT and (b) 50% WOT	126
5.71	Torque with speed for LPG along with steam at 6 deg. bTDC, (a) WOT and (b) 50% WOT	127
5.72	BTE with speed for LPG along with steam at 5 deg. bTDC, (a) WOT and (b) 50% WOT	127
5.73	BTE with speed for LPG along with steam at 6 deg. bTDC, (a) WOT and (b) 50% WOT	128
5.74	BSEC with speed for LPG along with steam at 5 deg. bTDC, (a) WOT and (b) 50% WOT	128

<b>Figure No.</b>	<b>Title</b>	<b>Page No.</b>
5.75	BSEC with speed for LPG along with steam at 6 deg. bTDC, (a) WOT and (b) 50% WOT	129
5.76	IMEP with speed for LPG along with steam at 5 deg. bTDC, (a) WOT and (b) 50% WOT	129
5.77	IMEP with speed for LPG along with steam at 6 deg. bTDC, (a) WOT and (b) 50% WOT	130
5.78	Pressure vs crank angle for LPG with steam at 5 deg. bTDC, 3500 rpm, (a) WOT & (b) 50% WOT	130
5.79	Pressure vs crank angle for LPG with steam at 6 deg. bTDC, WOT, (a) 3500 rpm & (b) 4500 rpm	131
5.80	Pressure vs crank angle for LPG with steam at 6 deg. bTDC, 50% WOT, (a) 3500 rpm & (b) 4500 rpm	131
5.81	COV of IMEP trends for LPG along with steam at 5 deg. bTDC, (a) WOT and (b) 50% WOT	132
5.82	COV of IMEP trends for LPG along with steam at 6 deg. bTDC, (a) WOT and (b) 50% WOT	132
5.83	COV of IMEP at (a) 3500 rpm and (b) 4500 rpm, WOT for LPG along with steam at various static ignition timings	133
5.84	COV of IMEP at (a) 3500 rpm and (b) 4500 rpm, 50% WOT for LPG along with steam at various static ignition timings	133
5.85	COV of heat release trends for LPG along with steam at 5 deg. bTDC, (a) WOT and (b) 50% WOT	134
5.86	COV of heat release trends for LPG along with steam at 6 deg. bTDC, (a) WOT and (b) 50% WOT	134
5.87	COV of heat release at (a) 3500 rpm and (b) 4500 rpm, WOT for LPG along with steam at various static ignition timings	135
5.88	COV of heat release at (a) 3500 rpm and (b) 4500 rpm, 50% WOT for LPG along with steam at various static ignition timings	135
5.89	CO with speed for LPG along with steam at 5 deg. bTDC, (a) WOT and (b) 50% WOT	136
5.90	CO with speed for LPG along with steam at 6 deg. bTDC, (a) WOT and (b) 50% WOT	136
5.91	CO emissions at (a) 3500 rpm and (b) 4500 rpm, WOT for LPG along with steam at various static ignition timings	137
5.92	HC with speed for LPG along with steam at 5 deg. bTDC, (a) WOT and (b) 50% WOT	138
5.93	HC with speed for LPG along with steam at 5 deg. bTDC, (a) WOT and (b) 50% WOT	138

<b>Figure No.</b>	<b>Title</b>	<b>Page No.</b>
5.94	HC at (a) 3500 rpm and (b) 4500 rpm, WOT for LPG along with steam at various static ignition timings.	139
5.95	NO <sub>x</sub> with engine speed at WOT and different static ignition timings for LPG along with steam	140
5.96	NO <sub>x</sub> with engine speed at 50%WOT and different static ignition timings for LPG along with steam	141
5.97	Percentage NO <sub>x</sub> reduction at 3500 rpm at 6 deg. bTDC, (a) WOT and (b) 50%WOT with steam induction along with LPG	142
5.98	Exhaust gas temperature with engine speed for LPG along with steam at WOT at (a) 5 deg. and (b) 6 deg. static ignition timings	143
5.99	CO <sub>2</sub> emissions with speed for LPG along with steam at (a) WOT and (b) 50%WOT at 6 deg. bTDC	143
5.100	CO <sub>2</sub> emissions at (a) 3500 rpm and (b) 4500 rpm, WOT for LPG along with steam at various static ignition timings	144
5.101	BTE for various fuels at WOT	145
5.102	BTE for various fuels at 50%WOT	146
5.103	COV of IMEP for various fuels at WOT	146
5.104	COV of IMEP for various fuels at 50%WOT	147
5.105	COV of heat release per cycle for various fuels at WOT	147
5.106	COV of heat release per cycle for various fuels at 50%WOT	148
5.107	CO for various fuels at WOT	149
5.108	CO for various fuels at 50%WOT	149
5.109	HC for various fuels at WOT	150
5.110	HC for various fuels at 50%WOT	150
5.111	NO <sub>x</sub> for various fuels at WOT	151
5.112	NO <sub>x</sub> for various fuels at 50%WOT	151

## **LIST OF TABLES**

<b>Table No.</b>	<b>Title</b>	<b>Page No.</b>
1.1	Production and import of crude oil in India	2
1.2	Gasoline and diesel consumption in India	2
1.3	Properties of Ethanol, LPG and gasoline	8
2.1	Some major literature on use of ethanol enriched gasoline	41
2.2	Some major literature on use of LPG in SI Engines	42
2.2	Some major literature on the use of NO <sub>x</sub> reduction techniques	43
4.1	Uncertainty of various parameters	74
5.1	Summary of performance, combustion and emission studies with ethanol enriched gasoline blends (at 3500 rpm)	152
5.2	Summary of performance, combustion and emission studies with LPG at various static ignition timings (at 3500 rpm)	153
5.3	Summary of performance, combustion and emission studies of LPG along with steam induction (At 6 deg. bTDC, 3500 rpm)	154
6.1	Experimentally optimized operating range of major parameters	159

## **LIST OF PLATES**

<b>Plate No.</b>	<b>Title</b>	<b>Page No.</b>
3.1	Engine setup with control panel	49
3.2	Gas injectors	52
3.3	Flame Arrestor	52
3.4.	Steam induction system	54
3.5	Steam induction to the intake manifold system	54
3.6	Copper coil over the exhaust pipe for production of steam	54



## NOMENCLATURE

### English

10%S	10% steam by mass of LPG
15%S	15% steam by mass of LPG
20%S	20% steam by mass of LPG
25%S	25% steam by mass of LPG
A/F	Air fuel ratio
BCM	Billion cubic meters
BSEC	Brake specific fuel consumption (MJ/kW-hr)
BSFC	Brake specific fuel consumption (kg/kW-hr)
bTDC	Before top dead centre
BTE	Brake thermal efficiency (%)
CA	Crank angle
CBC	Cycle by cycle
CNG	Compressed Natural Gas
CO	Carbon monoxide (% volume)
CO <sub>2</sub>	Carbon dioxide
COV	Coefficient of variation (%)
COV <sub>IMEP</sub>	Coefficient of variation of IMEP
deg.	Degree crank angle
DME	Dimethyl ether
DP	Differential pressure
E10	Ethanol 10%+gasoline 90% by volume
E15	Ethanol 15%+gasoline 85% by volume
E20	Ethanol 20%+gasoline 80% by volume
E5	Ethanol 5%+gasoline 95% by volume
EBP	Ethanol blended petrol
ECU	Electronic control unit

EGR	Exhaust gas recirculation
EGT	Exhaust gas temperature
HC	Hydrocarbon (ppm)
HR	Heat release (J/cycle)
hr	Hour
I.C	Internal combustion
IMEP	Indicated mean effective pressure (bar)
kW	Kilo watt
LPG	Liquefied petroleum gas
lph	Liters per hour
MJ	Mega joules
MMT	Million metric tonnes
MPFI	Multi point port fuel injection
MT	Metric tonnes
MTBE	Methyl tertiary butyl ether
NO <sub>x</sub>	Oxides of nitrogen (ppm)
O <sub>2</sub>	Oxygen (%)
P	Pressure (bar)
PFI	Port fuel injection
P <sub>max</sub>	Peak pressure
ppm	Parts per million
rpm	Revolution per minute
SCR	Selective catalytic reduction
SI	Spark ignition
T	Temperature
T <sub>Wall</sub>	Wall temperature
TWC	Three-way catalytic converter
ULEV	Ultra low emission vehicle

V	Volume
VOC	Volatile organic compounds
WOT	Wide open throttle
$\theta P_{\max}$	Crank angle of peak pressure
n	Number of combustion cycles
$C_v$	Specific heat at constant volume
Q	Heat transferred (Joules)
$Q_{\text{net}}$	Net heat release rate (Joules per degree)
h	Heat transfer coefficient ( $\text{W}/\text{m}^2\text{K}$ )
Greek symbols used	
$\Phi$	Equivalence ratio
$\sigma$	Standard deviation
$\mu$	Mean
$\theta$	Crank angle (degree)
$^\circ$	Degree
$\gamma$	Ratio of specific heats



## **CHAPTER 1**

### **INTRODUCTION**

The world is currently facing the twin crisis of depletion of fossil fuels with ever increasing oil prices and environmental degradation due to the harmful emissions. Engine manufacturers are currently working towards ways to increase fuel economy and reduce harmful emissions from internal combustion engines. In recent years there has been considerable growth in road transport, and this trend is set to continue for the foreseeable future. In view of the versatility of internal combustion engine (ICE), it will remain to lead the transportation sector as there is a significant restriction for the battery and fuel cell powered vehicles with respect to range and acceleration. The power to weight ratio of the ICE is much more than that of the battery powered or fuel cell operated vehicles. Today's transport is based almost exclusively on the consumption of petroleum products such as gasoline and diesel. Research shows that the contribution of transportation to the global anthropogenic emissions amount to 21% for CO<sub>2</sub>, 37% for oxides of nitrogen (NO<sub>x</sub>), 19% for volatile organic compounds (VOCs), 18% for carbon monoxide CO and 14% for black carbon (Myung et al. 2012). The search for alternative fuels, which promise a harmonious correlation with sustainable development, energy conservation, efficiency and environmental preservation has become highly pronounced in the present context (Agarwal 2007).

India's energy-mix comprises both non-renewable (coal, lignite, petroleum and natural gas) and renewable energy sources (wind, solar, small hydro, biomass, cogeneration bagasse etc.). The estimated reserves of crude oil and natural gas in India as on 31.03.2010 stood at 1206 million metric tonnes (MMT) and 1453 billion cubic meters (BCM), respectively. India is highly dependent on import for crude oil with more than 70% of its crude oil requirements and part of the petroleum products is met from imports. Oil import has been steadily rising over the years with the net import of crude oil increased from 11.68 MTs during 1970-71 to 159.26 MTs during 2009-10. There has been an annual increase of 19.9% during 2009-10 over 2008-09, as the net import of crude increased from 132.78 MTs to 159.26 MTs (Table 1.1). The import of petroleum products witnessed a decline of 27.8 % during 2009-10 over

2008-09 to 14.66 MTs, after continually increasing from 13.44 MTs during 2005-06 to 22.46 MTs during 2007- 08 (Das 2011).

Table 1.1: Production and import of crude oil in India (Das 2011)

Year	Production (MT)	Net import (MT)	Gross availability (MT)
1970-71	6.82	11.68	18.51
1980-81	10.51	16.25	26.76
1990-91	33.02	20.7	53.72
2000-01	32.43	74.10	106.52
2005-06	32.19	99.41	131.60
2006-07	33.99	111.50	145.49
2007-08	34.12	121.67	155.79
2008-09	33.51	132.78	166.28
2009-10	33.69	159.26	192.95

Table 1.2: Gasoline and diesel consumption in India (Das 2011)

Year	Gasoline consumption (MT)	Diesel consumption (MT)	Ratio of diesel/ gasoline
2000-01	6.61	37.96	5.74
2005-06	8.65	40.19	4.64
2006-07	9.29	42.9	4.61
2007-08	10.33	47.67	4.61
2008-09	11.26	51.67	4.59
2009-10	12.82	56.32	4.39

The estimated consumption of crude oil has regularly increased, from 18.38 MTs during 1970-71 to 160 MTs during 2009-10 with a cumulative annual growth rate of 5.6%. It decreased from 160.8 MTs in 2008-09 to 160 MTs in 2009-10. The estimated consumption of natural gas has shown a remarkable increase, from 0.7 BCM in 1970-71 to 47.2 BCM in 2009-10. The demand for high speed diesel has been estimated to be 56.32 MT which has accounted for 37.6% of total consumption of all types of petroleum products in 2009-10. This was followed by LPG (8.8%), gasoline (8.6%),

fuel oil (8.5%) and refinery fuel (7.8%). Sector-wise consumption of different petroleum products reveals that transport sector accounts for the lion's share (50%) of the total consumption with agriculture sector for 18%, 11% for industry and 7% for power generation. The diesel fuel consumption is about four times higher than gasoline fuel consumption as shown in table 1.2 (Das 2011).

In recent decades vehicles have undergone a number of changes aimed at achieving more environmentally friendly transport. Some of these changes have resulted from technology developments and cost optimization, but many were driven by government actions such as emission legislation. There are several technical options for future vehicles, all of them cleaner because they will have to comply with stringent emission norms. Gasoline was the prime fuel for propulsion of passenger cars until the 1970s. The oil crisis of 1973 led to an increase in awareness of the need for better fuel economy, and alternative fuels & propulsion systems received more attention. In the late 1980s and early 1990s environmental concerns began to increase, leading to the introduction of emission limits. The spark-ignited gasoline engine is still the main option for passenger cars and light-duty vehicles. Emissions from gasoline engines have been reduced dramatically with the introduction of the three-way catalyst, coupled with electronically controlled gasoline injection. With a renewed emphasis on fuel economy and reduction of CO<sub>2</sub> emissions which is linked to the fear of global warming, fuel-saving technologies such as gasoline direct injection (GDI) and variable valve actuation have gained interest. Diesel engines were mainly used in the past for stationary purposes or for heavy-duty vehicles. The shift from indirect injection to turbo diesel direct injection and the introduction of electronic diesel control (i.e. common rail) led to significant improvements in terms of fuel economy and emissions. Noise and performance, once the main drawback of diesel engines, have also improved tremendously in the latest diesel models.

### **1.1 ALTERNATIVE FUELS FOR ENGINES**

Alternative fuels came into the picture in the 1970s for reasons of security of energy supply. By the end of the 1980s growing concern about the environmental impact of automobiles stimulated the interest in alternative fuels. The popular alternative fuels at the moment are LPG, alcohols (ethanol and methanol), natural gas, and – for diesel

engines - biodiesel. Other fuels that have not so far reached the commercialization stage are hydrogen (particularly for use in fuel cells), dimethyl ether (DME) and synthetic fuels. Most vehicles operating on alternative fuels are also capable of using conventional fuels such as gasoline (in the case of LPG, natural gas, alcohols) or diesel (in the case of biodiesel). These vehicles are often referred to as bi-fuel, dual-fuel or flexible fuel vehicles. The two-fuel option increases their functionality, since alternative-fuel filling stations may be rare. The researchers recognized biofuels as a major renewable energy source to supplement declining fossil fuel resources. Especially, the alcohol fuels such as methanol, ethanol etc. have been accepted as good alternative fuels for the vehicles equipped with SI (spark ignition) engines because they are liquid and have several physical and combustion properties similar to gasoline. Generally gaseous fuels result in very low levels of pollutants and can be effectively utilized both in spark ignition (SI) and compression ignition (CI) engines. Gaseous fuels exhibit wide ignition limits and can easily form homogeneous mixtures with air to promote complete combustion with the possibilities of use of very lean mixtures. Also gaseous fuels have high hydrogen to carbon ratios, which will lead to reduction in carbon-based emissions. Promising gaseous alternate fuels are natural gas, liquefied petroleum gas (LPG), hydrogen, biogas and producer gas. Each of these has its own advantages and is suitable for specific application. Compressed natural gas (CNG) and LPG are readily available petroleum based fuels, which are mainly used for public transportation in urban areas in India, while hydrogen, biomass and producer gas can be obtained from renewable sources. In the last three decades, there is a progressive interest related with use of non-fossil fuel sources in vehicles. The properties and utilization of some potential alternatives are discussed below.

### **1.1.1 Ethanol enriched gasoline in SI engines**

Biofuels such as bio-ethanol and biodiesel have gained increased interest worldwide due to the concerns over climate change and also the energy security. While these fuels still represent a minor proportion of total fuel consumption in the world, their share is expected to grow sharply with research indicating that they have good qualities as alternate fuels. Alcohols are particularly attractive as alternative fuels because they are a renewable bio-based resource and oxygenated, thereby providing



the potential to reduce particulate emissions in spark ignition engines. Methanol and ethanol can be used in blends with petroleum based engine fuels (Ozsezen and Canakci 2011). Ethanol was the first fuel among the alcohols to be used to power vehicles in the 1880s and 1890s. Henry Ford presented it as the fuel of choice for his automobiles during their earliest stages of development. In the United States and also in many countries such as France and United Kingdom, many studies were achieved in the 1920's and 1930's with this fuel, before the wide diffusion of leaded gasoline induced a decrease in the interest in ethanol for years. Rising taxes on ethanol limited its use as a fuel. During World Wars I and II in both the United States and Europe, alcohol fuels were used as a supplement to oil-based fuels (usually around 20%). Following World War II, ethanol was unsuccessful as an economically competitive transportation fuel due to the reduction in oil prices. In Brazil and in the USA in particular, the 1970s oil crises gave birth to a governmental ethanol support strategy. During the last decades, a renewed interest for ethanol has grown, linked with the more and more stringent emission limits. Moreover, some economical aspects, such as agricultural development (in Brazil for instance) have also favoured to the use of ethanol. The Kyoto Protocol and the growing concern for greenhouse gas emissions will lead in the next coming years to an increase in bio-fuel productions, among which ethanol has an important role to play.

Ethanol ( $C_2H_5OH$ ), also called ethyl alcohol is a liquid derived from corn, grains or from a variety of other agricultural products, residues and waste. As such it is considered a renewable energy source. Over four million vehicles have operated on ethanol in Brazil as a result of a government programme to produce the fuel from sugar cane. In high concentrations ethanol is most typically used as a blend of 85% ethanol and 15% gasoline by volume, known as E85, which is appropriate for light-duty vehicles. Ethanol, however, is most commonly used to enrich gasoline as a blending component in a combination of 10% ethanol and 90% gasoline, commonly known as gasohol or E10. Ethanol can be blended in even lower concentrations with gasoline to produce oxygenated gasoline. Compared to gasoline, ethanol has a very high octane number, which induces a strong resistance to knock and consequently the ability to optimize the engine (compression ratio, spark advance). Its density is close to that of gasoline. The presence of oxygen in it can provide a more homogeneous

fuel/air mixing and consequently a decrease in unburnt or partially burnt molecule emissions (HC and CO). A high latent heat of vaporization of the alcohol enables a cooling effect of air and consequently can enhance the volumetric efficiency. But the oxygen included in the molecule (30%wt) induces an increase in the fuel volumetric consumption. The high latent heat of vaporization can induce running difficulties in cold conditions, especially cold start. Ethanol leads to azeotropes with light hydrocarbon fractions and can lead to volatility issues. Ethanol is miscible with water, which can cause non mixing problems when blended with hydrocarbons (Jeuland 2004). The high oxygen content of ethanol and its ability to oxidize into acetic acid induce compatibility problems with some materials used in the engine, such as metals or polymers. Ethanol combustion in engines induces aldehydes emissions, which can have a negative impact on health.

In India, plans have been developed to use ethanol enriched gasoline blends, and even ethanol-diesel oil blends. In 2003, the Ministry of Petroleum and Natural Gas launched the first phase of the Ethanol Blended Petrol (EBP) Program that mandated blending of 5% ethanol in gasoline in nine states (out of a total of 29) and four union territories (out of a total of 6). The second phase of the EPB program was launched in September 2006. It mandated 5% blending of ethanol with gasoline, subject to commercial viability, in 20 states and eight union territories with effect from November 2006. This would require about 550 million liters of ethanol over 2006/2007, all needing to be sourced domestically. Once the second stage of the ethanol program extends to all target states, the Government plans to launch the third stage when the ethanol blend ratio will be raised from 5% to 10% (Pohit et al. 2009). The ethanol production in India is mainly done using sugar cane as feedstock. For achieving the 5% blending EBP program in transport the estimated total sugarcane requirement in India of 545 million tones by 2011-12 which is more than the production of sugarcane in bumper years (approximately 355 and 340 million tonnes during 2006-07 and 2007-08 respectively) considering the different uses of ethanol in India (Ray et al. 2011). India being oil importing country and the oil prices escalate continuously; indigenous alternatives to gasoline will need to be used in higher proportions. Hence it is necessary to study the suitability of ethanol enriched gasoline blend ratios beyond E10 in unmodified SI engines so as to further reduce gasoline

consumption. This will help in future government program to make it mandatory to use higher percentages of ethanol enriched gasoline blends.

### **1.1.2 LPG as fuel in SI Engine**

From the point of view of the reduction of exhaust emission, liquefied petroleum gas (LPG) is a useful alternative fuel because of its comparatively higher heating value and also availability of sufficient supply infrastructure. LPG fuel also has merits in the operating characteristics under the high compression ratio because it has higher octane value and lower exhaust HC emission compared with the combustion of gasoline. The use of LPG as an alternative fuel for gasoline with low emissions has been studied extensively in recent years. The major attractions of LPG, in comparison with conventional liquid fuels, lie in their relatively low carbon content, causing them to burn cleanly with lower emissions of CO, CO<sub>2</sub> and HC. A higher thermal efficiency and therefore improved fuel economy can be obtained from internal combustion engines running on LPG when compared to gasoline (Ceviz and Yuksel 2006). The major reason for better performance of LPG is attributed to its high flame propagation speed compared to gasoline. The flame propagation speed of LPG is faster than that of gasoline at the range of lean to stoichiometric equivalence ratios, but at the rich mixtures range flame speed of gasoline is superior to that of LPG. Hence LPG has better combustion characteristics as lean burn engines (Lee and Ryu 2004). A common source of gaseous fuels involves the higher molecular weight components of natural gas in the form of Liquefied Petroleum Gases (LPG), which can be liquefied under pressure at ambient temperature. Usually, the main component of these fuel gases is n-propane. On this basis, often engine performance with pure or even commercial propane is considered to be represented adequately by engine operation with LPG gas mixtures. LPG is an environmentally friendly fuel for spark ignition engine which has potential emission advantages over gasoline. LPG refers to mixtures of hydrocarbons such as propane (C<sub>3</sub>H<sub>8</sub>), propene (C<sub>3</sub>H<sub>6</sub>), n-butane (C<sub>4</sub>H<sub>10</sub>), isobutene (methylpropane), and various butanes (C<sub>4</sub>H<sub>8</sub>). The composition Indian LPG is 70% of propane and 30% of butane. LPG is liquefied under pressure and compressed & stored in steel tanks under pressure that varies from 1.03 to 1.24 MPa. It is used for heating, cooking, and can be used as SI engine fuel. The fuel is liberated from lighter

hydrocarbon fraction produced during petroleum refining of crude oil and from heavier components of natural gas. It is also a by-product of oil or gas mining. LPG has some advantages over gasoline because it reduces engine maintenance, it offers faster cold starting and it provides overall lower operational cost. But the power output may decrease with LPG use since LPG displaces about 15–20% greater volume than gasoline. The properties of ethanol, LPG and gasoline are compared below in the table 1.3

Table 1.3: Properties of Ethanol, LPG and gasoline  
 \*(Kumar et al. 2009), \*\* (Loganathan and Ramesh 2007)

<b>Properties</b>	<b>Ethanol*</b>	<b>LPG**</b>	<b>Gasoline</b>
Composition (% vol.)	C <sub>2</sub> H <sub>5</sub> OH	70% C <sub>3</sub> H <sub>8</sub> –30% C <sub>4</sub> H <sub>10</sub>	C <sub>8</sub> H <sub>18</sub>
Heating value (MJ/kg)	26.8	45.7	44
Density ( kg/m <sup>3</sup> at 15 °C)	794	2.26	740
Research Octane number	120	103–105	88–100
Auto ignition temperature (°C)	425	405–450	371
Stoichiometric A/F ratio	8.95	15.5	14.2–14.8
Flame speed ( m/s)	--	0.382	0.375

## 1.2 CYCLE-BY-CYCLE VARIATIONS OF SI ENGINE

The combustion process in a spark ignition (SI) engine consists of the spark discharge and inflammation, initial flame development, and propagation of the flame in the combustion chamber. However, this combustion process does not repeat identically for each cycle even under steady state operation. This cyclic variation in the combustion process is generally accepted to be caused by variations in the mixture motion, in the amounts of air and fuel fed into the cylinder and their mixing, and in mixing with residual gases and exhaust gas recirculation (EGR), especially in the vicinity of the spark plug. Fuel lean operation is desired in spark ignition engines to reduce nitrogen oxides and hydrocarbon emissions as well as to improve fuel efficiency. Cycle by cycle (CBC) variation occurs more frequently with lean fueling

and EGR, resulting in large number of misfires and partial burns thus limits the potential benefits which can be derived from these operating modes. Therefore, minimization of CBC variations is a key requirement for operating near to or extending the effective lean limit. A small amount of CBC variations (slow burns) can produce undesirable engine vibrations. CBC variations are recognized as a limit for operating conditions with lean and highly diluted mixtures. Previous studies showed that if CBC variations could have been eliminated, there would be a 10% increase in the power output for the same fuel consumption (Litak et al. 2004). To maintain a fuel air mixture near the lean limit of combustion, the indicated mean effective pressure can be measured and interpreted as a measure of the combustion stability. The cyclic variations are caused because of the variations in the residual gas fraction, the air-fuel ratio, the fuel composition and the motion of unburned gas in the combustion chamber. The cylinder pressure-time history of consecutive cycles in an S.I engine shows that variations from one cycle to another exist. Since the pressure rate is uniquely related to the combustion, the pressure variations are caused by variations in the combustion process. The pressure related parameters which are useful from engine combustion diagnosis are the maximum cylinder pressure, the crank-angle at which maximum pressure occurs, the maximum rate of pressure rise, the crank-angle at which maximum rate of pressure rise occurs and the indicated mean effective pressure (IMEP). One important measure of CBC variations, derived from pressure data, is the coefficient of variation of indicated mean effective pressure ( $COV_{IMEP}$ ). It is the standard deviation in IMEP divided by the mean IMEP, and is usually expressed in percentage. This percentage defines the variability in indicated work per cycle, and it has been found that vehicle drivability problems usually results when  $COV_{IMEP}$  exceeds about 10% (Han 2000).

### **1.3 NO<sub>x</sub> REDUCTION TECHNIQUES**

Due to the stringent emission norms laid down by the governments the engine manufacturers are forced in to development of technologies to reduce harmful exhaust emissions. Exhaust gas after-treatment and optimized combustion are the two ways by which these emission regulations can be met without much fuel economy. LPG fueled spark ignition engines produce virtually zero emissions of particulate matter, very

little carbon monoxide, and moderate hydrocarbon emissions. A major disadvantage of the LPG is the oxides of nitrogen ( $\text{NO}_x$ ) emission which is greater than that for liquid fuels.  $\text{NO}_x$  comprise of nitric oxide (NO) and nitrogen dioxide ( $\text{NO}_2$ ) and both are considered to be toxic to humans as well as environmental health.  $\text{NO}_2$  is considered to be more toxic than NO. It affects human health directly and is precursor to ozone formation, which is mainly responsible for smog formation (Agarwal et al. 2011).  $\text{NO}_x$  emissions are mainly affected by the presence of oxygen in the charge and the reaction temperature, which promotes chemical activity during both the formation and destruction stages. During the formation stage, the reaction temperature is close to the adiabatic flame temperature, which is a consequence of the oxygen concentration in the charge, the initial temperature and pressure and the local fuel–air ratio. Pollutants from the exhaust gases in the engine exhaust system can be removed using after treatment systems. The catalytic converters used in spark-ignition engines consist of an active catalytic material in a specially designed metal casing which directs the exhaust gas flow through the catalyst bed (oxidizing catalysts for HC and CO, reducing catalysts for NO and three-way catalysts for all three pollutants). NO is removed by reduction using the CO, hydrocarbons, and  $\text{H}_2$  in the exhaust gas. In lean burn engines, the conventional three-way catalytic converters cannot be used. In this case Selective Catalytic Reduction (SCR) method is employed using urea, which converts to ammonia in the exhaust stream and reacts with  $\text{NO}_x$  over a catalyst to form harmless nitrogen gas and water. The catalyst is usually a mixture of titanium dioxide, vanadium pentoxide, and tungsten. SCR can remove up to 70% of  $\text{NO}_x$  from flue gases, but is very expensive (Shah et al. 2009).

An effective way for reducing  $\text{NO}_x$  emissions may be accomplished by changing the engine combustion process through the recycling of exhausted gases by adding combustion products to the fresh fuel-air mixture during the intake process. This technology is known as Exhaust Gas Recirculation (EGR) and has been applied in both spark ignition engines and compression ignition engines. EGR reduces the oxygen concentration in the charge and, consequently, the combustion pressure and temperature. The engine tests have demonstrated that  $\text{NO}_x$  is greatly suppressed when the oxygen concentration in the combustion chamber is reduced due to dilution effect. At part load EGR acts as an additional diluent in the unburned gas mixture, thereby

reducing the peak burned gas temperatures and NO formation rates. Substantial reductions in NO concentrations are achieved with 10–25% EGR. However, EGR also reduces the combustion rate, which makes stable combustion more difficult to achieve. EGR percentages in the 15–30% range are about the maximum amount of EGR a spark ignition engine will tolerate under normal part throttle conditions (Abd Alla 2002). Injection of water into the intake manifold has been found to be an effective way to reduce NO emission in SI, CI and LPG engines. Increasing the intake charge humidity was also reported as an efficient technique to control NO emission. It is a well known fact that water does not burn but it is excellent at absorbing heat due to water having a high specific heat capacity and latent heat of evaporation. Since it is a good absorber of heat, peak temperature in the cylinder will reduce so that the NO emissions will greatly reduce. Water injection is found to be a very effective strategy to reduce nitric oxide emission and to control hydrogen knocking, but it can certainly lead to many adverse effects like corrosion, lubricant contamination etc. (Subramanian et al. 2007).

#### **1.4 PRESENT WORK**

The present study deals with experimental investigations on the effect of steam induction with the intake air while using LPG as fuel on engine performance, combustion and emissions in a modified multi-cylinder SI engine. A 4 cylinder car engine of 44.5 kW capacity has been made in to a test rig with all necessary instrumentations for measuring performance, combustion and emission parameters. This test rig is modified to run with LPG injection after incorporating an aftermarket LPG injection kit. The engine is coupled to an eddy current dynamometer for measuring the load on engine. Series of experiments are carried out with the engine operating parameters of speed, throttle opening positions and idle ignition timings being varied. Experiments are also carried out on the engine test rig before modification with various ethanol enriched gasoline blends of 5, 10, 15 and 20%. To compare the results of the experiments with LPG, an ethanol enriched gasoline blend is optimized as a baseline fuel based on engine performance, combustion and emissions. With LPG combustion, the NO<sub>x</sub> emissions are higher. Hence to address this problem, the method of steam induction is employed. The waste heat from the

engine exhaust gas is used to heat water in a heat exchanger and it is converted into steam. The steam at various proportions of 10, 15, 20 and 25% of LPG consumption are inducted along with the intake air. Engine performance, combustion and emissions are studied. Finally a comparative study is done with LPG along with steam and ethanol enriched gasoline blend.

## **1.5 ORGANIZATION OF THE THESIS**

The thesis has been organized into 6 chapters starting with the introduction. This chapter gives the background of the problem definition. The second chapter deals with the detailed literature review covering mainly the various aspects related to combustion, performance and emissions of alternative fuels and the methods to improve the same. Previous works on the use of alcohol fuels like methanol, ethanol in SI engines and various gaseous fuels like LPG, CNG etc. are detailed in this chapter. Based on the literature, the objectives of the present work are described in this chapter. The third chapter presents the experimental work, covering the engine setup, instrumentation and measurements. Details of the original set up, the modifications done to run the engine with LPG and the steam induction system developed are given. The experimental procedures and experimental methodology are described in chapter four. The details of IMEP calculations and heat release rate calculations are given in this chapter. The uncertainty and errors involved in the experimentations are also analysed. Fifth chapter deals with the results obtained with detailed discussion. The results of engine operation with ethanol enriched gasoline blends are detailed in the beginning and an optimum blend is selected for further comparisons. The investigations with LPG as fuel are described in the next part, with various operating parameters. Results of combustion of LPG along with steam induction are described in the next part of this chapter. Finally a comparative study has been done with engine performance, combustion and emissions of LPG along with steam induction with ethanol enriched gasoline. The sixth chapter is devoted to bring out the important conclusions based on this work and the scope for future work.



## CHAPTER 2

### LITERATURE REVIEW

Exhaust gas emission regulations and fuel economy standards have become more stringent due to environmental problems caused by vehicle exhaust emissions. The rapidly diminishing oil reserves have also forced researchers to move towards the application of alternative fuels in internal combustion (IC) engines. In this context a review of literature on the use of various alternate fuels for spark ignition engines has been done in this chapter. Details of studies on the combustion, performance and exhaust emissions with the use of alternative fuels like LPG and ethanol have been presented. One of the major problems with burning gaseous fuel is the higher NO<sub>x</sub> emissions. Various NO<sub>x</sub> reduction techniques used have also been reported. Literature on the causes and estimation of cycle-by-cycle combustion variations and heat release rate analysis are given.

#### 2.2 USE OF ETHANOL IN SI ENGINES

Alcohols like ethanol and methanol are biofuels which can be used as an alternative fuel in internal combustion engines. Al-Farayedhi et al. (2004) have conducted experiments on a six-cylinder Mercedes-Benz engine of 2960 cm<sup>3</sup> capacity with different oxygenates viz MTBE, methanol and ethanol in three ratios of 10, 15, and 20 vol. % with a base unleaded fuel. When compared to the base and leaded fuels, the oxygenated blends improved the engine brake thermal efficiency. Overall, the methanol blends performed better than the other oxygenated blends in terms of engine output and thermal efficiency. Sadiq Al-Baghdadi (2001) has studied the effect of the amount of hydrogen/ethyl alcohol addition on the performance and pollutant emission of a Ricardo E6/US carbureted single cylinder spark ignition engine. The results of the study show that all engine performance parameters have been improved when operating the gasoline spark ignition engine with dual addition of hydrogen and ethyl alcohol. The important improvements of alcohol addition are the reduced NO<sub>x</sub> emission while increasing the higher useful compression ratio and output power of hydrogen-supplemented engine. When ethyl alcohol is increased over 30%, it causes unstable engine operation which can be related to the fact that the fuel is not

vaporized, and this causes a reduction in both brake power and efficiency. Shenghua et al. (2007) have adopted a 3-cylinder port fuel injection engine with the fuel of low fraction methanol in gasoline. Without any retrofit of the engine, experiments show that the engine power and torque will decrease with the increase fraction of methanol in the fuel blends under wide open throttle (WOT) conditions. However, if spark ignition timing is advanced, the engine power and torque can be improved under WOT operating condition. Engine thermal efficiency is thus improved in almost all operating conditions. Engine combustion analyses show that the fast burning phase becomes shorter; however, the flame development phase is a little delay. When methanol/gasoline fuel blends being used, the engine emissions of CO and HC decrease, NO<sub>x</sub> changes little prior to three-way catalytic converter (TWC). The non-regulated emissions, unburned methanol and formaldehyde, increase with the fraction of methanol, engine speed and load, and generally the maximum concentrations are less than 200 ppm. Methanol addition to gasoline improves the SI engine cold start. Srinivasan and Saravanan (2010) have investigated the effects of ethanol-blended gasoline with oxygenated additives of cycloheptanol and cyclooctanol on a 3 cylinder SI Engine. The experimental results proved that the blend increased brake thermal efficiency more than a sole fuel, such as gasoline. The emission tests found that the CO slightly decreased, while HC and O<sub>2</sub> increased moderately and CO<sub>2</sub> and NO<sub>x</sub> appreciably decreased. Eyidogan et al. (2010) have investigated the effects of ethanol–gasoline (E5, E10) and methanol–gasoline (M5, M10) fuel blends on the performance and combustion characteristics of a spark ignition (SI) engine. A vehicle with four-cylinder multi-point injection system SI engine was used. The tests were performed on a chassis dynamometer while running the vehicle at two different vehicle speeds (80 km/h and 100 km/h), and four different wheel powers (5, 10, 15, and 20 kW). The results indicated that when alcohol–gasoline fuel blends were used, the brake specific fuel consumption increased; cylinder gas pressure started to rise later than gasoline fuel. Almost in the all test conditions, the lowest peak heat release rate was obtained from the gasoline fuel use.

Various researchers have investigated the use of ethanol in SI engines and have found that using ethanol as a fuel additive to unleaded gasoline causes an improvement in engine performance and exhaust emissions. Yuksel and Yuksel (2004) have designed

a new carburetor to realize of a stable homogeneous liquid phase which is a problem for the successful application of gasoline–alcohol mixtures as a motor fuel in a 1668 cc Opel record L engine. By using ethanol–gasoline blend, the availability analysis of a spark-ignition engine was experimentally investigated. Using 60% ethanol–40% gasoline blended fuel, the torque output of the engine increased slightly, the CO and HC emissions decreased dramatically as a result of the leaning effect caused by the ethanol addition, and the CO<sub>2</sub> emission increased because of the improved combustion. It was found that using ethanol-gasoline blended fuel, the CO and HC emissions would be reduced approximately by 80% and 50%, respectively, while the CO<sub>2</sub> emission increases 20% depending on the engine conditions. Test results on a KIA 1.3 four cylinder engine by Najafi et al. (2009) has indicated that using ethanol–gasoline blended fuels up to 20% by volume, the torque output and fuel consumption of the engine slightly increase; CO and HC emissions decrease as a result of the leaning effect caused by the ethanol addition. In contrast, the concentration of CO<sub>2</sub> and NO<sub>x</sub> was found to be increased when ethanol is introduced. Al-Hasan (2003) has conducted experiments on a four cylinder, Toyota-Tercel-3A engine using gasoline–ethanol blends with different percentages up to 25% by volume at three-fourth throttle opening position and speed range of 1000 to 4000 rpm. It was found that using ethanol as a fuel additive to unleaded gasoline causes an improvement in engine performance and exhaust emissions. Ethanol addition results in an increase in BP, brake thermal efficiency and volumetric efficiency by about 8.3%, 9.0% and 7% mean average values respectively and the BSFC and equivalence air–fuel ratio decrease by about 2.4% and 3.7% mean average value respectively. The exhaust emissions have been reduced by about 46.5% and 24.3% of the mean average values of CO and HC emission, respectively, for all engine speeds while the CO<sub>2</sub> emissions increase by about 7.5%. The 20% ethanol fuel blend gave the best results of the engine performance and exhaust emissions. Bayraktar (2005) has investigated experimentally and theoretically the effects of ethanol addition to gasoline on a 763 cm<sup>3</sup> SI engine for performance and exhaust emissions. A quasi-dimensional SI engine cycle model has been adapted for SI engines running on gasoline–ethanol blends. Experiments have been carried out with the blends containing up to 12% ethanol at 1500 rpm for compression ratios of 7.75 and 8.25 at full throttle setting. Blend of

7.5% ethanol was the most suitable from the engine performance and CO emissions points of view. However, theoretically 16.5% ethanol blend was the most suited. Hsieh et al. (2002) have experimentally investigated the engine performance and pollutant emission of a commercial SI engine using ethanol–gasoline blended fuels of 5%, 10%, 20% and 30%. It was found that with increasing the ethanol content, the Reid vapor pressure of the blended fuels initially increases to a maximum at 10% ethanol addition, and then decreases. Results indicate that torque output and fuel consumption of the engine slightly increase; CO and HC emissions decrease significantly as a result of the leaning effect caused and CO<sub>2</sub> emission increases because of the improved combustion while it was concluded that NO<sub>x</sub> emission depends on the engine operating condition rather than the ethanol content.

Many researchers have conducted experiments to find out the effect of compression ratio with ethanol enriched gasoline. Abdel-Rahman and Osman (1998) have experimented in a variable compression ratio engine to study the effect of varying the compression ratio using different ethanol-gasoline fuel blends up to 40%, on SI engine performance. The results show that the engine indicated power improves with the percentage addition of the ethanol in the fuel blend. The maximum improvement occurs at 10% ethanol-90% gasoline fuel blend. Topgul et al. (2006) have conducted studies on a Hydra single-cylinder SI engine by varying the compression ratio (8:1, 9:1 and 10:1) and ignition timing at a constant speed of 2000 rpm at wide open throttle which has shown that blending unleaded gasoline with ethanol slightly increases the brake torque and decreases CO and HC emissions. It was also found that blending with ethanol allows increasing the compression ratio without knock occurrence. Celik (2008) has used ethanol blends of E25, E50, E75 and E100 as fuels at high compression ratio to improve performance and to reduce emissions in a Lombardini LM 250 engine. The results showed that engine power increased by about 29% when running with E50 fuel compared to the running with E0 fuel. Moreover, the specific fuel consumption, and CO, CO<sub>2</sub>, HC and NO<sub>x</sub> emissions were reduced by about 3%, 53%, 10%, 12% and 19%, respectively.

Huang et al. (2000) have investigated the use of ethanol blended gasoline and have shown that combustion characteristics and hydrocarbon emissions improve in a spark

ignition engine. Calculation results, based on the recorded pressure diagram, show that the flame development angle and rapid burn angle decrease when the fraction of alcohol fuels in gasoline is small, whereas they increase when the fraction of alcohol fuels is large. The experimental results show that engine exhaust hydrocarbon emissions can be reduced by blending oxygenated fuels in gasoline rather than operating on neat gasoline. The use of alcohol blends in port fuel injected SI engines has been studied by many researchers. Brusstar et al. (2002) at EPA have used a turbocharged, PFI spark-ignited 1.9 L, 4-cylinder engine with 19.5:1 compression ratio. The engine was operated unthrottled using stoichiometric fueling from full power to near idle conditions, using EGR and intake manifold pressure to modulate engine load. Operating on methanol fuel, the engine demonstrates better than 40% brake thermal efficiency from 6.5 to 15 bar BMEP at speeds ranging from 1200 to 3500 rpm, while achieving low steady state emissions using conventional after treatment strategies. Similar emissions levels were realized with ethanol fuel, but with slightly higher BSFC due to reduced spark authority at this compression ratio. These characteristics make the engine attractive for hybrid vehicle applications. Knapp et al. (1998) have tested the emissions from a fleet of 11 vehicles at temperatures of 75, 0, and -20°F with base gasoline and E10. The testing followed the Federal Test Procedure, and regulated emissions -CO, total hydrocarbons (THC), and nitrogen oxides (NO<sub>x</sub>) - CO<sub>2</sub>, speciated organics, and fuel economy were measured. The data obtained indicated that with most vehicles, at the temperatures tested, improvements in both CO and THC emissions were obtained with the use of E10 fuel. At the lowest temperature used, -20 °F, most vehicles had an increase in NO<sub>x</sub> emissions with the use of E10 fuel. At the other temperatures, however, more vehicles showed a decrease in NO<sub>x</sub> emissions with the use of E10. With all vehicles at all temperatures tested, the emissions of acetaldehyde increased significantly when E10 fuel was used. The highest increase was about 8 to 1. Benzene, formaldehyde, and 1,3 butadiene showed both increases and decreases in the emissions when using E10 fuel. Unexpected results were obtained with the fuel economy, with about half of the tests showing an increase in fuel economy with the use of E10 fuel.

Kadam (2002) has conducted a life cycle assessment to quantify the environmental benefits of diverting excess bagasse to ethanol production in India as opposed to

disposing it through the current practice of open-field burning. The results demonstrated that the use of ethanol has the lower net values for carbon monoxide, hydrocarbons (except methane), SO<sub>x</sub>, NO<sub>x</sub>, particulates, carbon dioxide, methane, and fossil energy consumption. Reduced carbon dioxide and methane emissions for the ethanol scenario also lower its greenhouse potential. The lower values observed for the depletion of natural resources, air acidification potential, eutrophication potential, human toxicity potential, and air odor potential are advocating the ethanol scenario. Niven (2005) has studied the five environmental aspects of ethanol enriched gasoline: (1) its purported reduction in air pollutant emissions; (2) its potential impact on subsurface soils and groundwater; (3) its purported reduction in greenhouse gas emissions; (4) the energy efficiency of ethanol; and (5) the overall sustainability of ethanol production. The study indicates that E10 is of debatable air pollution merit; offers little advantage in terms of greenhouse gas emissions, energy efficiency or environmental sustainability; and will significantly increase both the risk and severity of soil and groundwater contamination. In contrast, E85 offers significant greenhouse gas benefits, however it will produce significant air pollution impacts, involves substantial risks to biodiversity, and its groundwater contamination impacts and overall sustainability are largely unknown.

Following the global trend, India has also adopted ethanol policy to promote ethanol production and utilization in the country%. In 2003, the Ministry of Petroleum and Natural Gas launched the first phase of the Ethanol Blended Petrol (EBP) Program that mandated blending of 5% ethanol in gasoline in nine states (out of a total of 29) and four union territories (out of a total of 6). The second phase of the EPB program was launched in September 2006. It mandated 5% blending of ethanol with gasoline, subject to commercial viability, in 20 states and eight union territories with effect from November 2006. Once the second stage of the ethanol program extends to all target states, the Government plans to launch the third stage when the ethanol blend ratio will be raised from 5% to 10 (Zhou and Thomson 2009). India has cost disadvantage in ethanol production in comparison with Brazil and the USA. Keeping in pace with the rise in domestic demand for petrol and the proposed hike in mandatory blending requirement of ethanol, India is unlikely to meet the demand for ethanol in the near future, unless more focused approach is adopted by the

Government. Keeping in view the high potential of the cellulosic ethanol, India should make collaborative research on this area with other countries like Canada that have made substantial advances in cellulosic technology (Pohit et al. 2009).

### **2.3 USE OF LPG IN SI ENGINES**

Gaseous fuels in general are promising alternative fuels due to their economical costs, high octane numbers, high calorific values and lower polluting exhaust emissions. During the last decade, gaseous fuels such as liquefied natural gas (LNG) and liquefied petroleum gas (LPG) have been widely used in commercial vehicles, and promising results have been obtained from the fuel economy and exhaust emissions points of view. LPG is a very clean fuel by comparison to petrol and diesel. Burning LPG in an internal combustion engine produces virtually no particulate material, and much lower emissions of hydrocarbons (HC) and carbon monoxide (CO) than either petrol or diesel. Because of the improved emissions, the governments have chosen to promote the use of LPG as a road fuel by allowing generous tax reduction on the purchase of LPG, in order to encourage vehicle owners to convert in to LPG.

Lee and Ryu (2004) have investigated the combustion process of the heavy duty LPG engine, the flame propagation and combustion characteristics using a CVCC (constant volume combustion chamber) and a port injection type heavy duty LPLi (Liquefied Petroleum Liquid injection) engine system. Both the laser deflection method and the high-speed Schlieren photography method were employed to measure the flame propagation speed of LPG fuel. According to the CVCC and heavy duty LPLi engine experimental results, the flame propagation reached a maximum speed at the stoichiometric equivalence ratio, regardless of operating conditions, and the effect of the equivalence ratio on both flame propagation and combustion characteristics was greater than that of ambient conditions and also the coefficient of variation of combustion duration increased when the equivalence ratio decreased. Furthermore, the combustion stability worsened as the equivalence ratio moved into the lean region. Dagaut and Ali (2003) have reported a kinetics study of gas-phase oxidation of a LPG blend mixture in a jet-stirred reactor at 1 atm, over the temperature range 950–1450 K and for equivalence ratios of 0.25, 0.5, 1, 1.5, 2 and 4. These measurements were used to validate a detailed kinetic reaction mechanism consisting of 112 species and 827

reactions (most of them reversible). Overall, the modeling is in very good agreement with the experimental measurements and showed that the oxidation of this LPG blend follows the general oxidation paths already delineated for simple alkanes.

Over the past few decades research on alternative fuels are going on to explore the possibility of availability, cost, lower emissions, and lower dependency on petroleum. Liquefied Petroleum Gas (LPG) is among the many alternatives proposed to replace gasoline in the short term due to its excellent characteristics as a fuel for spark ignition (SI) engines. Yamin and Badran (2002) have studied the parameters that affect the engine's heat losses mainly during power stroke, with suggestions to minimize it using a mathematical model, which was validated by experimentations in a single cylinder engine while using LPG as fuel. Increasing compression ratio, the need for near-central spark locations, larger valve areas and the aim for leaner air-fuel equivalence ratios are shown to have a favourable effect on reducing heat losses. Caton et al. (1997) have discussed the development of dedicated LPG fueled SI engine. It was intended to advance the development of LPG to encourage the use of propane in vehicles. Beroun et al. (2001) have given details of the conversion of diesel engines to SI engines to burn LPG, LNG with an intention to reduce the emissions and cyclic variability. Gas fuelled SI engines seems to be very attractive although its cyclic variability is higher because of lower emission. Johnson (2003) has believed that LPG should play a greater role in road-transport-fuel policy in Western Europe, because (1) it is more secure than conventional and most alternative road-transport fuels; (2) it is superior to most road-transport fuels with respect to public health and environmental impact, and (3) it is available commercially today, which most alternatives are not. Further he says policy makers should target a 2010 market share for LPG at 3–5% of road-transport fuel, up from its current level of about 1%. IMPCO Technologies (1998) in their report describes the last in a series of three projects designed to develop a commercially competitive LPG light duty passenger car that meets California ULEV standards and corporate average fuel economy (CAFE) energy efficiency guidelines for such a vehicle. In this project, IMPCO upgraded the vehicle's LPG vapor fuel injection system and performed emissions testing. The vehicle met the 1998 ULEV standards successfully, demonstrating the feasibility of meeting ULEV standards with a dedicated LPG vehicle.



Oh et al. (2002) have investigated combustion and flame propagation characteristics of the liquid phase LPG injection (LPLI) engine in a single cylinder optical engine. In this study, the effects of piston geometry along with injection timing and swirl ratio on flame propagation characteristics were investigated. The results show the correlation between the flame propagation characteristics, which is related to engine performance of lean region, and engine design parameters such as swirl ratio, piston geometry and injection timing. Stronger swirl resulted in faster flame propagation under open valve injection. The flame speed was significantly affected by injection timing under open valve injection conditions; supposedly due to the charge stratification. Piston geometry affected flame propagation through squish effects. Badr et al. (1998) have conducted a parametric study on the lean operational limits of a Ricardo E6 engine using propane and LPG as fuels and have shown that the lean misfiring limit increased with increasing engine speed. As the spark timing was advanced the lean knocking and misfiring limits were reduced. Murillo et al. (2005) in their research adapted two different outboard engines for operation with bottled LPG dosed in gaseous form to determine the basic parameters and quantify the emission index for carbon monoxide, unburned hydrocarbons, and nitric oxides when LPG is used instead of gasoline. The results obtained indicate that with the use of LPG, specific fuel consumption and CO emissions were much lower without noticeable power loss while HC emissions are shown to be little affected by fuel substitution. In contrast, NO<sub>x</sub> emissions were higher, but could be kept below current and future emission limits.

Bae et al. (2001) have investigated the effects of EGR variables on combustion characteristics in a 2 liter, 4 cylinder spark ignition LPG fuelled engine. The effects of EGR on the reduction of thermal loading at exhaust manifold were also investigated because the reduced gas temperature is desirable for the reliability of an engine in light of both thermal efficiency and material issue of exhaust manifold. The steady-state tests show that decreasing EGR temperature by 180°C enabled the reduction of exhaust gas temperature by 15°C in cooled EGR test at 1600rpm / 370kPa BMEP operation, and consequently the reduction of thermal load at exhaust. All COV<sub>IMEP</sub> values distributed within 3% except the case of lower engine speed and load operation during the entire tests, and they meant a stable combustion through reduced cyclic

variations. Jothi et al. (2008) have experimentally investigated the effect of EGR on homogeneous charge ignition engine. A stationary four stroke, single cylinder, direct injection diesel engine capable of developing 3.7 kW at 1500 rpm was modified to operate in HCCI mode with LPG. The LPG has a low cetane number ( $<3$ ), therefore Diethyl ether was added to the LPG for ignition purpose. Results showed that by EGR technique, at part loads the brake thermal efficiency increases by about 2.5% and at full load, NO concentration could be considerably reduced to about 68% as compared to LPG operation without EGR. However, higher EGR percentage affects the combustion rate and significant reduction in peak pressure at maximum load. Woo and Bae (2007) have examined lean burn of LPG with stratified EGR to attain lower emissions and better fuel economy. The stratification of EGR along the vertical distance from the spark plug was observed through a concentration measurement by a planar laser-induced fluorescence (PLIF) technique. Properly stratified EGR showed faster combustion and improved combustion stability for both stoichiometric and lean mixtures compared to those from homogeneous EGR. With a 30% EGR rate, the peak heat release was 10% higher, accompanied by shorter combustion duration in the stratified EGR (SEGR) case than in the homogeneous EGR (HEGR) case. More EGR could be admitted and NO<sub>x</sub> emission further reduced with less increase in hydrocarbon emission with stratified EGR than with homogeneous EGR. Those results are due to the dominance of stratified EGR over homogeneous EGR in combustion speed and stability. Zhaoda et al. (2002) have developed an emission control technology by using universal wide range exhaust gas oxygen sensor (UEGO) for LPG engine. The UEGO is used mainly controlling the air/fuel ratio to make the combustion process in cylinder under the lean burn condition. The results show that the better emission characteristics can be got. Under the lean burn condition the control of NO<sub>x</sub> emission still is difficult for LPG engine because of lower NO<sub>x</sub> catalysis transmissible efficiency. In order to reduce the NO<sub>x</sub> emission, a special TWC should be set up for lean burn of LPG engine.

Goto et al. (2000) report that lean burn operation of an LPG SI engine has resulted in improved fuel consumption for both the full and half load cases. As the in-cylinder flow was made more turbulent by suitable piston cavity modification, the cyclic variation and combustion duration both declined. High swirl improved combustion

stability and thermal efficiency, and enabled engine operation at low  $\text{NO}_x$  levels. Enhanced combustion by high swirl was also clearly observed at the low load range, where air motion was not very vigorous. The propane butane fuel content was varied to determine its effect on engine performance. For the 100% load case, as the propane composition increased, cyclic variation declined and  $\text{NO}_x$  emissions increased. Mustafa and Briggs (2098) have examined a LPG fueled four-stroke spark ignition engine to determine and quantify the exhaust emissions from the engine. The volume percentage of LPG fuel in gasoline used in the experiments was varied at 5%, 10% and 20%, and the amount of LPG fuel injected is controlled electronically at an idling speed of 4000rev/min. It was found that the level of carbon dioxide ( $\text{CO}_2$ ) peaked at around relative air-fuel ratio of 1.0 and carbon monoxide (CO) exhibits a sharp decrease as the relative air-fuel ratio increases. Unburned hydrocarbons (UHC) also shows marked reduction as the relative air-fuel ratio exceeds stoichiometric and nitrogen oxides ( $\text{NO}_x$ ) exhibits an increasing trend as the relative air-fuel ratio increases.

Loganathan and Ramesh (2007) have injected gasoline and LPG into the manifold of a 145 cc two stroke engine using a specially developed electronic circuit to have a close control over the air fuel ratio. Experiments were carried out at 3000 rpm and fixed throttle positions of 10, 15, 25, 40, 50 and 100% of full opening. The amount of fuel injected (air fuel ratio), injection timing and injection pressure were varied. The maximum brake thermal efficiency with LPG was 25% and that with gasoline was 23%. The engine could generally operate with much leaner mixtures with LPG due to its good mixture formation capability. HC levels and exhaust gas temperature were slightly higher with LPG while NO levels were comparable. It was found that the injection pressure had to be reduced at part throttle conditions in order to get better engine stability and performance. The maximum power output with LPG was lesser than that with gasoline. Gumus (2011) has investigated the effects of variation in volumetric efficiency on the 4 cylinder dual fuel engine (gasoline and LPG) performance and emissions with different LPG usage levels. The engine was operated with new generation closed loop, multi-point and sequential gas injection system. The volumetric efficiency decreased considerably at the use of 25% LPG level. As for the 50%, 75% and 100% LPG usage, volumetric efficiency decreased in proportion to

LPG usage level. Air–fuel ratio decreases with the increase in LPG usage level and the minimum air–fuel ratio value was obtained at 100% LPG usage. At the use of mixture containing 25% LPG, brake specific fuel and energy consumption decreased while the brake thermal efficiency was maintained. Positive results were obtained at all LPG usage levels in terms of exhaust emissions. Best results were achieved at using 100% LPG for exhaust emissions of CO and HC. Kowalewicz (2000) has analysed the thermodynamic cycle of IC engine from the point of view of economy and emissions. From this analysis potential capability of engine development was derived. Several different modes of fuelling were proposed and tested on one cylinder test engine from the point of view of extending lean operating limit of the engine, emissions and fuel economy. Among them were: fuelling with evaporated preheated gasoline, with gas (LPG evaporated) and with liquid butane. From these modes, fuelling with liquid butane injected to inlet port was selected and finally tested. This novel system of fuelling offered better than standard engine performances and emissions at lean operating limit. These results were validated on full-scale two-cylinder engine.

Price et al. (2004) have investigated the thermodynamic performance of the evaporator used in the Ford Focus with LPG over the engine power range. In-vehicle tests were performed at two extreme operating temperatures so that the switchover (from gasoline to LPG) characteristics could be examined. Approximately 300 kW of thermal energy from the LPG, (6 g/s), is needed to realize maximum engine power output. The effect of LPG composition on engine performance was also studied, and was found to be minimal due to the fuel components having similar calorific values. Engine coolant temperatures (into and out of the evaporator) are discussed and for maximum power, using energy balance, the temperature difference was found to be about 6 K. Masi and Gobatto (2012) have conducted experimental investigations on a 5 cylinder passenger car SI engine equipped with a ‘‘third generation’’ LPG kit for the dual-fuel operation using a dynamometer test rig. A single-stage pressure reducer was selected as LPG evaporator, to take advantage of an additional pre-heating of the liquid LPG that allows higher power output than a two-stage device of the same size. Engine performance, volumetric efficiency and change of LPG thermodynamic states in the evaporator were measured both in steady-state and transient operation of the

engine. Steady-state measurements show the advantage of LPG in terms of engine efficiency, and quantify the drop in steady-state brake torque due to the volume swept by gaseous fuel in the fresh charge admission process. On the other hand, transient measurements show that a single-stage evaporator device is capable to match overall simplicity and satisfactory performance during strong changes in engine load.

Bayraktar and Durgun (2005) have investigated the combustion, cycle, performance parameters and exhaust emissions of an SI engine running on gasoline and LPG by means of the quasi-dimensional spark ignition (SI) engine cycle model. In the case of using LPG in SI engines, the burning rate of fuel is increased, and thus, the combustion duration is decreased thus the cylinder pressures and temperatures predicted for LPG are higher than those obtained for gasoline. The maximum cylinder pressures and temperatures predicted for LPG are higher. This may cause some damages on engine structural elements. LPG reduces the engine volumetric efficiency and, thus, engine effective power. Furthermore, the decrease in volumetric efficiency also reduces the engine effective efficiency and consequently increases specific fuel consumption. LPG decreases the mole fractions of CO and NO included in the exhaust gases. Khatri et al. (2009) have developed a sequential gas injection system working on the master-slave concept for hydrogen with compressed natural gas (HCNG) as an automotive fuel in a car fitted with a 4 cylinder, 1.3 liter, S.I. engine. The effect of gas pressure and gas temperature on the duration gas injection was considered in the control strategy. Different parameters like injector pulse width and ignition timing were optimized under idling and different load conditions. Detailed testing was conducted on idling operation to analyze the idle stability and emission. Hoekstra et al. (1996) have determined the NO<sub>x</sub> emissions and efficiency of hydrogen, natural gas and hydrogen/natural gas blended fuels. The results indicate that use of hydrogen/natural gas fuel has a potential of meeting highly restrictive NO<sub>x</sub> levels. Lee et al. (2009) have investigated a 2.7 liter spark ignition engine operated with DME blended LPG fuel at 1800 and 3600 rpm. Results showed that stable engine operation was possible for a wide range of engine loads up to 20% by mass DME fuel. Up to 10% DME, output engine power was comparable to that of pure LPG fuel. Exhaust emissions measurements showed that hydrocarbon and NO<sub>x</sub> emissions were slightly increased when using the blended fuel at low engine speeds.

However, engine power output was decreased and break specific fuel consumption (BSFC) severely deteriorated with the blended fuel since the energy content of DME is much lower than that of LPG. Furthermore, due to the high cetane number of DME fuel, knocking was significantly increased with DME. Bielaczyc et al. (2001) have reviewed the exhaust emissions from automotive engines fuelled with petrol or LPG and CNG alternatively. In case of LPG fuelled vehicles differences in CO and HC emissions compared to gasoline were not so visible, but the main problem is difficulty with calibration of LPG fuelling systems of II generation and I. The increase of HC and CO emissions during cold start and warm-up of LPG vehicles is accompanied by increased CO<sub>2</sub> emissions and fuel consumption. CO<sub>2</sub> emission is lower for LPG and CNG fuelled vehicles compare to gasoline fuelled vehicles. Saraf et al. (2009) have investigated emissions of newly introduced gasoline/LPG bifuel 1.8 liter, 4 cylinder automotive engine in Indian market. Emissions were tested as per LPG-Bharat stage III driving cycle for urban cycle and extra urban cycle. Corrected emissions were computed by deducting ambient reading from sample reading. CO emissions in both urban & extra urban cycle are less in LPG mode as compared to gasoline mode. CO emissions were 147.89 ppm in gasoline mode & 103.1 ppm in LPG mode. In extra urban cycle CO emissions were 43.11 in gasoline mode & 38.8 ppm in LPG mode. Hydrocarbon emissions were 53.8 ppm in urban cycle & 11.1 ppm in extra urban cycle in gasoline mode. These values were 37.7 ppm & 5.5 ppm in LPG mode. NO<sub>x</sub> emissions were 5.76 ppm in urban cycle & 3.043 ppm in extra urban cycle in gasoline mode. These values were 3.4 & 0.7 in LPG mode. CO<sub>2</sub> emissions were 8950.3 ppm in urban cycle & 16509.32 ppm in extra urban cycle in gasoline mode. These values were 8051 ppm & 14693.3 ppm in LPG mode.

Yousufuddin and Mehdi (2008) have evaluated the performance and emission characteristics of a single cylinder variable compression ratio spark ignition engine when fuelled with LPG in the form of propane at different compression ratios. The results obtained show that the engine running on an LPG fuel system delivered a substantial improvement in power and torque in a high-load condition. Conversion of the engine using LPG as fuel showed an average reduction of CO and HC exhaust gas emissions in comparison to the original fuel. Seshaiyah (2010) has conducted experiments on a variable compression ratio spark ignition engine tested with pure

gasoline, LPG (Isobutene), gasoline blended with ethanol 10%, 15%, 25% and 35% by volume and gasoline mixed with kerosene at 15%, 25% and 35% by volume without any engine modifications. It has been observed that the petrol mixed with ethanol at 10% by volume performed better at all loads and compression ratios. It also been observed that the variation in thermal efficiency for all the tested fuels is approximately 5%, and well within the experimental error. At medium loads, the efficiency variation is small. He recommended that the petrol should not be mixed with the commercially available kerosene as it gives high carbon monoxide emission. LPG combustion has shown lowest CO emissions at all test points.

#### **2.4 CYCLE-BY-CYCLE COMBUSTION VARIATION**

Lean burn is one of several effective methods for improving fuel consumption and reducing NO<sub>x</sub> emissions in an automotive SI engine. However, lean burn operation increases the cyclic combustion variation and in the worst case deteriorates vehicle drivability. Cyclic variability is recognized as a limit for operating conditions with lean and highly diluted mixtures. The cyclic variations are caused by both chemical and physical phenomena. Of these phenomena, the variations in the residual gas fraction, the fuel–air ratio, the fuel composition and the motion of unburned gas in the combustion chamber can be taken into consideration. Cyclic variability is recognized as a limit for operating conditions with lean and highly diluted mixtures. Previous studies showed that if cyclic variability could have been eliminated, there would be a 10% increase in the power output for the same fuel consumption and power pollution of emissions from the engine.

An extensive literature survey has been done by Young (1981) to assess the state of the art relative to cyclic dispersion in combustion and its effect on the subsequent pressure development in the cylinder of a homogeneous charge SI engine. He has conducted survey ranging from 1950 to 1980. The study includes the effect of chemical factors such as equivalence ratio, charge dilution and fuel type. The physical factors include ignition system, combustion chamber geometry, engine speed, compression ratio, swirl and turbulence. A more detailed review of literature on cyclic variability in SI engines has been done by Ozdor et al. (1994), which review the effect of various parameters and their contributions. They also give an insight regarding the

various indicators used for measurements of cycle-by-cycle variations. Accordingly the pressure related parameters such as  $P_{\max}$ ,  $\theta_{P_{\max}}$  and IMEP are still most valuable in estimating in quantitative terms, the effect of various variables on the cycle-by-cycle variations. They have also distinguished between the factors causing and influencing the cycle-by-cycle variations. Gatowski et al. (1984) have developed a heat release analysis procedure of SI engine which includes the effects of heat transfer, crevice flow and fuel injection. The model developed has been validated with experimental results. Cycle-by-cycle application of the model tend to predict small negative heat release rates at the end of combustion for fast burning cycles. The possible sources of error include the heat transfer correlation, the method used to represent the thermodynamic properties, or thermal effects in the pressure transducer. Kalghatgi (1987) has shown that the advanced ignition systems are of practical interest for automotive applications as they influence the cyclic variations. The cyclic variations in SI engines can be reduced at source by reducing the variations in combustion. The influence of non homogeneity on CBC variations was studied by Pundir et al. (1981) and shown that cyclic variations increases with increase in charge non homogeneity at a given mixture strength.

Lean burn is one of several methods for improving efficiency however increases the cyclic variations. Yamamoto and Misumi (1987) has analyzed the cyclic combustion variation in a lean operation SI engine with the IMEP variation being subjected to multiple regression analysis to identify the causes of the cyclic variations, and found that the main cause of IMEP variations in the lean operating SI engine was the released heat quantity variations. Ishli et al. (1997) have investigated the cyclic variations of IMEP under lean burn operations. They have identified three major reasons for cyclic variations of IMEP namely the burning speed during initial stage of combustion, maximum fuel mass fraction burned and variation in the late burning during late expansion stroke. Whitelaw and Xu (1995) have investigated the cyclic variations in a lean burn SI engine without and with swirl. Measurements of cylinder pressure and flame travel velocity in the lean limit have been done. The extent to which residual burned gas retarded the combustion rate and increased cyclic variability are quantified. Einewall and Johansson (2000) have studied the influence of spark gap and fuel injection strategies to improve lean burn limit and shown that



combustion chamber geometry is a problem in lean burn engines. Slow burn combustion chamber, with low turbulence results in high cycle to cycle variations. Kowalewicz (2001) has proposed several modes of fuelling and testing on single cylinder engine to extend the lean operating limit fuelling with preheated gasoline, LPG and with liquid butane. Liquid butane showed better at lean burning limit. Cheng et al. (1993) gave an over view of UBHC emission and shown that reduction in HC emission will produce lesser cyclic variations and improved engine performance, efficiency.

Ceviz and Yuksel (2005) have investigated on a FIAT, 1801cm<sup>3</sup>, carbureted four cylinder spark ignition engine and showed that using ethanol–unleaded gasoline blends as a fuel decreased the coefficient of variation in indicated mean effective pressure, and CO and HC emission concentrations, while increased CO<sub>2</sub> concentration up to 10vol.% ethanol in fuel blend. On the other hand, after this level of blend a reverse effect was observed on the parameters aforementioned. The unleaded gasoline was blended with ethanol to get five test blends ranging from 0% to 20% ethanol with an increment of 5%. COV<sub>IMEP</sub> was observed as 3.077, 2.970, 2.352, 3.085 and 3.317 for pure gasoline and 5%, 10%, 15% and 20% ethanol in fuel blend experiments. The relative air–fuel ratio was the highest at the 10vol. % ethanol ratio and COV<sub>IMEP</sub> was the lowest. After the 10vol.% ethanol in blend, the relative air–fuel ratio started to decrease and COV<sub>IMEP</sub> started to increase in the experiments due to the increase in the temperature of the intake manifold and decrease in the volumetric efficiency. Ceviz\_ and Yuksel (2006) have investigated the use of liquefied petroleum gas (LPG) as a fuel for spark ignition engine in terms of lean operation, and focuses on the cyclic variations and exhaust emissions and showed that use of LPG decreased the coefficient of variation in the indicated mean effective pressure, and emission. They concluded that the higher laminar flame speed of LPG and good mixing of gaseous fuels with air causes a decrease in cyclic variations, and higher H/C ratio of LPG decreases the engine emissions.

Lee and Kim (2001) have concluded that it is necessary to understand the combustion process and cycle-by-cycle variation in combustion to improve the engine stability and consequently to improve the fuel economy and exhaust emissions. The pressure

related parameters instead of mass fraction burned were compared for the effect of initial combustion pressures on the following combustion and the analysis of cycle-by-cycle variation in combustion for two port injected SI engines. The correlation between IMEP and pressures at referenced crank angles showed almost the same trends for equivalence ratios, but the different mixture preparations indicated different tendency. The dependency of IMEP on pressure at the referenced crank angles increases as the mixture becomes leaner for both engines. Villarroel (2004) has investigated the effects of cycle-to-cycle variations (ccv) on nitric oxide (NO) emissions with an engine simulation model. The simulation determines engine performance and NO emissions as functions of engine operating conditions, engine design parameters, and combustion parameters. An automotive, spark-ignition engine at part load and 1400 rpm was examined in this study. The engine cycle simulation employed three zones for the combustion process: (1) unburned gas, (2) adiabatic core region, and (3) boundary-layer gas. The use of the adiabatic core region has been shown to be especially necessary to capture the production of nitric oxides which are highly temperature dependent. The result indicates that cyclic variations must be considered when calculating the overall NO emissions.

Zervas (2004) has determined the coefficient of covariation of the in-cylinder pressure on each crank angle of a number of cycles, in the case of a natural gas feed SI engine operating under lean conditions. The resulting curve of COV versus crank angle was explored and three points of this curve show particular interest, as they correspond to the combustion beginning, combustion end and the point where the mass burned fraction is 50% (half combustion duration). The hypothesis concerning the combustion limits is proved by the comparison of the covariation curves of fired and motored cycles and by the determination of the combustion beginning and end using different methods. The hypothesis of the half combustion duration point is verified from a burn rate analysis of the cycle. The integral of the covariation curve in the combustion region is proposed as a criterion of the cyclic dispersion quantification. The integrals of the first and second combustion periods are explored as a function of the engine operating parameters. Kaminski et al. (2004) have analyzed the experimental time series of internal pressure in a four cylinder spark ignition engine. They performed for different spark advance angles; apart from usual cyclic changes of

engine pressure they observed oscillations. These oscillations are with longer time scales ranging from one to several hundred engine cycles depending on engine working conditions. Basing on the pressure time dependence they have calculated the heat released per cycle. Using the time series of heat release to calculate the correlation coarse-grained entropy we estimated the noise level for internal combustion process. Results show that for a smaller spark advance angle the system is more deterministic. Litak et al. (2009) have analyzed the cycle-to-cycle variations of peak pressure  $P_{max}$  and peak pressure angle  $\theta_{P_{max}}$  in a four-cylinder spark ignition engine by examining the experimental time series of  $P_{max}$  and  $\theta_{P_{max}}$  for three different spark advance angles. Using standard statistical techniques such as return maps and histograms it has been shown that depending on the spark advance angle, there were significant differences in the fluctuations of  $P_{max}$  and  $\theta_{P_{max}}$ . The multi-scale entropy of the various time series has been calculated to estimate the effect of randomness in these fluctuations. It explained how the information on both  $P_{max}$  and  $\theta_{P_{max}}$  can be used to develop optimal strategies for controlling the combustion process and improving engine performance. Blazek (2004) has described the problems of the combustion process in SI engine which is attribution cyclic variability of the combustion process, manifested by variations combustion pressure near the peaks of the pressure. Variability of the velocity of burning is given variability parameters Vibe characteristic formula. This work describe to interpretation of the process burning and its variability in-cylinder pressure measurement.

## **2.5 NO<sub>x</sub> REDUCTION METHODS**

The peak cycle temperature shoots up whenever the load is increased, which tends to accelerate NO formation. Several techniques have been tried to inhibit NO formation, the use of exhaust gas recirculation (EGR) being on among them. Agrawal et al. (2004) have conducted an experimental investigation to observe the effect of exhaust gas re-circulation on the exhaust gas temperatures and exhaust opacity on a two-cylinder, direct injection, air-cooled, compression ignition engine. It is seen that the exhaust gas temperatures reduce drastically by employing EGR. This indirectly shows the potential for reduction of NO<sub>x</sub> emission. Thermal efficiency and brake specific fuel consumption are not affected significantly by EGR. However particulate matter

emission in the exhaust increases, as evident from smoke opacity observations. EGR is proved to be one of the most efficient methods of  $\text{NO}_x$  reduction in diesel engines. The increase in particulate matter emissions due to EGR can be taken care by employing particulate traps and adequate regeneration techniques. Vianna et al. (2005) have reported that increasing the compression ratio of a SI engine that employs EGR technology is an effective way to correct the loss in the performance. Some degree of recirculation was enough to keep emissions down to an acceptable level. Increasing the compression ratio from 8.2:1 to 8.9:1, with 6% recirculation ratio led to a 50% reduction in the emission of  $\text{NO}_x$ , combined to a 10% increase in power output of the engine.

These days EGR is commonly used also in spark-ignition engines since this technique is able to both limit the  $\text{NO}_x$  formation rate and improve engine thermodynamics at some operating points. The EGR technique, since a long time adopted in reducing the  $\text{NO}_x$  formation rate, could be an effective system for fuel economy improvement. Mainly, a de-throttle effect and decreased heat losses to the walls can be obtained in this way. Furthermore, lower exhaust gas temperatures can be reached thus avoiding damages to the noble metals of catalytic converters. Fontana and Galloni (2010) have investigated the effect of EGR in a naturally aspirated, spark-ignition engine. In particular, at full or high load operation, attention has been paid to the combustion development and the influence of EGR rate on the values of spark advance, at knock onset limit, tolerated by the engine has been assessed. Due to lower temperature levels within the combustion chamber, the obtained results show a decreased octane requirement, thus an optimal choice of spark advance is possible. Hence a significant increase of engine efficiency has been obtained. Kim and Bae (1999) have measured speciated hydrocarbon emissions and combustion performances in a gas fueled 2-liter four-cylinder SI engine under lean burn conditions. The emission characteristics of natural gas and LPG fuels were compared as a function of mixture strength mainly under lean burn conditions for two compression ratios and various EGR ratios. At the same air/fuel ratio, increasing the EGR (%) resulted in less  $\text{NO}_x$  emission. However HC emission, engine efficiency and the production of the ozone were not greatly affected by the change of EGR (%). Woo et al. (2004) have investigated the effect of EGR in a modified single cylinder SI engine with EGR in both homogeneous mode

and stratified mode. The thermodynamic heat release analysis showed that the burning duration was decreased in case of stratified EGR. It was found that the stratification of EGR hardly affected the emissions. Almost same amount of nitrogen oxides ( $\text{NO}_x$ ) reduction was attained with and without the EGR stratification process.

The usefulness of water–diesel emulsion on performance improvement and emission reduction of diesel engines has been reported by several researchers. Water added diesel can reduce  $\text{NO}_x$  and smoke simultaneously. Maiboom and Tauzia (2011) have conducted an experimental study on a modern automotive 1.5 liter HSDI Diesel engine while injecting a water-in-diesel emulsion (WDE) with a volumetric water-to-fuel ratio of 25.6%. When used in combination with EGR, water diesel emulsion allows reducing both  $\text{NO}_x$  and PM emissions, the relative reduction being approximately the same whatever the EGR rate. Thus, the traditional  $\text{NO}_x$ -PM trade-off is largely improved and very low emission level can be achieved.

Nguyen and Wu (2009) have introduced the process of intake port modification to develop a lean burn system. It also studies about applicable technique –water-gasoline emulsions - used in this engine for reducing the  $\text{NO}_x$ . To reach the lean combustion, the original intake port of a four-stroke spark-ignition (SI) engine was modified to generate tumble by using various flow control baffles. Water-gasoline emulsion has a positive effect on  $\text{NO}_x$  reduction with a suitable water concentration at 5% by mass and the  $\text{NO}_x$  emissions has been decreased 35.0% approximately in comparison with lean-burn engine using pure gasoline. Rajan and Saniee (1983) have experimented with water/ethanol/gasoline mixture containing up to 6 vol.% of water in the ethanol and found that it constitutes a desirable motor fuel with power characteristics similar to those of the base gasoline. It was found that the emissions of oxides of nitrogen and the unburnt hydrocarbons with the water/ethanol/gasoline mixture were lower compared to the base gasoline under identical operating conditions. Experiments were conducted by Subramanian (2011) to compare the effects of water–diesel emulsion and water injection into the intake manifold on performance, combustion and emission characteristics of a DI diesel engine under similar operating conditions. The water to diesel ratio for the emulsion was 0.4:1 by mass. The same water–diesel ratio was maintained for water injection method in order to assess both potential benefits.

The emulsion was prepared using the surfactant of HLB: 7. The emulsion was injected using the conventional injection system during the compression stroke. The second phase of work was that water was injected into the intake manifold of the engine using an auxiliary injector during the suction stroke. An electronic control unit (ECU) was developed to control the injector operation such as start of injection and water injection duration with respect to the desired crank angle. At full load, NO emission decreased drastically from 1034 ppm with base diesel to 645 ppm with emulsion and 643 ppm with injection. But, NO emission reduction is lesser with injection than emulsion at part loads. However, CO and HC levels were higher with emulsion than water injection. As regards NO and smoke reduction, the emulsion was superior to injection at all loads. Peak pressure, ignition delay and maximum rate of pressure rise were lesser with water injection as compared to the emulsion.

Several techniques have been tried to inhibit NO<sub>x</sub> formation and addition of diluents or water injection along with the intake charge is being one. Injection of water into the intake manifold has been found to be an effective way to reduce NO emission in SI, CI and LPG engines. Subramanian et al. (2006) have conducted experiments to study the effect of water injection and spark timing on the nitric oxide emission and combustion parameters of hydrogen fuelled single cylinder spark ignition engine run at different equivalence ratios at full throttle. NO levels were found to rise after an equivalence ratio of 0.55; maximum value was about 7500 ppm. High reductions in NO emission were not possible without a significant drop in thermal efficiency with retarded spark ignition timings. Drastic drop in NO levels to even as low as 2490 ppm were seen with water injection. In spite of the reduction in heat release rate (HRR) no loss in brake thermal efficiency (BTE) was observed. There was no significant influence on combustion stability or HC levels. Ozcan and Soylemez (2005) have studied about the effect of water injection on a S.I engine's thermal balance and performance. A four cylinder conventional engine was used with LPG as fuel. Different water to fuel ratios by mass was used with variable engine speed ranging from 1000 to 4500 rpm. The results showed that as the water injection level to the engine increased, the percentage of useful work increased, while the losses other than unaccounted losses decreased. Additionally, the specific fuel consumption decreases, while the engine thermal efficiency increases. The average increase in the brake

thermal efficiency for a 0.5 water to fuel mass ratio is approximately 2.7% over the use of LPG alone for the engine speed range studied. Since both the exhaust gas temperatures as well as the peak cylinder temperature are lower in the case of water added operations, there was less heat loss through these channels, and as such, more useful work was available at the engine crankshaft.

Ozcan and Soylemez (2005a) have experimentally investigated the effects of water addition on the exhaust emissions of a naturally aspirated, liquefied-petroleum-gas-fueled engine. The manifold induction method is used for water addition in this study. The exhaust emissions, ignition timing, and exhaust temperature values were measured for different equivalence ratio values. The water induction is accomplished over a wide range of water to fuel mass ratios of 0.2-0.5. The results showed that water addition worked as a cooling mechanism for the fuel-air charge and slowing the burning rates, yielding a reduction of the peak combustion temperature, which in turn provides a 35% reduction in peak NO<sub>x</sub> emissions without any significant change in CO and HC emissions. In addition, greater ignition advance is obtained. Larbi and Bessrouer (2008) have carried out in the measurement and simulation of pollutant emissions from marine diesel combustion engine and their reduction by water injection. An analytical model based on detailed chemical kinetics employed to calculate the pollutant emissions of a marine diesel engine gave results, in general, satisfactory compared to experimentally measured results. Especially the NO emission contents are found higher than the standards limiting values set out by the International Maritime Organization. Thus, this study is undertaken in order to reduce as much as possible these emissions. In studying the reduction of pollutant emissions of the diesel engine by the use of water injection, substantial decrease in NO was observed which allows the unit to meet IMO regulation. Furuhata et al. (2010) have investigated experimentally the effect of steam addition on NO reduction in kerosene combustion. Three steam addition pathways: (i) steam was directly introduced into the fuel spray; (ii) it was pre-mixed with the combustion air and introduced into the combustor and (iii) it was introduced through side holes of the combustor. NO, O<sub>2</sub>, CO, CO<sub>2</sub> and temperature distributions in the combustor were analyzed for these steam pathways. It was clearly observed that the maximum temperature was reduced and high temperature region in the combustion chamber become narrow with steam

addition. It was considered that the suppression of NO formation in just after ignition region was necessary to reduce NO emission from the combustor.

Lanzafame (1999) has investigated the effects of water injection in the intake pipe are investigated from both a theoretical and experimental viewpoint. Pressure vs. time diagrams were recorded on a single-cylinder CFR engine. Tests were performed according to Research and Motor Method (ASTM). Water was supplied by a continuous injection system inclusive of comparatively high pressure pump. The engine was fed with low O.N. base gasoline (cheap products, intermediate of refinery processes). The water to fuel mass flow rate ratio was varied in the range 0 to 1.5. The NO<sub>x</sub> emissions measurements confirm the tremendous effectiveness of water injection in reducing the engine environmental impact. Test data have been used to implement a detonation model that allows predicting water injection effects. Results have shown that water injection really represents a new way to avoid detonation, to reduce compression work and to control NO<sub>x</sub> formation in SI engines. Gadallah et al. (2009) have examined experimentally the effect of direct water injection strategies on performance and NO<sub>x</sub> emissions of a hydrogen fuelled direct injection engine. Three water injection timing strategies were used, at the suction stroke, at the compression stroke and at the expansion stroke. The quantity and time of water injection were varied during every strategy. Also the effect of water injector sprays location inside the combustion chamber relative to the spark plug position was studied. The results showed that the reduction of NO<sub>x</sub> emissions was most strongly dependent on the water injection timing. The optimum water injection timing, for maximum NO<sub>x</sub> reduction, was depended on the change in the water injection quantity and this optimum water injection timing was advanced with the increase of water quantity.

Xavier Tauzia et al. (2010) have described an experimental study conducted on a modern high speed common-rail automotive diesel engine in order to evaluate the effects on combustion and pollutant emissions of water injected as a fine mist in the inlet manifold. The influence of WI on ignition delay, rate of heat release, nitrogen oxides (NO<sub>x</sub>) and particulate matter (PM) emissions and engine efficiency is analyzed for various engine operating conditions (speed and load) and various amount of water (up to 4 times the amount of fuel injected). A large reduction of NO<sub>x</sub> emissions can



be achieved with high WI rates, at low load as well as high load conditions. A water mass of about 60-65% of the fuel is needed to obtain a 50% NO<sub>x</sub> reduction. However, WI seems to increase heat losses at cylinder wall, which can affect negatively the engine global efficiency. Adnan et al. (2012) have carried out experimental investigations to determine the optimum water injection timing for power augmentation and emission control of a single cylinder hydrogen fueled compression ignition engine. It was concluded that NO<sub>x</sub> emission was less for longer injection duration. This is because of the fact that longer injection duration introduces more water droplets into the cylinder that reduces in-cylinder charge temperature. Tesfa et al. (2012) have carried out investigations on the combustion, performance and emission characteristics of a 4 cylinder, turbocharged CI engine running with biodiesel with an integrated water injection system under steady state operating conditions. The results indicate that water injection at a rate of 3 kg/h results in the reduction of NO<sub>x</sub> emission by about 50% without causing any significant change in the specific fuel consumption. Furthermore, the water injection in the intake manifold has little effect on the in-cylinder pressure and heat release rate of the CI engine under different operating conditions.

Franz and Roth (2000) have conducted experiments by injecting hydrogen peroxide (H<sub>2</sub>O<sub>2</sub>) dissolved in water into the combustion chamber of a direct injection (DI) diesel engine at different crank angles. For both, the spray of H<sub>2</sub>O<sub>2</sub>/water and pure water, a clear decrease in soot emission was observed for early injection at crank angles  $-40^\circ < CA < -10^\circ$  before top dead center (bTDC), which is associated with an increase in the exhaust gas HC concentration. For these conditions, the soot removal is mainly an effect of compressed air cooling, which increases the induction time of the diesel spray, thus resulting in a shift toward more premixed combustion. At injection crank angles  $CA > +10^\circ$ , the water and the H<sub>2</sub>O<sub>2</sub>/water sprays show an opposite behavior with respect to the exhaust gas soot. The in-cylinder measurements clearly show an increase of OH radiation during cycles with H<sub>2</sub>O<sub>2</sub>/water injection compared to the standard engine conditions. The H<sub>2</sub>O<sub>2</sub> decomposition product OH influences the chemistry of the in-cylinder soot oxidation, which results in a decrease of the soot mass in the engine exhaust gas flow. Concentrations of HC and NO<sub>x</sub> are not significantly affected. Mafra et al. (2010) have investigated the influence of swirl

number and fuel equivalence ratio on NO emission in an LPG-fired chamber. A burner was designed and used to investigate the influence of swirl number and fuel equivalence ratio on nitric oxide concentration formed in a cylindrical combustion chamber. Liquefied petroleum gas was always fired in the experiments. Temperature, O<sub>2</sub> and NO concentration were monitored in 42 different radial and axial positions along the chamber at four different operating conditions in terms of NO formation. The effect of increasing the swirl number and reducing the fuel equivalence ratio was to reduce approximately 31% and 33% the nitric oxide emission, respectively.

## **2.6 HEAT RELEASE RATE ANALYSIS**

Brown (2001) has presented the initial work on building a combustion analysis system. The project was started by making a thorough review of current acquisition and analysis technology. This has highlighted the importance of good quality data being collected if meaningful analysis is to be carried out. In particular, errors in locating TDC introduce a large error in calculated parameters such as IMEP. Hardware and software has been developed to put this theory into practice, and validation has been carried out to compare results with other researchers. Additionally, several pieces of unique work were carried out: Calibration of dynamometer outputs, Development of a cylinder volume equation allowing for wrist pin offset, handling of acquisition at incorrect TDC, handling of cylinder angular offset, determination of thermodynamic loss angle. Eriksson et al. (2002) have developed and validated an analytic model for cylinder pressures in spark ignited engines. The main result is a model expressed in closed form that describes the in-cylinder pressure development of an SI engine. The method is based on a parameterization of the ideal Otto cycle and takes variations in spark advance and air-to-fuel ratio into account. The model consists of a set of tuning parameters that all have a physical meaning. Experimental validation on two engines show that it is possible to describe the in-cylinder pressure of a spark ignited combustion engine operating close to stoichiometric conditions, as a function of crank angle, manifold pressure, manifold temperature and spark timing.

Goering (1998) describes that calculation of rates of heat release from engine fuels provides a useful diagnostic tool. As one example, the technique was useful in

discovering that retarding injection timing will reduce the proportion of premixed combustion and thereby reduce  $\text{NO}_x$  emissions from a diesel engine. The technique for calculating heat release rates was proposed more than 30 years ago. Initially a cumbersome technique, it has been simplified over the years. He has presented equations which allow calculation of heat release rates within a spread sheet. Ramachandran (2009) has described the classical two-zone thermodynamic model for the simulation of a spark ignition engine running on alternate hydrocarbon fuel wherein parameters like heat transfer from the cylinder, blowby energy loss and heat release rate are computed. The general fuel is specified by way of its C-H-O-N values. Curve-fit coefficients are then employed to simulate air and fuel data along with frozen composition and practical chemical equilibrium routines. The calculated data is then used to plot the various thermodynamic parameters with respect to crank angle.

Mendera (2004) describes that the cylinder pressure gives valuable information about the combustion process and the analysis of cylinder data over a closed part of engine cycle is a classical tool for engine studies. He has developed and applied heat release analysis for SI engine pressure data. Mass fraction burned (MFB) is used to interpolate the in-cylinder gas properties for the burned and unburned charge. Ghojel and Honnery (2005) have developed relatively simple single-zone model to calculate heat release characteristics in internal combustion engines using diesel oil emulsions and standard diesel fuel. The output from the model includes the apparent heat release, fraction of fuel burned, fuel burning rate, heat losses, indicated parameters and average gas temperature. The model is a suitable tool for quick evaluation and interpretation of the performance of different engines with different configurations or fuels and for the same engine under variable operating conditions.

Shiao and Moskwa (1995) have estimated cylinder pressures and combustion heat releases of a multi cylinder SI engine using sliding observer. Since a problem of system observability arises in pressure estimation when the cylinder piston moves to its TDC, means of reducing estimation errors in this condition are described. The detection of cylinder misfire or abnormal combustion is also achieved by utilizing the estimated heat release or heat release rate. A load torque observer can be added to the engine speed dynamic equation to further reduce modeling errors. Prasath et al.

(2010) have developed a computer code using "C" language for compression ignition (CI) engine cycle and modified in to low heat rejection (LHR) engine through wall heat transfer model. Combustion characteristics such as cylinder pressure, heat release, heat transfer and performance characteristics such as work done, specific fuel consumption (SFC) and brake thermal efficiency (BTE) were analysed. On the basis of first law of thermodynamics the properties at each degree crank angle was calculated. Preparation and reaction rate model was used to calculate the instantaneous heat release rate. The effect of coating on engine heat transfer was analysed using a gas-wall heat transfer calculations and total heat transfer was based on Annand's combined heat transfer model. The predicted results are validated through the experiments on the test engine under identical operating conditions on a turbocharged D.I diesel engine.

Kuo(1996) attempts to accurately predict the gas pressure changes within the cylinder of a spark-ignition engine using thermodynamic principles. The model takes into account the intake, compression, combustion, expansion and exhaust processes that occur in the cylinder. Comparisons with actual pressure data show the model to have a high degree of accuracy. The model is further evaluated on its ability to predict the angle of spark firing and burn duration. Tazerout et al. (2000) have done simulation studies, which indicated that the start and end of combustion in an internal combustion engine could be determined from the points of minimum and maximum entropy in the cycle. This method was further used to predict the beginning and end of the combustion process from experimentally obtained pressure crank angle data from a natural gas operated, single cylinder, spark ignition engine. The end of combustion always matched well with the point of maximum entropy. The start of combustion could be determined easily from the rate of change of entropy, which showed a sharp change at ignition. Results closely agreed with those obtained from a heat release analysis.

The following tables 2.1, 2.2 and 2.3 give the summary of some important literature on the use of ethanol enriched gasoline, LPG and NO<sub>x</sub> reduction techniques respectively.

Table 2.1: Some major literature on use of ethanol enriched gasoline

<b>Author(s)</b>	<b>Engine</b>	<b>Fuel</b>	<b>Results</b>
Hsieh et al. (2002)	1600 cm <sup>3</sup> multi-point injection gasoline engine	Ethanol–gasoline blended fuels of 5%, 10%, 20% and 30%.	Torque of the engine slightly increase; CO and HC decrease, CO <sub>2</sub> emission increases, NO <sub>x</sub> emission depends on the engine operating condition.
Al-Hasan (2003)	Toyota-Tercel-3A	Ethanol–gasoline blended fuels up to 25%	Increase in BP, brake thermal efficiency and volumetric efficiency, BSFC and equivalence air–fuel ratio decrease. CO and HC decrease.
Al-Farayedhi et al. (2004)	Six-cylinder Mercedes-Benz engine of 2960 cm <sup>3</sup>	MTBE, methanol and ethanol in three ratios of 10, 15, and 20 vol. %	Oxygenated blends improved the engine brake thermal efficiency. Methanol blends performed better.
Ceviz and Yuksel (2005)	FIAT, 1801cm <sup>3</sup> , carbureted four cylinder SI engine	Ethanol–unleaded gasoline blends	Decreased the COV of IMEP, CO and HC emission concentrations up to E10.
Najafi et al. (2009)	KIA 1.3 four cylinder engine	Ethanol–gasoline blended fuels up to 20%	Torque output and fuel consumption slightly increase; CO and HC emissions decrease CO <sub>2</sub> and NO <sub>x</sub> , increased.
Srinivasan and Saravanan (2010)	3 cylinder SI Engine	Ethanol-blended gasoline + cycloheptanol and cyclooctanol	Increased brake thermal efficiency. CO decreased, HC and O <sub>2</sub> increased and CO <sub>2</sub> and NO <sub>x</sub> appreciably decreased.
Eyidogan et al. (2010)	4 cylinder MPI SI Engine	E5, E10, M5, M10	Brake specific fuel consumption increased.

Table 2.2: Some major literature on use of LPG in SI Engines

<b>Researcher</b>	<b>Engine</b>	<b>Fuel</b>	<b>Results</b>
Goto et al. (2000)	LPG SI engine (High swirl)	LPG	Low NO <sub>x</sub> levels.
Bae et al. (2001)	2 liter, 4 cylinder spark ignition	LPG with EGR	Reduced cyclic variations.
Lee and Ryu (2004)	Port injection type heavy duty LPLi engine (Schlieren photography)	LPG	Flame propagation reached a maximum speed at the stoichiometric equivalence ratio. Combustion stability worsened as the equivalence ratio moved into the lean region.
Ceviz_ and Yuksel (2006)	SI engine	LPG	LPG decreased the coefficient of variation in the indicated mean effective pressure, and emission.
Yousufuddin and Mehdi (2008)	Single cylinder variable compression ratio SI engine	LPG	Improvement in power and torque in a high-load condition, reduction of CO and HC.
Mustafa and Briggs (2008)	SI engine	Gasoline+ LPG at 5%, 10% and 20%	CO, UHC decreased as the relative air-fuel ratio increases, and increased NO <sub>x</sub> .
Gumus (2011)	4 cylinder dual fuel engine	Gasoline and LPG	Volumetric efficiency decreased. Best results were achieved at using 100% LPG for exhaust emissions of CO and HC.
Masi and Gobbato (2012)	5 cylinder passenger car SI engine	Gasoline and LPG	Engine efficiency improved, brake torque dropped due to reduced volumetric efficiency.

Table 2.2: Some major literature on the use of NO<sub>x</sub> reduction techniques

Researcher	Engine	NO <sub>x</sub> reduction technique	Results
Kim and Bae (1999)	LPG 2-liter four-cylinder SI engine	EGR	Increasing the EGR (%) resulted in less NO <sub>x</sub> emission.
Agrawal et al. (2004)	2 cylinder CI engine	EGR	Thermal efficiency and brake specific fuel consumption are not affected significantly by EGR, but particulate matter emission increased.
Ozcan and Soylemez (2005a)	LPG SI engine	Manifold water induction, water to fuel mass ratios of 0.2-0.5	35% reduction in peak NO <sub>x</sub> emissions.
Subramanian et al. (2006)	Hydrogen fuelled single cylinder SI engine	Water injection	Drastic drop in NO levels from 7500 ppm to even as low as 2490 ppm.
Nguyen and Wu (2009)	Four-stroke SI engine	Water-gasoline emulsions	Water concentration at 5% by mass and the NO <sub>x</sub> emissions has been decreased 35.0%.
Fontana and Galloni (2010)	Naturally aspirated, spark-ignition engine	EGR	Decreased octane requirement, significant increase of engine efficiency.
Maiboom and Tauzia (2011)	Modern automotive 1.5 liter HSDI Diesel engine	Injecting a water-in-diesel emulsion (WDE) 25.6%.	Reducing both NO <sub>x</sub> and PM emissions.
Subramanian (2011)	DI diesel engine	Water-diesel emulsion and water injection.	At full load, NO emission decreased drastically from 1034 ppm with base diesel to 645 ppm with emulsion and 643 ppm with injection.

## **2.7 RESEARCH GAPS**

On the basis of the extensive literature work detailed above, the following research gaps have been identified.

- Most of the previous studies have been carried out in different type of engines. The engines include carburetor type SI engines, 2, 3 and 4 cylinder engines, and PFI engines. There are numerous test results with ethanol enriched gasoline compared gasoline and LPG separately. But comparative studies of ethanol enriched gasoline and LPG injection are limited.
- Extensive research work has been reported on the use of EGR as a NO<sub>x</sub> reduction technique. Most research indicates that NO<sub>x</sub> emission can be brought down with this method with a marginal compromise with engine performance. The use of steam/ water injection to control NO<sub>x</sub> emissions is not a novel idea. But the use of same in car engines has not been reported adequately. Specifically literature on the use of steam induction with LPG fuel in SI engines is inadequate.

## **2.8 OBJECTIVES OF THE RESEARCH**

In India the use of ethanol enriched gasoline blend E10 is made mandatory. The government will increase the level of blending from 10% by volume to higher %ages in view of the increasing oil import bills. Thus ethanol enriched gasoline is the long term alternative fuel for SI engines. LPG is the short term alternative fuel due to the abundant availability at this point in time. But the emission of NO<sub>x</sub> is a concern with LPG combustion. Therefore LPG can be used with some kind of NO<sub>x</sub> reduction technique. Thus an extensive study on the performance, combustion and emissions of a SI engine with LPG as fuel in along with a NO<sub>x</sub> reduction method compared to ethanol enriched gasoline is conceived.

A thorough and careful review of the available literature on the use of ethanol enriched gasoline, LPG injection in SI engine and use of various NO<sub>x</sub> reduction techniques is performed. Based on the literature it is found that comparative studies with LPG along with steam induction and ethanol enriched gasoline blends are limited. The present study deals with experimental investigations on the effect of steam induction with the intake air while using LPG as fuel on engine performance,



combustion and emissions in a modified multi-cylinder SI engine. The engine operating parameters of speed, throttle opening positions and static ignition timings are varied. To compare the results of the above experiments, an ethanol enriched gasoline blend is optimized as a baseline fuel based on engine performance, combustion and emissions.

Specific objectives of the research work:

1. To study the performance, combustion and emission characteristics of the four-cylinder SI engine fueled with ethanol enriched gasoline at various throttle opening positions & speeds and to optimize the baseline ethanol enriched gasoline blend which is to be used for comparative studies.
2. To modify the existing 4 cylinder MPFI SI Engine to run with injection of gaseous LPG as fuel. An LPG injection system is to be added to the existing setup. The modified setup can be run either with ethanol enriched gasoline or LPG alone.
3. To study the performance, combustion and emission characteristics of the four-cylinder SI engine with injection of gaseous LPG at various throttle opening positions, static ignition timings and speeds. The WOT tests give the full load characteristics, while the other throttle opening condition operations give the part load characteristics. The emissions are to be sampled without any after treatment devices.
4. To develop a steam induction system in the inlet manifold using waste exhaust heat from the engine and to study the effect of various proportions of steam to LPG fuel mass ratios on the performance, combustion and emissions of the test engine at various static ignition timings. Steam rates of 10, 15, 20 and 25% are to be used.
5. To make a comparative study of the LPG- steam characteristics with ethanol enriched gasoline based on engine performance, combustion and emission characteristics.

## **2.9 SCOPE**

The experimental investigation was carried out on a 4-cylinder spark ignition car engine converted into a stationary test rig. The engine was loaded with an eddy current type dynamometer. The cylinder pressure of the first cylinder was sampled through the piezo-electric pressure transducer, which is used for the combustion studies. The exhaust emissions were measured in real time with a AVL 444 analyser, with the samples being taken as raw sample i.e., without any exhaust after treatment devices in between the sampling point and the engine exhaust manifold. For the production of steam the waste heat from exhaust gas of the engine was used in a heat exchanger coiled around the exhaust pipe.

## **CHAPTER 3**

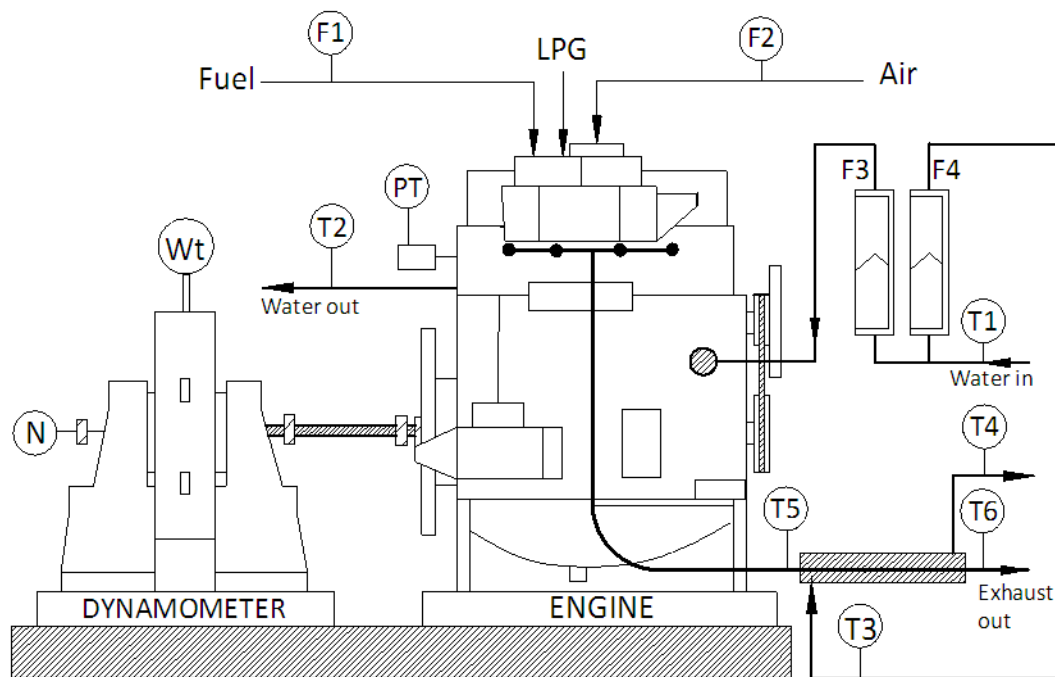
### **EXPERIMENTAL TEST RIG AND INSTRUMENTATION**

The principles, instrumentation and measurement systems used during the course of the research are described in this chapter. The experiments are carefully planned in a manner to fulfill the objectives framed under present research. The entire work carried out in the research can be divided into three phases. Initially the engine tests are conducted with gasoline and ethanol enriched gasoline blends of E5, E10, E15 and E20 to evaluate the engine combustion, performance and emissions characteristics to determine the baseline ethanol enriched fuel. The tests are conducted with preset (factory set) static ignition timing of 5deg. Before top dead center (bTDC) at the throttle opening positions of quarter, half, three fourth and wide open (WOT). The engine speed is varied from 2000 rpm to 4500 rpm in the interval of 500 rpm. In the next phase, the engine setup is modified to operate with LPG injection. Four solenoid operated gas injectors are fit to the engine manifold connecting each cylinder. Various controlling signals are used by a separate gas ECU which is coupled to the main ECU. The amount of LPG being injected for various load and speed conditions is decided by the gas ECU. Experiments are conducted with LPG at the 5deg. bTDC static ignition timing. Later the experiments are conducted at various static ignition timings (viz: 3, 4 and 6deg. bTDC) to study the effect of static ignition timing on the engine performance and emissions with LPG fuel. In the final phase of the research, a steam induction system for the LPG engine is developed using waste exhaust gas to reduce the emissions of oxides of nitrogen. The engine combustion, performance and emissions are studied with various steam to LPG mass ratios. A comparative study is performed with LPG along with steam induction and ethanol enriched gasoline blends.

#### **3.1 TEST ENGINE DESCRIPTION**

A one liter inline four cylinder engine of Maruti Suzuki Zen (max. power of 44.5 kW at 6000 rpm) with multi point port fuel injection (MPFI) system was used to acquire experimental data for this project. The engine has a single overhead camshaft layout with 4 valves per cylinder (2 intake and 2 exhaust). Fuel is injected into the intake

port by a single fuel injector located in each intake runner. The engine is connected to an eddy current type dynamometer which is used to absorb power and regulate engine speed. The test rig is provided with necessary instruments for combustion pressure and crank-angle measurements, airflow, fuel flow, temperatures and load measurements. These signals are interfaced to a digital computer through an 8 channel engine interface. The set up has a stand-alone panel box consisting of air box, fuel tank, manometer, fuel measuring unit, differential pressure transmitters for air and fuel flow measurements, process indicator and engine indicator. Rotameters are provided for cooling water and calorimeter (for heat balance sheet) water flow measurement. Figure 3.1 shows the Schematic of the experimental setup, while plate 3.1 gives a view of the engine test rig.



F1- Fuel Flow Differential Pressure (DP) unit  
 F2- Air Intake DP unit  
 F3- Rotameter (Engine)  
 F4- Rotameter (Calorimeter)  
 T1- Cooling water inlet temperature  
 T2- Cooling water outlet temperature

T3- Calorimeter water inlet temperature  
 T4- Calorimeter water outlet temperature  
 T5- Exhaust gas inlet temperature  
 T6- Exhaust gas outlet temperature  
 N – rpm decoder  
 PT- Pressure transducer  
 Wt – Load on Dynamometer

Fig. 3.1 Schematic of the experimental setup

The setup enables study of engine performance for brake power, indicated power, frictional power, BMEP, IMEP, brake thermal efficiency, indicated thermal efficiency, mechanical efficiency, volumetric efficiency, specific fuel consumption and air-fuel ratio (A/F). Windows based engine performance analysis software package 'Engine Soft' is provided by the supplier of the test rig - M/s Apex Innovation Pvt. Ltd. Sangli, India, for online performance evaluation. The detailed specifications of the gasoline engine and other instrumentation mounted on the test-rig are given as Appendix I. The lower calorific value and the fuel density are input to the software for the computation of various performance parameters.



Plate 3.1 Engine setup with control panel

### **3.2 MODIFICATION OF THE ENGINE SETUP FOR OPERATION WITH LPG**

The engine is modified to operate with liquefied petroleum gas (LPG) fuel. Separate four gas injectors are attached to the inlet manifold near the inlet port of each cylinder for injecting LPG. The gas injectors are operated by solenoid valves driven by 12V DC power supply. The nozzle diameter of each gas injector is determined based on the power output per cylinder and for the given engine nozzle diameter of 2 mm is used. A

separate gas ECU has been used for driving the solenoid valves and the signals from the gas ECU controls the activation period of the gas injectors. The after market LPG injection system manufactured by M/s Europe gas (Europe gas v 2.5 LPG) is used. The block diagram of the LPG injection system is shown in the Fig. 3.2. Domestic LPG stored in cylinders at a pressure of about 10 bar (Max. Vapour Pressure at 40° C is 1050 KPa gauge) which weighs 14.2 kg is used in the experiments. An unreduced pressure regulator is fitted to LPG cylinder which allows the gas to pass through it at high pressure. A copper pipe is used to supply the LPG from the cylinder to the vaporiser. An electromagnetic strainer is provided in the supply line to absorb the iron particles from the LPG cylinder which may travel along LPG. Power supply from the battery is given to activate the electromagnet. A LPG vaporiser which is provided in the supply line serves the purpose of vaporizing the fuel and supplies it at the required pressure. The function of the vaporiser is to transfer thermal energy into the LPG and to reduce the LPG (tank) pressure to the much lower system pressure such that the LPG evaporates to the superheated gas phase (Price et al. 2004). The thermal energy required is supplied by the engine cooling water which is made to pass through the vaporiser after the engine jacket circulation. To supply the required amount of gas at the required pressure for meeting the various load conditions a reference pressure from the engine inlet manifold is also connected to the evaporator.

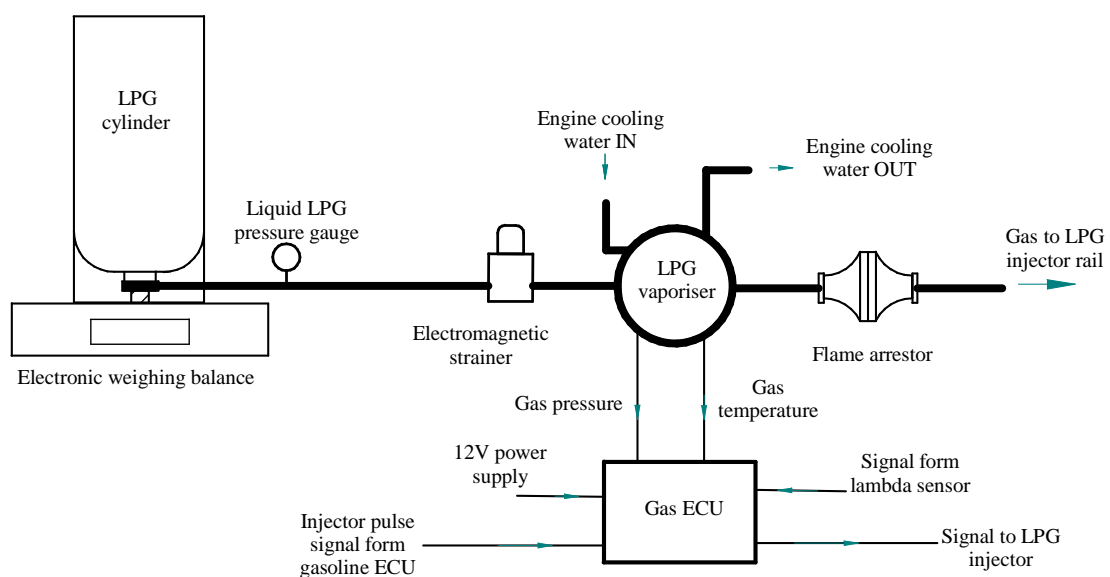


Fig. 3.2. Block diagram of LPG injection system.

### **3.2.1 LPG engine control unit (Gas ECU)**

The function of the gas ECU is to open and close the gas injector at appropriate time to control the duration of injection. Concept of working of gas ECU for bi-fuel application is based on master slave theory (Khatri et al. 2009). A sequential gas injection controller of IV generation OSCAR-N OBD CAN is used. The gasoline injector opening signal pulse from the pre-installed Gasoline ECU is fed to gas ECU as an input. The gas ECU modifies the gasoline pulse width using a correction factor and sends it to gas injectors. This correction factor is calculated based on the density of liquid gasoline and gaseous LPG. It also takes into account the signals from the other sensors such as exhaust lambda sensor (indicating oxygen content in the exhaust gases) and inlet manifold absolute pressure indicating the engine load. When the engine is running with LPG as fuel, the emulator system in the gas ECU cuts off gasoline injector signals and gives the emulated signal to the gasoline ECU so that it doesn't give a fault signal. A switch provided in the control panel is use to switch between LPG and gasoline fuel operation. The specifications of the gas ECU is given as Appendix II.

### **3.2.2 Safety measures and flame arrestor**

Gaseous fuels are difficult to handle compared to liquid fuels and thus they are considered to be more dangerous than liquid fuels. Hence at most care has been taken while handling the gaseous fuels. LPG is mainly a mixture gaseous fuel of propane and butane. Both these fuels have very low ignition temperature normally in the range of 40<sup>0</sup>C. So the contingencies of auto ignition and thus explosion are rather more here. Also the flames may propagate back into the pipeline which may trigger the fuel in the gas cylinder to explode. To avoid flash back, a flame arrestor is connected in series in the fuel supply line. From the flame arrestor LPG is passed to the gas injector rail. Flame arrestors are the equipments which quench flames that are propagating back to the cylinder. They prevent the propagation of flame from the exposed side of the unit to the protected side by the use of wound crimped metal ribbon type flame cell element called as Honeycomb. This construction produces a matrix of uniform openings that are carefully constructed to quench the flame by absorbing the head of the flame. This provides an extinguishing barrier to the ignited vapour mixture. Under

normal operating conditions the flame arrester permits a relatively free flow of gas or vapour through the piping system. If the mixture is ignited and flame begins to travel back through the piping, the arrester will prohibit the flame from moving back to the gas source. Plates 3.2 and 3.3 respectively show the gas injectors and the flame arrester used in the LPG system.

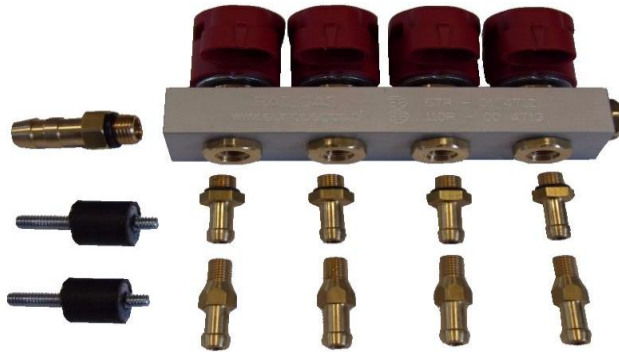


Plate 3.2 Gas injectors



Plate 3.3 Flame Arrester

The leakage in LPG pipeline can happen in two ways. One such chance is through the injector to the cylinder and other one is through any leaks in the pipeline. The safety measure to avoid this leakage is by conducting the periodic leak checking of both the injector and the pipelines. The new injector may not have any leakage problems but as the time progress due wear and tear of the parts, the injectors may be subjected to some leakage problems. These leakages may be of very small quantity but are sufficient enough to auto ignite. Since the LPG gas molecules are denser than the air, it will settle down inside the cylinder and during cranking it may auto ignite and thus causes trouble. Use of ordinary pipes increases the chances of leakage of gases to the atmosphere which may enhance the chances for LPG to mix with the air. This may even led to hazardous explosions. Hence seam-less copper pipes are used to avoid the chances of leakage of gas through the pipes to the atmosphere.

### **3.3 STEAM INDUCTION SYSTEM DEVELOPMENT**

LPG combustion in SI engine results in higher emissions of harmful  $\text{NO}_x$  even though the emissions of CO and HC are reduced substantially. Use of after treatment



devices may reduce the NO<sub>x</sub> emissions. In this work a method of reduction of NO<sub>x</sub> in the engine itself is described. Among several in cylinder reduction techniques, the method of steam induction with intake air is used by developing a device to supply steam at various proportions. The steam is produced with the help of heat of engine exhaust gases, which is otherwise is lost to the surroundings. De-ionized water is stored in a container and a low power pump is used to pass the water through a copper tube of 3/4<sup>th</sup> inch size. The copper tube is coiled around the engine exhaust pipe such that the water and exhaust gases pass in a counter flow way so as to maximize the heat transfer between the two fluids. Since the flow rate of the available pump was higher than the required water flow rate (max. 3 liters per hour), a bypass system is provided after pump so that the excess water returns back to the sump. Sufficient length of copper coiling is provided so that the water will be completely vaporized and dry steam is inducted in to the engine manifold. The amount of steam to be inducted is decided based on the LPG fuel flow rate at each operating condition. Before admitting steam in to the engine manifold at each operating condition with a specific steam flow rate, it is ensured that water is completely converted into steam. Fig.3.3 represents the schematic block diagram of the steam induction setup.

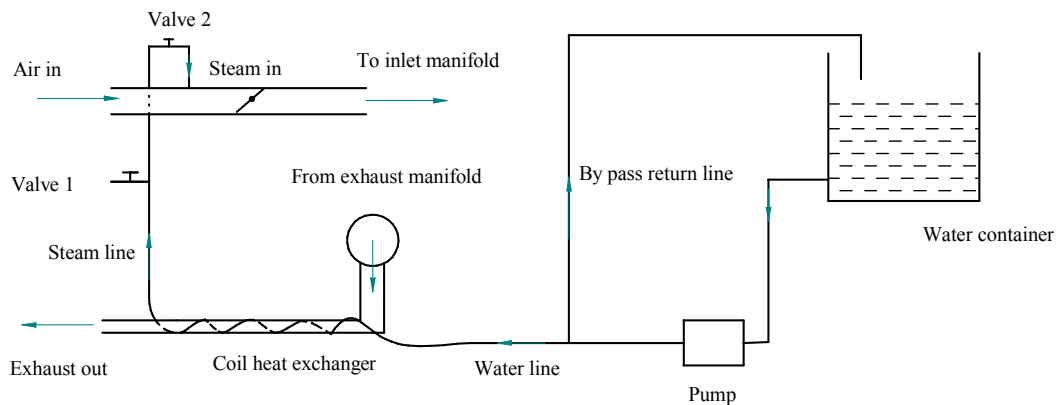


Fig. 3.3 Block diagram of steam induction system



Plate 3.4. Steam induction system

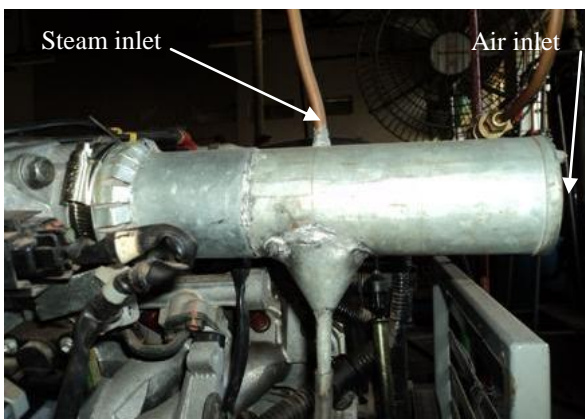


Plate 3.5 Steam induction to the intake manifold system

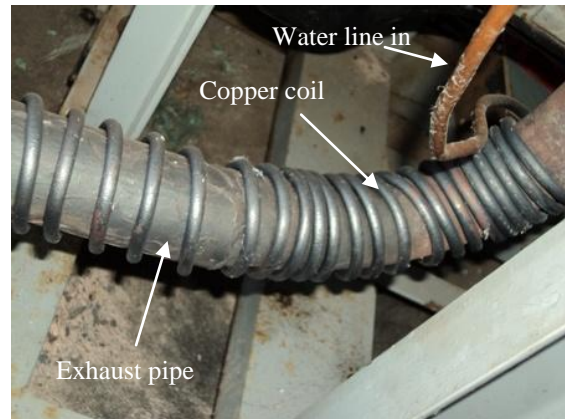


Plate 3.6 Copper coil over the exhaust pipe for production of steam

Steam to LPG fuel mass ratios of 0.1, 0.15, 0.20 and 0.25 are used at each operating condition. A provision is made in the inlet manifold just before the throttle valve to induct steam continuously to ensure good mixing of steam with the intake air. The water flow rate is measured and controlled manually by a water rotameter of range 0.2 lph to 2.5 lph with a least count of 0.1 lph. Plates 3.4, 3.5 and 3.6 detail the various systems.

### 3.4 MEASUREMENT SYSTEM

The test bed is fully instrumented to measure the different parameters during the experiments on the engine. A detailed description of the different measurement

systems used for evaluating the engine performance and emission is given in this section.

#### **3.4.1 Cylinder pressure measurement**

A piezo-electric pressure transducer is used for recording the cylinder pressure for number of consecutive cycles for combustion variability studies. A PCB Piziotronics Inc, built piezoelectric pressure transducer is installed in the engine cylinder head of 1<sup>st</sup> cylinder. The sensor is flush mounted and it measures the pressure trace in the cylinder with 1degree crank-angle resolution. The pressure crank-angle data is acquired on a digital computer operating on windows XP system that contains a “Dyналog” make data acquisition board. The software provided is capable of data logging a maximum of 25 consecutive combustion cycles. The sensor body is continuously circulated with cooling water so as to maintain the sensor at a constant temperature. A rotary encoder is fitted on the engine output shaft for crank angle signal. Both signals are simultaneously scanned by an engine indicator (electronic unit) and communicated to computer. The software in the computer draws pressure crank-angle and pressure volume plots and computes indicated power of the engine.

#### **3.4.2 Air and fuel flow measurements**

As the air flow during engine suction is pulsating, for satisfactory measurement of air consumption an air box of suitable volume fitted with orifice is used for damping out the pulsations. The differential pressure across the orifice is measured by water manometer and pressure transmitter. The flow across the orifice is connected via a parallel section to the U- tube manometer and the air intake differential pressure (DP) unit. The DP unit senses the pressure difference across the orifice, which is sent to the transducer. The transducer gives a proportional output as DC voltage (analog signal), which is converted into digital signal by analog to digital convertor (ADC) which will be in turn processed by the computer software program to get the air flow rate in kg/h.

The fuel consumed by the engine is measured by determining the volume flow of the fuel in a given time interval and multiplying it by the density of the fuel. A glass burette having graduations in ml is used for volume flow measurement. Time taken by the engine to consume this volume is measured by stopwatch manually. Alternatively

a differential pressure transmitter working on hydrostatic head principles is used for fuel consumption measurement. The fuel tank is connected to a burette for manual fuel flow measurement and to a fuel flow DP transmitter unit. The fuel line is connected to a two-way fuel cock which can be kept either in tank position or measuring position. When kept in measuring position, the fuel to the engine goes from the burette. The pressure head difference is sensed by the fuel DP transmitter. It gives proportional analog signal, which through the ADC card goes to the 'Engine soft' which calculates the fuel flow rate in kg/h. It is essential to enter the values of density and the lower calorific value of each test fuel to the software 'Engine soft' before operating with that test fuel. LPG flow rate is measured on the mass basis, to minimize the error in measurement while operating the system under varying pressures. An electronic weighing balance of 30 kg capacity with a least count of 1 gram and a stopwatch is used to measure the flow rate of LPG. For the experiment, the LPG cylinder is placed in upside down direction, so that LPG will be flowing in liquid form to the vapouriser which can provide the required amount of fuel.

### **3.4.3 Engine speed measurement**

Engine speed is sensed and indicated by an inductive pickup sensor in conjunction with a digital rpm indicator, which is a part of the eddy-current dynamometer controlling unit. The dynamometer shaft rotating close to inductive pickup rotary encoder sends voltage pulse whose frequency is converted to rpm and displayed by digital indicator in the control panel, which is calibrated to indicate the speed directly in number of revolution per minute.

### **3.4.4 Load measurement**

The brake load is measured by an eddy current dynamometer. It consists of a stator on which a number of electromagnets are fitted and a rotor disc coupled to the output shaft of the engine. When rotor rotates eddy currents are produced in the stator due to magnetic flux set up by the passage of field current in the electromagnets. These eddy currents oppose the rotor motion, thus loading the engine. These eddy currents are dissipated in producing heat so that this type of dynamometer needs cooling arrangement. Regulating the current in electromagnets controls the load. A moment arm measures the torque with the help of a strain gauge type load cell mounted

beneath the dynamometer arm. The analog load cell signal through the ADC card is fed to the computer to give load in kg. The dynamometer is loaded by the dynamometer loading unit situated in the control panel.

### **3.4.5 Temperature measurement**

Chromel-Alumel thermocouples connected to digital panel meter are positioned at different locations to measure the following temperatures: jacket water inlet temperature ( $T_1$ ), jacket water outlet temperature ( $T_2$ ), inlet water temperature at calorimeter ( $T_3$ ), outlet water temperature at calorimeter ( $T_4$ ), exhaust gas temperature before calorimeter ( $T_5$ ) and exhaust gas temperature after calorimeter ( $T_6$ ). All sensors, which sense the temperatures of respective locations, are connected to the control panel, which gives the digital reading of the respective temperatures. These are also interfaced to the computer.

### **3.4.6 Static ignition timing measurement**

Static ignition timing is varied in this work when running the engine with LPG. To measure the static ignition timing an ignition timing gun is used which illuminates the pulley connected to the engine flywheel. The static ignition timing can be read on a scale having 10 divisions with a range of 0-20 deg. bTDC with the help of timing gun light. To change the static ignition timing, the ignition distributor assembly is loosened and is rotated slightly in the direction of rotation of flywheel to retard the timing and in the direction opposite of rotation of flywheel to advance the timing.

### **3.4.7 Exhaust emission measurement**

An AVL Digas 444 exhaust gas analyzer is used to measure the various exhaust emissions of carbon monoxide (CO, % volume), carbon dioxide ( $\text{CO}_2$ , % volume), unburnt hydrocarbons (HC, ppm) oxygen ( $\text{O}_2$ , % volume) and oxides of nitrogen ( $\text{NO}_x$ , ppm). The five gas analyzer is calibrated by the supplier AVL prior to the use and necessary precautions are taken to see the proper working of it by regular check up of all types of filters and cleanliness of probe was maintained. Leakage test and zero adjustments are done regularly. The engine test rig has no catalytic converter, and thus the emission readings taken are raw emissions, without being treated. The specifications of the analyzer are given as Appendix III.

### **3.4.8 Calibration of instruments**

All instruments are calibrated prior to their use in the tests. The dynamometer, five gas exhaust gas analyser and pressure sensor are factory calibrated by the suppliers. The temperature sensors are calibrated with reference to standard thermometers. Rotameters are calibrated by manual measurement of the liquid flow through a known time. When conducting the experiments due care is taken to check the repeatability of readings. At each test point the engine is allowed to reach steady state operating condition by allowing it to run for sufficient time. Average of at least three readings at each test point is taken to minimize the experimental error.

## CHAPTER 4

### EXPERIMENTAL METHODOLOGY

#### 4.1 SCHEME OF ENGINE EXPERIMENTAL STUDIES

The engine experimental study involves three distinct stages. The first stage of the experiment involves the steady state engine performance, combustion and emission characteristics evaluation with ethanol enriched gasoline fuels (gasoline, E5, E10, E15 and E20). E5 is 95% by volume gasoline and 5% by volume ethanol. From these experiments an optimal blend ratio is determined and used as baseline ethanol enriched gasoline fuel for comparison with LPG fuel operation in the later stages. The fuel blends are prepared on the volume basis just before starting the experiment to ensure that the fuel mixture is homogenous and also to avoid the reaction of ethanol with water. The original fuelling strategy controlled by the factory-fit gasoline engine control unit (ECU) is used while running the engine with ethanol enriched gasoline blends. Experiments are conducted at wide open throttle (WOT) and part throttle conditions while the load on the dynamometer is varied at these throttle openings to vary the engine speed from 2000 rpm to 4500 rpm. Figure 4.1 gives the scheme of experiments in this phase of research work.

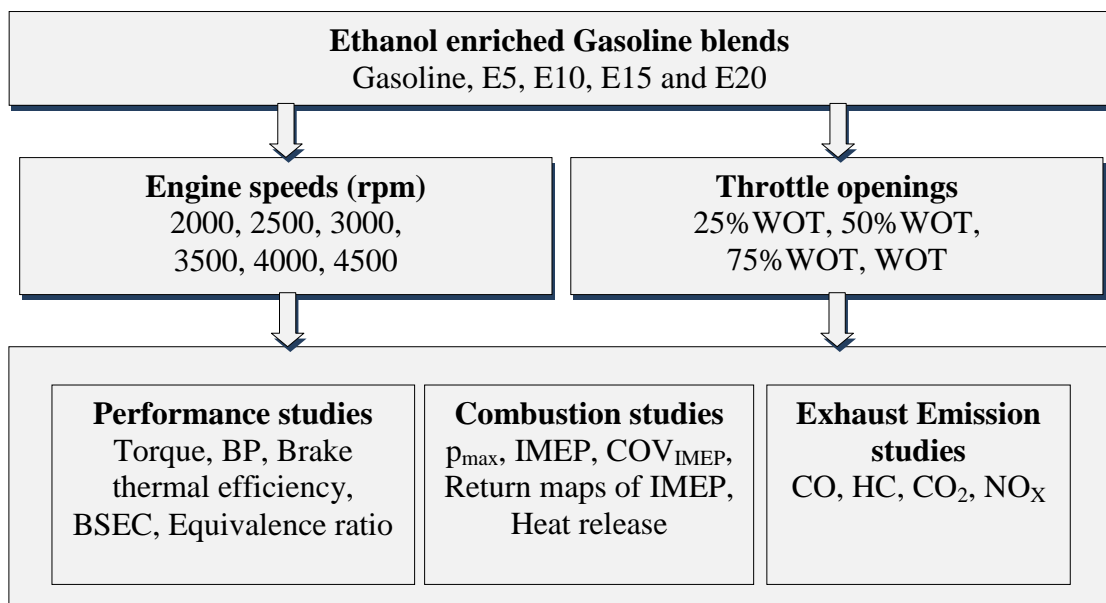


Fig. 4.1 Scheme of experiments with ethanol enriched gasoline blends.

The recorded pressure-crank angle data for 25 consecutive cycles are used for calculating the indicated mean effective pressures (IMEP) and  $COV_{IMEP}$  with the help of a computer program which is coded using Visual C++ platform. Another program computes the heat release (HR) per cycle based on the recorded cylinder pressure. Analysis of the obtained data is performed and results are plotted.

In the second stage the engine testing is performed with gaseous LPG injection in the modified engine test rig with various operating parameters of speed, throttle opening positions and static ignition timings of 3, 4 5 and 6 deg. bTDC where 5deg. bTDC is the pre-set static ignition timing. Figure 4.2 shows the scheme of experiments for various static ignition timings viz: 3, 4, 5 and 6 deg. bTDC respectively with LPG fuel operation. LPG consumption rate is measured on the mass basis to minimize the error in measurement while operating the system under varying pressures. To check the static ignition timing, an “ignition timing gun” (timing light) is used. It is connected to the battery positive and negative terminals. Another probe of the timing gun is hooked to the cable connected to the spark plug of the first cylinder.

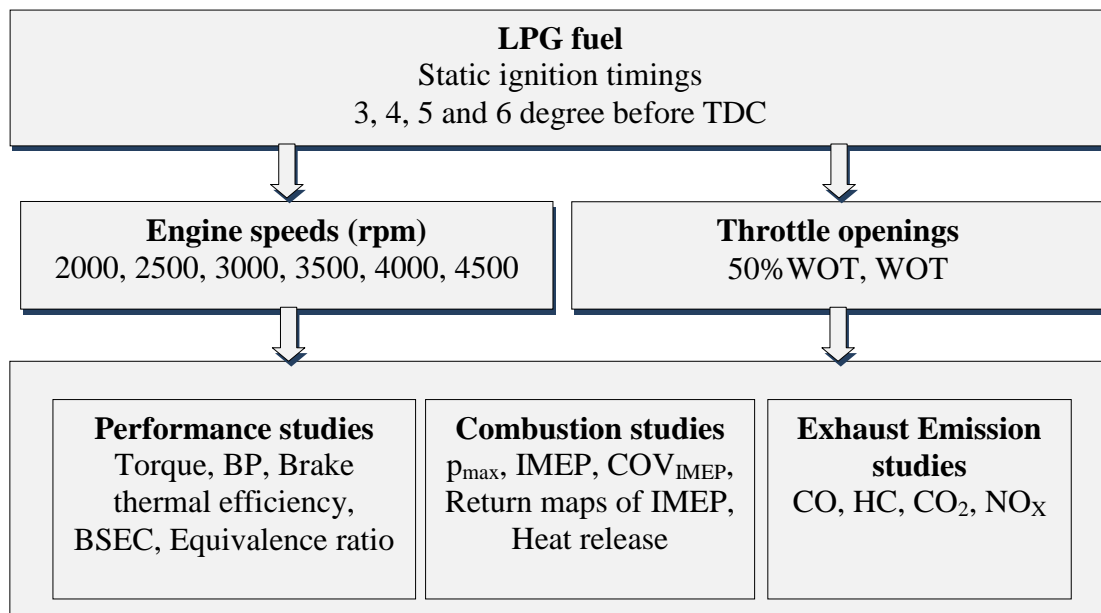


Fig. 4.2 Scheme of experiments with LPG at different static ignition timings



The engine is started and kept at static condition for 2-3 minutes. Now the timing gun is used to illuminate the pulley connected to the engine flywheel and the static ignition timing can be read on a scale with the help of timing gun light. To change the static ignition timing, the ignition distributor assembly is loosened and is rotated slightly in the direction of rotation of flywheel to retard the timing (4 and 3 degree bTDC since the pre-set static ignition timing of the engine is 5 degree bTDC) and in the direction opposite of rotation of flywheel to advance the timing (6 degree bTDC). Again the mark on the flywheel pulley is checked against the scale in the light of the timing gun. Once the required timing is set, the engine is shut and the diagnostic connector short circuit is removed.

In the last stage of the engine testing is performed with gaseous LPG injection with steam induction. Fig 4.3 shows the scheme of experiments for various static ignition timings viz: 3, 4, 5 and 6 degree bTDC respectively with LPG and steam at different rates. Steam is produced from deionized water using waste heat from exhaust gases.

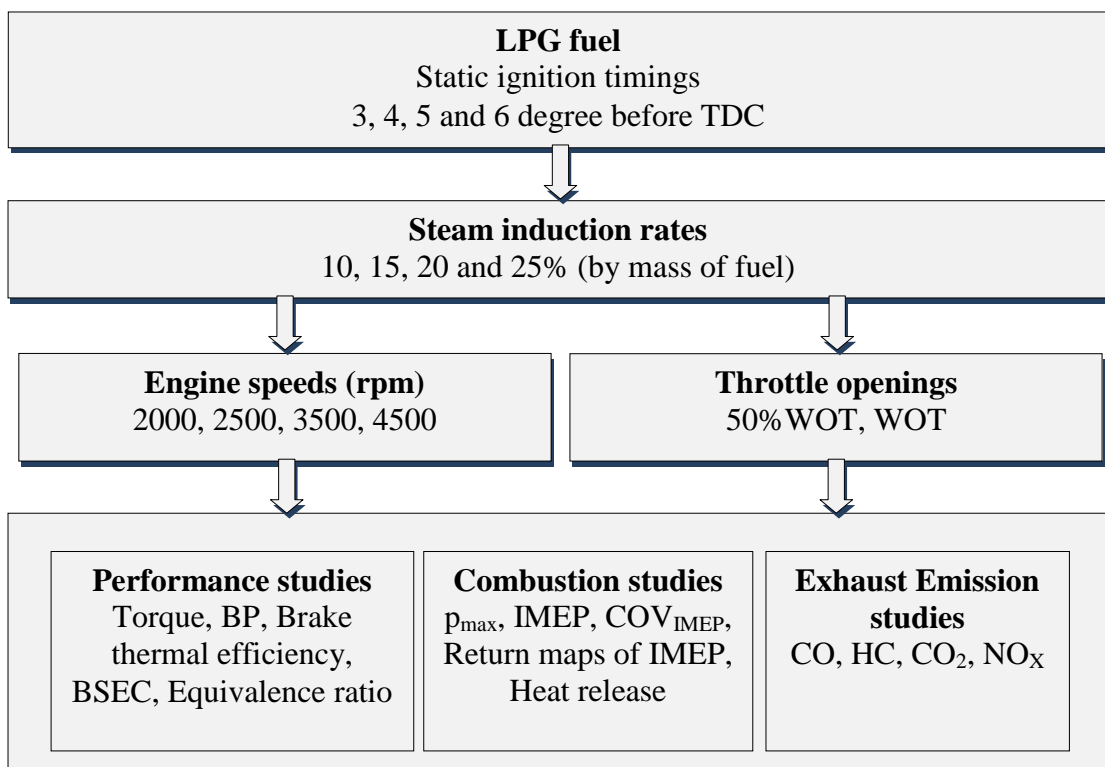


Fig.4.3 Scheme of experiments at different static ignition timings with LPG and steam

Precisely measured water at rates of 10, 15, 20 and 25% by mass of LPG is converted in to steam and is inducted in to the intake air stream. The performance, combustion and emission characteristics of the test engine at various static ignition timings are evaluated. Experiments are carried out with 50% WOT and WOT conditions and the engine speeds of 2000, 2500, 3500 and 4500 rpm are used at the static ignition timings of 3, 4, 5 and 6deg. bTDC.

#### 4.2 DETERMINATION OF IMEP AND $COV_{IMEP}$

The area enclosed by the p-v diagram of an engine gives the indicated work done by the gas on the piston. The IMEP is a measure of the indicated work output per unit swept volume, a parameter independent of the size and number of cylinders in the engine and engine speed.

IMEP is defined as:

$$IMEP = \frac{W_i}{V_s} \quad (4.1)$$

where  $W_i$  is the indicated work in Newton metres

$V_s$  is the swept volume per cylinder in cubic metres

The IMEP can be computed by experimental pressure & volume data for a 0-720° crank angle by the following equation (Brown 2001):

$$IMEP = \frac{\Delta\theta}{V_s} \int_{i=n_1}^{i=n_2} p(i) \frac{dV(i)}{d\theta} \quad (4.2)$$

$p(i)$  is cylinder pressure at crank angle I in Pascals

$V(i)$  is cylinder volume at crank angle I in cubic metres

$V_s$  is cylinder swept volume in cubic metres

$n_1$  is BDC induction crank angle

$n_2$  is BDC exhaust crank angle

A computer program is coded in visual C++ for the computation of IMEP for consecutive cycles from the measured pressure history. The input for the program is the cylinder pressure and volume for each crank angle from 0 to 720 degrees. The software uses the pressure crank-angle history for the determination of the indicated

mean effective pressure (IMEP). When logging consecutive combustion cycles the software calculates the average IMEP. But for the cycle-by-cycle combustion study since IMEP of each of the consecutive cycles is required, it is necessary to write a computer program which takes consecutive pressure crank-angle history and calculates the IMEP of each cycle. Initially the indicated power is computed by calculating the area under the pressure volume diagram of each cycle. The cylinder swept volume is calculated by the engine geometry. Finally the indicated mean effective pressure is calculated by dividing the indicated power by the swept volume. Fig. 4.4 gives the flow chart of the computer program to find IMEP and COV of IMEP

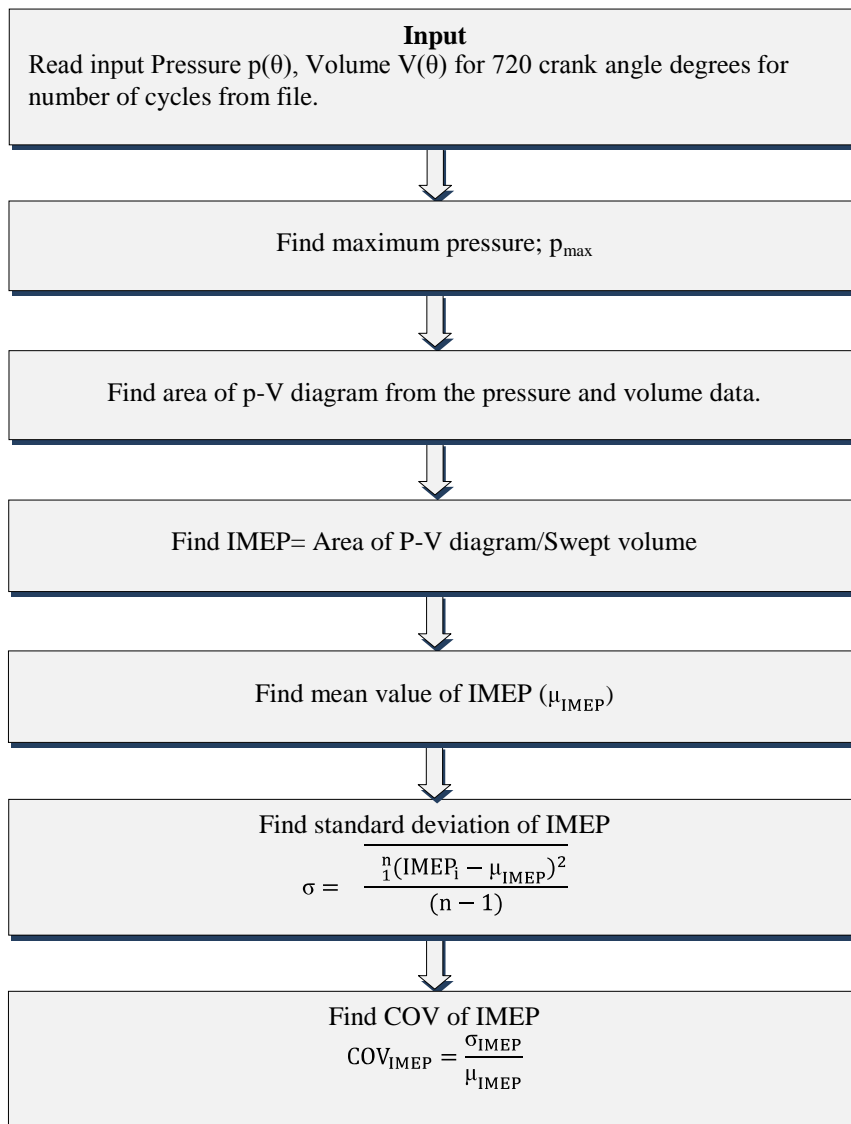


Fig. 4.4 Flow chart to find IMEP and COV of IMEP

The program also computes the mean IMEP and the coefficient of variation (COV). The coefficient of Variation (COV) is the standard deviation in IMEP divided by the mean IMEP (Ceviz and Yuksel 2006), and is usually expressed in percent. It is defined as

$$\text{COV}_{\text{IMEP}} = \frac{\sigma_{\text{IMEP}}}{\mu_{\text{IMEP}}} \quad (4.3)$$

Where  $\sigma$  is the standard deviation and  $\mu$  is the mean value.

The standard deviation is given by

$$\sigma = \frac{\sqrt{\sum_1^n (\text{IMEP}_i - \mu_{\text{IMEP}})^2}}{(n - 1)} \quad (4.4)$$

Where n= Number of combustion cycles.

### 4.3 HEAT RELEASE RATE

In-cylinder combustion pressure data is very useful information, which could be used to quantify the combustion behavior of the fuels inside the engine. Traditionally, engineers, during the engine design and optimization process, perform in-cylinder pressure measurements to determine peak pressure, rate of change in pressure, estimated rate of heat release, mass-burned fraction, and the charge temperature. Rate of heat release analysis shows the estimated rate of heat release during the combustion process. The results provide a quantified assessment of combustion rate and the means to diagnose combustion process (Catania et al. 2001). Heat release analysis is generally applied to compression ignition engines, although there is no reason why it cannot be used in spark ignition applications. Heat release analysis computes how much heat would need to have been added to the cylinder contents, in order to produce the observed pressure variations. In the present work, an effort is made to determine a single zone heat release rate and combustion temperature in a SI engine, using experimentally obtained average pressure-crank angle data. A computer program is developed using standard heat release rate equations, correlations and constants discussed below. The program is coded in Visual C++ flat form. Heat release rate is computed for 25 consecutive combustion cycles at every test point. The program also determines the coefficient of variation of heat release rate.

### 4.3.1 Thermodynamics of heat release

The heat-release analysis is carried out within the framework of the first law of thermodynamics when the intake and exhaust valves are closed, i.e. during the closed part of the engine cycle. The simplest approach is to regard the cylinder contents as a single zone, whose thermodynamic state and properties are modeled as being uniform throughout the cylinder and represented by average values. The basis for the majority of the heat-release models is the first law of thermodynamics, i.e. the energy conservation equation. For an IC engine, the cylinder contents are a single open system. The First law of thermodynamics as applied to this case is given by:

$$\frac{dQ}{dt} - p \frac{dV}{dt} + \sum_i m_i h_i = \frac{dU}{dt} \quad (4.5)$$

Where Q is the heat transferred in Joules, p is the pressure in pascals, V is the volume m<sup>3</sup>, m<sub>i</sub> is the mass of fuel injected, h<sub>i</sub> is the enthalpy in J/kg and U is the internal energy in J. Since the only mass crossing the system boundary is the fuel injected, the mass-enthalpy term reduces to a "mass of fuel enthalpy" term. Assuming that the enthalpy and internal energy are sensible terms (using a baseline of 298 K) and that the net heat released defined as the difference between the energy released through combustion and the energy lost to heat transfer from the system walls, the equation 4.5 can be rewritten as:

$$\frac{dQ}{dt} = p \frac{dV}{dt} + \frac{dU}{dt} \quad (4.6)$$

The heat transfer dissipated through the system boundary presents a problem only at the end of combustion where temperatures have risen. If we further assume that the contents of the cylinder can be modeled as an ideal gas, then the equation 4.6 can be rewritten as:

$$\frac{dQ}{dt} = p \frac{dV}{dt} + m C_v \frac{dT}{dt} \quad (4.7)$$

Where C<sub>v</sub> is the specific heat at constant volume. Differentiation of the perfect gas law with R assumed constant provides a means of eliminating the temperature term which is generally unavailable in pressure analysis to give

$$\frac{dQ_{Net}}{dt} = \left(1 + \frac{c_v}{R}\right)p \frac{dV}{dt} + \left(\frac{c_v}{R}\right)V \frac{dp}{dt} \quad (4.8)$$

Substituting the specific heat ratio  $\gamma$ , provides the final equation used in the analysis with the result being equally valid when substituting the independent variable  $\theta$ , or crank angle, for time,  $t$ , the net heat release combustion model of Krieger and Borman is obtained (Eyidogan et al. 2010).

$$\frac{dQ_{Net}}{d\theta} = \frac{\gamma}{\gamma-1} p \frac{dV}{d\theta} + \frac{1}{\gamma-1} V \frac{dp}{d\theta} \quad (4.9)$$

where  $\gamma$  is the ratio of specific heats,  $Q_{net}$  is the net heat release rate in Joules per degree,  $p$  is the in-cylinder pressure in Pascals,  $V$  is the in-cylinder volume in  $m^3$ .

The in-cylinder heat transfer occurs by both convection and radiation, where convection constitutes the major part. Heat is transferred by both convection and radiation occurring between in-cylinder gases and cylinder head, valves, cylinder walls, and piston during the engine cycle. By taking into account the effects of heat transfer to the cylinder walls, the gross heat release can be calculated as follows:

$$\frac{dQ_{Gross}}{d\theta} = \frac{dQ_{Net}}{d\theta} + \frac{dQ_{ht}}{d\theta} \quad (4.10)$$

$$\frac{dQ_{ht}}{d\theta} = hA_{\theta}(T - T_{wall}) \quad (4.11)$$

Where  $h$  is the heat transfer coefficient ( $W/m^2K$ ),  $T$  is the mean gas temperature in Kelvin, obtained from the equation of state ( $pV = mRT$ ) and  $T_{wall}$  is the mean cylinder wall temperature in Kelvin. In the present analysis the  $T_{wall}$  is assumed to be 450K and  $A_{\theta}$  is the instantaneous heat transfer surface area of the combustion chamber in cubic meters.

Considerable part of cylinder wall, piston crown and cylinder head are exposed to heat transfer during later part of the combustion. Therefore, the heat transfer rate must be estimated accurately while calculating the net heat release. Over the years, various papers have been published in the area of in-cylinder heat transfer aiming to quantify the heat transfer coefficient to easily measure or derive engine parameters. In the

current research heat transfer coefficient  $h$  [ $\text{Wm}^{-2}\text{K}^{-1}$ ] is calculated by using the Annand's correlation given below.

$$h = \frac{a \cdot \lambda}{B} \text{Re}^{0.3} + c \frac{(T^4 - T_{\text{wall}}^4)}{T - T_{\text{wall}}} \quad (4.12)$$

where,  $0.35 < a < 0.8$

$c = 0$  during intake and compression

$c = 0.075\sigma$  for SI engine combustion and expansion

$\sigma = 5.67 \times 10^{-8} \text{ W.m}^{-2}.\text{K}^{-4}$ , is the Stefan-Boltzmann constant.

$\lambda$  = Gas thermal conductivity,  $\text{kJ.m/s/K}$

The Reynold's number is given as:

$$\text{Re} = \frac{Sd\rho}{\mu} \quad (4.13)$$

where

$S$  is the mean velocity in the pipe (mean piston speed) in  $\text{m/s}$ .

$d$  the characteristic length (=engine bore,  $B$ ) in  $\text{m}$ .

$\rho$  is the density of the fluid in  $\text{kg/m}^3$ .

$\mu$  is the dynamic fluid viscosity in  $\text{kg/m-s}$ .

Mean piston speed is calculated from engine speed

$$S = \frac{2NL}{60} \quad (4.14)$$

where  $N$  is engine speed in  $\text{rpm}$  and  $L$  is engine stroke in  $\text{m}$ .

The density of the fluid is given as:

$$\rho = \frac{p}{RT} \quad (4.15)$$

The gas thermal conductivity is given as:

$$\lambda = \frac{C_p \mu}{0.7} \quad (4.16)$$

The specific heat at constant pressure is given as:

$$C_p = \frac{R}{1 - \frac{1}{\gamma}} \quad (4.17)$$

A temperature dependent equation for specific heat ratio  $\gamma$  obtained from experimental data is used (Shehata 2010).

$$\gamma = 1.338 - 6E^{-10}T + 1E^{-8}T^2 \quad (4.18)$$

The dynamic fluid viscosity is given as:

$$\mu = 4.702 E^{-7} T^{0.645} \quad (4.19)$$

Constants  $a=0.45$  and  $R=241.1$  J/kgK

The cylinder volume from crank angle for a slider-crank mechanism is as follows (Heywood 1988).

$$V = V_C + \frac{\pi B^2}{4} (l + R - R \cos \theta - \sqrt{l^2 - R^2 \sin^2 \theta}) \quad (4.20)$$

Where,  $R$  is crank throw in meters (= stroke/2),  $l$  is connecting rod length in meters,  $V_C$  is clearance volume at TDC in cubic meter,  $B$  is bore in meter,  $\theta$  is crank angle measured from the beginning of the induction stroke in radians.

$$V_c = \frac{\pi B^2}{4} \frac{2R}{CR} \quad (4.21)$$

Where,  $CR$  is the compression ratio

When computing the heat transfer rate, the instantaneous combustion chamber surface area  $A_\theta$  through which the heat transfer occurs is computed from

$$A_\theta = A_{Ch} + A_p + A_{lat(\theta)} \quad (4.22)$$

Where  $A_{ch}$  is the cylinder head surface area and  $A_p$  is the piston crown surface area. For flat-topped pistons,  $A_c = \pi B^2/4$ . The lateral surface area  $A_{lat(\theta)}$  is approximated by the lateral surface of a cylinder, and  $A_{ch}$  is assumed to be equal to  $A_p$ . The instantaneous combustion chamber surface area can then be expressed as:

$$A_\theta = \frac{\pi B^2}{2} + \pi B (l + R - R \cos \theta - \sqrt{l^2 - R^2 \sin^2 \theta}) \quad (4.23)$$

Equation 4.23 ignores the area associated with the piston cup, but the approximation has little effect on the heat release results (Goering 1998).

The mean charge temperature  $T$  for the single-zone model is found from the state equation  $pV = mRT$ , assuming the total mass of charge  $m_c$  and the mass specific gas



constant  $R$  to be constant. These assumptions are reasonable since the molecular weights of the reactants and the products are essentially the same. If all thermodynamic states ( $p_{ref}$ ,  $T_{ref}$ ,  $V_{ref}$ ) are known or evaluated at a given reference condition such as Inlet Valve Close (IVC), the mean charge temperature  $T$  is computed as

$$T = pV \frac{T_{ref}}{p_{ref}V_{ref}} \quad (4.24)$$

The cylinder volume at IVC is computed using the cylinder volume given in the above equation for  $\theta_{IVC}$  and is therefore considered to be known. The two other states at IVC ( $P_{IVC}$ ,  $T_{IVC}$ ) are considered unknown and have to be estimated.

Fig. 4.5 below gives the flow chart of the computer program to find heat release per cycle and COV of heat release.

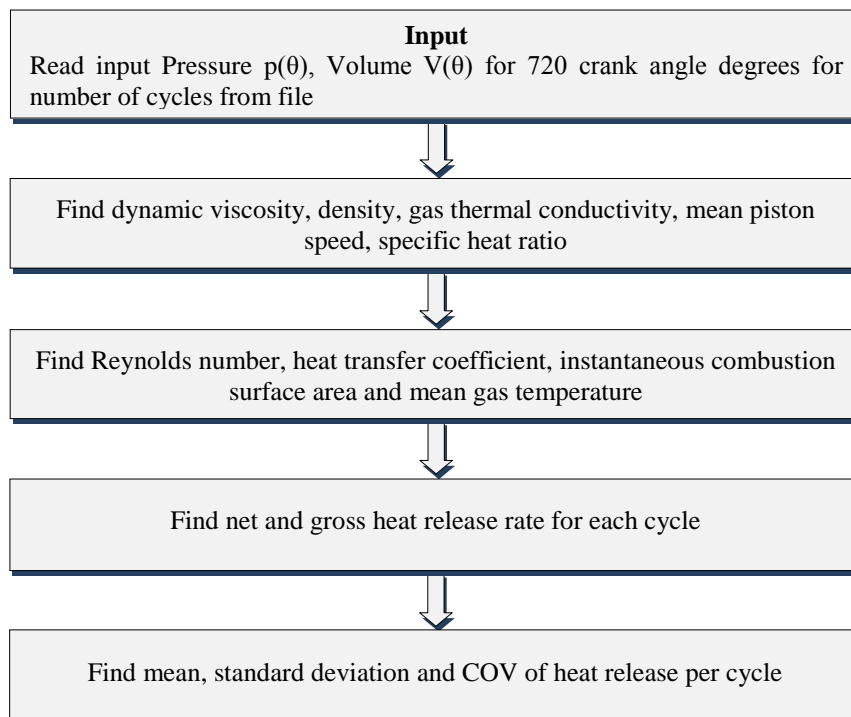


Fig. 4.5. Flow chart to find heat release rate and COV of heat release per cycle.

The rate of pressure rise is calculated using a simple numerical differentiation:

$$\frac{dp}{d\theta} = \frac{p_{i+1} - p_{i-1}}{\theta_{i+1} - \theta_{i-1}} \quad (4.25)$$

Once the rate of heat release rate is computed for 25 consecutive combustion cycles for a given test point, the gross heat release per cycle (HR) is computed for every combustion cycle. This heat release for 25 cycles is used to compute coefficient of variation of heat release per cycle (COV of heat release).

$$\text{COV}_{\text{heat release}} = \frac{\sigma_{\text{heat release}}}{\mu_{\text{heat release}}} \quad (4.26)$$

Where  $\sigma$  is the standard deviation and  $\mu$  is the mean value.

The standard deviation is given by

$$\sigma = \frac{\sqrt{\sum_1^n (\text{Heat release}_i - \mu_{\text{heat release}})^2}}{(n - 1)} \quad (4.27)$$

Where n= Number of combustion cycles.

#### 4.4 ERROR AND UNCERTAINTY ANALYSIS

Error is associated with various primary experimental measurements and the calculations of performance parameters. Errors and uncertainties in the experiments can arise from instrument selection, condition, calibration, environment, observation, reading and test planning. Uncertainty analysis is needed to prove the accuracy of the experiments.

The uncertainty in any measured parameter is estimated based on Gaussian distribution method with confidence limit of  $\pm 2\sigma$  (95.45% of measure data lie within the limits of  $\pm 2\sigma$  of mean). Thus uncertainty of any measured parameter is given by:

$$w_i = \frac{2\sigma_i}{x} 100 \quad (4.28)$$

Experiments are conducted to obtain the mean ( $x$ ) and standard deviation ( $\sigma_i$ ) of any measured parameter ( $x_i$ ) for a number of readings. This is done for speed, load, time for a specified amount of air and fuel flow etc. For the analysis, 20 sets of readings are taken at the same operating condition. The uncertainty values for speed, load, air

flow rate, fuel flow rate, exhaust gas temperature and emissions of NO<sub>x</sub>, HC, CO are calculated using equation (4.28).

A method of estimating uncertainty in experimental results has been presented by Kline and McClintock (1953). The method is based on careful specifications of the uncertainties in the various primary experimental measurements. Suppose a set of measurements is made and the uncertainty in each measurement may be expressed with the same odds. These measurements are then used to calculate some desired results of the experiments. The uncertainty in the calculated result can be estimated on the basis of the uncertainties in the primary measurements.

If an estimated quantity R depends on 'n' independent measured parameters x<sub>1</sub>, x<sub>2</sub>, x<sub>3</sub>, ... , x<sub>n</sub>. Then R is given by

$$R=R(x_1, x_2, x_3, \dots, x_n) \quad (4.29)$$

Let w<sub>R</sub> be the uncertainty in the result and w<sub>1</sub>, w<sub>2</sub>, ..., w<sub>n</sub> be the uncertainties in the independent measured parameters. R is the computed result function of the independent measured parameters x<sub>1</sub>, x<sub>2</sub>, x<sub>3</sub>...x<sub>n</sub> as per the relation x<sub>1</sub>±w<sub>1</sub>, x<sub>2</sub>±w<sub>2</sub>,... x<sub>n</sub>±w<sub>n</sub>). If the uncertainties in the independent variables are all given with the same odds, then the uncertainty in the result having these odds is given as (Adnan et al. 2012):

$$w_R = \sqrt{\left(\frac{\partial R}{\partial x_1} w_1\right)^2 + \left(\frac{\partial R}{\partial x_2} w_2\right)^2 + \dots + \left(\frac{\partial R}{\partial x_n} w_n\right)^2} \quad (4.30)$$

Using the equation (4.30) for a given operating condition, the uncertainties in the computed quantities such as mass flow rates of air and fuel, brake power, brake thermal efficiency are estimated.

The estimated uncertainty values at a typical operating condition are given in the next section.

#### 4.4.1 Sample Calculations

The sample calculation is shown for the E20 at 3500 rpm, WOT condition

Speed=3505 rpm

Fuel=144 cc/min

Weight on dynamometer W = 33.03 kg

Fuel consumption rate = 6.48864 kg/hr

Calorific value = 40561 kJ/kg

##### (i) Brake Power (BP)

In the experimentation, brake power is obtained from:

Brake Power:

$$BP = \frac{2\pi NWgR}{60000} \text{ kW} \quad (4.31)$$

Where, N = Engine speed in rpm,

R = Arm length of dynamometer =0.21 m

$$BP = \frac{2\pi \times 3505 \times 33.03 \times 9.81 \times 0.21}{60000} = 24.98 \text{ kW}$$

##### (ii) Brake Specific Energy Consumption

Brake specific energy consumption

$$BSEC = \frac{m_f CV}{BP} \text{ MJ/kWh} \quad (4.32)$$

Where,  $m_f$  = Mass flow rate of fuel in kg/hr

BP = Brake power in kW

$$BSEC = \frac{6.48 \times 40561}{24.98} \\ = 10.53 \text{ MJ/kWh}$$

### (iii) Brake Thermal Efficiency

Brake Thermal Efficiency (%)

$$BTE = \frac{BP \times 3600 \times 100}{Cv \times m_f} \quad (4.33)$$

$$\begin{aligned} BTE &= \frac{24.98 \times 3600 \times 100}{40561 \times 6.48} \\ &= 34.16\% \end{aligned}$$

### (iv) Uncertainty analysis

BP=f(N, W)

$$BP = \frac{2\pi \times N \times W \times 9.81 \times 0.21}{60000} = NW \times 2.16E^{-4}$$

$$w_{BP} = \frac{\partial BP}{\partial N} w_N^2 + \frac{\partial BP}{\partial W} w_W^2 \quad 1/2$$

$$w_N = 0.25$$

$$w_W = 0.32$$

$$\frac{\partial BP}{\partial N} = 7.13E^{-3}$$

$$\frac{\partial BP}{\partial W} = 0.757$$

$$w_{BP} = 7.13E^{-3} \times 0.25^2 + 0.757 \times 0.32^2 \quad 1/2$$

$$= 0.24 \text{ kW}$$

$$= 0.96\%$$

Table 4.1: Uncertainty of various parameters

<b>Sl. No.</b>	<b>Parameter</b>	<b>Uncertainty (%)</b>
1	Speed	$\pm 0.25$
2	Torque	$\pm 0.32$
3	Air flow rate	$\pm 1.05$
4	Fuel flow rate	$\pm 0.81$
5	Exhaust gas temperature	$\pm 0.50$
6	NO <sub>x</sub> emission	$\pm 5.91$
7	HC emission	$\pm 5.50$
8	CO emission	$\pm 3.77$
9	Brake power	$\pm 0.96$
10	Brake thermal efficiency	$\pm 0.5$

## CHAPTER 5

### RESULTS AND DISCUSSION

The engine performance, combustion characteristics and exhaust emissions with LPG, LPG with steam and ethanol enriched gasoline blends are presented in this chapter. First part of the chapter details the studies with the ethanol enriched gasoline blends of E5, E10, E15 and E20 while the second section explains the results with LPG fuel. The last section describes the results of experiments with LPG along with steam induction. Tests are conducted at different throttle opening positions and speeds to evaluate the engine performances and emissions. Studies are conducted and results obtained are analyzed with graphs.

#### 5.1 PERFORMANCE, COMBUSTION AND EMISSION STUDIES WITH ETHANOL ENRICHED GASOLINE BLENDS

This section gives the results of experiments conducted with gasoline and various ethanol enriched gasoline blends of E5, E10, E15 and E20 at wide open throttle (WOT) and part throttle conditions (i.e., quarter, half and three-fourth throttle open conditions). The WOT condition results give the full load test results. For representing the part load performances 50%WOT condition is selected. The engine speed range selected for the results are 2000 to 4500 rpm. Addition of ethanol to the gasoline raises engine volumetric efficiency and causes leaner operation. As a result, combustion becomes more complete or more stoichiometric, therefore, flame temperature and cylinder pressure rise to their maximum values as equivalence ratio approaches 1.

##### 5.1.1 Torque

The influence of the ethanol addition to gasoline on engine torque with engine speeds of 2000 to 4500 rpm at WOT and 50% WOT conditions are shown in figures 5.1 (a) and (b) respectively. It is observed that at WOT, torque with blended fuels are higher than that of gasoline. Even though the ethanol addition to the gasoline decreases its heating value, the increase in torque and power are obtained. Beneficial effect of

ethanol as an oxygenated fuel is a possible reason for more complete combustion, thereby increasing the torque. In addition, a larger mass of fuel for the same volume is injected to the cylinder due to higher density of ethanol. This results in increase of torque and power.

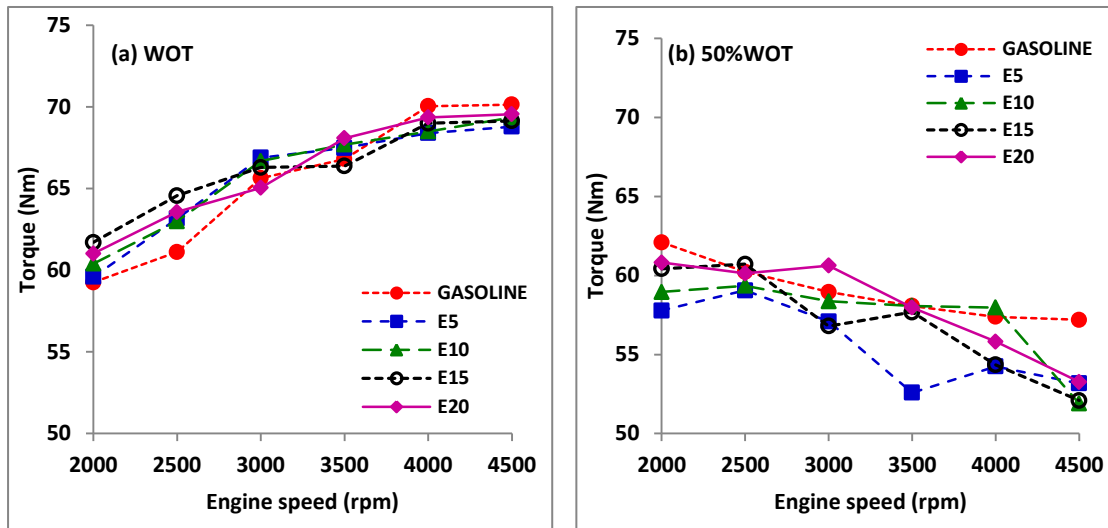


Fig. 5.1 Torque with engine speed for ethanol blends at (a) WOT and (b) 50% WOT

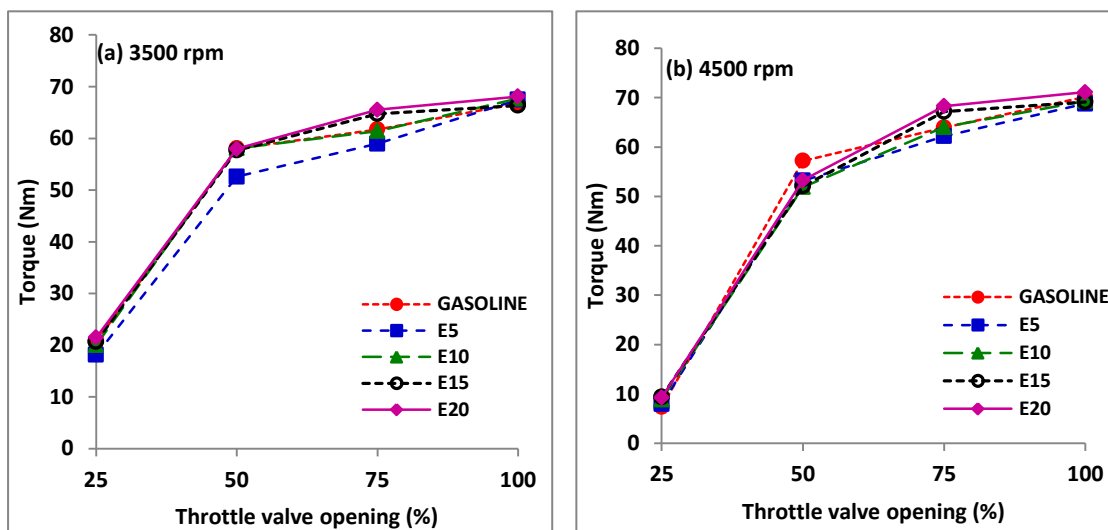


Fig. 5.2 Torque with ethanol blends at (a) 3500 rpm and (b) 4500 rpm

Figures 5.2 (a) and (b) respectively shows the torque output of the test engine at different throttle valve opening conditions with various ethanol enriched gasoline blends at speeds of 3500 and 4500 rpm. The engine torque at a fixed speed increases with increase in throttle valve opening. It is seen that at lower engine speed the torque



output is more sensitive to ethanol blends as compared to at higher engine speeds. It is observed that gasoline has the highest torque at speed of 3500 rpm, while E15 has the highest torque at lower engine speeds and has comparable torque with gasoline. At 4500 rpm, E20 has the highest torque. It is seen that at higher throttle valve openings, there is a lot of variation in output torque with blended fuels as compared to lower throttle openings. Under the conditions of low throttle valve openings or high engine speeds, the original fuel injection strategy tends to operate the engine in fuel- rich burning conditions. Therefore, the added ethanol will produce the leaning effect to increase the air–fuel equivalence ratio to a higher value, and make the burning closer to be stoichiometric. The original fuel injection strategy controlled by the ECU is set based on the use of pure gasoline. The stoichiometric air– fuel ratio for pure gasoline is 14.7 approximately, and that for the blended fuel is less than 14.7. The amount of intake air remains constant, when the engine speed and the throttle valve opening are kept the same. However, according to the gasoline fueling strategy, the ECU must reduce the fuel supply to achieve the stoichiometric air–fuel ratio being 14.7, when ethanol is added. This ultimately makes the air–fuel mixture of the ethanol enriched gasoline blend to go leaner. The oxygen in ethanol gives an additional assistance to achieve lean burning in the engine. Its final result is that better combustion can be achieved and higher torque output can be acquired. Engine operating speed of 3500 rpm is taken as representative speed since the maximum speed of the engine is 6000 rpm.

### **5.1.2 Brake power**

Variation of brake power for the various fuel blends with engine speeds at WOT and 50%WOT conditions are shown in the figures 5.3 (a) and (b) respectively. It is observed that ethanol blends have resulted in a marginal increase in brake power at all speed conditions, with E20 showing the highest increase in the brake power as compared with gasoline. As the ethanol content in the blend increases the contribution to the net energy output from the blend also increases. As the throttle valve opening and speed increases brake power increases.

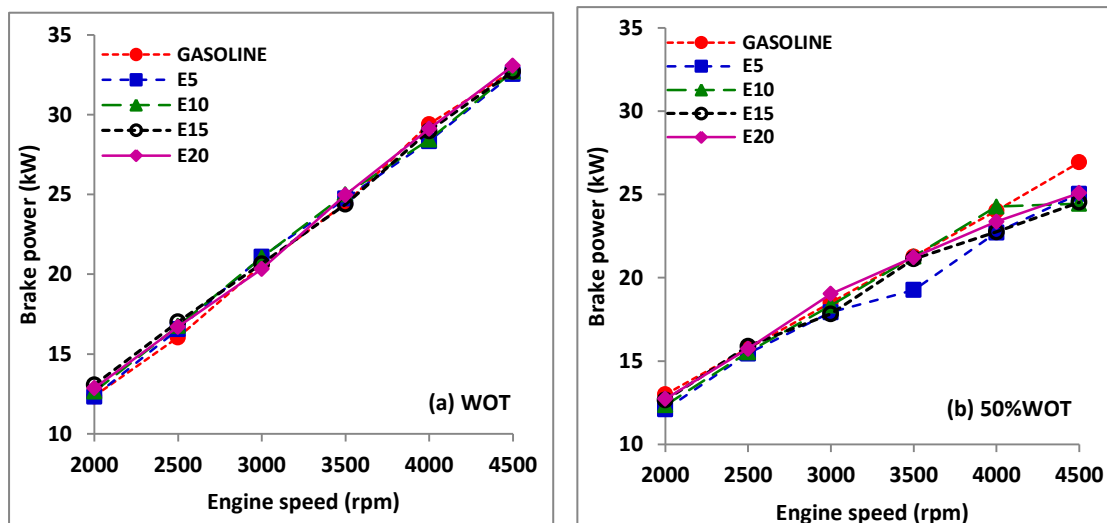


Fig. 5.3 Brake power with engine speed for ethanol blends at (a) WOT and (b) 50% WOT

### 5.1.3 Brake thermal efficiency(BTE)

The variation of brake thermal efficiency for various blends at WOT and 50%WOT operation for different ethanol gasoline blends are shown in figures 5.4 (a) and (b) respectively. It may be observed that blended fuels of E15 and E20 gave better engine performances for all speeds when compared to baseline gasoline fuel operation. E20 blend has an increasing trend when compared to other blends. The presence of oxygen in the blended fuel may be attributed to the higher thermal efficiency. However at WOT condition blends of E5 and E10 have shown falling trend as the engine speed increases. At 50%WOT condition; the blends perform better than the baseline gasoline, with E15 and E20 showing overall improved performance.

The variation of brake thermal efficiency for various blends at different throttle valve opening conditions is shown in figures 5.5 (a) and (b) at engine speeds of 3500 and 4500 rpm. At the speeds of 3500 and 4500 rpm, the blends show a similar increase in thermal efficiency when compared to E0. At 50% throttle opening, E15 blend gives the maximum efficiency while at WOT condition E20 has the highest efficiency. It can be seen that blended fuels gave better engine performances for all speeds when compared to baseline gasoline fuel operation. E20 blend has an increasing trend when compared to other blends at all throttle conditions. The presence of oxygen in the

blended fuel leading to complete combustion may be attributed to the higher thermal efficiency.

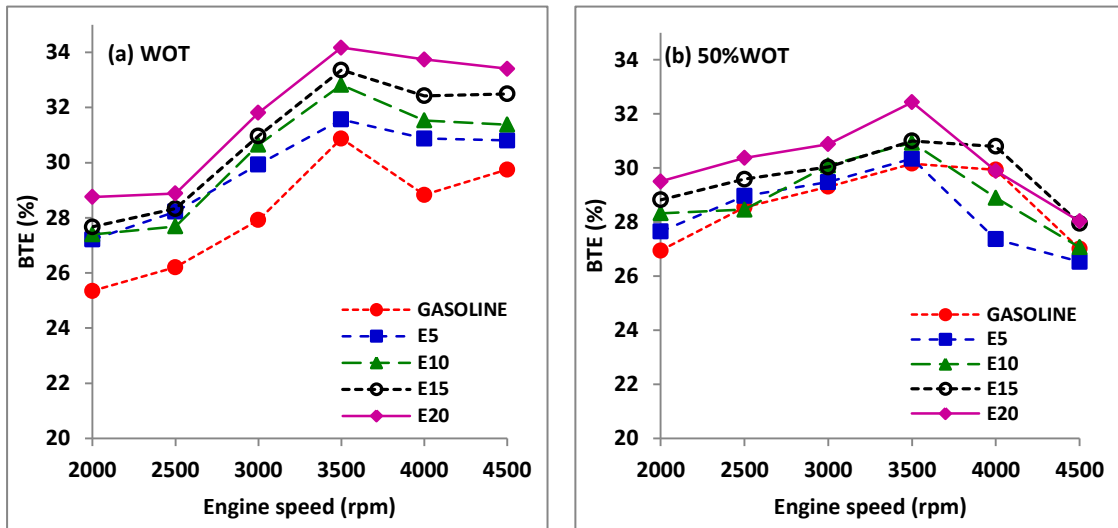


Fig. 5.4 Brake thermal efficiency (BTE) with engine speed for ethanol blends at (a) WOT and (b) 50% WOT

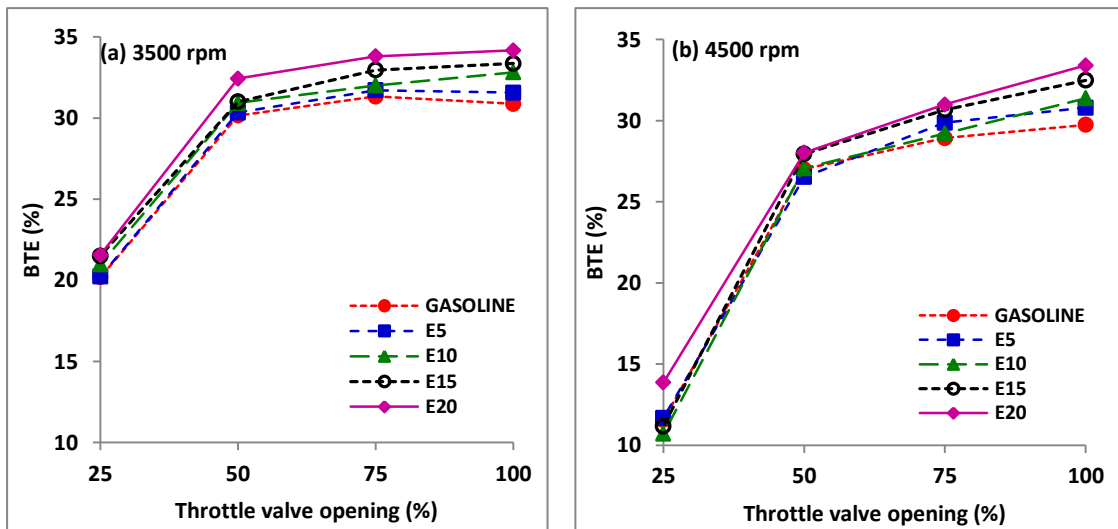


Fig. 5.5 Brake thermal efficiency with ethanol blends at (a) 3500 rpm and (b) 4500 rpm

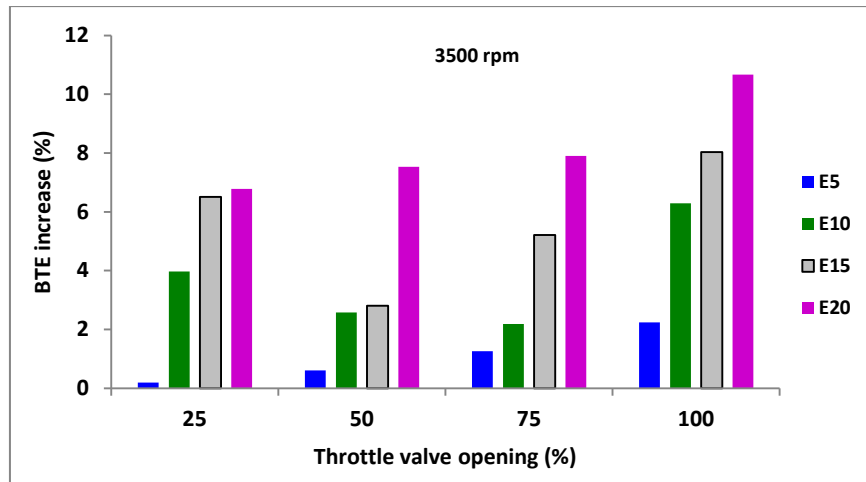


Fig. 5.6 Influence of ethanol blends on brake thermal efficiency at 3500 rpm

Figure 5.6 shows the influence of blending ethanol on the brake thermal efficiency at 3500 rpm. At 50%, 75% WOT and WOT conditions; there is a clear increase in thermal efficiency with the increase in the ethanol content in the blend. At WOT condition E20 has increased the thermal efficiency by 10.67 %. Even though the ethanol addition to the gasoline decreases its heating value, the increase in torque and power are obtained. Beneficial effect of ethanol as an oxygenated fuel is a possible reason for more complete combustion, thereby increasing the torque and hence the power.

#### 5.1.4 Brake specific energy consumption (BSEC)

The figures 5.7(a) and (b) respectively shows the variation of brake specific energy consumption (BSEC) for the various fuel blends at WOT and 50% WOT operations. At WOT condition generally the BSEC values have decreased with increase in the speed. Favorable effect of ethanol as an oxygenated fuel is a possible reason for more complete combustion, thereby reducing the total energy consumption. In addition, a larger fuel for the same volume is injected to the cylinder due to higher density of ethanol. This results in increase of torque and power. At 50% WOT condition towards the higher speed range the BSEC tends to increase, which is in agreement with the decreasing trend of BTE explained earlier.

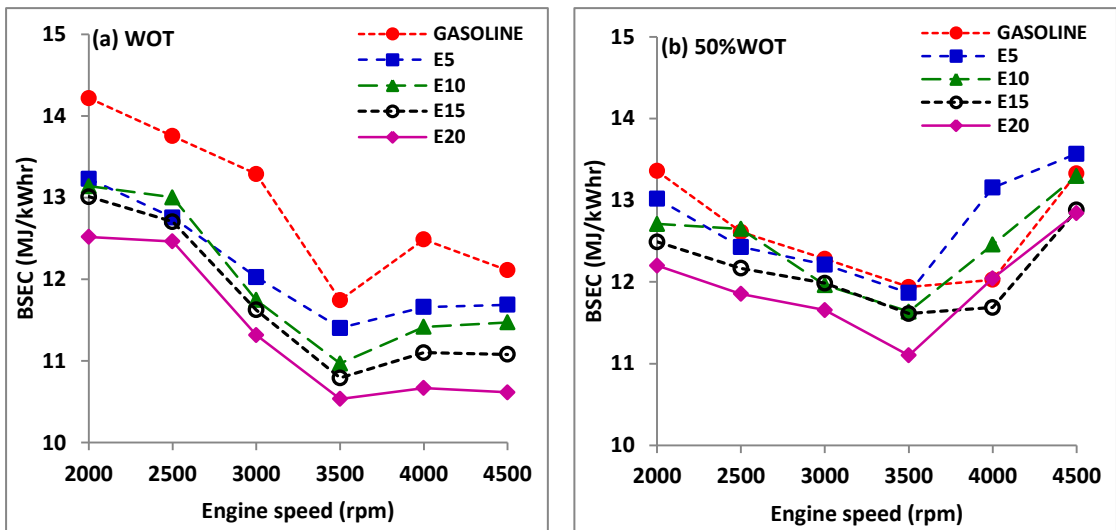


Fig. 5.7 BSEC with engine speed for ethanol blends at (a) WOT and (b) 50% WOT

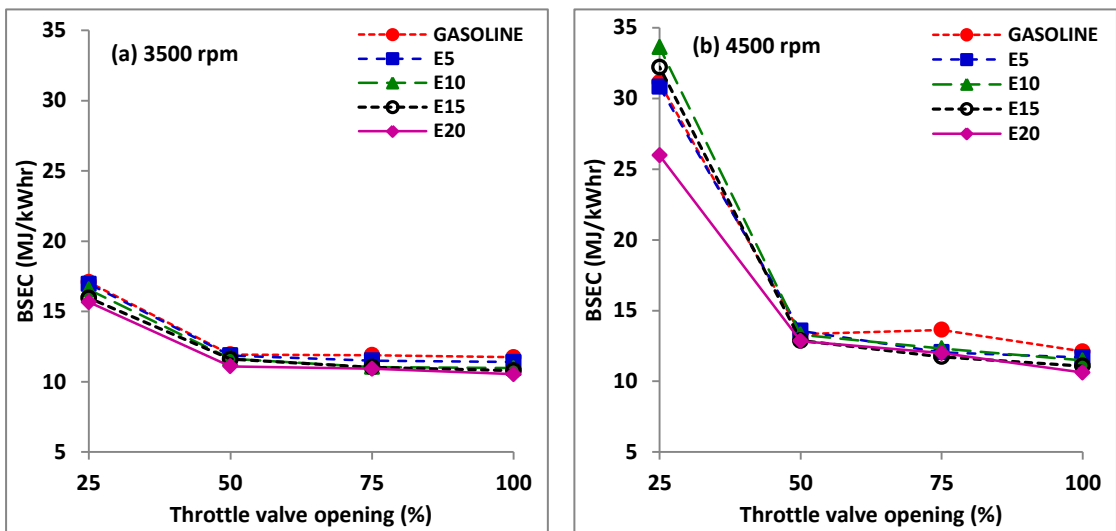


Fig. 5.8 BSEC with ethanol blends at (a) 3500 rpm and (b) 4500 rpm

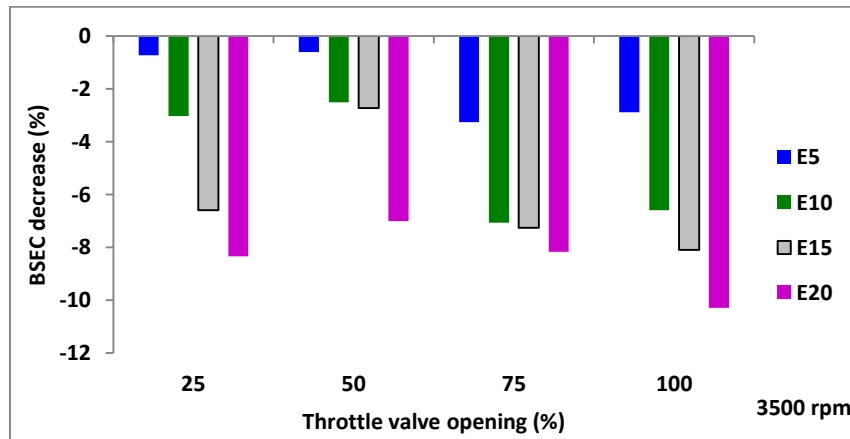


Fig. 5.9 Influence of ethanol blends on BSEC at 3500 rpm

Figures 5.8(a) and (b) shows the variation of BSEC at different throttle valve openings at speeds of 3500 and 4500 rpm respectively. The BSEC values have increased with increase in the speed generally. For higher engine speeds at 50% throttle opening, E15 and E20 fuels have registered the lowest BSEC, while at WOT conditions E10 and E15 blends have resulted in lowest values. Figure 5.9 shows the influence of ethanol blending on BSEC at 3500 rpm. It can be observed that at 25% throttle openings, the BSEC has increased for blends while it has reduced at 50%, 75% and WOT conditions. At WOT, the maximum reduction is for E20 blend is by 10.3%, followed by other blends of E15, E10 and E5 respectively by 8.1, 6.6 and 2.9%. The theoretical air fuel ratio of gasoline is 1.6 times that of ethanol, therefore the BSFC should be increased with the increase of ethanol content. However, the fuel injection strategy tends to operate the engine at fuel-rich condition, and the ethanol addition produces leaning effect to enhance the combustion of fuel.

#### **5.1.5 Equivalence ratio ( $\Phi$ )**

The trends of fuel-air equivalence ratios calculated for the various ethanol blends are shown in figures 5.10(a) and (b) respectively at WOT and 50%WOT for different engine speeds. At lower engine speeds, the combustion is lean, while at higher speeds like 4500 rpm, it reaches towards stoichiometric and then to rich mixture zone. Ethanol blends at WOT have shown lean burning especially E15 and E20. At 4500 rpm, E20 has equivalence ratio of 0.98 while the other blends have values more than 1 indicating richer than stoichiometric combustion. Engine performance parameters such as brake power, torque and brake thermal efficiency are increased when the ethanol amount in the blended fuel is increased which is due to the reduction in the equivalence ratio. At 50%WOT condition also it has been observed that gasoline burns richer than any other fuel blends, while E20 burns overall lean compared to others.

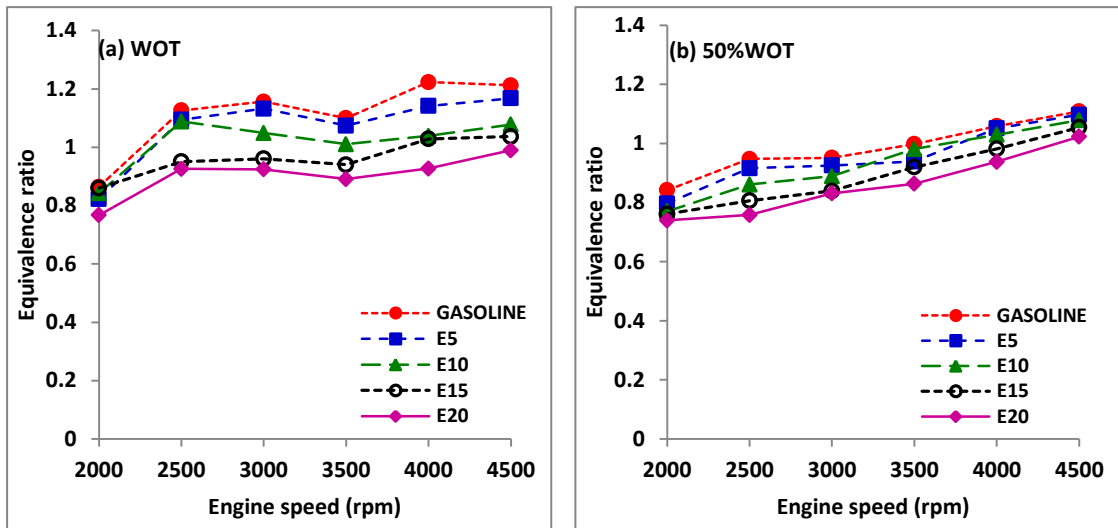


Fig. 5.10 Equivalence ratio with engine speed for ethanol blends at (a) WOT and (b) 50%WOT

The equivalence ratio decreases as the ethanol percentage increases to 20%. This effect is attributed to two factors: (1) the decrease in the stoichiometric air–fuel ratio of the fuel blends, since the stoichiometric air–fuel ratio of ethanol fuel is usually lower than that of gasoline fuel and (2) the increase of actual air–fuel ratio of the blends as a result of the oxygen content in ethanol.

### 5.1.6 Pressure-crank angle diagrams

Figures 5.11 (a) and (b) show the variation of the cylinder pressure for 25 consecutive combustion cycles with gasoline fuel at WOT and 50%WOT and 3500 rpm. It can be observed that there is considerable variation in the pressure for the same operating conditions from one cycle to another. The dark line indicates the average pressure at this operating condition. Figures 5.12 (a) and (b) respectively show the variation of the maximum cylinder pressure of each cycle ( $P_{max}$ ) and IMEP of each cycle for 25 consecutive combustion cycles with gasoline fuel. It is observed from the figures that there is considerable variation in the pressure related parameters for the same operating conditions from one cycle to another. Compared to the peak pressure, the cycle to cycle variation of IMEP is less.

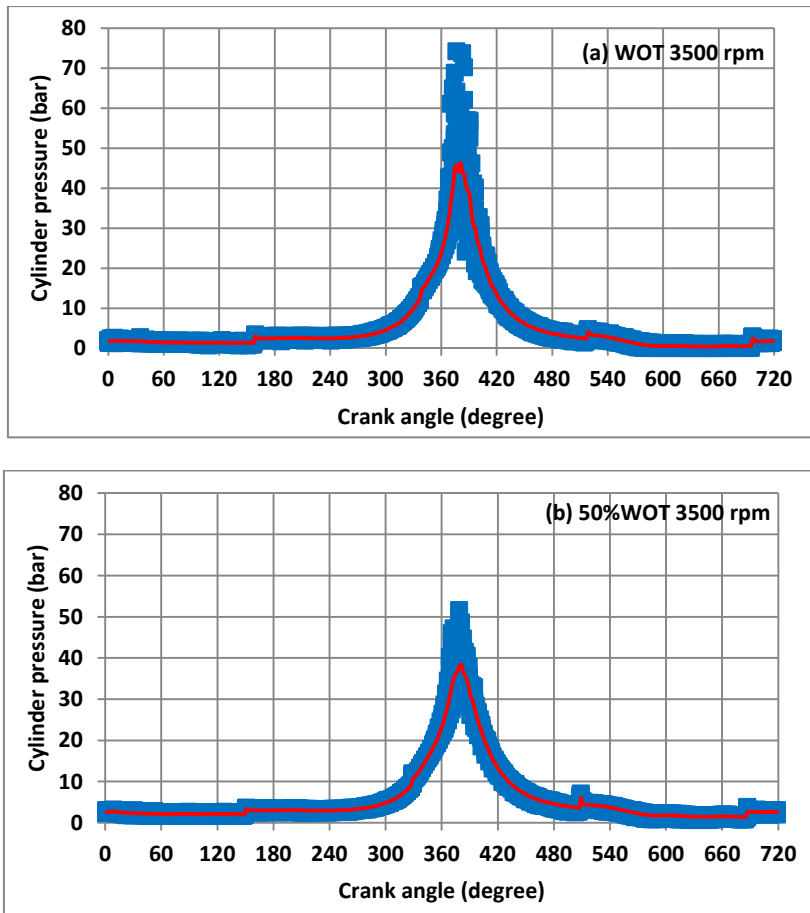


Fig. 5.11 Cylinder pressure of 25 combustion cycles vs crank angle for gasoline at 3500 rpm (a) WOT and (b) 50% WOT.

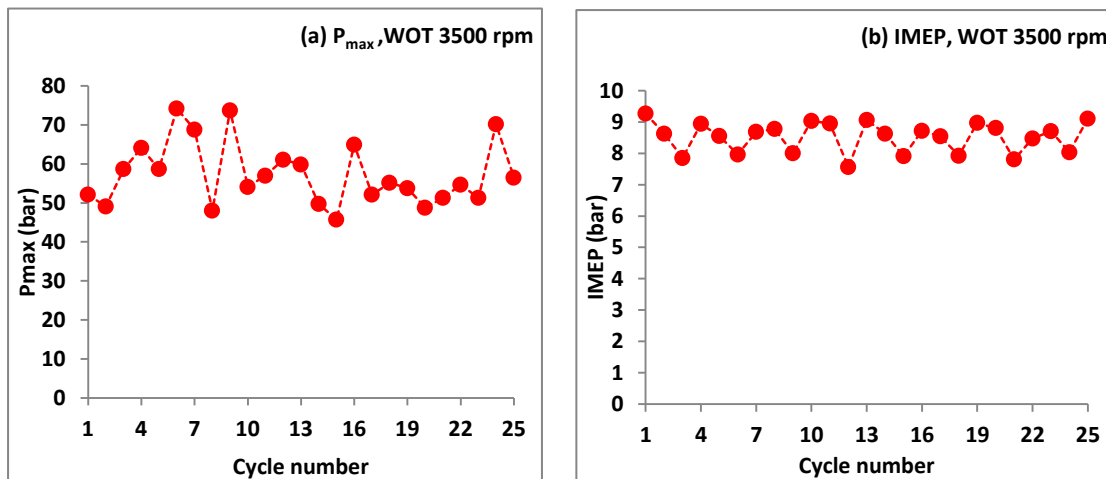


Fig. 5.12 (a)  $P_{max}$  and (b) IMEP for 25 consecutive cycles for gasoline at WOT & 3500rpm.



The average pressure- crank angle diagrams for various ethanol enriched gasoline blends at WOT and 50%WOT are shown in figures 5.13 (a) & (b) and 5.14 (a) & (b) respectively for 3500 and 4500 rpm.

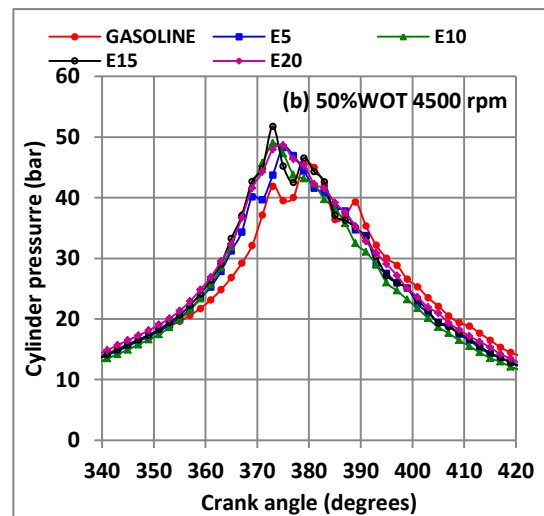
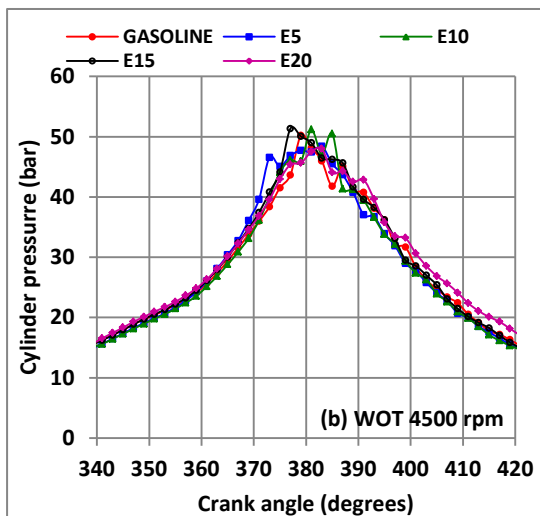
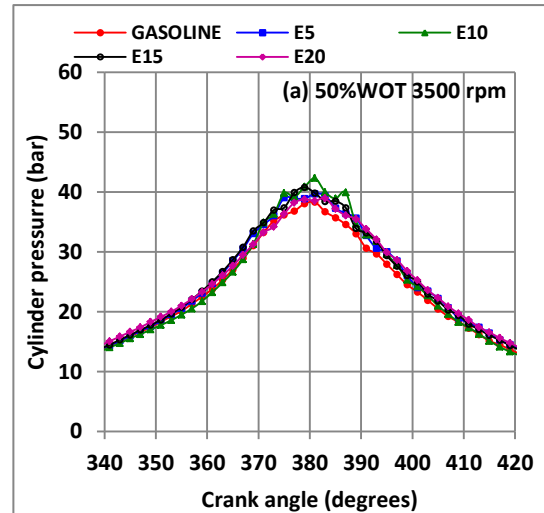
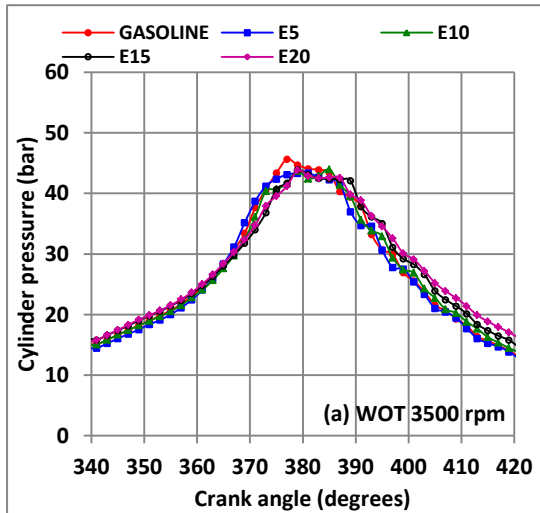


Fig. 5.13 Pressure vs crank angle for ethanol blends at WOT, (a) 3500 rpm & (b) 4500 rpm

Fig. 5.14 Pressure vs crank angle for ethanol blends at 50% WOT, (a) 3500 rpm & (b) 4500 rpm

At WOT condition, as the engine speed is increased the peak pressure for various fuels are observed to be occurring nearer to TDC. The blending of ethanol above 10% has increased the peak pressure when compared to gasoline fuel operation.

### 5.1.7 Variation of peak pressure and IMEP

Combustion variations are presented with the generalized plots of peak pressure ( $P_{max}$ ) and indicated mean effective pressure (IMEP) for 25 consecutive cycles at 3500 rpm

when the engine was operated at WOT and 50%WOT conditions in figures 5.15 and 5.16 respectively. Considerable variations in the peak pressure and IMEP trends are observed for various fuels. From the peak pressure trends it can be observed that the fluctuations are high for gasoline followed by E20 blend. The IMEP trends also ascertain this fact, but the mean IMEP was higher for gasoline fuel operation. The ethanol- gasoline blends of E5, E10 and E15 show relatively low fluctuations in both  $P_{max}$  and IMEP.

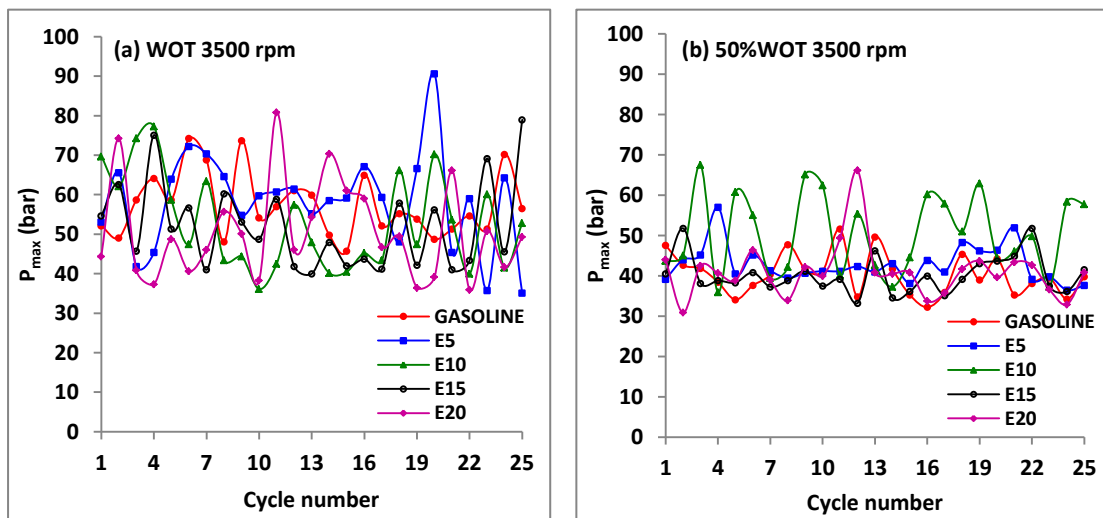


Fig. 5.15  $P_{max}$  of 25 cycles for ethanol blends at 3500 rpm, (a) WOT & (b) 50%WOT

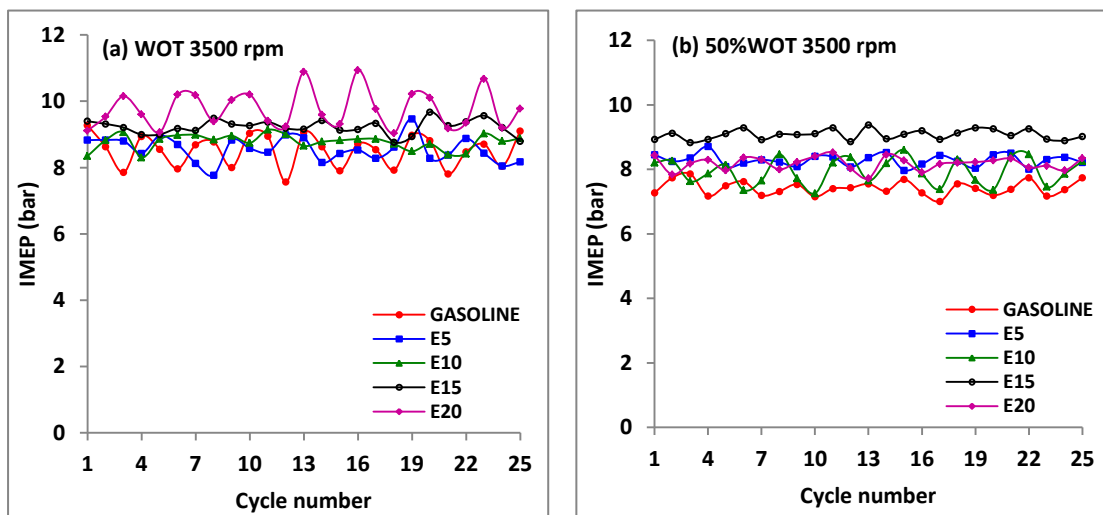


Fig. 5.16 IMEP of 25 cycles for ethanol blends at 3500 rpm, (a) WOT & (b) 50%WOT

Time return maps are commonly used for investigating the structure of nonlinear dynamic data and are typically constructed by plotting an observed variable against itself lagged in time. The return map presented here was constructed by plotting the  $P_{max}$  at cycle  $(i+L)$  versus the  $P_{max}$  at cycle  $i$ , where  $L$  is the return lag and typically has a value of one. Similar return map was prepared for IMEP also. For Gaussian random data, such a map will exhibit a circular, unstructured pattern. A significantly different pattern may indicate the presence of determinism. The appearance of structure in return maps is very robust for low dimensional dynamics, even in the presence of high levels of noise. Time return map of IMEP at 3500 rpm and at various throttle openings are shown in figures 5.17(a) & (b) while the figures 5.18(a), (b) & (c) shows the return maps at WOT condition for various speeds. The IMEP values give an insight of combustion as it is derived from the cylinder pressure signals. At WOT condition, the IMEP of the engine increases with speed. The ethanol blending has improved the combustion by which the IMEP values increases as ethanol content in the blend increases. The 50%WOT trends are having differing trends with speed and it decreases with speed. But blends have indicated better IMEP development, which is the reason for better engine performance with blends. In both the cases E20 blend has resulted in the maximum IMEP gain.

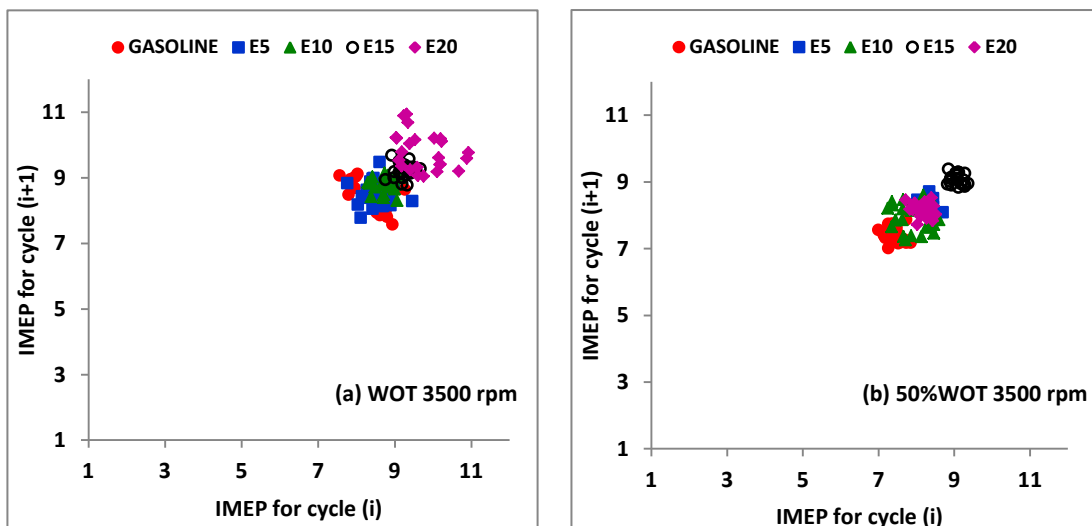


Fig. 5.17 Time return map of IMEP of 25 cycles for ethanol blends at 3500 rpm, (a) WOT & (b) 50% WOT

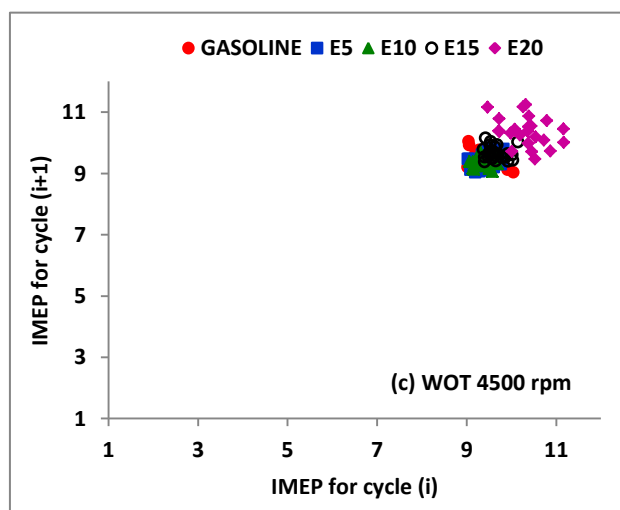
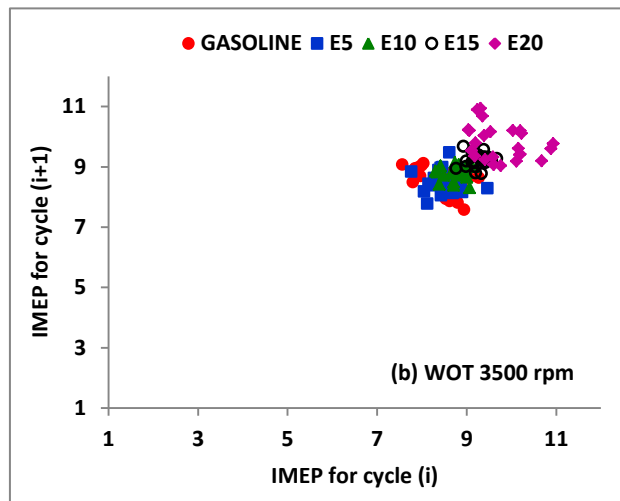
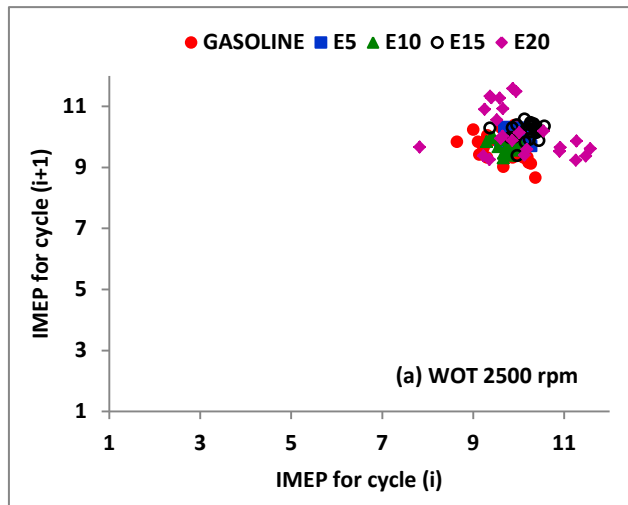


Fig. 5.18 Time return map of IMEP of 25 cycles for ethanol blends at WOT, (a)2500 rpm, (b) 3500 rpm & (c) 4500 rpm.

From the above figures it can be observed that IMEP return map for gasoline are more scattered and they are exhibiting asymmetric pattern compared to the blended fuels. The return maps for the blend E15 are more symmetric. As the blend ratio is increased beyond 15%, there is higher scattering of return maps. The IMEP return map indicates that blending ethanol with gasoline results in more consistent power outputs.

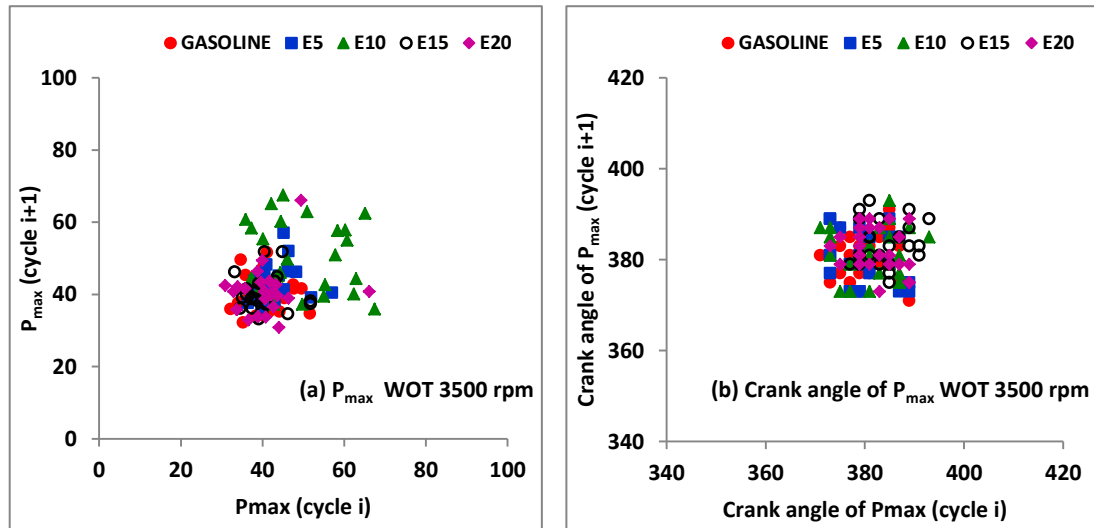


Fig. 5.19 Time return map of (a)  $P_{max}$  and (b) crank angle of  $P_{max}$  of 25 cycles for ethanol blends at 3500 rpm.

Figures 5.19 (a) & (b) respectively gives the return maps of peak pressure ( $P_{max}$ ) and crank angle of  $P_{max}$  at 3500 rpm and WOT condition. It is observed that higher blends of ethanol in gasoline have reduced the peak pressure as well the scatter. The average crank angle of peak pressure occurrence has not changed much.

#### 5.1.8 COV of IMEP and COV of $P_{max}$

The variation of IMEP at WOT and 50% WOT are given in figures 5.20 (a) and (b) respectively. It is observed that enriching the gasoline with ethanol improves the IMEP. As the blend ratio is increased the IMEP also increase with speed. The trends of coefficient of variation of IMEP ( $COV_{IMEP}$ ) with engine speeds for various throttle openings are shown in figures 5.21 (a) & (b). It can be observed that generally the  $COV_{IMEP}$  increases as the speed increases for all throttle opening conditions.

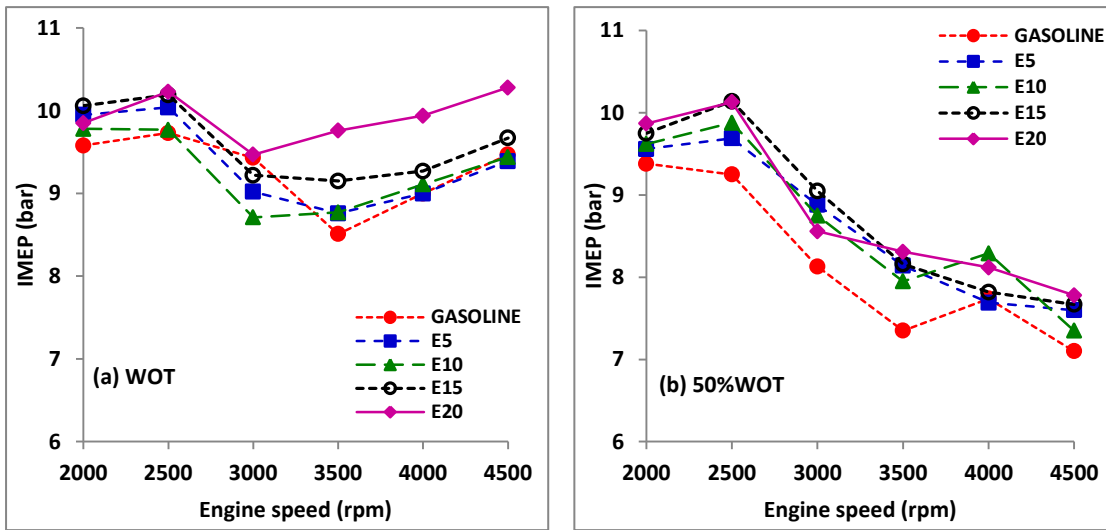


Fig. 5.20 IMEP with engine speed for ethanol blends at (a) WOT and (b) 50%WOT

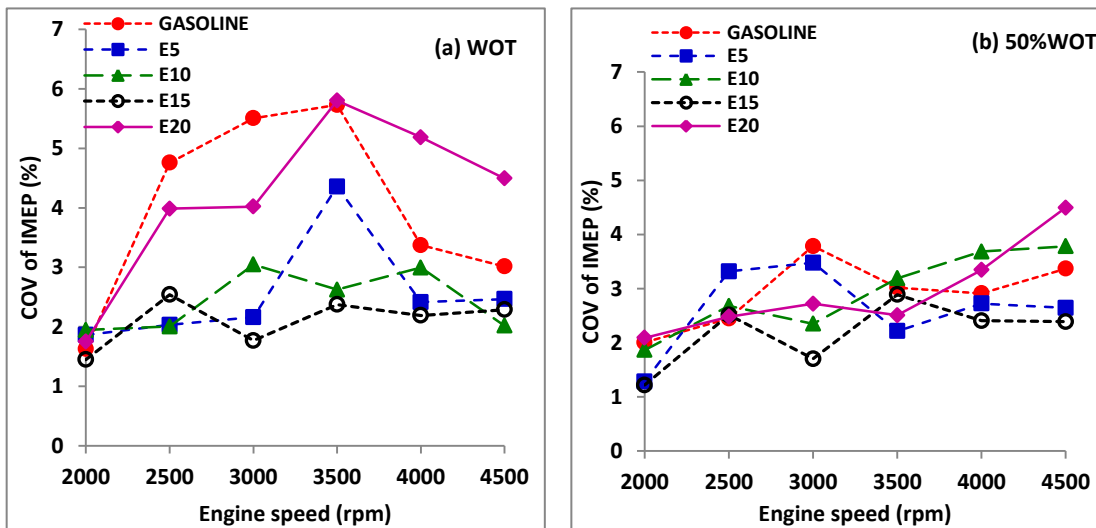


Fig. 5.21  $COV_{(IMEP)}$  with engine speed for ethanol blends at (a) WOT and (b) 50%WOT

At WOT conditions the average  $COV_{IMEP}$  was 4.0% for gasoline as compared to 2.55% for E5, 2.43% for E10, 2.1% for E15 and 4.21 for E20 fuel operations respectively. However the  $COV_{IMEP}$  values were below the 10% mark after which the engine operation becomes rough and the engine output decreases. At WOT operation ethanol blending reduces the COV of IMEP for all speeds and E15 exhibits minimum variation trend. At half throttle open operation also blend E15 has resulted in lowest COV of IMEP. The percentage of ethanol in fuel blend affects the volatility and the

latent heat of fuel blend. The latent heat of ethanol (840 kJ/kg) is higher than that of gasoline (305 kJ/kg) which makes the temperature of intake manifold lower, and increases the volumetric efficiency. Moreover, ethanol decreases the stoichiometric air–fuel ratio of the fuel blends, because the stoichiometric relative air–fuel ratio of ethanol fuel is lower than that of the unleaded gasoline fuel, as a result of the oxygen content in ethanol. These may have resulted in better combustion leading to the reduction in  $COV_{IMEP}$  for the lower blends. From the above trends it can be concluded that E15 is the blend which has relatively better  $COV_{IMEP}$  characteristics for all operating conditions among all the blends tested. Figure 5.22 shows the variation of COV of IMEP at 3500 rpm for various throttle valve openings. The engine operates smoothly except at 1/4<sup>th</sup> throttle opening when compared to other throttle opening conditions. At 3/4<sup>th</sup> throttle open operation the blend E10 was having lowest variation.

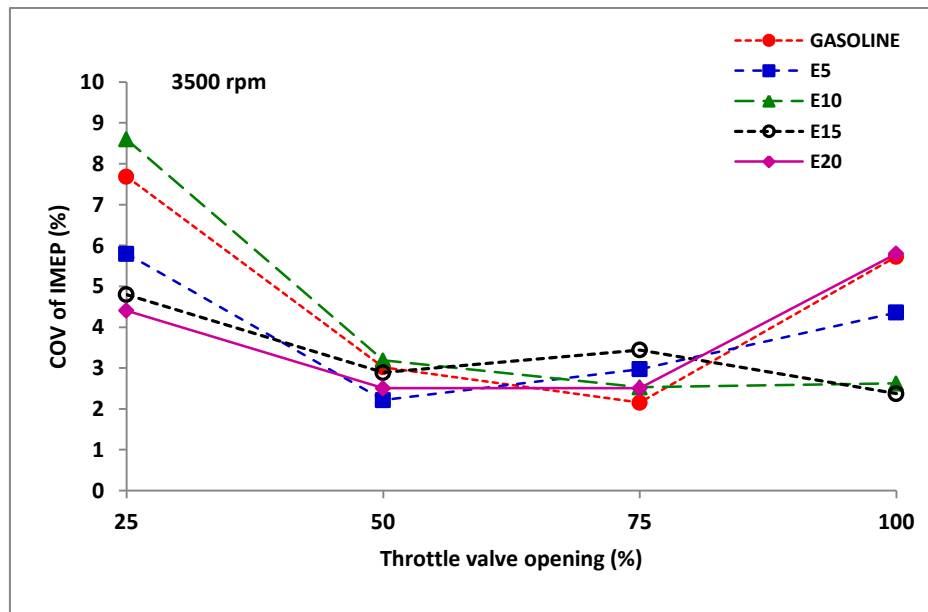


Fig. 5.22 Variation of COV of IMEP at 3500 rpm for ethanol blends

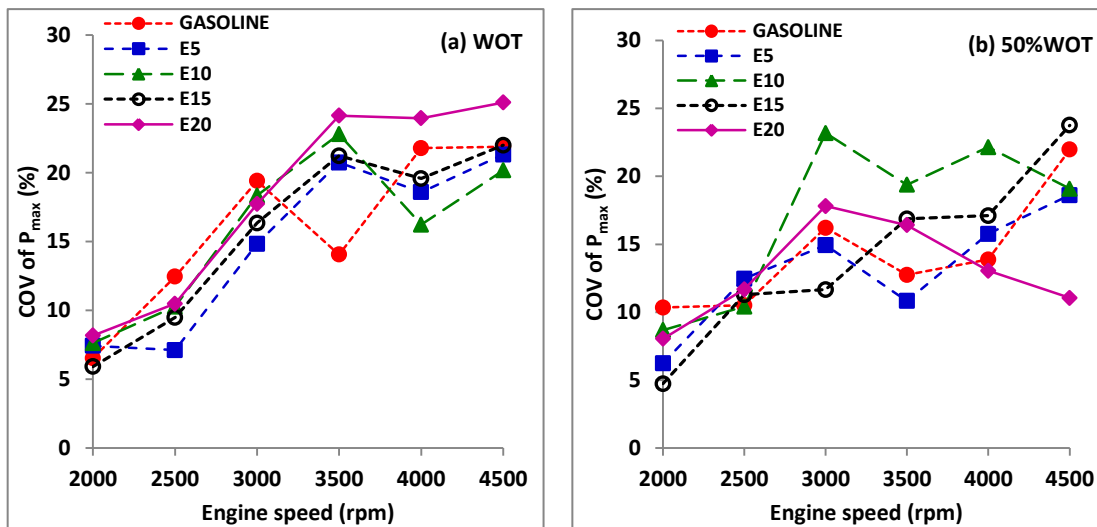


Fig. 5.23 Variation of COV of  $P_{\max}$  with engine speed for ethanol blends at (a) WOT and (b) 50%WOT

The variation of COV of  $P_{\max}$  at WOT and 50%WOT conditions are shown in figure 5.23(a) & (b) respectively.

### 5.1.9 Heat release rate analysis

The gross heat release trends for various speeds of 2500, 3500 and 4500 rpm are given in figures 5.24 (a), (b) & (c) and 5.25 (a), (b) & (c) at WOT and 50%WOT respectively. Heat release calculations are an attempt to get some information about the combustion process in an engine. Heat release rate is used in both engine performance influences in various operating conditions and same engine performances under the equal conditions. Moreover, physical and chemical properties of the fuel used in internal combustion engines are one of the main parameters which affect the heat release rate. As seen in the figures, except at 4500 rpm engine speed, the heat release rate for gasoline fuel began to rise earlier than that of alcohol-gasoline fuel blends at the both throttle openings. And also, the peak locations of heat release rate of alcohol-gasoline blends are wider than that of pure gasoline. This may be due to the fact that ethanol has one type of hydrocarbon and a single boiling point. The other reason may be that the alcohol fuels which contain oxygen in their structures improve combustion and a large amount of fuel burn takes place in the areas close to TDC. For the all test fuels, heat release rate takes place in the areas close to TDC with the increasing speed.



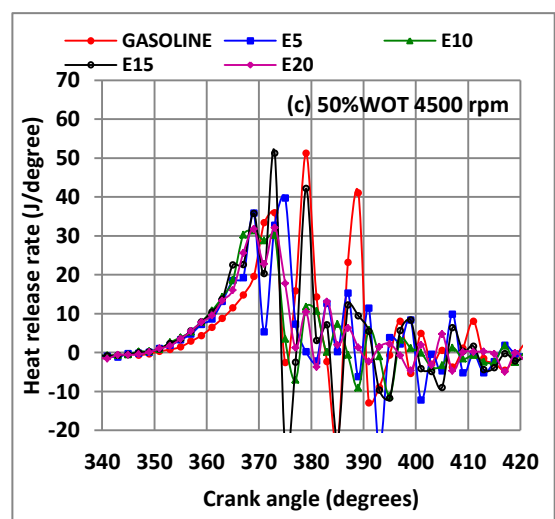
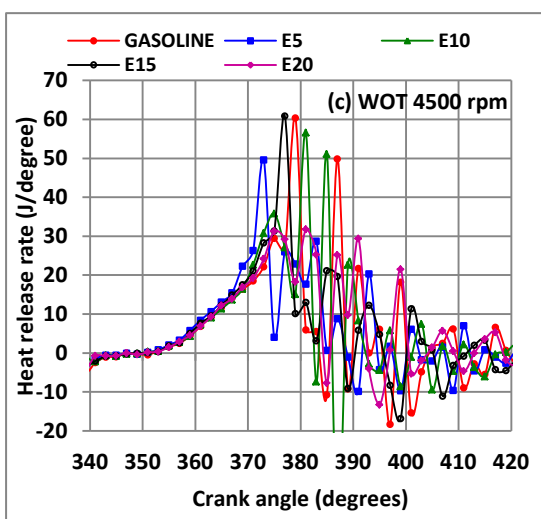
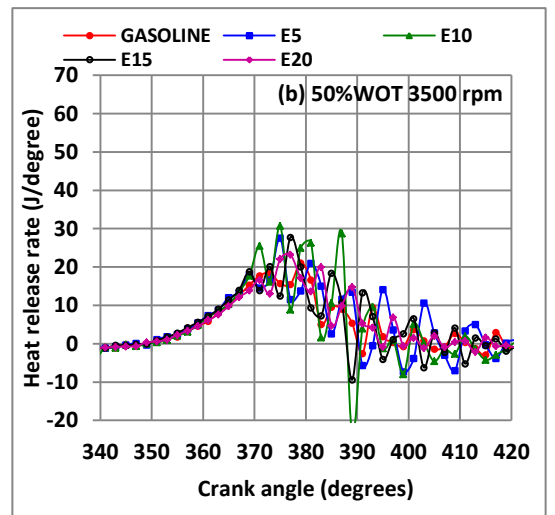
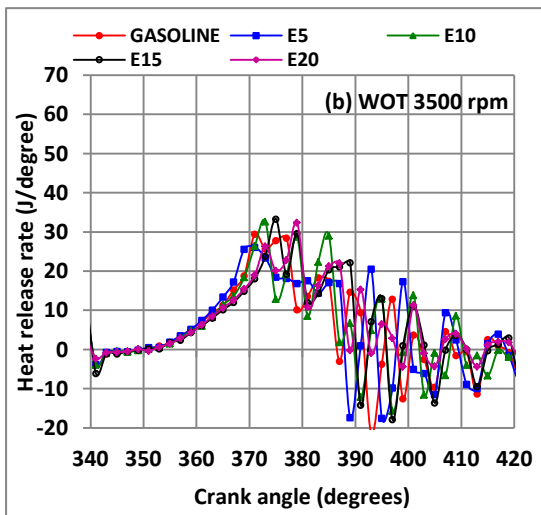
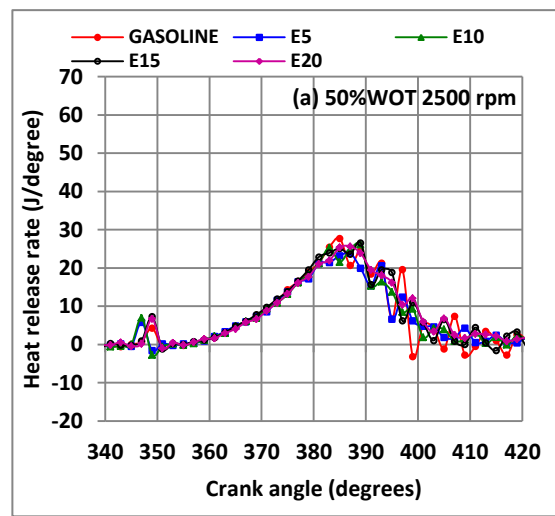
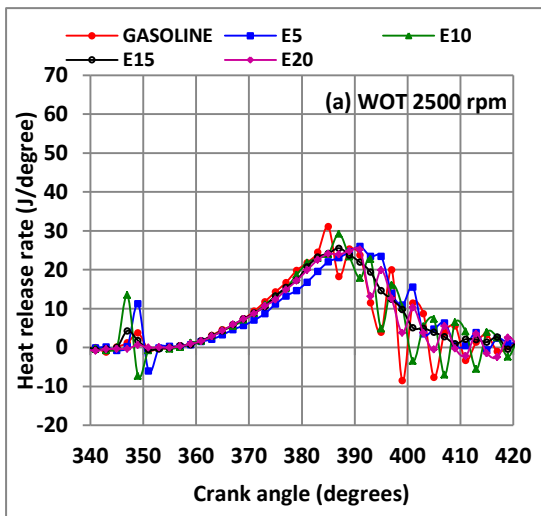


Fig. 5.24 Gross heat release rate for ethanol blends at WOT, (a) 2500, (b) 3500 & (c) 4500 rpm

Fig. 5.25 Gross heat release rate for ethanol blends at 50% WOT, (a) 2500, (b) 3500 & (c) 4500 rpm

At 3500 rpm and WOT for the sole fuel, the rate of heat release was faster and reached a peak at 12 deg. after TDC which was 10 deg. earlier than that of the ethanol enriched gasoline fuel E20. Subsequently, the heat release rate came down sharply on account of the amount of unburnt fuel available due to the quenching effect. This is one of the main reasons for the reduction in the heat release rate in ethanol–gasoline blended fuels. The COV of heat release per cycle is computed from average cylinder pressures at various throttle openings for blends are shown in fig. 5.26 (a) & (b).

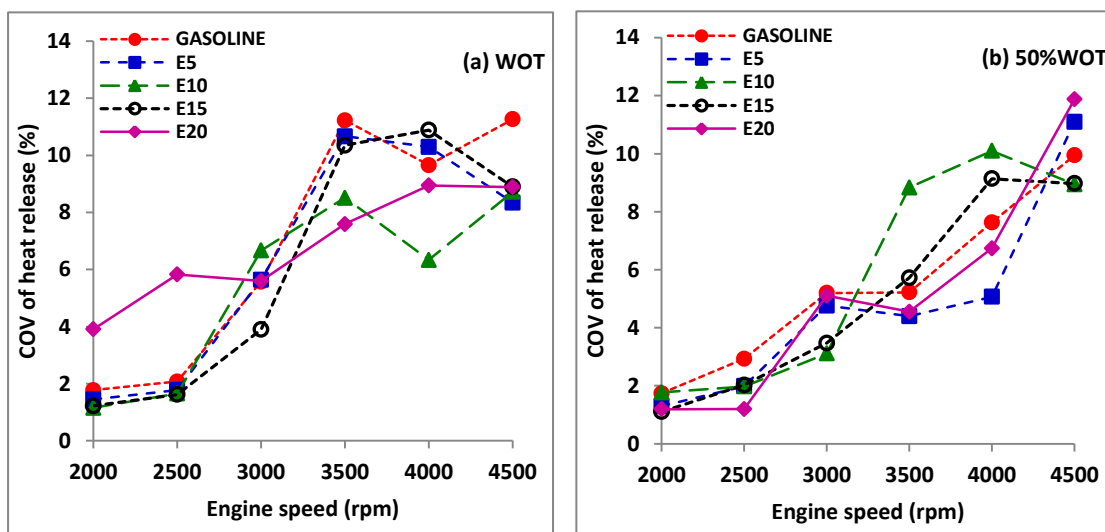


Fig 5.26 COV of heat release per cycle for ethanol blends at (a) WOT and (b) 50% WOT

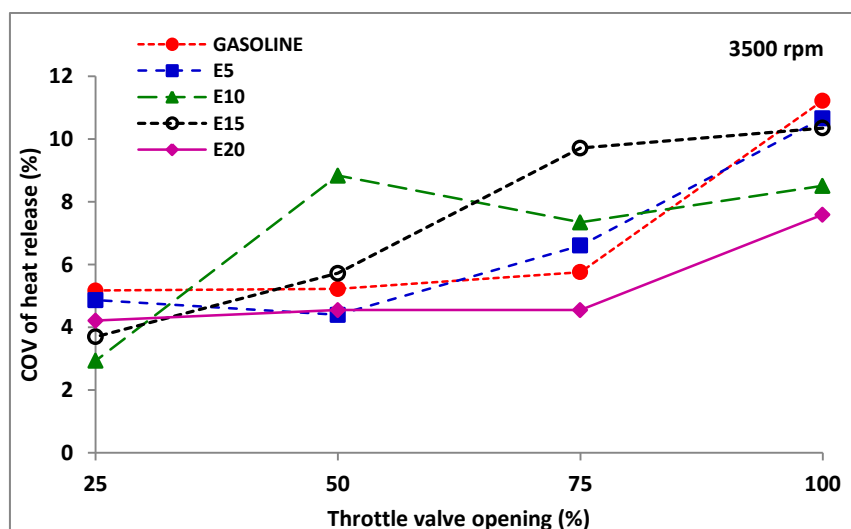


Fig. 5.27 COV of heat release per cycle at 3500 rpm for ethanol blends

The addition of ethanol to gasoline generally reduces the variation of heat release. E15 blend shows consistent better characteristics at lower throttle openings, while E20 at higher throttle openings and speeds more than 3000 rpm. Figure 5.27 shows the COV of heat release per cycle at 3500 rpm for various throttle opening positions.

The time return maps of gross heat release on cycle basis at 3500 rpm for various throttle opening conditions is shown in figure 5.28. At lower throttle opening of 25% and 50%, the gross heat release return maps indicate a more compact pattern. At WOT, the blended fuels have increased the gross heat release, but are more scattered.

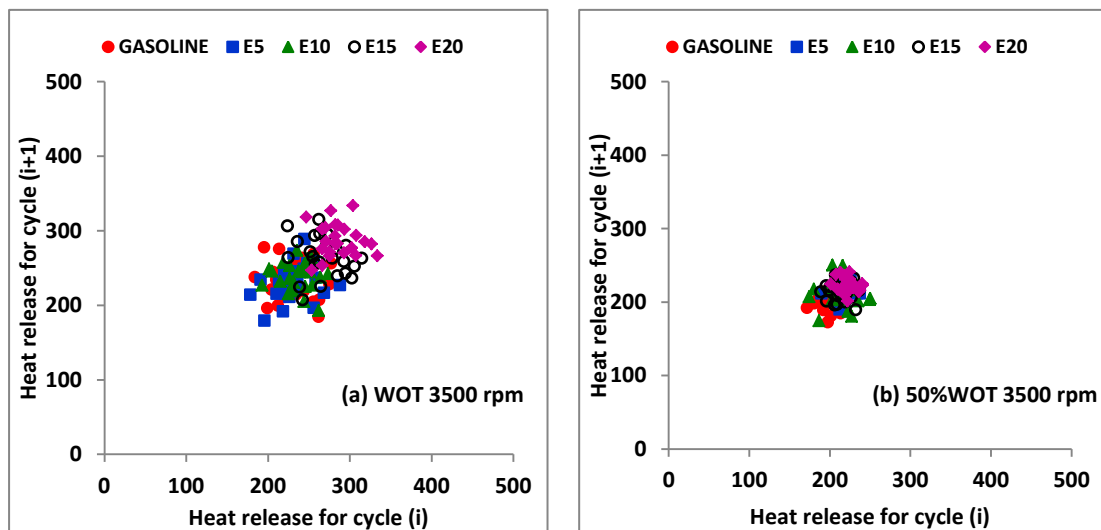


Fig 5.28 Time return map of heat release per cycle for ethanol blends at 3500 rpm, (a) WOT & (b) 50% WOT

### 5.1.10 Carbon monoxide (CO)

The engine exhaust emissions are measured for various fuels at different engine speeds using an AVL exhaust gas analyser. Variation of CO at different operating speed and different throttle valve opening can be observed in the following figures 5.29(a) and (b) respectively for various throttle operations. It is clearly visible that the CO emissions are considerably reduced as compared to the gasoline at all engine speeds and different throttle valve opening conditions. The Oxygen available in the ethanol has led to the better combustion which in turn reduced CO emissions. As the ethanol content increases the CO emission decreases. Figures 5.30 (a) and (b) shows the variation of CO emissions with throttle positions at engine speeds of 3500 rpm

and 4500 rpm respectively. At both the engine operating conditions, CO emissions have reduced comparably. At WOT condition, E15 and E20 blends have improved the combustion which has resulted in CO reduction.

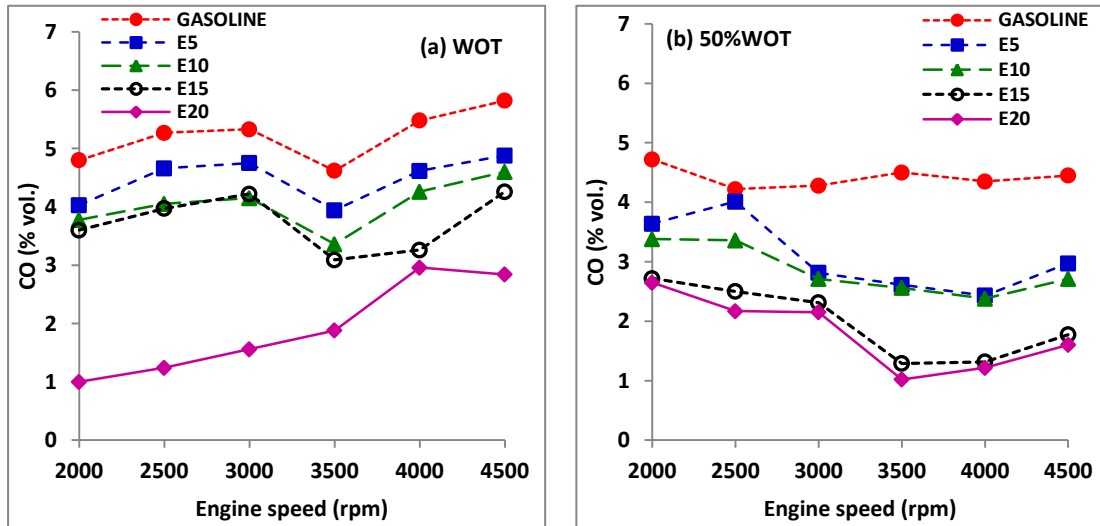


Fig. 5.29 CO with engine speed for ethanol blends at (a) WOT and (b) 50%WOT

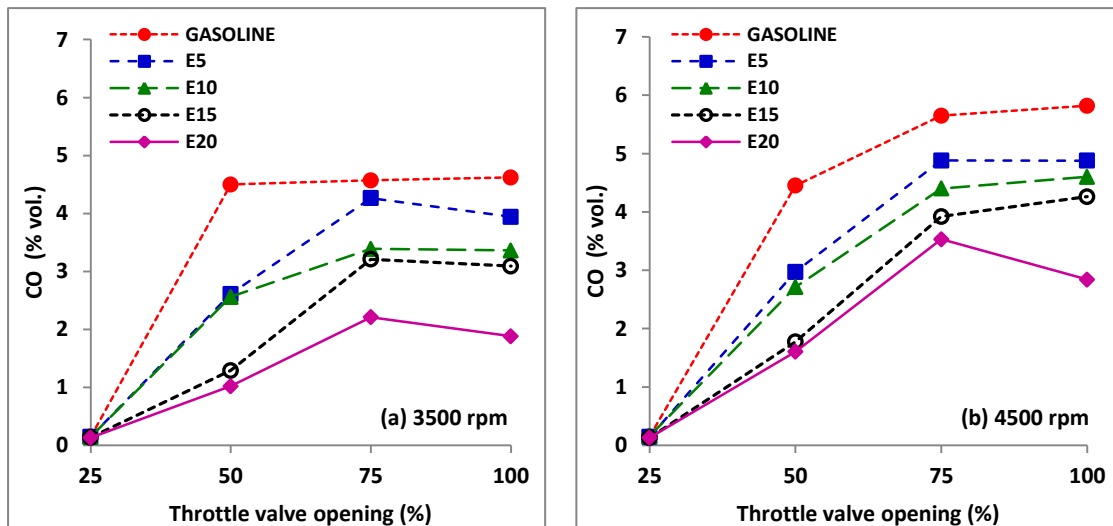


Fig. 5.30 CO with ethanol blends at (a) 3500 rpm and (b) 4500 rpm

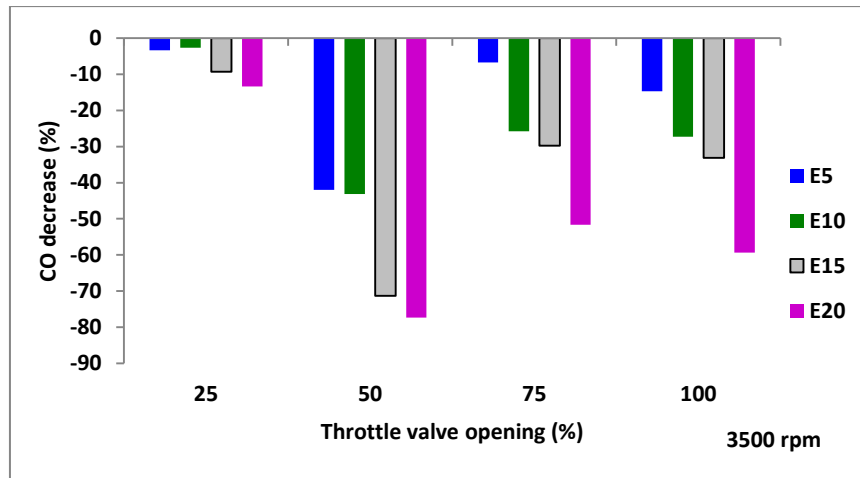


Fig. 5.31 Influence of ethanol blends on CO at 3500 rpm

Figure 5.31 shows the influence of ethanol blending on CO emission decrease at an engine speed of 3500 rpm for different throttle positions. It is found that the reduction of CO emission grows as the ethanol content increases. This indicates that the addition of ethanol can reduce the concentration of CO emission efficiently. The concentration of CO emission can be reduced up to 80% depending on the operating condition of the engine. Maximum reduction in CO with blends is observed at 50% WOT condition.

#### 5.1.11 Hydrocarbon (HC)

Figures 5.32(a) and (b) respectively shows the variation of Hydrocarbon (HC) emissions from the engine in ppm under at WOT and 50%WOT opening conditions. It is observed that the HC emissions have substantially reduced with all the blends compared to that of gasoline for all speeds. Among the blends E15 and E20 showed less emission as compared to gasoline and other blends. This means additional ethanol has led to better combustion of petrol for all operating conditions which resulted in the reduction in HC emissions. This is because of the lean burning with ethanol blending. Lower value of HC emissions was observed at higher operating speeds. At 50%WOT condition, reduction in HC emissions are more pronounced compared to gasoline. E15 and E20 are better blends in the emissions reduction point of view of CO and HC. Figures 5.33(a) and (b) shows the variation of HC emissions with throttle positions at engine speeds of 3500 rpm and 4500 rpm respectively. Figure 5.34 below

shows the influence of ethanol blending on HC emission decrease at an engine speed of 3500 rpm for different throttle positions. It can be observed that increasing the ethanol content, the concentration of HC emission has decreased by 50 to 60% in comparison with pure gasoline at 50% WOT.

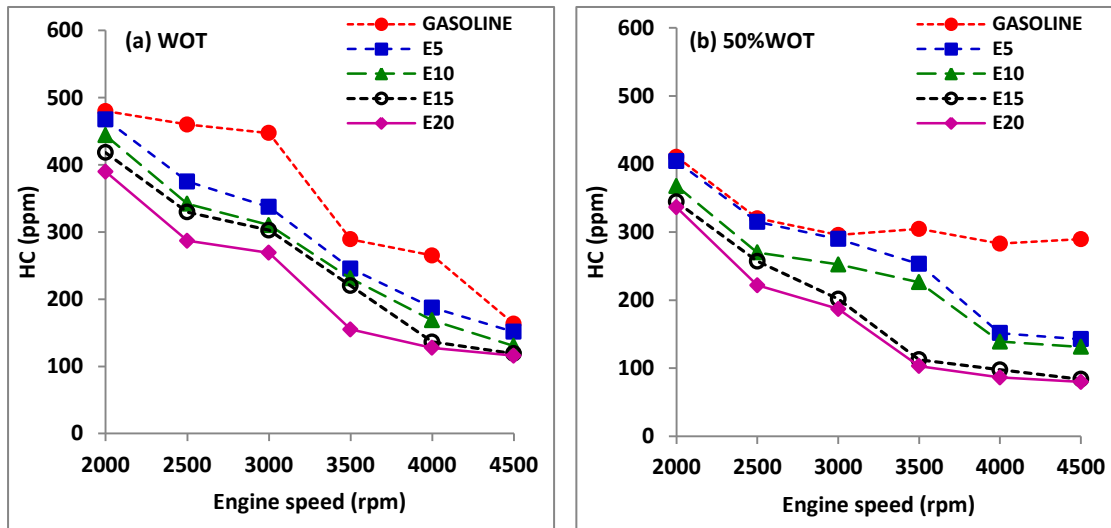


Fig. 5.32 HC with engine speed for ethanol blends at (a) WOT and (b) 50% WOT

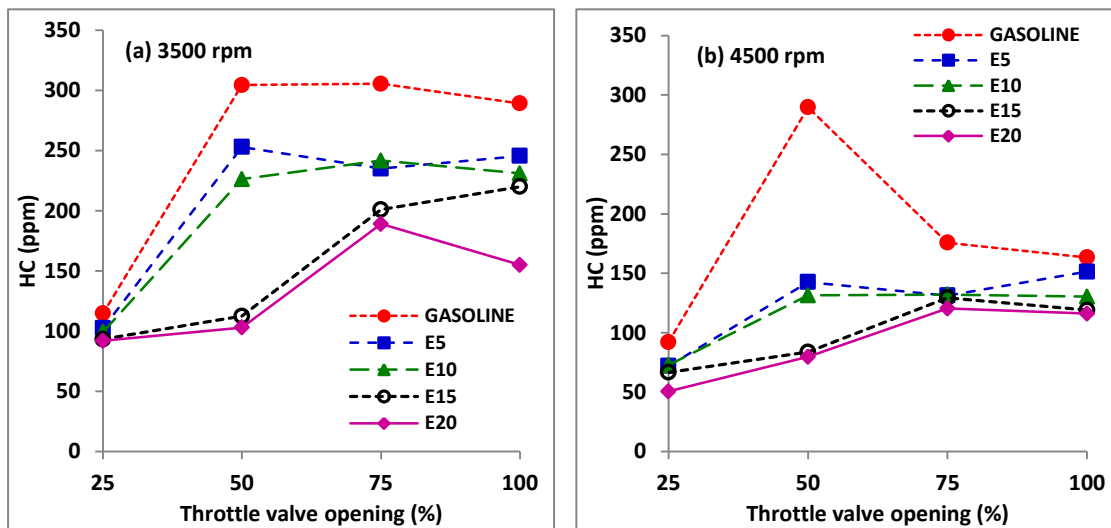


Fig. 5.33 HC with ethanol blends at (a) 3500 rpm and (b) 4500 rpm

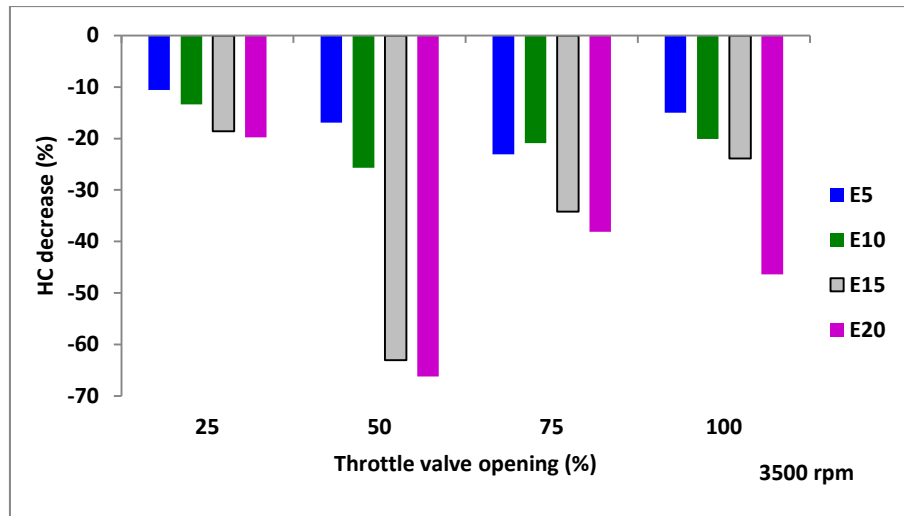


Fig. 5.34 Influence of ethanol blends on HC at 3500 rpm

### 5.1.12 Oxides of Nitrogen (NO<sub>x</sub>)

Variation of NO<sub>x</sub> are shown in the following figures 5.35(a) and (b) at different speeds at WOT and 50%WOT conditions respectively. NO<sub>x</sub> has increased at all operating conditions as NO<sub>x</sub> is the function of temperature. The presence of ethanol in the blend which makes combustion better than gasoline and as a result, the peak temperature increases which in turn increases NO<sub>x</sub> emissions. All the blends showed increase in NO<sub>x</sub> higher the ethanol content better combustion higher the NO<sub>x</sub> emissions.

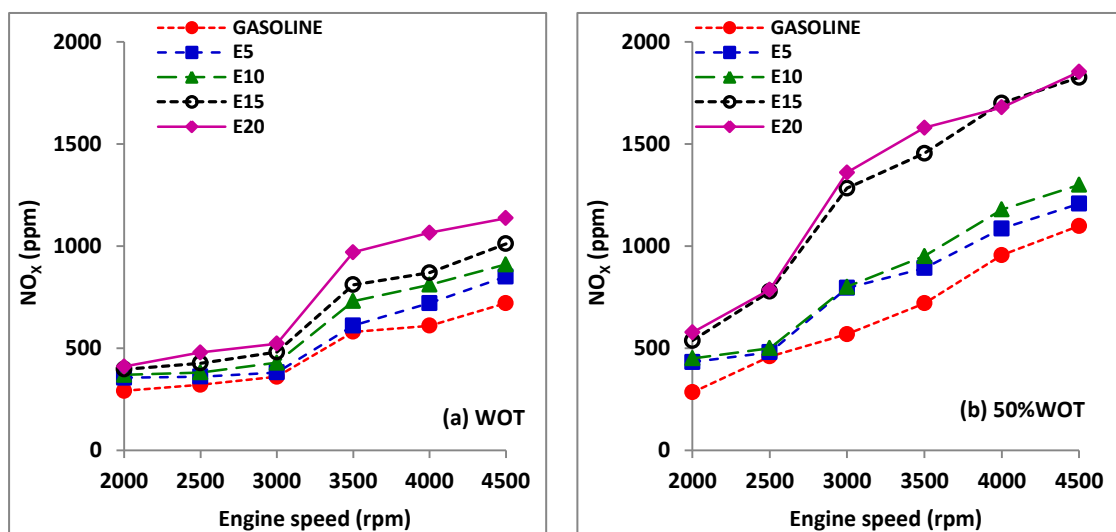


Fig. 5.35 NO<sub>x</sub> with engine speed for ethanol blends at (a) WOT and (b) 50%WOT

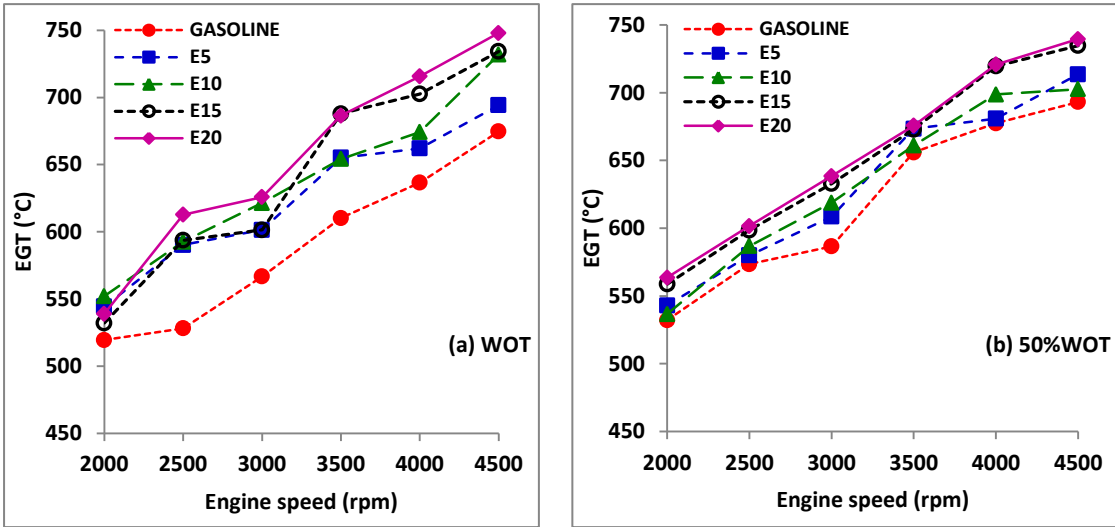


Fig. 5.36 EGT with engine speed for ethanol blends at (a) WOT and (b) 50% WOT

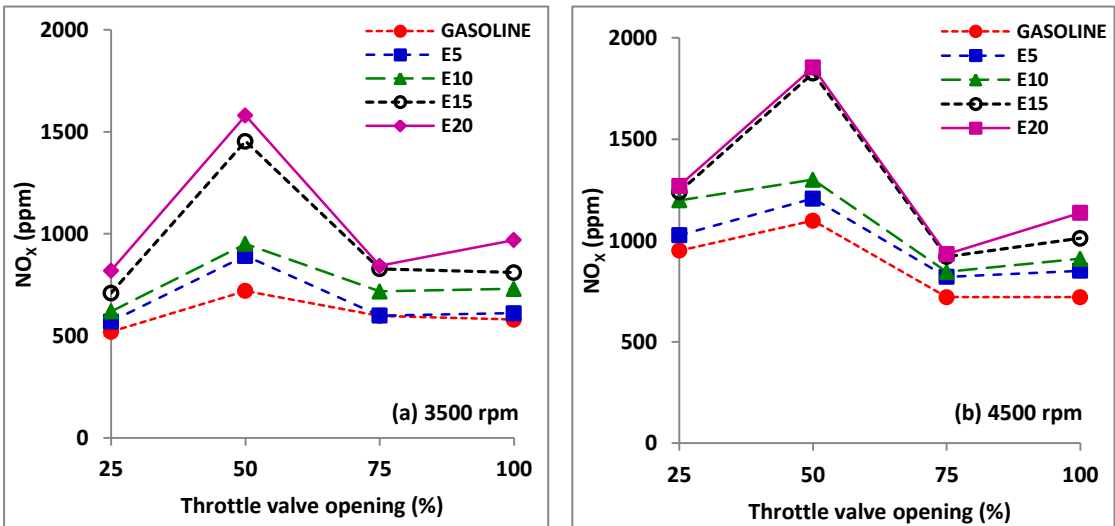


Fig. 5.37 NO<sub>x</sub> with ethanol blends at (a) 3500 rpm and (b) 4500 rpm

These emissions are the only disadvantages of ethanol blended fuel, which is harmful. As the temperature increases NO<sub>x</sub> value increases. The variation of engine exhaust temperature measured at WOT and 50%WOT conditions are shown in figures 5.36(a) and (b) respectively. It is evident that with ethanol blending the combustion temperature hence the exhaust temperature increases. This trend explains the reason for NO<sub>x</sub> increase with ethanol blending. Figures 5.37 (a) and (b) shows the variation of NO<sub>x</sub> emissions with throttle positions at engine speeds of 3500 rpm and 4500 rpm respectively. The emissions at part throttle condition are more concerning than at



WOT. Figure 5.38 shows the influence of ethanol blending on NO<sub>x</sub> emission increase at an engine speed of 3500 rpm for different throttle positions. At 50%WOT condition, ethanol blending has resulted in considerable increase in NO<sub>x</sub> emission, with E20 the value increased by more than 100%. This necessitates some technique to be employed for NO<sub>x</sub> reduction. At WOT condition, E20 blend resulted in about 60% increase in NO<sub>x</sub>.

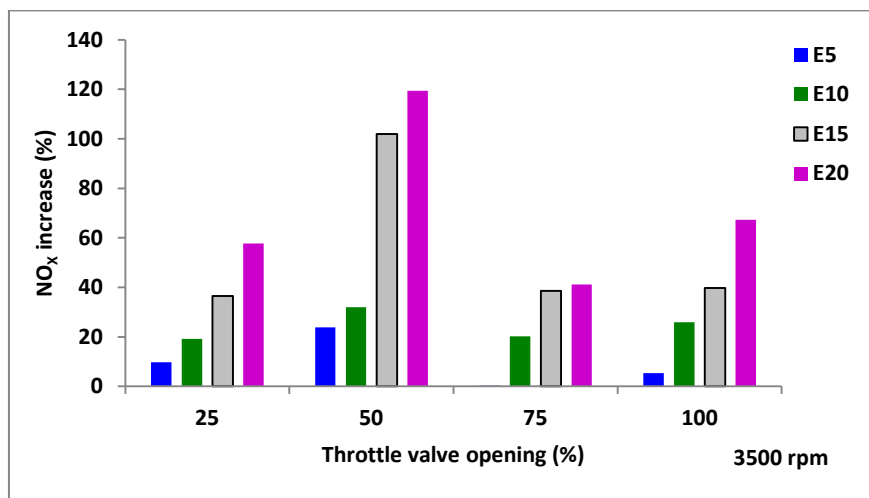


Fig. 5.38 Influence of ethanol blends on NO<sub>x</sub> at 3500 rpm

### 5.1.13 Carbon Dioxide (CO<sub>2</sub>)

Carbon dioxide emissions with engine speeds at WOT and 50%WOT conditions are shown in figures 5.39 (a) and (b) respectively. Due to complete combustion on account of lean burning, it is observed that ethanol blends have resulted in slight increase in CO<sub>2</sub> emission. With increase in ethanol content CO<sub>2</sub> emissions increase with E20 showing maximum of 13.3% at 4500 rpm at WOT condition. At 50%WOT conditions, similar trends are observed, with gasoline showing reduction in CO<sub>2</sub> emissions with increase in speed, while ethanol blends emitting marginally higher CO<sub>2</sub>.

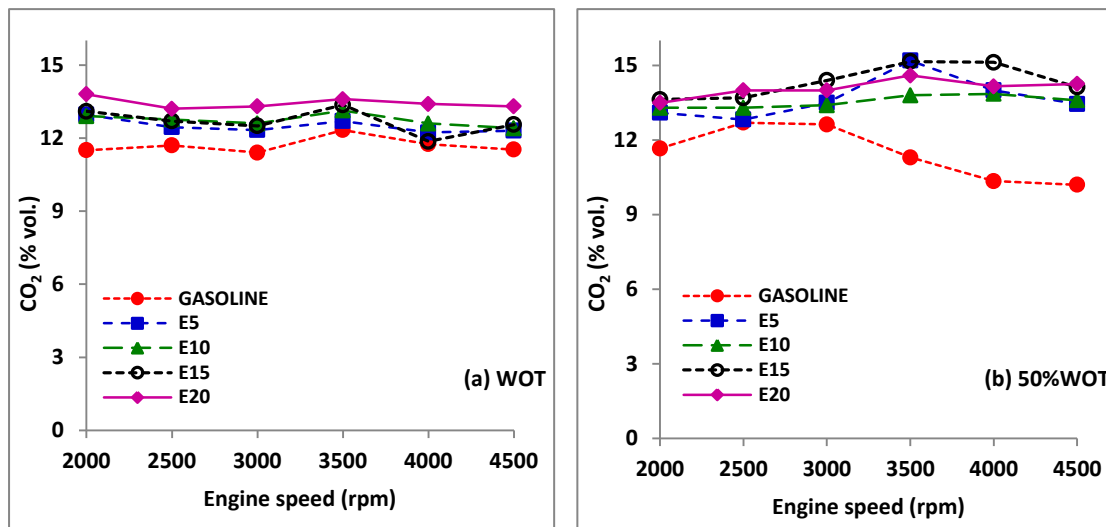


Fig. 5.39 CO<sub>2</sub> with engine speed for ethanol blends at (a) WOT and (b) 50%WOT

The results of the experiments with ethanol enriched gasoline blends can be summarized as follows:

- Results have shown that among the various ethanol enriched gasoline fuel blend E20 was the most suitable one from the engine performance and CO & HC emissions points of view. Hence it can be taken as optimized ethanol enriched gasoline at preset idle ignition timing of 5 deg. bTDC.
- The engine performance has improved with the addition of ethanol, and for E20 at WOT & 3500 rpm, torque increases by 2% and BTE increases by 10.67% when compared to gasoline.
- All the ethanol enriched gasoline fuels have lower COV<sub>IMEP</sub> values compared to gasoline fuel operation. At WOT and 3500 rpm blend E15 shows an average reduction by 2% over the entire speed range.
- Significant reductions in the CO & HC emissions were achieved while the NO<sub>x</sub> emissions have shown an increasing trend with ethanol enriched gasoline fuels. With E20 at WOT & 3500 rpm value of CO has reduced by 59%, HC reduced by 46% and NO<sub>x</sub> increased by 67%.

## 5.2 PERFORMANCE, COMBUSTION AND EMISSION STUDIES OF LPG AT STATIC IGNITION TIMING OF 5 deg. bTDC

In this section the results of engine tests conducted with LPG injection at WOT and 50% WOT condition are presented. Initially the results of the engine test conducted with LPG injection at the preset static ignition timing of 5deg. bTDC at engine speeds of 2000-4500 rpm are given.

### 5.2.1 Torque

The engine torque characteristics with LPG injection at WOT and 50%WOT condition are shown in figures 5.40(a) and (b) respectively. At WOT it can be seen that LPG and gasoline combustion produces near identical torque, but at part throttle operation, LPG has resulted in a lower torque for all the engine speeds. At 50%WOT, the torque trends for both the fuels are dropping with the increase in engine speed.

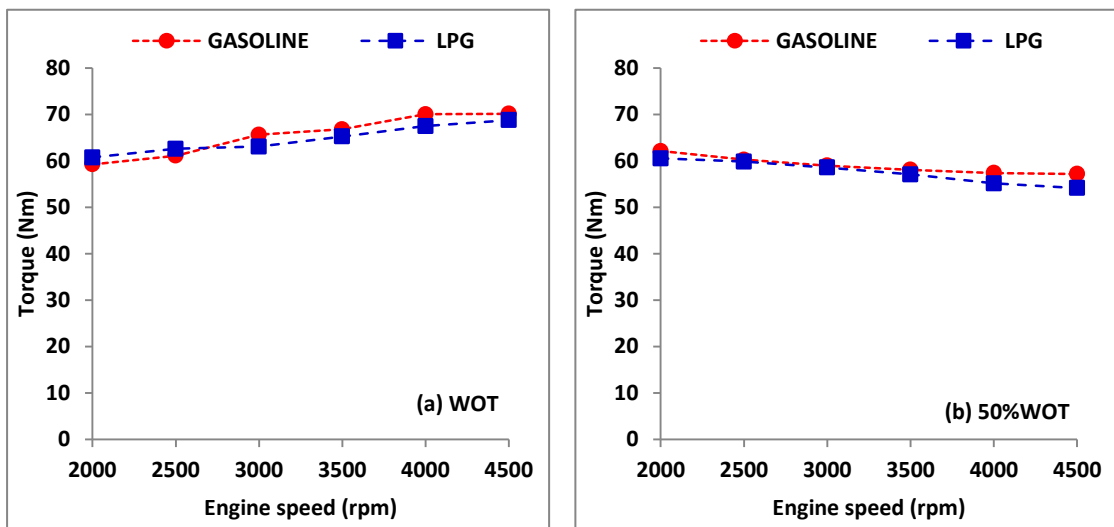


Fig. 5.40 Torque with engine speed for LPG at (a) WOT & (b) 50% WOT

### 5.2.2 Brake power

The variation of brake power with the engine speeds at different throttle valve openings are shown in figures 5.41(a) & (b). At WOT condition, the engine generates constant torque with the increase in engine speed. Hence the brake power increases linearly with engine speeds at higher throttle valve opening position. The influx of fuel is more at wide open throttle compared to part throttles. This results in the higher

power generation with the larger throttle valve openings. LPG produces brake power equivalent to that of gasoline at WOT condition. At part throttle operation, torque and mean effective pressure decreases more rapidly with increasing speeds. This may be attributed to the reduced air flow in to the cylinder as the throttle area is reduced. The pumping component of total friction also increases as the engine is throttled, thus decreasing the mechanical efficiency (Heywood 1988). At 50%WOT, at higher engine speed, the brake power produced by LPG drops slightly when compared to gasoline.

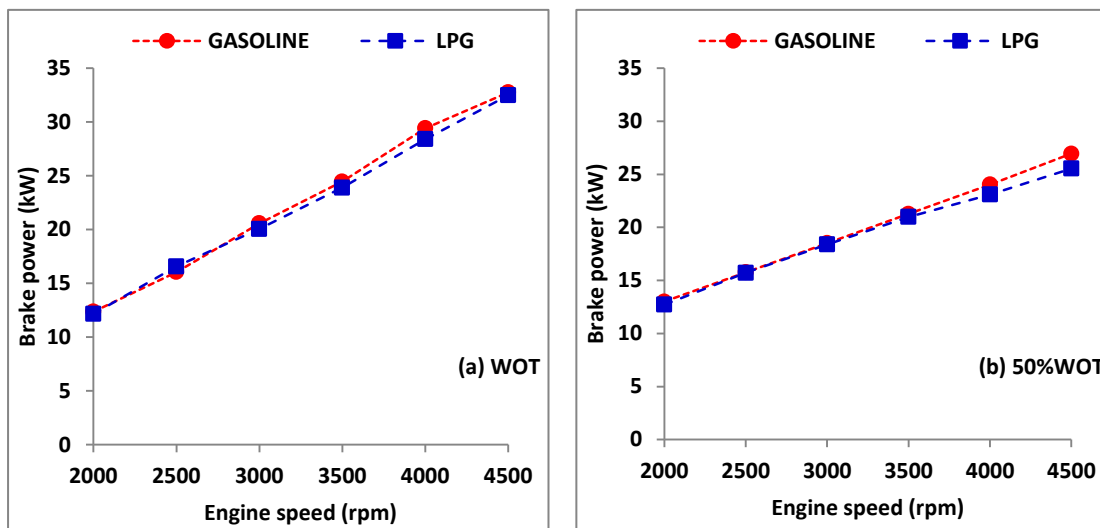


Fig. 5.41 Brake power with engine speed for LPG at (a) WOT & (b) 50%WOT

### 5.2.3 Brake thermal efficiency (BTE)

The variation of brake thermal efficiency (BTE) for gasoline and LPG fuels at WOT and 50%WOT operating condition are shown in figures 5.42 (a) and (b) respectively. It can be observed that at WOT, the brake thermal efficiency is more for gasoline at lower speeds. LPG combustion exhibits higher thermal efficiency than gasoline after 3500 rpm. Since the ignition temperature of LPG is higher than that of gasoline, ignition delay and thus combustion duration is more for LPG (Ceviz 2005) which decreases the average burning rate. To contain this effect, the fuel consumption of the engine increases which in turn decreases the thermal efficiency at lower engine speeds. At higher engine speeds, the higher flame propagation speed of LPG negates the effect of ignition temperature. Here the time duration for each cycle is very low which demands more rate of combustion to get the complete combustion of the fuel.

The lower propagation speeds of gasoline flames cannot afford the requisite combustion rate; instead the engine takes more fuel to generate the required torque. The collective outcome of these factors lowers brake thermal efficiency of the engine for gasoline at higher engine speeds. The highest BTE of 31.36% is achieved at 3500 rpm for LPG at WOT condition. The 50%WOT trends of BTE show that gasoline combustion has resulted in higher brake thermal efficiency for the entire operating speed range with near constant BTE of 30% for speeds of 3000-4000 rpm. The LPG thermal efficiency at 50%WOT is similar to the WOT trend, with maximum BTE of 29.84% at 3500 rpm.

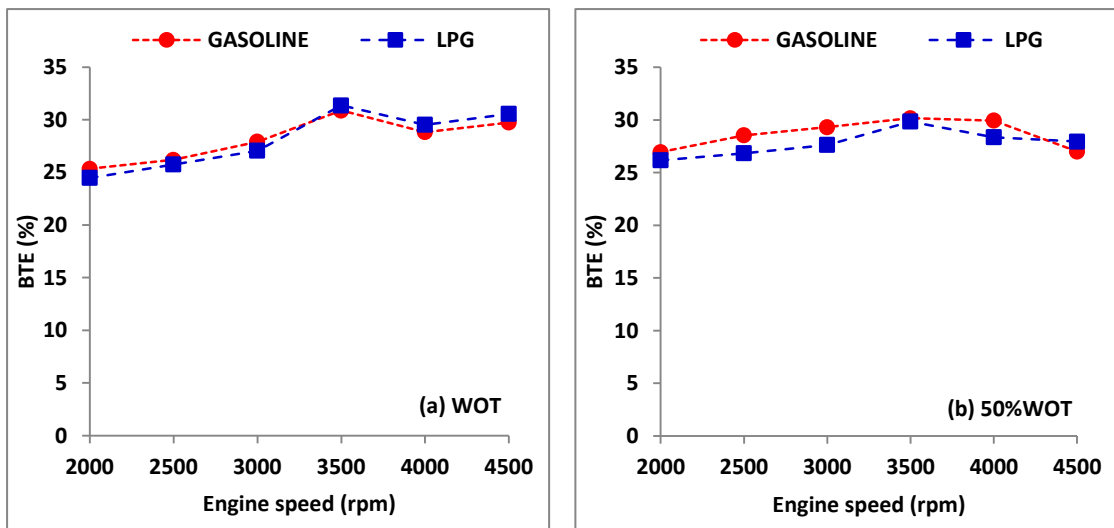


Fig. 5.42 BTE with engine speed for LPG at (a) WOT & (b) 50%WOT

#### 5.2.4 Brake specific energy consumption (BSEC)

Brake specific energy consumption of LPG and gasoline at various throttle opening conditions are shown in figures 5.43(a) & (b). At higher throttle valve openings, the BSEC of LPG is lower than that of gasoline at higher engine speeds. This could be a result of the higher flame propagation speed and better miscibility of gaseous LPG with the air. The equivalence ratio is too lean at lower engine speed for both fuels which decreases its burning rate. The higher combustion duration demands more quantity of fuel for LPG. Hence LPG has lower BSEC at lower engine speeds. At 50% WOT; the BSEC of gasoline is lower throughout the speed range when compared to LPG.

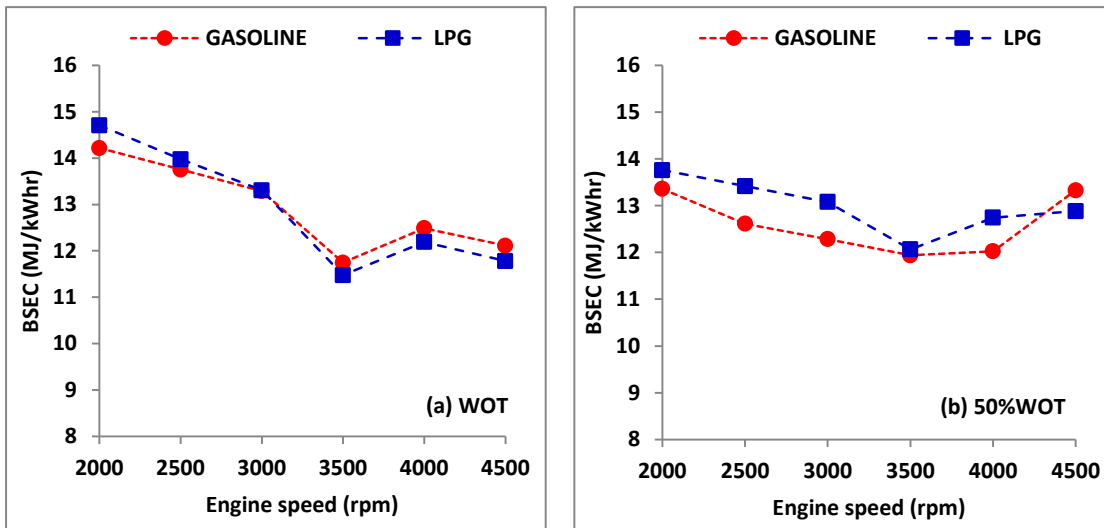


Fig. 5.43 BSEC with engine speed for LPG at (a) WOT & (b) 50% WOT

### 5.2.5 Indicated Mean Effective Pressure(IMEP)

Figures 5.44 (a) and (b) shows the variations of IMEP at different engine speeds at WOT and 50%WOT conditions respectively. The indicated mean effective pressure developed by the engine remains constant at higher throttle valve opening positions.

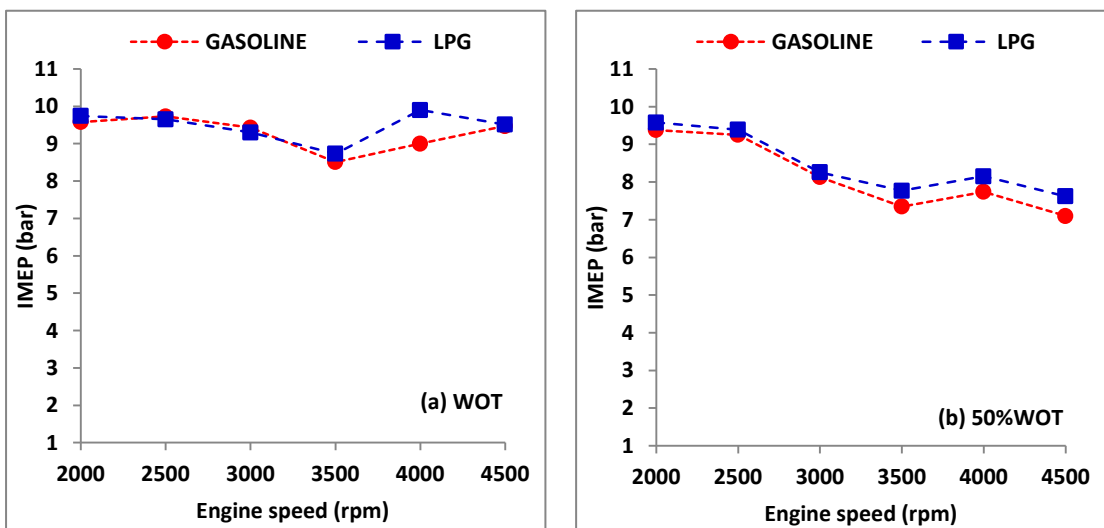


Fig. 5.44 IMEP with engine speed for LPG at (a) WOT & (b) 50% WOT

It can be observed that LPG fuel combustion develops slightly lower IMEP at lower engine speeds and marginal increased IMEP at higher engine speeds compared to gasoline fuel combustion. As the variation in IMEP is marginal, the engine doesn't

suffer much power loss. Minimum IMEP for both the fuels occur at 3500 rpm. At WOT the average IMEP for LPG is 9.5 bar. The trends of 50%WOT indicate that IMEP drops with increase in engine speed.

The time return maps of IMEP for successive combustion cycles with LPG combustion has been shown in figures 5.45 (a) & (b) for various throttle valve openings at 3500 rpm. The IMEP developed by the engine with LPG is higher than that for gasoline at higher throttle openings. At WOT, the map reveals that LPG combustion has resulted in increased variation than gasoline IMEP. At 50%WOT condition the combustion with LPG has stabilized as the grouping of IMEP is symmetric. At lower throttle openings the IMEP with LPG combustion shows a circular pattern with inconsistent IMEP development. From these maps it can be inferred that LPG use at part load conditions are far better with smooth combustion with increased IMEP. At WOT however the variations are higher, which may result in knocking combustion.

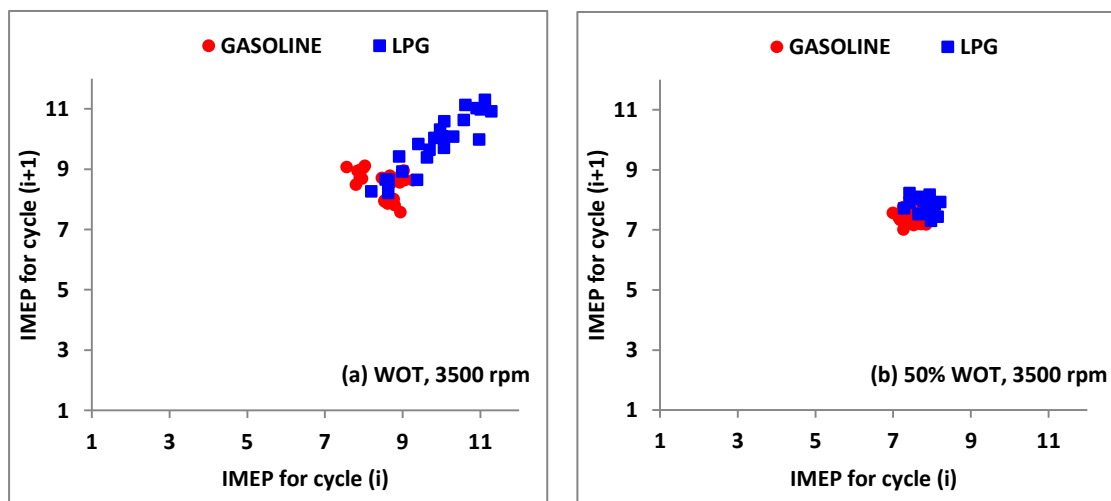


Fig. 5.45 Time return map of IMEP for LPG at 3500 rpm at (a) WOT & (b) 50%WOT

The coefficient of variation of IMEP (COV of IMEP) plots with engine speeds for various throttle openings are shown in figures 5.46 (a) & (b). The combustion variations are higher with LPG with COV of IMEP reaching as high as 12% at speed range of 3000-3500 rpm at WOT. The part throttle variations of COV of IMEP for LPG and gasoline are comparable, indicating stable operating zone. At 50%WOT condition, stable combustion at higher speeds is resulted with LPG. Figure 5.47 show

the COV of IMEP trends for 3500 rpm at various throttle openings. Part throttle combustion variations with LPG are 3% while that for gasoline are also in the same range. At WOT, the COV of IMEP has doubled with LPG.

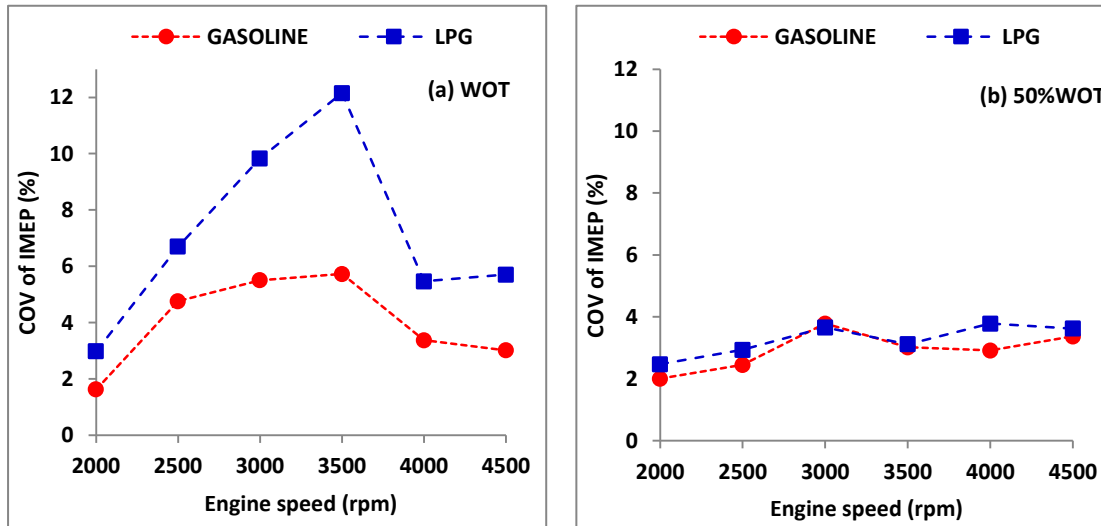


Fig. 5.46 COV of IMEP for LPG at (a) WOT & (b) 50%WOT

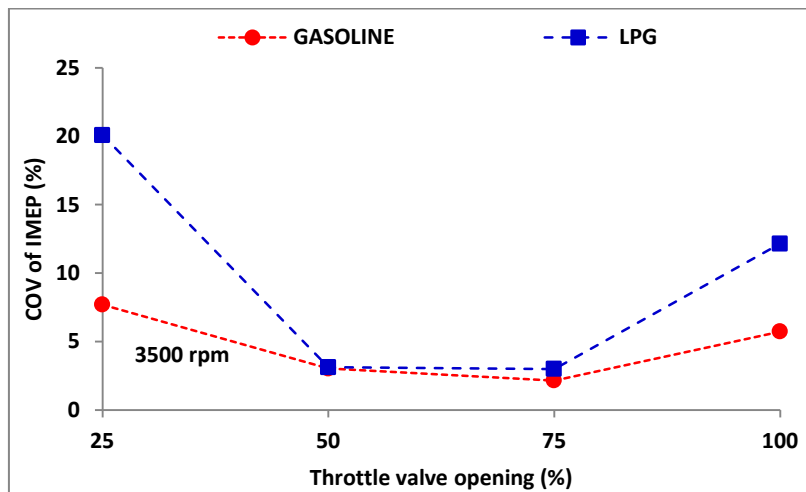


Fig. 5.47 COV of IMEP for LPG at 3500 rpm and different throttle valve openings

### 5.2.6 Heat release rate analysis

The gross heat release per cycle has been computed based on the pressure - crank angle data for LPG and presented in the form of time return maps in figures 5.48 for (a) & (b) 3500 rpm at various throttle openings. The heat release with LPG is on the higher side to that of gasoline. At WOT condition for LPG the average heat release is



300 J/cycle for where as for gasoline the mean heat release is 250 J/cycle. At 50% WOT condition both the fuels have released same amount of heat explaining the similar powers developed.

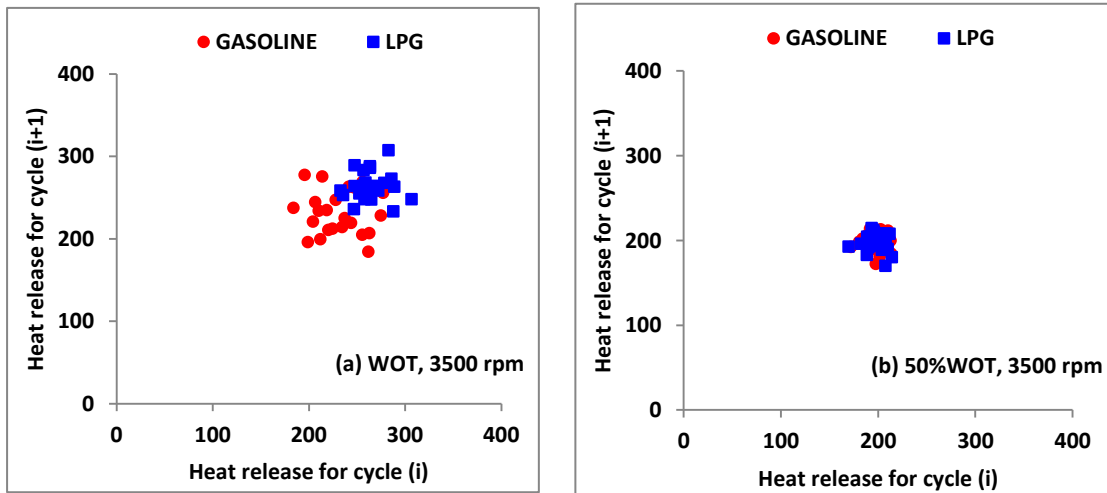


Fig. 5.48 Time return map of heat release per cycle for LPG at 3500 rpm at (a) WOT & (b) 50% WOT

The COV of heat release /cycle has been shown in figures 5.49 (a) & (b) at 3500 rpm & different throttle openings. This plot reveals that variation in heat release rate with LPG is lower when compared to that with gasoline at different throttle openings. At WOT in the operating range of 3500 to 4500 rpm LPG combustion has a constant COV of about 6%. At 50%WOT also LPG combustion has stabilized in this speed range.

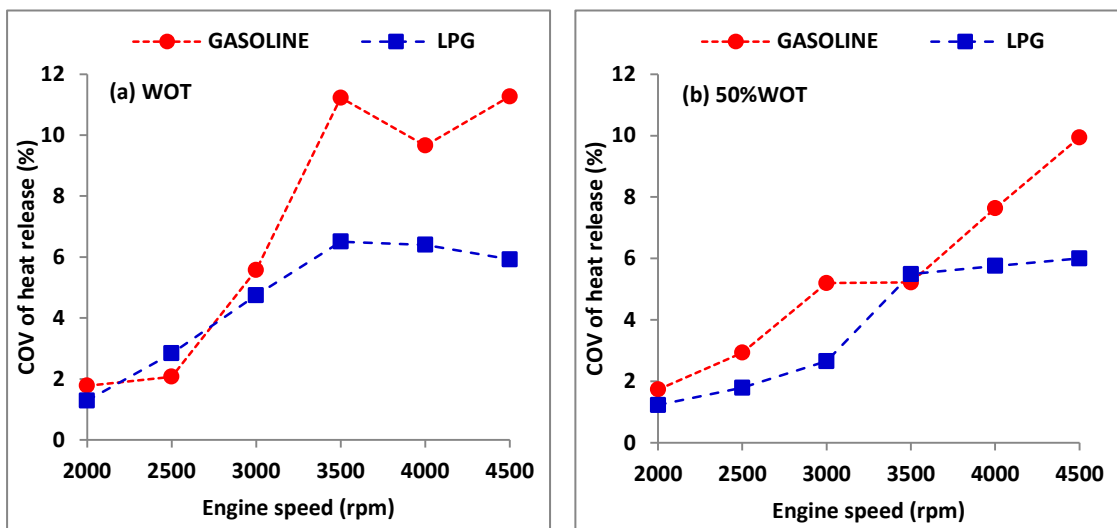


Fig. 5.49 COV of heat release per cycle for LPG at (a) WOT & (b) 50% WOT

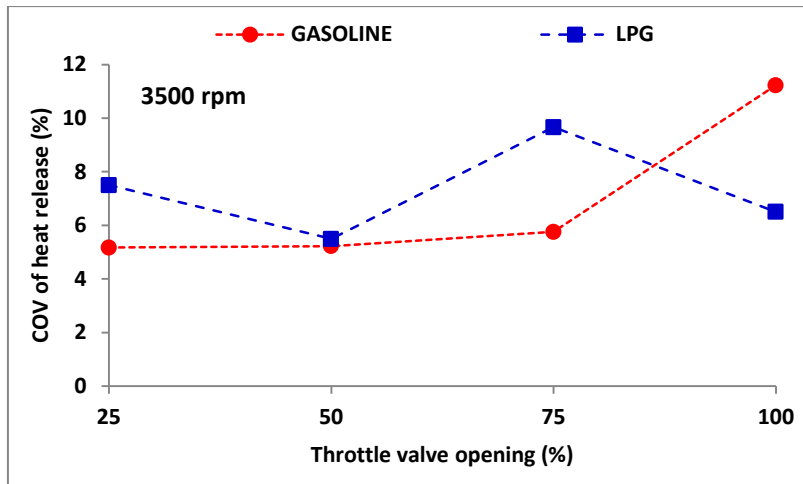


Fig. 5.50 COV of heat release per cycle for LPG at 3500 rpm and different throttle valve openings

The COV of gross heat release per cycle at 3500 rpm at various throttle openings are shown in figure 5.50. It can be observed that at 75%WOT condition the COV of heat release for LPG is comparatively higher than that for gasoline. But the average COV is lower than that for gasoline.

### 5.2.7 Carbon monoxide (CO)

The variation of carbon monoxide (CO) emission with speed at WOT and 50% WOT conditions are shown in figures 5.51 (a) & (b) respectively. It is observed that CO emissions with LPG are far less than that with gasoline. The CO emissions are reduced from an average value of 5.2% to 1.33% with the use of LPG compared to that with gasoline. For LPG, at all throttle positions the CO emissions is found to be less than 2% which is well within the limits of EURO V pollution norms. The higher flame propagation speed and better mixing of gaseous LPG with the air enhances the combustion and thus reduces the CO emissions. At wide throttle valve opening positions, the total quantity of air and fuel which is inducted into the engine is more than that of half or quarter throttle positions. The lower combustion duration at higher engine speeds is not sufficient for the complete combustion of fuel. As a result of this, CO emissions increase at higher engine speeds for gasoline. But with LPG being in homogeneous mix with air, the CO sharply decreases with increase in engine speed.

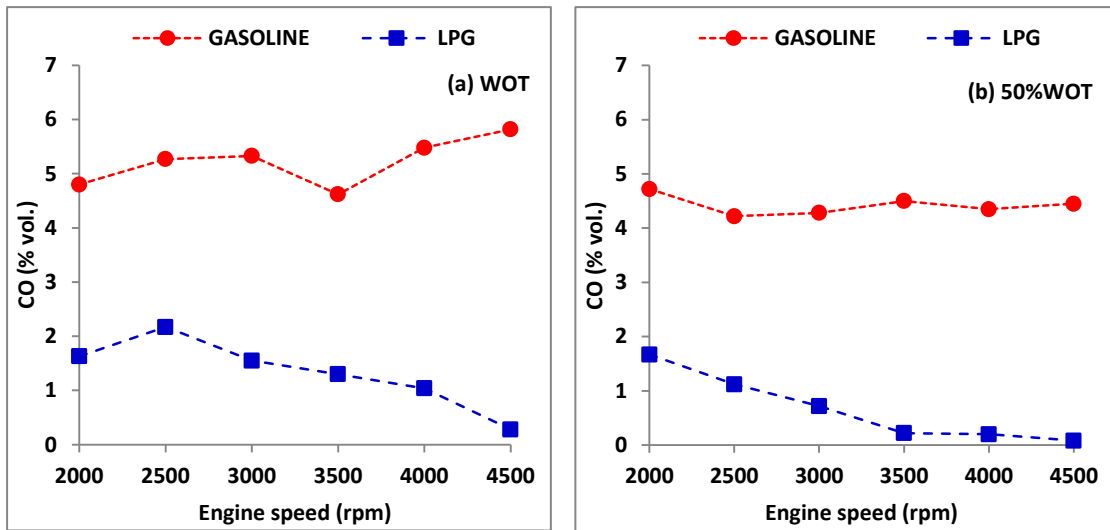


Fig. 5.51 CO with engine speed for LPG at (a) WOT & (b) 50%WOT

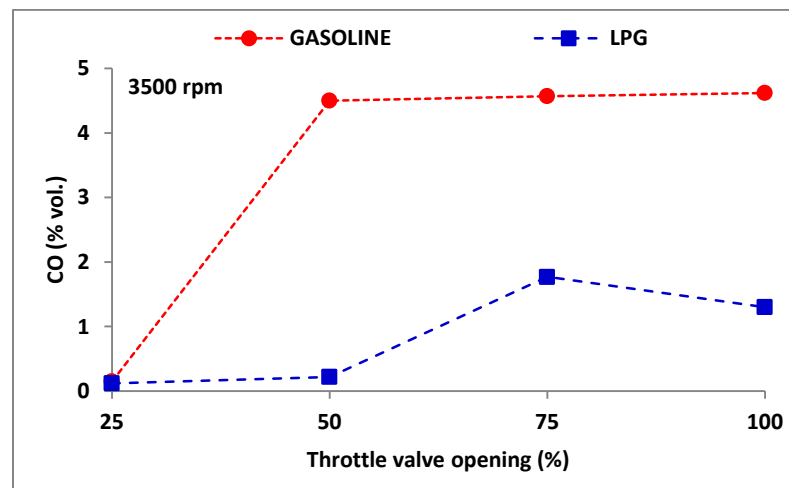


Fig. 5.52 CO at different throttle valve openings for LPG at 3500 rpm

The CO variation with different throttle openings at 3500 rpm as shown in figure 5.52 indicate that very low CO emissions can be achieved with LPG, which is one of the highlight of LPG applications in ultra low emission vehicles. At less that 50%WOT conditions the CO emissions are near zero with LPG.

## 5.2.8 Hydrocarbon (HC)

Figures 5.53 (a) & (b) depicts the variation of un-burnt hydrocarbon emissions with engine speed at different throttle openings. Contrary to gasoline which shows a drastic reduction trend of HC as the engine speed increases, HC emissions with LPG are almost constant. LPG combustion results in drastic reduction in HC emissions when

compared to gasoline values at all the operating speeds. Enhanced oxidation of unburned HC within the cylinder and in exhaust pipe line at higher speeds may be the reason for the gasoline HC emission trend, since expansion and exhaust stroke gas temperatures increases significantly due to reduced heat transfer.

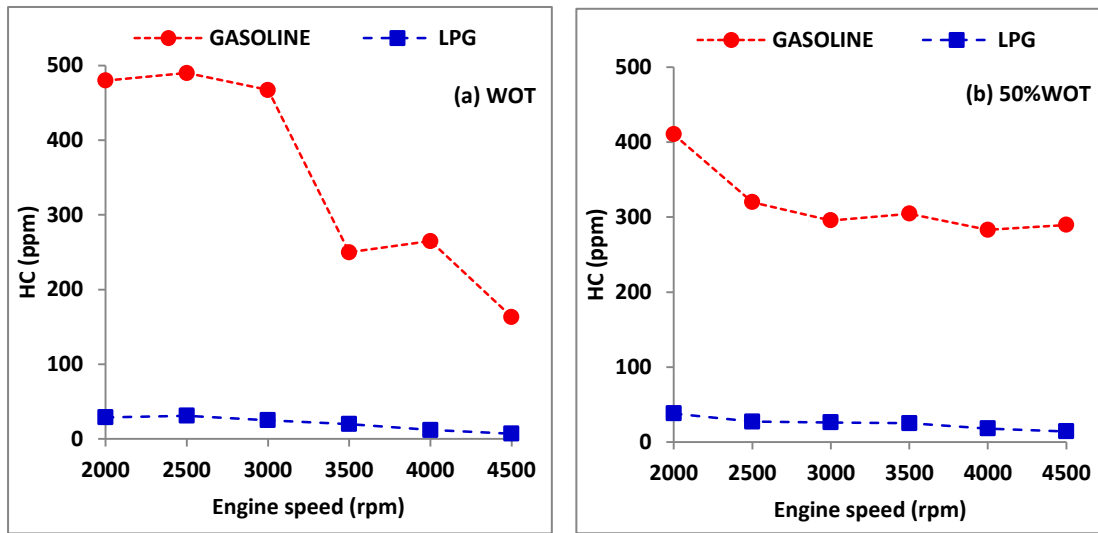


Fig. 5.53 HC with engine speed for LPG at (a) WOT & (b) 50%WOT

Complete combustion due to homogeneous mixture formation might have resulted in almost 95% reduction in HC emissions when compared to gasoline. Substantial reductions in HC emission at all throttle open conditions as confirmed by figure 5.54 at 3500 rpm is one of the reason for LPG being the choice of a clean burning alternative fuel.

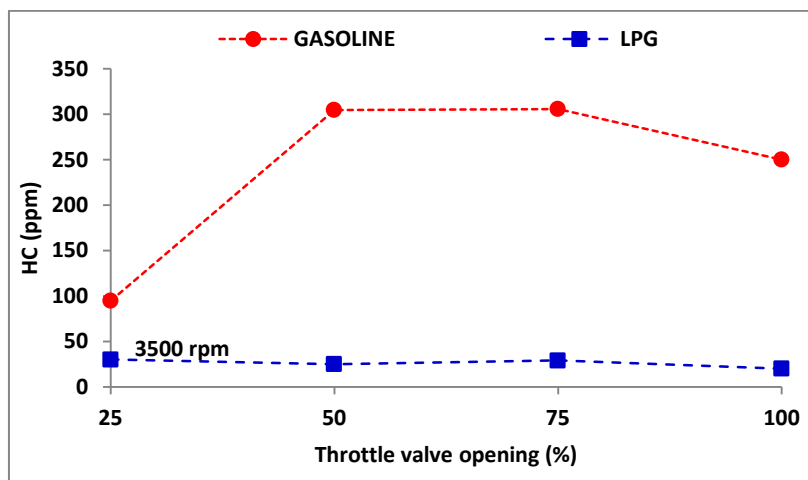


Fig. 5.54 HC at different throttle valve openings for LPG at 3500 rpm

### 5.2.9 Oxides of Nitrogen (NO<sub>x</sub>)

The variation of NO<sub>x</sub> at different engine speeds with various throttle opening is shown in figures 5.55(a) & (b) respectively. Generally as the engine speed increases the NO<sub>x</sub> emissions also show an increasing trend. But LPG combustion results in more elevated NO<sub>x</sub> emissions compared to gasoline at higher engine speeds after 3500 rpm. Higher flame propagation speed of LPG at higher engine speeds where the equivalence ratio reaches stoichiometric value, and proper mixing of gaseous fuels with air causes an increase in the burning rate of the fuel and thus results in the complete combustion of the fuel. Hence the cylinder pressures and combustion temperatures of LPG are higher than those obtained for gasoline. As a final outcome of this, more NO<sub>x</sub> emissions occur in LPG combustion at higher speeds. The value of NO<sub>x</sub> emission of LPG is almost double the emission of gasoline at all throttle positions at a speed of 4500 rpm. The reason for lower NO<sub>x</sub> emissions for gasoline and LPG at lower engine speeds may be attributed to lower peak combustion temperature due to too lean mixtures as it might result in quenching effect. Fig. 5.56 indicates the NO<sub>x</sub> emissions at 3500 rpm with various throttle openings. The adverse effect of NO<sub>x</sub> is more pronounced at part load operation, where it reaches almost three times higher level when compared to gasoline operation.

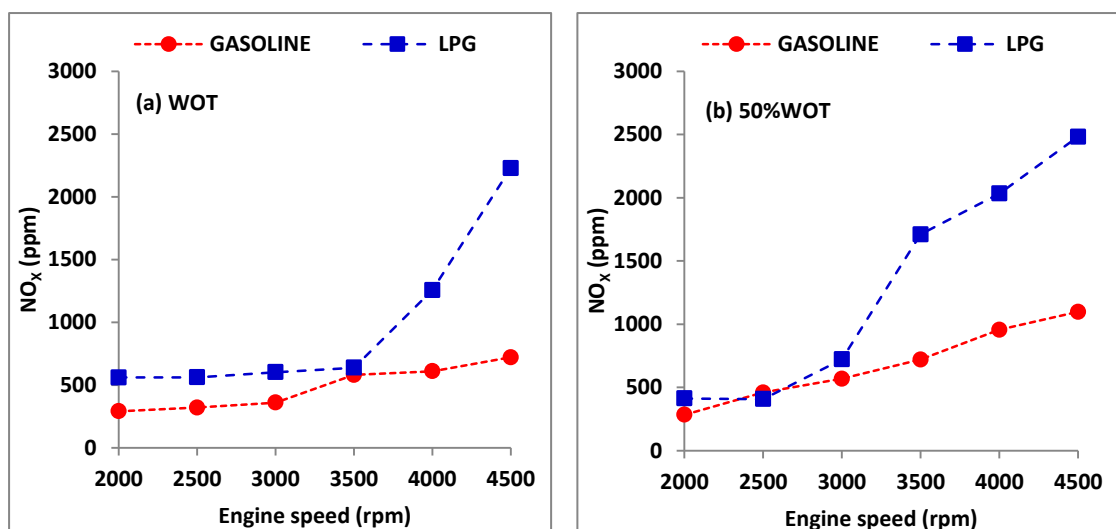


Fig. 5.55 NO<sub>x</sub> with engine speed for LPG at (a) WOT & (b) 50%WOT

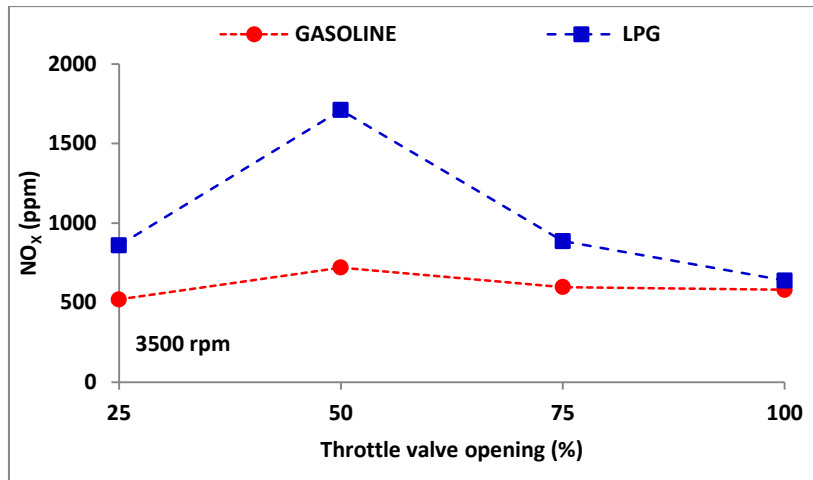


Fig. 5.56 NO<sub>x</sub> at different throttle valve openings for LPG at 3500 rpm

From the results of the experiments with LPG at preset static ignition timing of 5 deg. bTDC it is observed that there is reduction in the brake thermal efficiency at lower engine speeds compared to gasoline. The engine exhaust emissions of CO and HC are very much reduced. In fact this is the major factor for advocating the use of LPG as an alternative SI engine fuel. But it is observed that the NO<sub>x</sub> emissions have increased steeply at higher engine speeds and at 4500 rpm NO<sub>x</sub> emission with LPG has increased by two folds compared to that for gasoline.

- At pre set static ignition timing of 5 deg. bTDC at WOT condition, brake thermal efficiency is more for gasoline at lower engine speeds and it is more for LPG at higher engine speeds.
- The CO emission has reduced from an average value of 5.2% to around 1.33% and corresponding change in HC is noticed was from 350 ppm to 21 ppm when LPG is used instead of gasoline.
- The NO<sub>x</sub> emission with LPG is more than double when compared to that with gasoline at higher engine speeds.

To investigate the possibility of improving the thermal efficiency at lower engine speeds experiments are conducted with LPG at various static ignition timings other than preset static ignition timing of 5 deg. bTDC.

### 5.3 LPG PERFORMANCE, COMBUSTION AND EMISSIONS AT VARIOUS STATIC IGNITION TIMINGS

To unearth the possibilities of enhancing the performance of LPG at lower engine speeds, experiments have been conducted at different static ignition timings. The different static ignition timings set for LPG are 3, 4 and 6 deg. bTDC. Performances are found to be reducing drastically at 3 deg. bTDC and tendency of knocking was observed when ignition timing was set above 6deg. bTDC. Hence experimental studies on performances and emission characteristics of LPG at different static ignition timings are limited to the range of 3 to 6 deg. bTDC.

#### 5.3.1 Torque

The variation of torque at WOT and 50%WOT conditions at various static ignition timings are shown in figure 5.57 (a) and (b). It is observed that retarded timings have resulted in reduction of torque, while advancing to 6 deg. bTDC has increased the torque. At both the operating conditions 6 deg. bTDC has resulted in increase of torque at lower speeds. But at 50%WOT as the speed is increased the torque output is reduced when compared to preset timing.

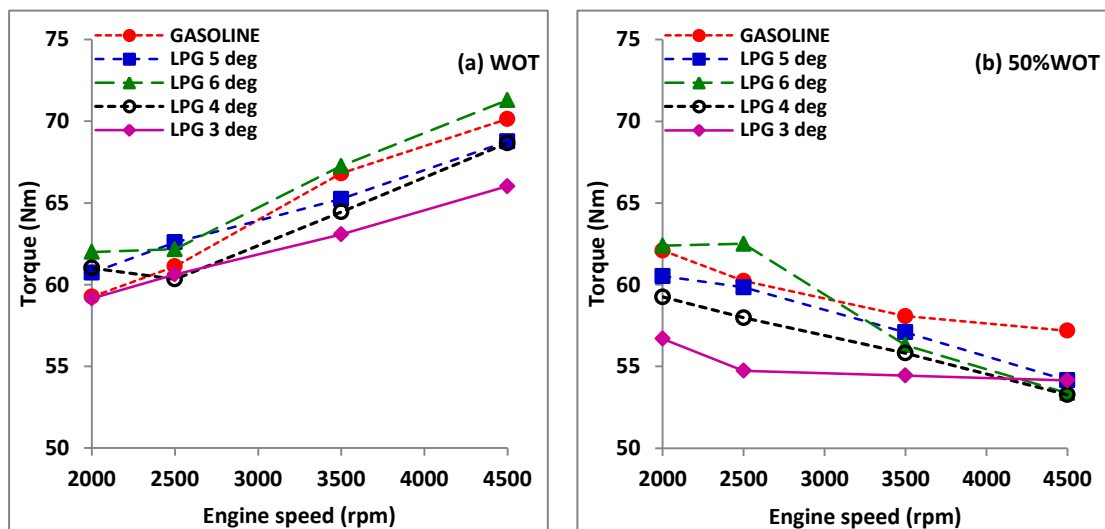


Fig. 5.57 Torque with engine speed for LPG at 5, 6, 4 & 3 deg. bTDC, (a) WOT & (b) 50%WOT

#### 5.3.2 Brake thermal efficiency (BTE)

Figures 5.58 (a) & (b) shows the variations of the brake thermal efficiency with engine speed for various ignition timings at WOT and 50%WOT respectively. Advancing the ignition timing increases the combustion duration which helps to overcome the effect of ignition delay. This enhances the cylinder pressure and power output at lower engine speeds. Hence efficiency is highest for 6 deg. bTDC at lower engine speeds. The equivalence ratio is nearly stoichiometric at higher engine speeds at all ignition timings. At higher engine speeds, the high propagation speeds of LPG flames allow the fuels to burn with high rate of combustion. Hence at higher engine speeds, the efficiency is more or less same irrespective of the ignition timing. The observations from the graph show that the combustion of fuel with 6 deg. bTDC provides the maximum average efficiency over the given range of engine speeds.

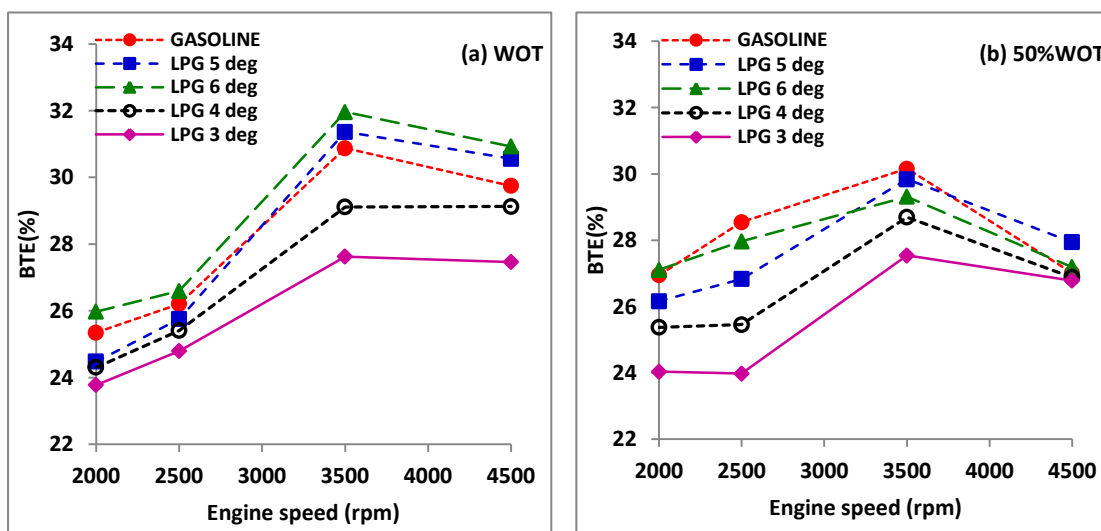


Fig. 5.58 BTE with engine speed for LPG at 5, 6, 4 & 3 deg. bTDC, (a) WOT & (b) 50%WOT

### 5.3.3 Brake specific energy consumption (BSEC)

The variation of BSEC with engine speeds at various ignition timings is depicted in figures 5.59 (a) & (b) at different throttle opening conditions. The incomplete combustion of fuels results in the higher specific energy consumptions for 3 deg. bTDC and 4 deg. bTDC. The optimal energy consumption can be achieved by running the engine at 3500 rpm with ignition timing being set at 6 deg. bTDC. This is also valid in comparison with gasoline at WOT.



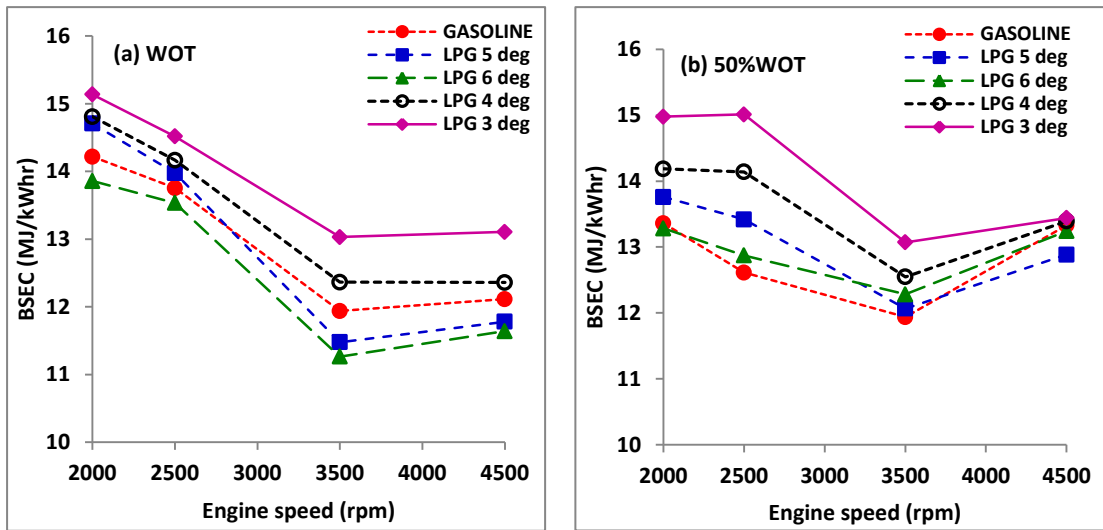


Fig. 5.59 BSEC with engine speed for LPG at 5, 6, 4 & 3 deg. bTDC, (a) WOT & (b) 50% WOT

### 5.3.4 Indicated Mean Effective Pressure (IMEP)

The indicated mean effective pressure generated by the engine will remain constant for a particular throttle valve position. The figure 5.60 shows the general trend in the variations of IMEP at different engine speeds at (a) WOT & (b) 50%WOT. The time return map of IMEP at WOT and 50%WOT is shown in fig. 5.61. At WOT the LPG combustion at advanced ignition timing shows better grouping. But at 50%WOT condition, preset ignition timing results in better combustion.

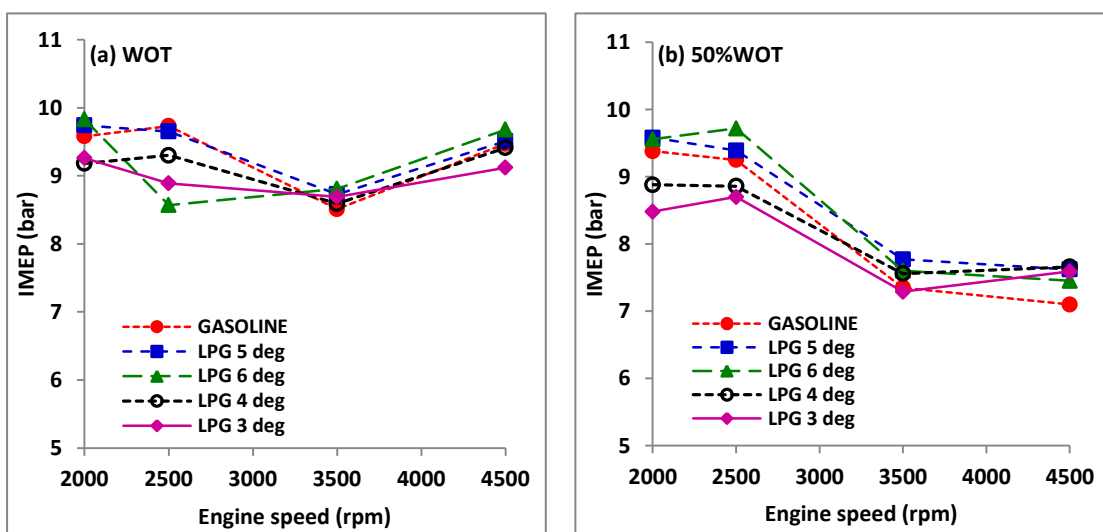


Fig. 5.60 IMEP with engine speed for LPG at 5, 6, 4 & 3 deg. bTDC, (a) WOT & (b) 50% WOT

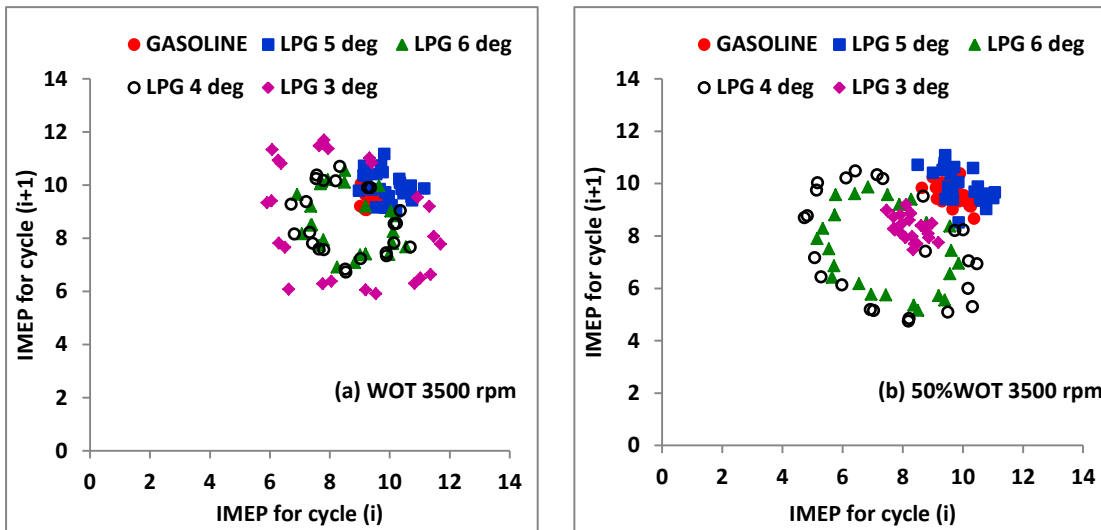


Fig. 5.61 Time return map of IMEP for LPG at 5, 6, 4 & 3 deg. bTDC, 3500 rpm, (a) WOT & (b) 50% WOT

At WOT condition the IMEP return map shows that changing the static ignition timing from the preset timing results in scattered pattern. This might result in unstable power output at these operating conditions. Similar trends are observed at 50%WOT also.

The COV of IMEP with various engine speeds at WOT and 50%WOT are shown in figures 5.62 (a) and (b) respectively. At WOT condition, advancing the ignition timing has reduced the combustion fluctuations in the operating speed range.

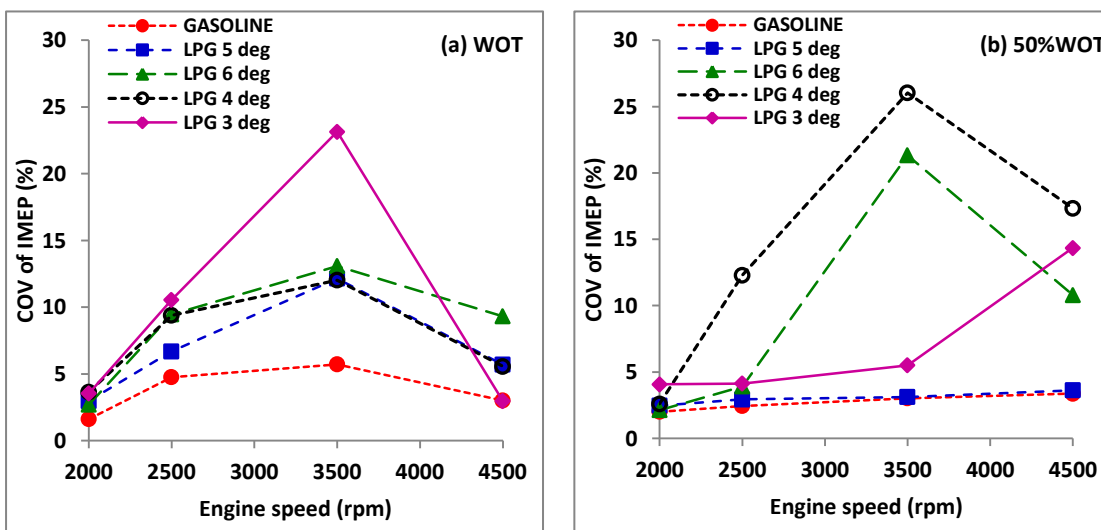


Fig. 5.62 COV of IMEP for LPG at 5, 6, 4 & 3 deg. bTDC, (a) WOT & (b) 50% WOT

At 3500 rpm & 6 deg. bTDC, the COV of IMEP for LPG is 13% when compared to gasoline it is higher by 7%. At 50%WOT condition changing the static timing adversely effects the combustion as the COV of IMEP increases steeply.

### 5.3.5 Equivalence ratio

Figures 5.63 (a) & (b) indicate the variations of equivalence ratio of LPG and gasoline at various static ignition timings. This equivalence ratio will determine the weather engine is working in leaner, stoichiometric or richer mixture. As the engine speed increases the equivalence ratio will also increases for both gasoline and LPG. At higher throttle valve openings, equivalence ratio for LPG will be lower than that of gasoline at all speeds. The equivalence ratio is lean for gasoline in the lower speed range but beyond speed of 2500 rpm it is rich mixture and richest mixture at 4500 rpm. This is because to get maximum power for a given volumetric efficiency is obtained with rich-of-stoichiometric mixture. But equivalence ratio for LPG is leaner in the speed range of 2000 rpm to 4000rpm and at 4500rpm it is just above stoichiometric mixture. Advancing the static timing has resulted in leaning the mixture throughout the speed range at WOT condition.

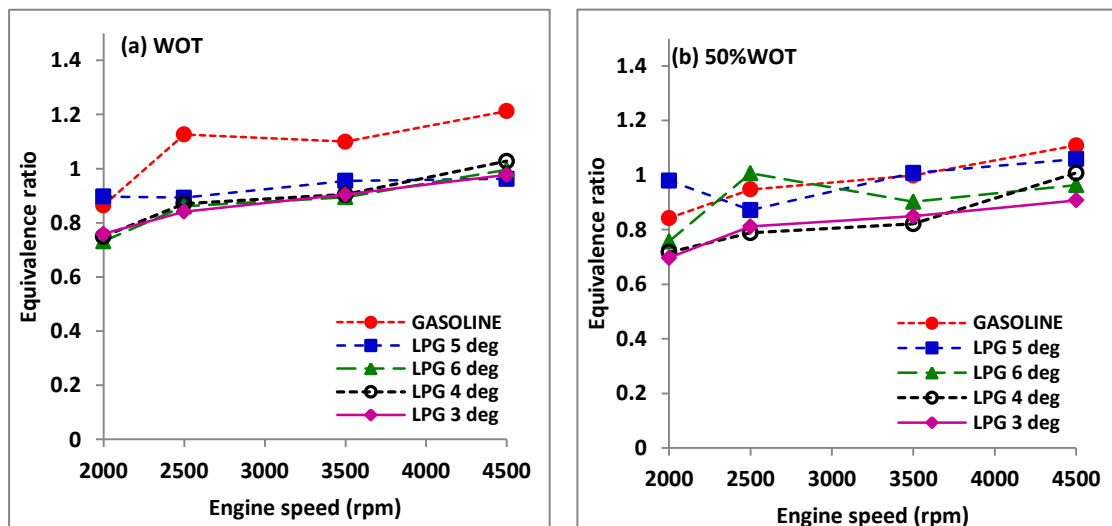


Fig. 5.63 Equivalence ratio for LPG at 5, 6, 4 & 3 deg. bTDC, (a) WOT & (b) 50% WOT

### 5.3.6 Heat release analysis

The time return map of gross heat released per cycle has been shown in figures 5.64(a) & (b) for WOT and 50%WOT condition. It indicates with 6 deg. bTDC ignition timing the heat release per cycle is more consistent. At 50%WOT condition the LPG combustion at 3 deg. bTDC is showing good grouping.

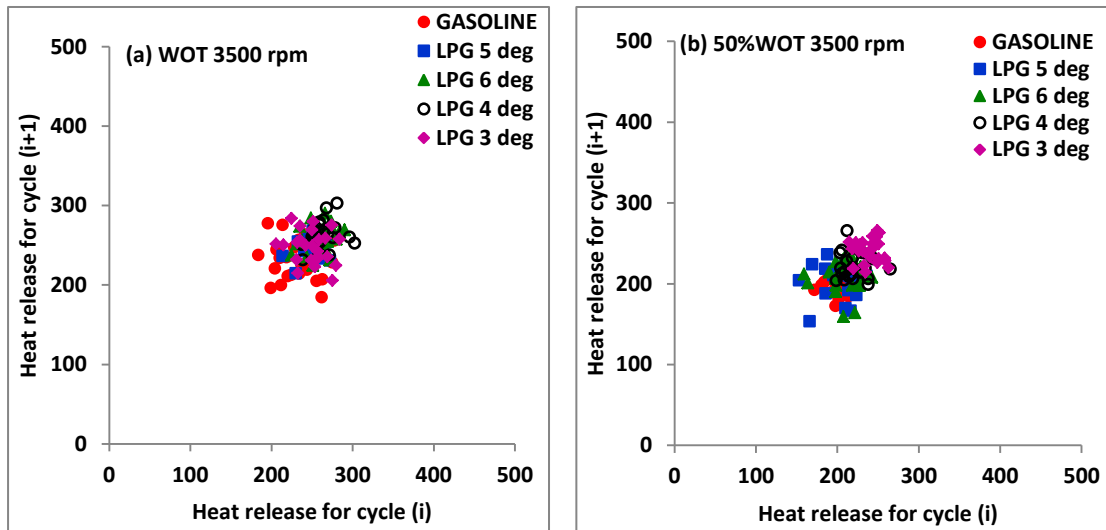


Fig. 5.64 Time return map of heat release per cycle for LPG at 5, 6, 4 & 3 deg. bTDC, 3500 rpm, (a) WOT & (b) 50%WOT

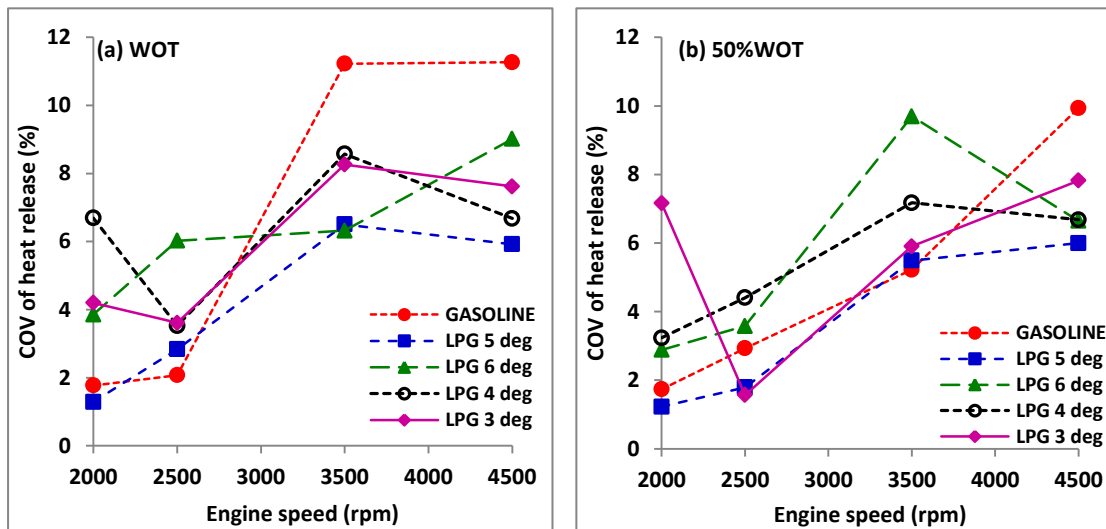


Fig. 5.65 COV of heat release per cycle for LPG at 5, 6, 4 & 3 deg. bTDC, (a) WOT & (b) 50%WOT

The COV of heat release per cycle at WOT and 50%WOT for LPG at different ignition timings are shown in figures 5.65(a) and (b) respectively. At WOT the trends

suggests that advancing the static timing reduces the COV, while at 50%WOT the same condition yields COV less than that for preset timing at lower engine speeds.

### 5.3.7 Carbon monoxide (CO)

The trends of CO emissions of LPG at various static ignition timings are shown in the figures 5.66 (a) & (b) at WOT and 50%WOT condition respectively. The combustion of fuel primarily depends on two factors. Air-fuel ratio being the first and flame speed is the other one. A fine trade-off between these two factors gives better results. At lower engine speeds, equivalence ratio is too lean at all throttle positions which results in complete combustion of the fuel and hence CO emissions are less. As speed increases air-fuel ratio increases and hence the CO emissions increase. At higher engine speeds, equivalence ratio is stoichiometric and hence flame propagation speed is higher. The high flame propagation speed results in complete combustion of fuel and thus engine produces very low values of CO emissions. This trend can be observed at higher engine speeds at half throttle. At wider throttle valve opening positions, the total quantity of air and fuel which is inducted into the cylinder is more than that of half or quarter throttle positions.

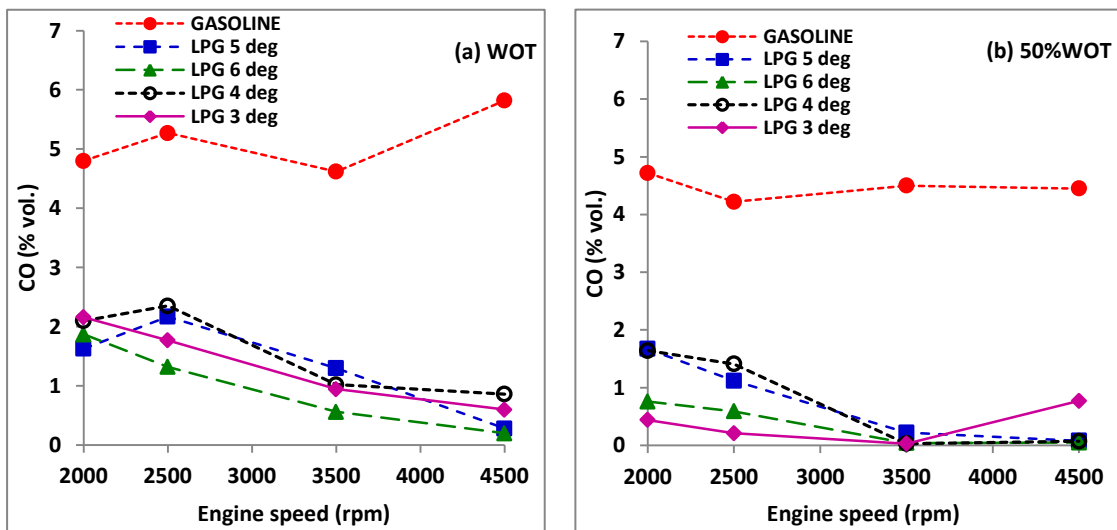


Fig. 5.66 CO for LPG at 5, 6, 4 & 3 deg. bTDC, (a) WOT & (b) 50%WOT

The lower combustion duration at higher engine speeds is not sufficient for the complete combustion of fuel. As a result of this, CO emissions increase at higher engine speeds. Retarding the ignition timings enhances the chances of incomplete

combustion which increases the CO emissions. Hence higher CO emissions are observed at 3 deg. bTDC and 4 deg. bTDC. The effective combustion may be the reason for reduced CO emissions when the static ignition timing is advanced to 6 deg. bTDC.

### 5.3.8 Hydrocarbon (HC)

Figures 5.67(a) & (b) depicts the variation in hydrocarbon emissions at various static ignition timing at WOT and 50%WOT. When engine runs with 6 deg. bTDC, combustion duration is more. This increases the chances of complete combustion and thus reduces the HC emissions. Hence HC emissions are found to be less when static ignition timing is set at 6 deg. bTDC. The incomplete combustion of fuel results in the higher emissions of hydrocarbons at 3 deg. bTDC and 4 deg. bTDC static ignition timings. The highest HC emissions are observed when ignition timing is set at 3 deg. bTDC. As the speed increases, both equivalence ratio and flame propagation speeds also increases. At lower engine speeds, the effect of flame propagation speed is less which results in incomplete combustion. Hence HC emission increases at lower engine speeds. The high flame propagation speeds at higher engine speeds drive the engine to complete combustion and thus reduces the HC emissions.

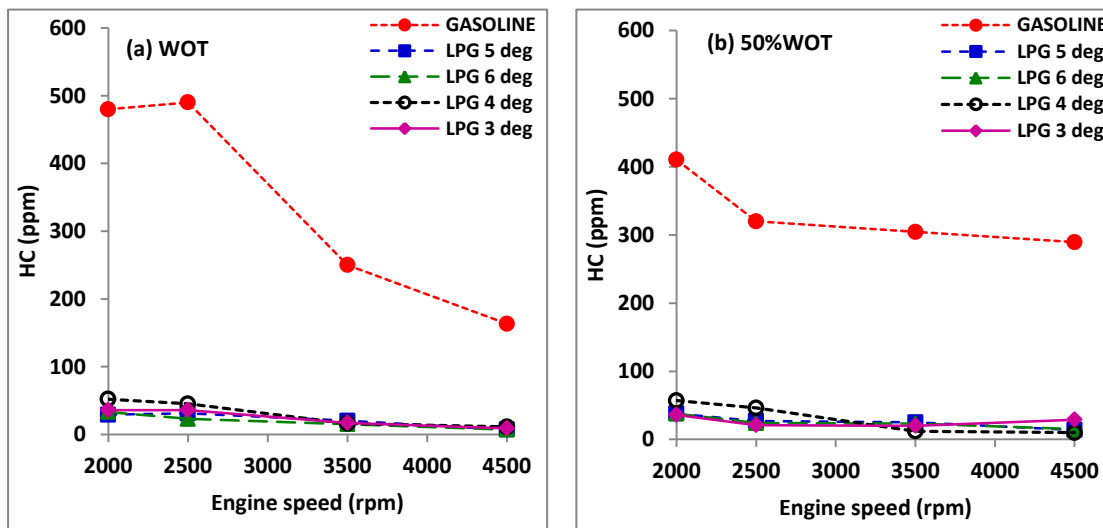


Fig. 5.67 HC for LPG at 5, 6, 4 & 3 deg. bTDC, (a) WOT & (b) 50%WOT

### 5.3.9 Oxides of Nitrogen (NO<sub>x</sub>)

Variation of NO<sub>x</sub> with engine speeds at various static ignition timing at WOT and 50%WOT are shown in figures 5.68 (a) & (b) respectively. At lower engine speeds

mixture is lean for all throttle positions. Hence at lower rpm, combustion of fuel remains same irrespective of the ignition timings and so is the case of combustion temperature. The combustion temperature at lower engine speeds is low at all throttle valve positions. As the engine speed increases, the air-fuel ratio of the mixture gradually increases and eventually becomes stoichiometric. LPG has higher flame speed at stoichiometric ratio than that at lean mixture. Since  $\text{NO}_x$  is a function of temperature, its value increases with engine speed and is highest at 4500 rpm for all operating conditions. As the ignition timing retards afterburning increases at higher rpm which lower the value of combustion temperature. The lower value of  $\text{NO}_x$  emission at 3 deg. bTDC attributes to its lower value of combustion temperature due to incomplete combustion. It can be observed that at wide open throttle, the value of  $\text{NO}_x$  emission for 4500 rpm at 6 deg. bTDC is around 2800 ppm where as it is nearly 1600 ppm at 3 deg. bTDC.

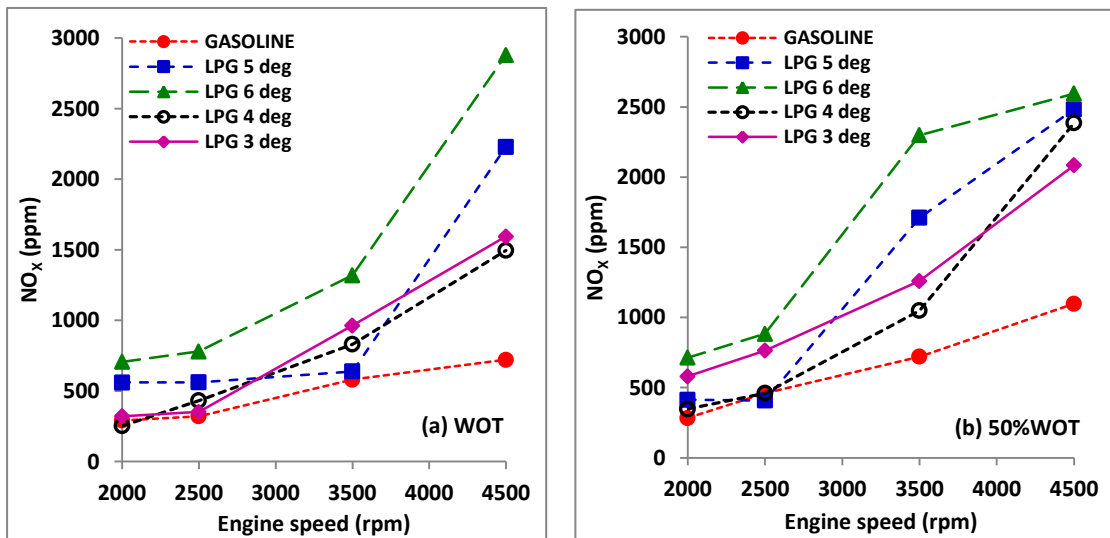


Fig. 5.68  $\text{NO}_x$  for LPG at 5, 6, 4 & 3 deg. bTDC, (a) WOT & (b) 50%WOT

### 5.3.10 Carbon dioxide( $\text{CO}_2$ )

The  $\text{CO}_2$  emissions with LPG at various ignition timings at WOT and 50%WOT are shown in figures 5.69 (a) & (b) respectively. LPG combustion has resulted in lower  $\text{CO}_2$  emissions. By advancing the static ignition timing the  $\text{CO}_2$  emission has further reduced. Even the retardation of ignition timing also has reduced the  $\text{CO}_2$  emissions.

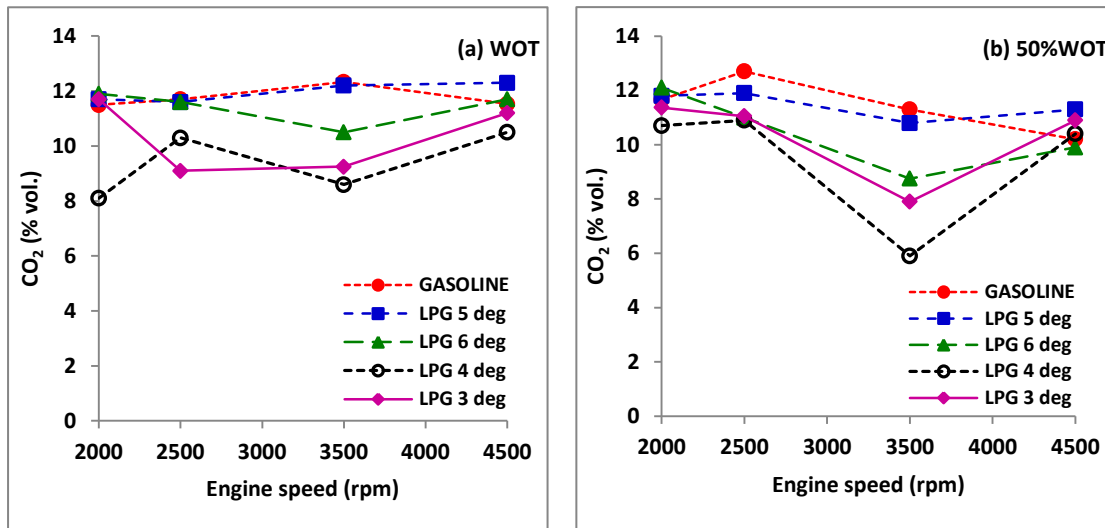


Fig. 5.69 CO<sub>2</sub> for LPG at 5, 6, 4 & 3 deg. bTDC, (a) WOT & (b) 50%WOT

The results of LPG fuel operation at various static ignition timings indicate that advancing the timing from 5 deg. bTDC to 6 deg. bTDC has resulted in better thermal efficiency and reduced emissions of CO and HC, compared to retarding the static ignition timing to 4 deg. bTDC and 3 deg. bTDC. However advanced static ignition timing has an adverse effect on NO<sub>x</sub> emissions as it increases further.

- When engine runs with LPG, better performance has been observed when ignition timing is set at 6 deg. bTDC with a marginal increase in brake thermal efficiency.
- The COV of IMEP has slightly increased with advancing the static ignition timing. At 50% WOT and 3500 rpm, COV has increased from 3 to 21%.
- CO emissions have reduced with advancing the ignition timing. At WOT and 3500 rpm, the reduction is from 5.6% to 1.3%.
- HC emissions have not much changed with change in static ignition timings.
- NO<sub>x</sub> emission has increased with advanced ignition timing. At WOT and 3500 rpm, it has increased from 638 ppm to 1319 ppm, where as at 50% WOT and 3500 rpm the increase is from 1710 to 2229 ppm compared to preset ignition timing. At WOT and 4500 rpm condition NO<sub>x</sub> emission at 6 deg. bTDC is 2800 ppm where as it is 1600 ppm at 3 deg. bTDC.



## **5.4 PERFORMANCE, COMBUSTION AND EMISSION STUDIES OF LPG WITH STEAM INDUCTION**

As a result of higher combustion temperature, comparatively more  $\text{NO}_x$  emissions occur in LPG combustion than in gasoline combustion. In order to address the problem of increase in the emissions of  $\text{NO}_x$  at all operating static ignition timings some kind of  $\text{NO}_x$  reduction technique has to be incorporated. Various methods that have been employed for this purpose include catalytic converter, exhaust gas recirculation (EGR), turbo-charging with inter-cooling, addition of diluents or steam injection along with the intake charge etc.

Injection of water into the intake manifold has been found to be an effective way to reduce NO emission in SI, CI and LPG engines. Increasing the intake charge humidity was also reported as an efficient technique to control NO emission. Hot steam from a steam generator is mixed with the intake charge at different proportions and the effect on performance, emission and combustion parameters have been reported. The concept of water addition as a supplement to the internal combustion engine has been around for over 50 years. It is a well-known fact that steam does not burn but it is excellent at absorbing heat due to steam having a high specific heat capacity and latent heat of evaporation. The latent heat of evaporation of steam is 2256 kJ/kg, which is approximately 6 times greater than that for gasoline under standard atmospheric pressure and temperature. Since it is at good absorbing heat, peak temperature in the cylinder will reduce so that the NO emission will greatly reduce.

For the reduction of  $\text{NO}_x$  emission steam induction to the intake manifold has been used. Steam is produced from the pressurized water using the waste heat in exhaust gases. To reduce the  $\text{NO}_x$  emission, the experiments have been carried out by varying amount of steam flow rate based on LPG fuel consumption. Steam flow rates of 10%, 15 %, 20% and 25% LPG fuel consumed are used in the experiments and beyond 25% steam flow rate; the engine performance has drastically reduced. Hence the experimental study on performances and emission characteristics of LPG with steam induction with different percentage of steam flow rate was limited to the range of 10% to 25% of fuel consumption. And also experiments have been conducted at 50%WOT and WOT (wide open throttle) positions.

### 5.4.1 Torque

The variation of brake torque with steam induction at 5 deg. static ignition timing for WOT and 50%WOT are shown in figure 5.70 (a) and (b), while figure 5.71(a) and (b) indicate the torque trends at 6 deg. static ignition timing condition. It can be observed that with the induction of steam, brake torque slightly reduces over the entire speed range. At 6 deg. bTDC the average decrease in engine torque are 1.35%, 2.4%, 3.89% and 5.08% respectively for 10, 15, 20 and 25% steam induction. With baseline 5 deg. bTDC static ignition timing, the effect of steam induction is marginal with 2.59%, 2.25%, 3.69% and 4.12% respectively for 10, 15, 20 and 25% (by mass) steam induction compared with no steam induction condition. At 4 deg. bTDC, the average torque itself is lower and the reduction with steam induction is very marginal. At 3 deg. bTDC with 25% steam, the decrease in average torque is 8.16% compared with no steam induction. With 50% WOT operating condition, generally the torque decreases with engine speed.

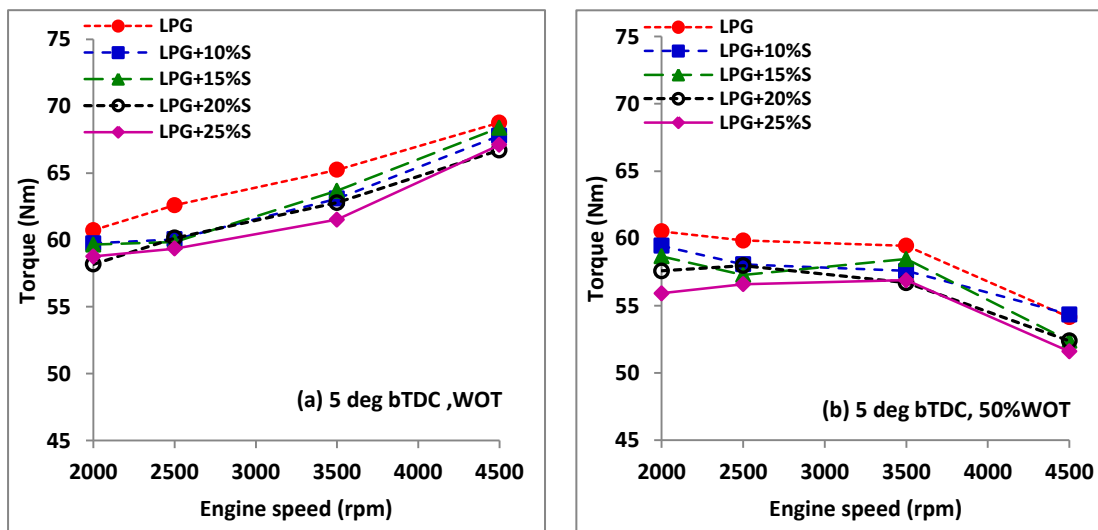


Fig. 5.70 Torque with speed for LPG along with steam at 5 deg. bTDC, (a) WOT and (b) 50%WOT

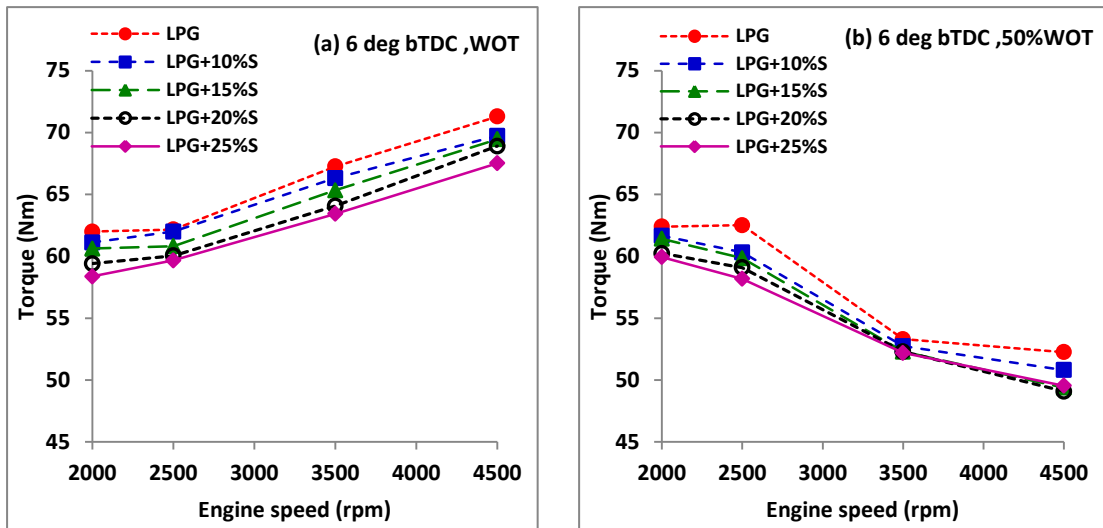


Fig. 5.71 Torque with speed for LPG along with steam at 6 deg. bTDC, (a) WOT and (b) 50% WOT

#### 5.4.2 Brake thermal efficiency (BTE)

The variation of BTE with steam induction along with LPG at 5 deg. static ignition timing for WOT and 50% WOT are shown in figure 5.72 (a) and (b), while figure 5.73 (a) and (b) indicate the BTE trends at 6 deg. static ignition timing condition. At WOT operating condition, the average brake thermal efficiency has decreased from 28.87% without steam induction to 28.43%, 28.10%, 27.44% and 27.13% at 6 deg. bTDC with 10, 15, 20 and 25% (by mass) steam induction respectively.

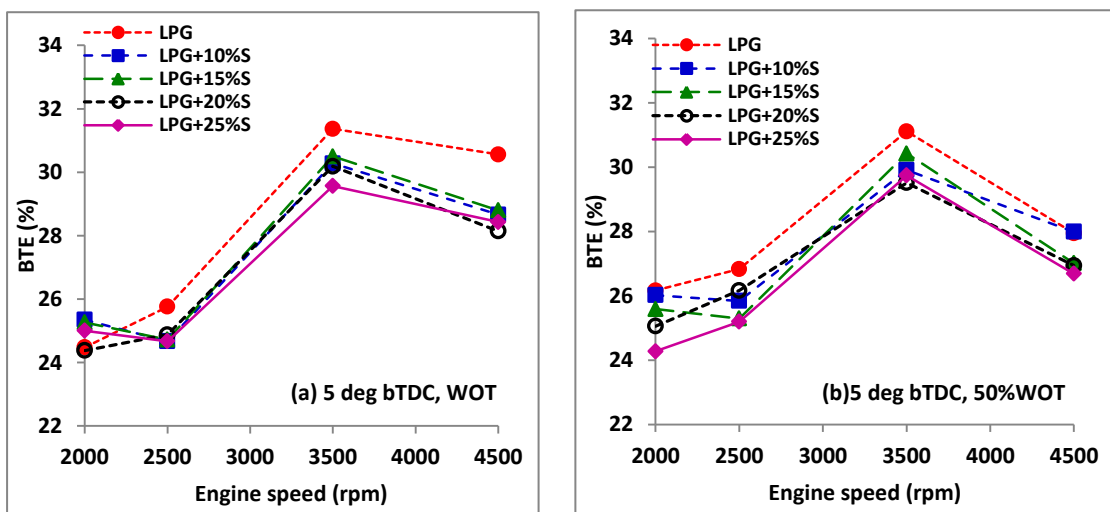


Fig. 5.72 BTE with speed for LPG along with steam at 5 deg. bTDC, (a) WOT and (b) 50% WOT

With 10 and 15% steam induction, there is no much decrease in BTE when compared to LPG, while there is a decrease of about 2% in BTE with 25% steam induction.

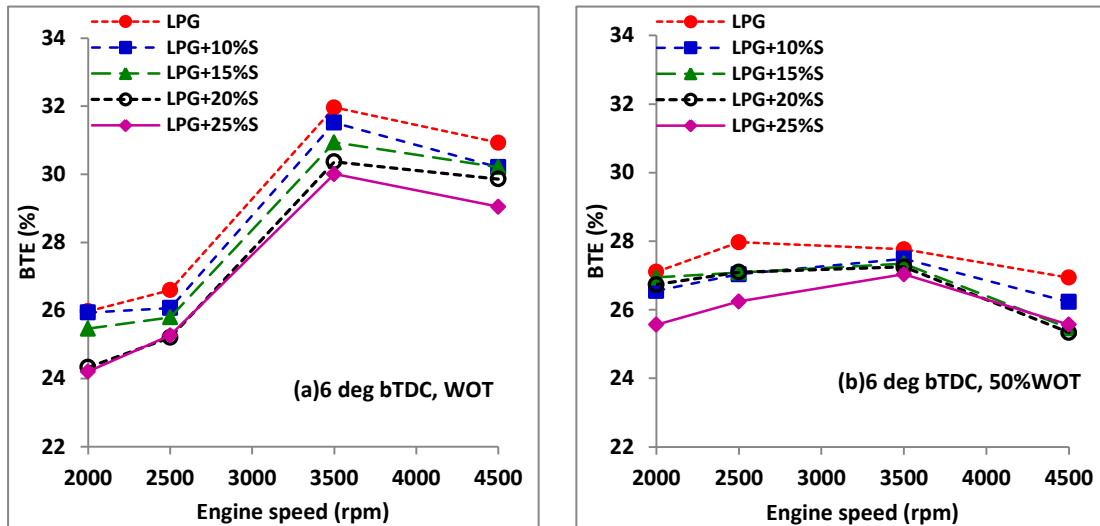


Fig. 5.73 BTE with speed for LPG along with steam at 6 deg. bTDC, (a) WOT and (b) 50% WOT

### 5.4.3 Brake specific energy consumption (BSEC)

The variation of BSEC with steam induction at 5 deg. static ignition timing for WOT and 50% WOT are shown in figure 5.74 (a) and (b), while figure 5.75 (a) and (b) indicate the BSEC trends at 6 deg. static ignition timing condition.

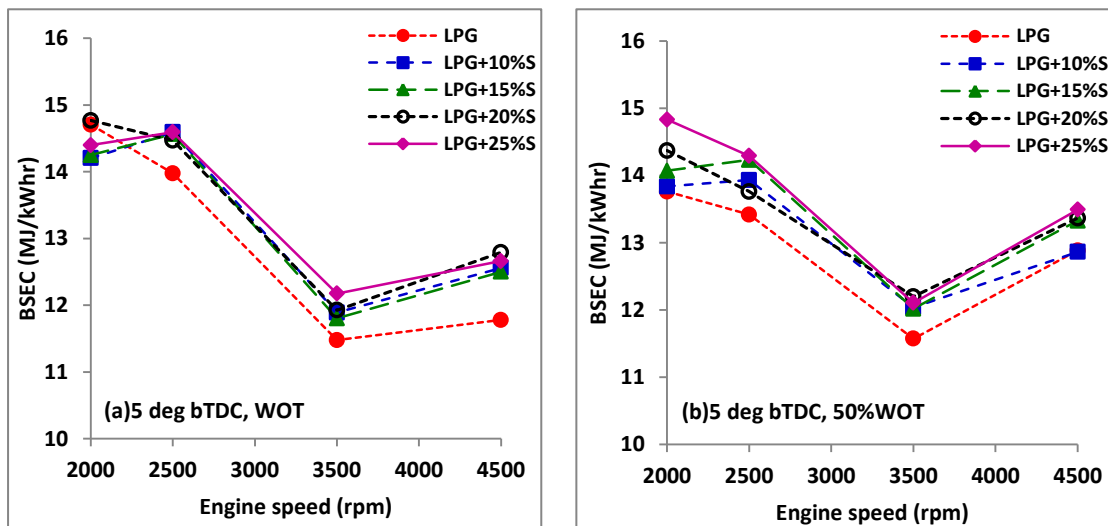


Fig. 5.74 BSEC with speed for LPG along with steam at 5 deg. bTDC, (a) WOT and (b) 50% WOT

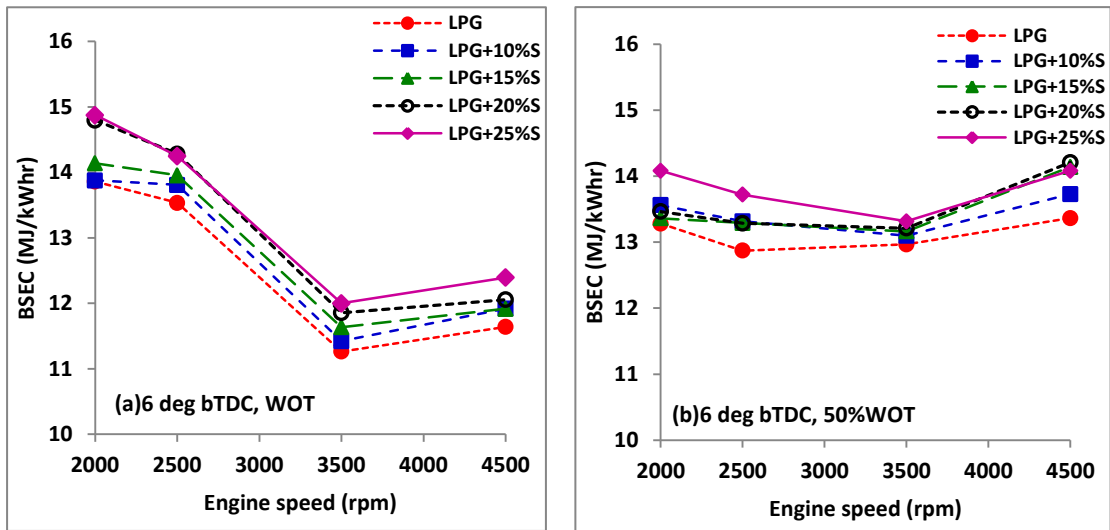


Fig. 5.75 BSEC with speed for LPG along with steam at 6 deg. bTDC, (a) WOT and (b) 50% WOT

At WOT condition, the average increase in BSEC when compared to LPG without steam induction at 6 deg. bTDC are 1.45%, 2.68%, 5.35% and 6.39% respectively with 10, 15, 20 and 25% (by mass) steam induction.

#### 5.4.4 Indicated mean effective pressure (IMEP)

The variation of IMEP with steam induction at 5 deg. bTDC static ignition timing for WOT and 50% WOT are shown in figure 5.76 (a) and (b), while figure 5.77 (a) and (b) indicate the IMEP trends at 6 deg. bTDC static ignition timing condition.

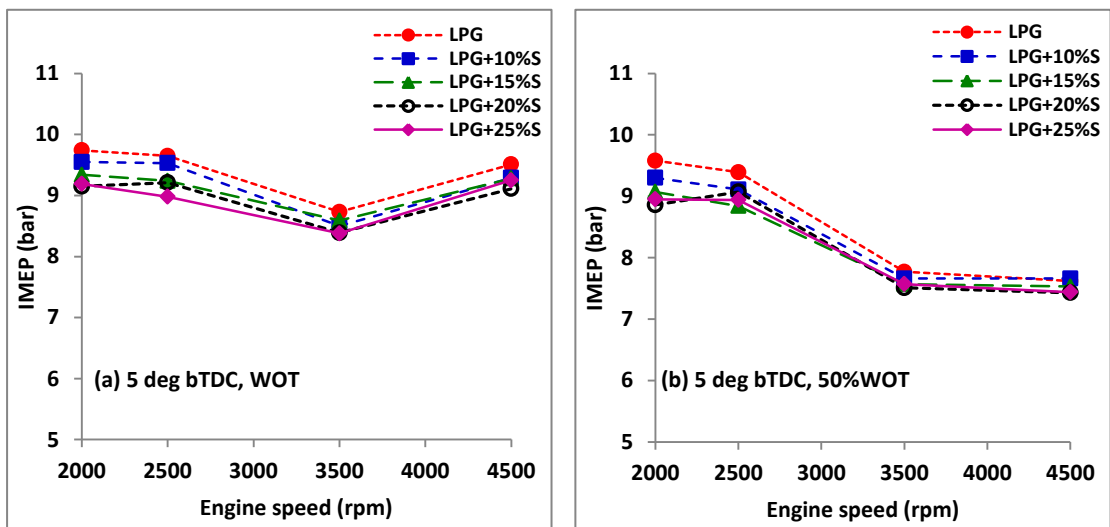


Fig. 5.76 IMEP with speed for LPG along with steam at 5 deg. bTDC, (a) WOT and (b) 50% WOT

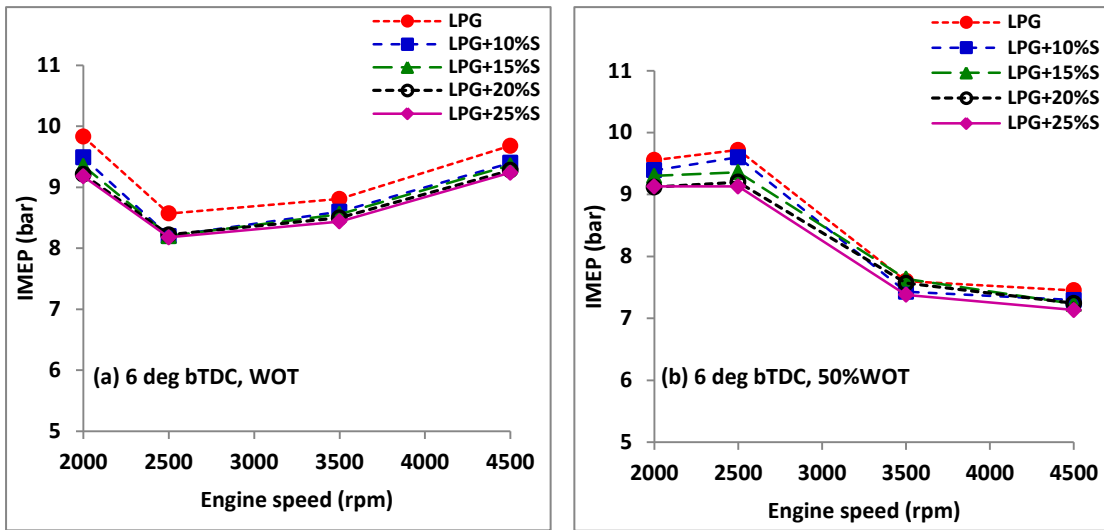


Fig. 5.77 IMEP with speed for LPG along with steam at 6 deg. bTDC, (a) WOT and (b) 50% WOT

At WOT condition, the IMEP remains almost constant throughout the operating speed range. The induction of steam to the intake charge has a marginal effect on IMEP reduction. At 6 deg. bTDC and 50% WOT there is a considerable reduction in IMEP with the engine speed, and the increase in steam proportion reduces IMEP marginally.

#### 5.4.5 Pressure-crank angle diagrams

Figure 5.78(a) & (b) shows the variation of in-cylinder pressure for LPG with steam induction at 5 deg. bTDC and 3500 rpm condition.

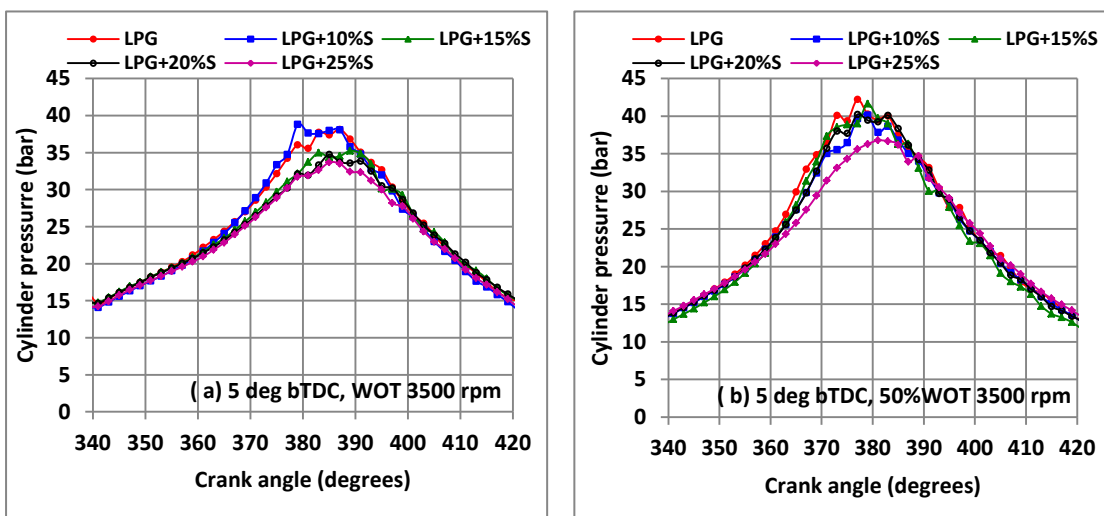


Fig. 5.78 Pressure vs crank angle for LPG with steam at 5 deg. bTDC, 3500 rpm, (a) WOT & (b) 50% WOT

The pressure trends at various speeds, WOT & 6 deg. bTDC condition are depicted in figures 5.79(a) & (b), while figure 5.80(a) & (b) shows the trends for 50%WOT condition at 3500 and 4500 rpm. It can be observed that induction of steam resulted in peak pressure occurrence further away from TDC while compared to LPG operation without steam induction. This may be the possible reason for reduction in the peak cylinder temperature which has resulted in reduced NO<sub>x</sub> emissions as discussed later.

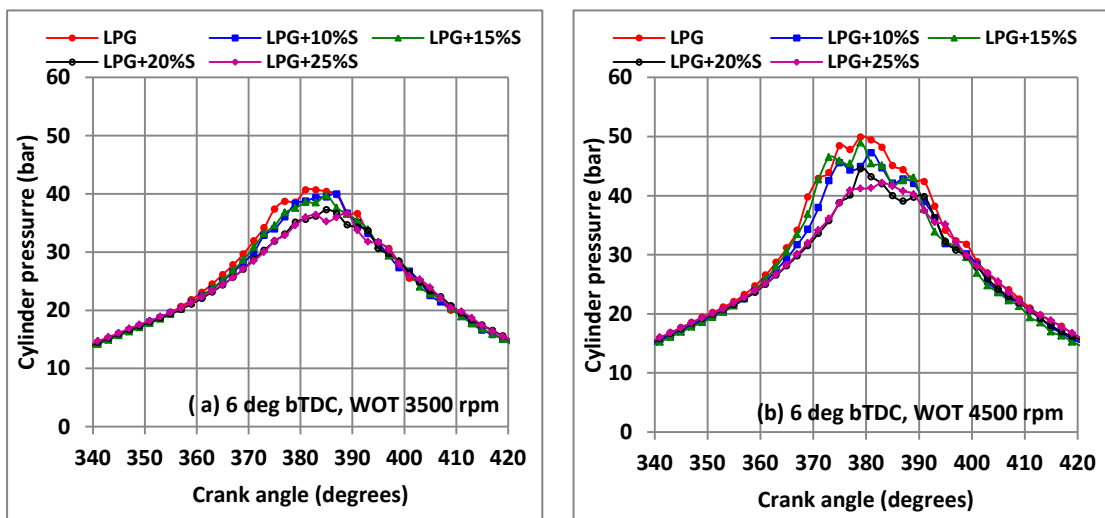


Fig. 5.79 Pressure vs crank angle for LPG with steam at 6 deg. bTDC, WOT, (a) 3500 rpm & (b) 4500 rpm

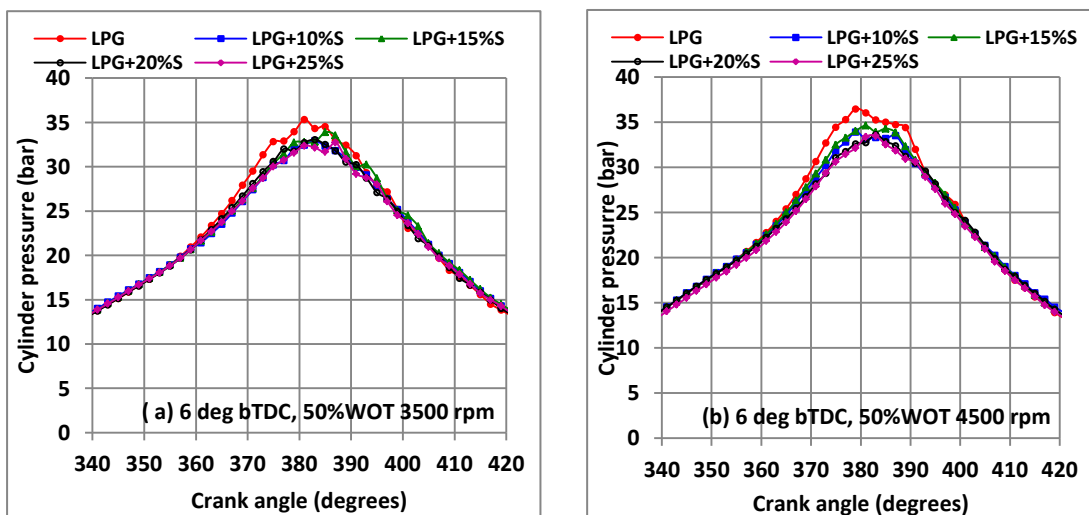


Fig. 5.80 Pressure vs crank angle for LPG with steam at 6 deg. bTDC, 50%WOT, (a) 3500 rpm & (b) 4500 rpm

### 5.4.6 COV of IMEP

The COV of IMEP variations with steam induction at WOT and 50%WOT conditions for 5 and 6 deg. bTDC conditions are shown in figures 5.81 (a) & (b) and 5.82 (a) & (b) respectively. At 5 deg. bTDC condition, steam induction at WOT has increased the COV. But comparatively 20% steam operation has given better results among the steam induction cases. At 50%WOT condition, as the steam induction increases, COV also increases.

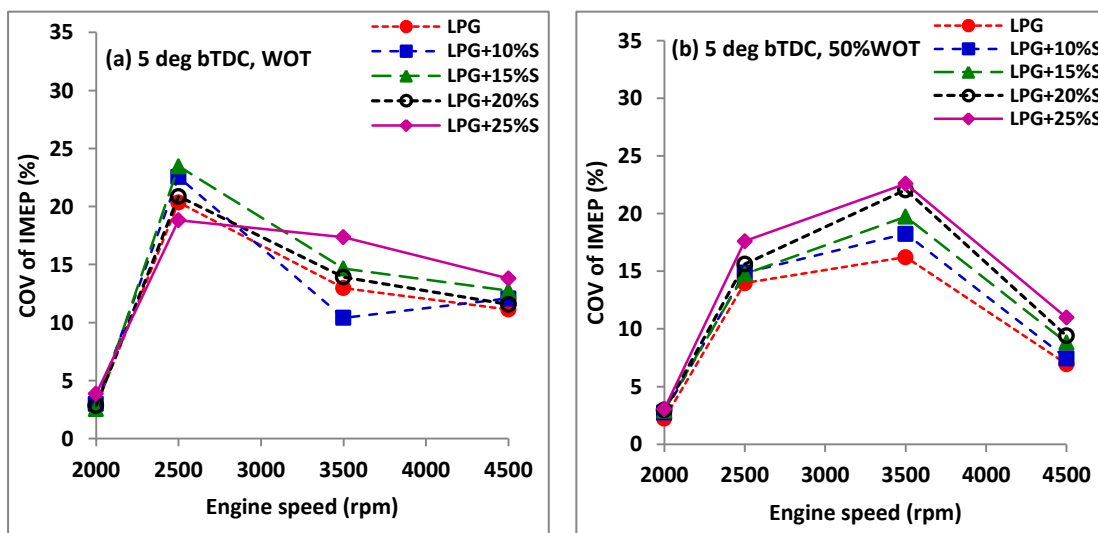


Fig. 5.81 COV of IMEP trends for LPG along with steam at 5 deg. bTDC, (a) WOT and (b) 50%WOT

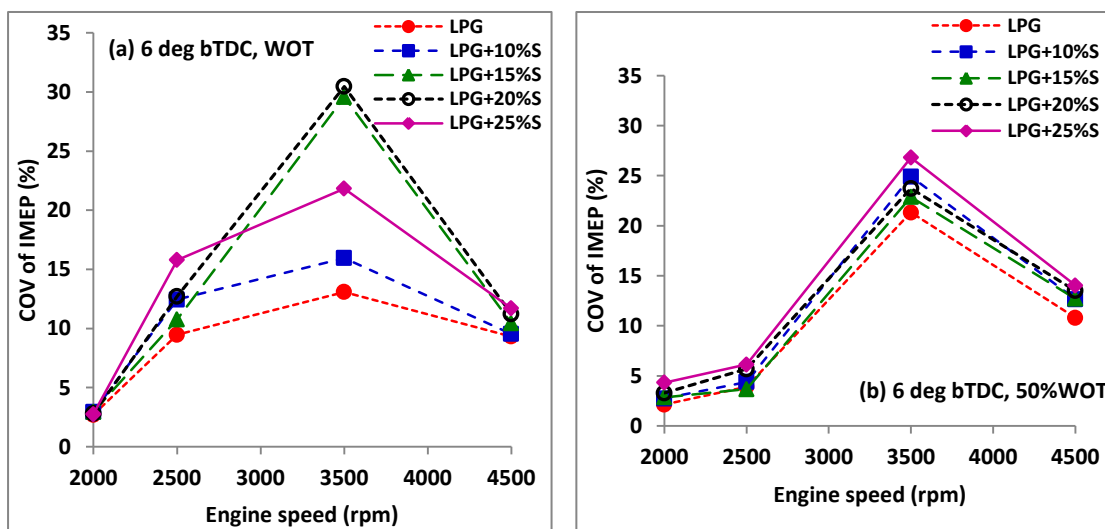


Fig. 5.82 COV of IMEP trends for LPG along with steam at 6 deg. bTDC, (a) WOT and (b) 50%WOT



At 6 deg. bTDC operating condition, 15-20% steam induction has better COV trends. Figures 5.83 and 5.84 shows the COV of IMEP variations with various static ignition timings for WOT and 50% WOT conditions at 3500 rpm & 4500 rpm. It can be observed that steam induction results in increased COV at all static ignition timings. At WOT condition, 15-20% steam induction rate has shown near equal COV of 20% at 6 deg. bTDC timing. Comparatively the COV of IMEP are lower with values up to 15% at 50%WOT condition.

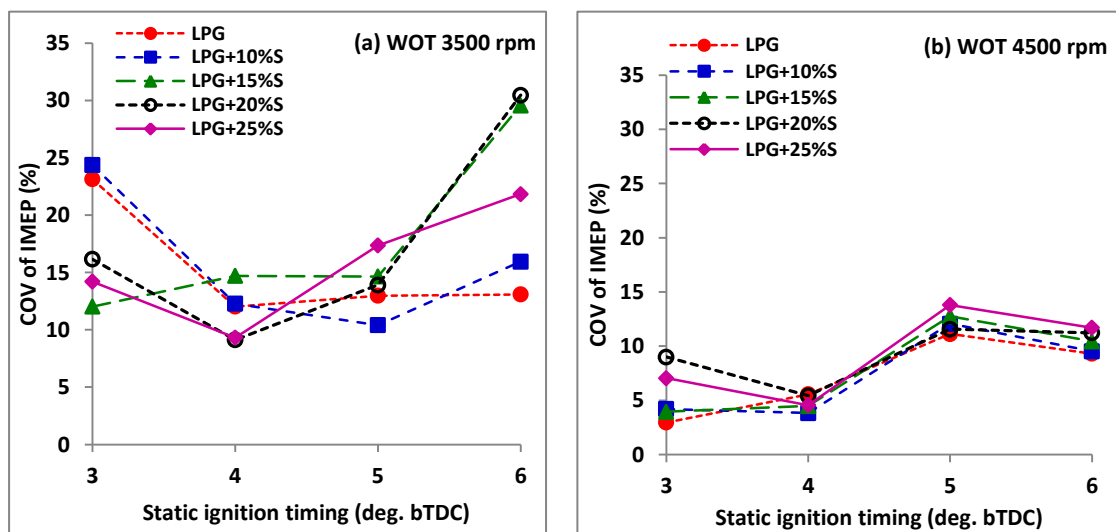


Fig. 5.83 COV of IMEP at (a) 3500 rpm and (b) 4500 rpm, WOT for LPG along with steam at various static ignition timings

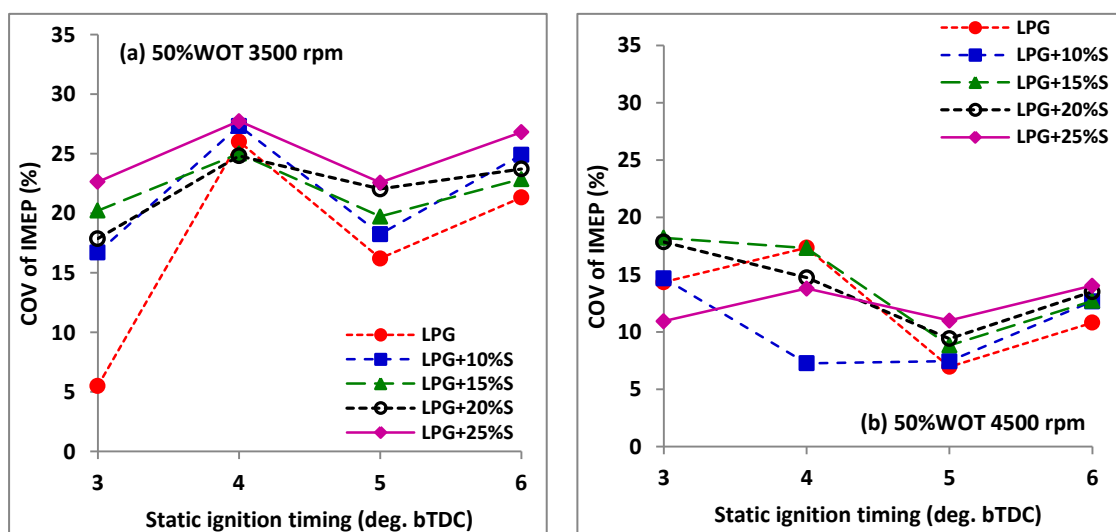


Fig. 5.84 COV of IMEP at (a) 3500 rpm and (b) 4500 rpm, 50% WOT for LPG along with steam at various static ignition timings

### 5.4.7 COV of Heat release

The heat release computed for 25 consecutive cycles are used to determine the coefficient of variation of heat release rate. The variations of COV of gross heat release per cycle at WOT and 50%WOT conditions for 5 and 6 deg. bTDC conditions are shown in figures 5.85 (a) & (b) and 5.86 (a) & (b) respectively. The heat release per cycle is higher with low percentage steam induction at WOT condition. But at 50%WOT condition induction of steam reduces the heat release per cycle.

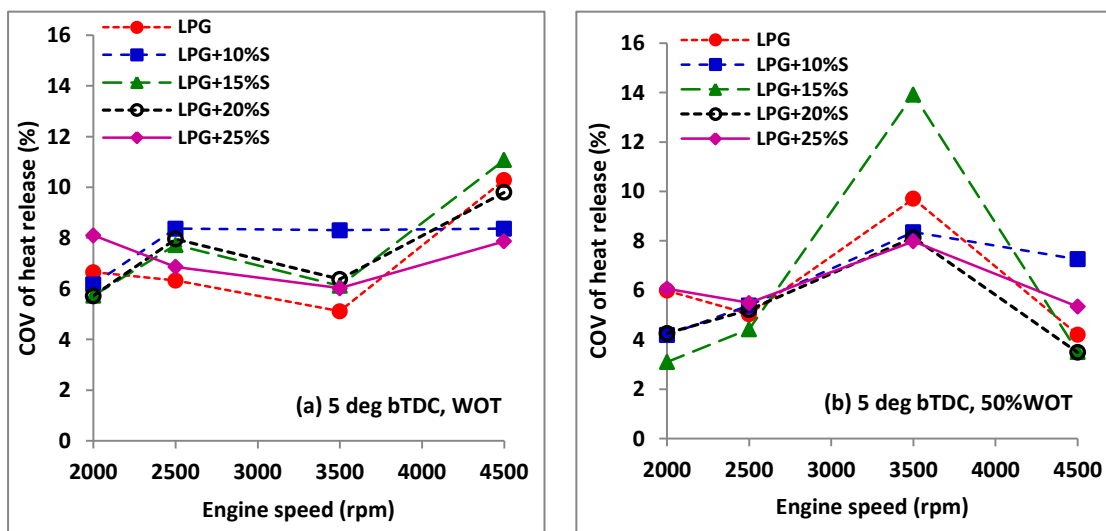


Fig. 5.85 COV of heat release trends for LPG along with steam at 5 deg. bTDC, (a) WOT and (b) 50%WOT

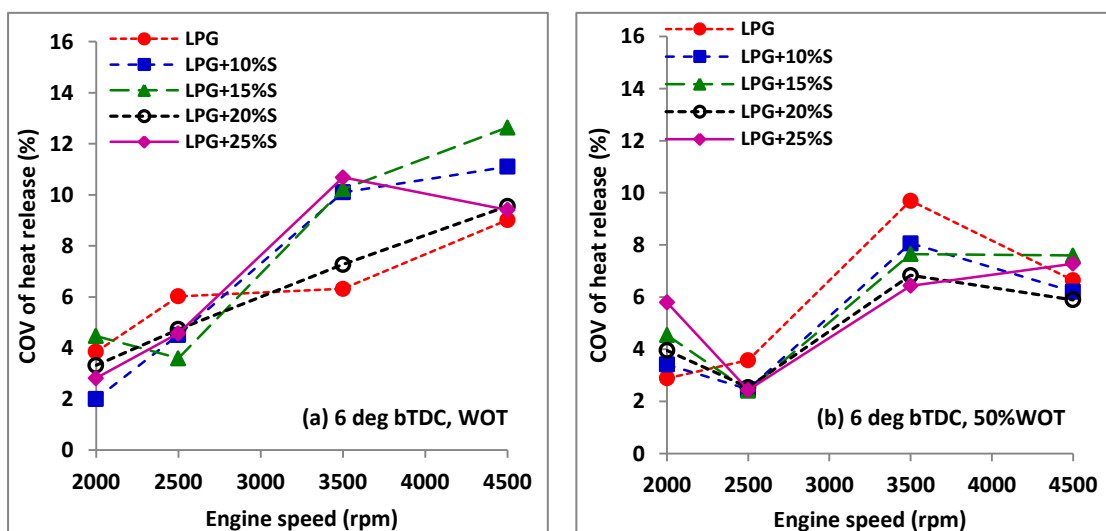


Fig. 5.86 COV of heat release trends for LPG along with steam at 6 deg. bTDC, (a) WOT and (b) 50%WOT

Figures 5.87 and 5.88 shows the COV of heat release rate variations with various static timings for WOT and 50%WOT conditions at 3500 rpm & 4500 rpm respectively. At 3500 rpm, steam induction at the rates of 15-20% has resulted in reduction of COV, with minimum COV recorded at static timing of 4 deg. bTDC. At 4500 rpm, the COV reduces as the steam rate increases, with 25%steam at 6 deg. bTDC giving COV value of 9.4%. At 50%WOT condition, again at 6 deg. bTDC, the addition of steam reduces the COV.

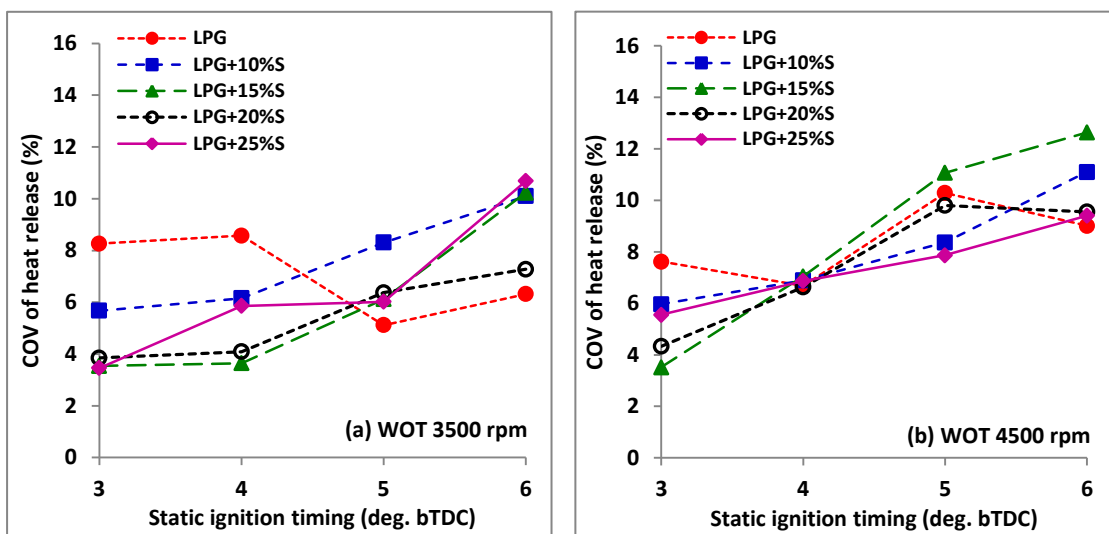


Fig. 5.87 COV of heat release at (a) 3500 rpm and (b) 4500 rpm, WOT for LPG along with steam at various static ignition timings

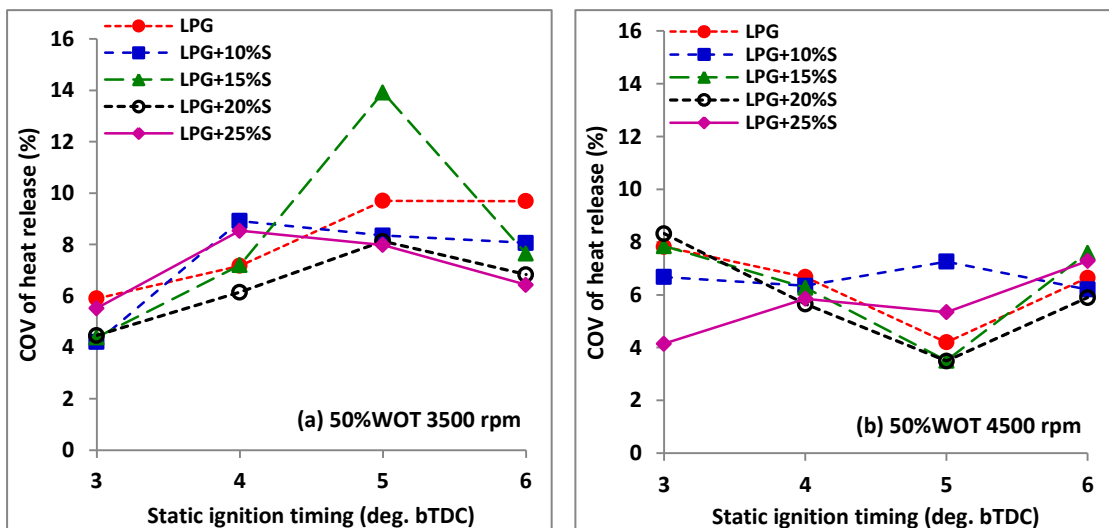


Fig. 5.88 COV of heat release at (a) 3500 rpm and (b) 4500 rpm, 50%WOT for LPG along with steam at various static ignition timings

### 5.4.8 Carbon monoxide (CO)

Figure 5.89 (a) and (b) depicts the variation of CO emissions with engine speed for different steam to LPG mass ratio at 5 deg. bTDC at WOT and 50%WOT respectively while figures 5.90 (a) & (b) shows the trends at 6 deg. bTDC. Induction of steam results in a marginal increase in the concentration of CO emissions.

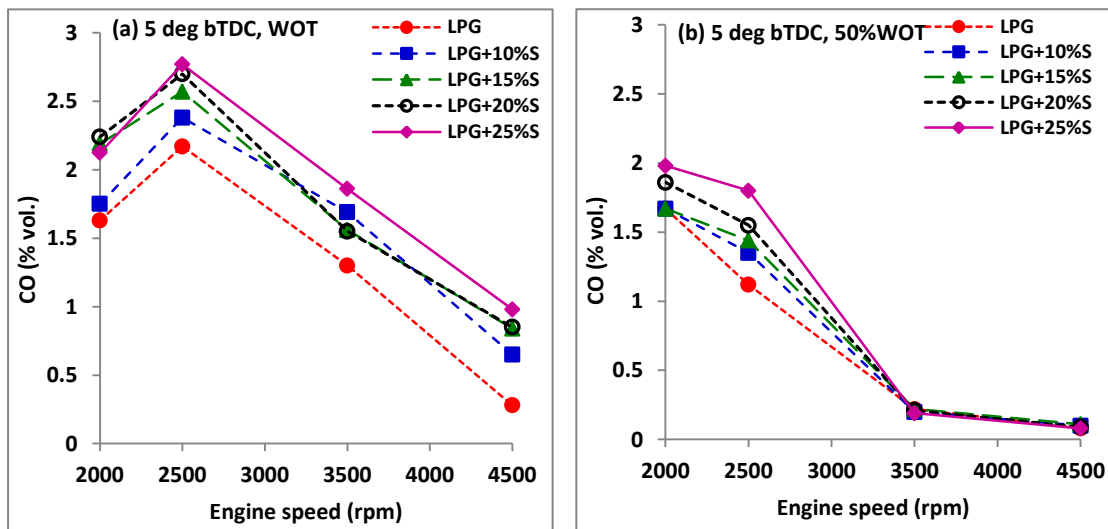


Fig. 5.89 CO with speed for LPG along with steam at 5 deg. bTDC, (a) WOT and (b) 50% WOT

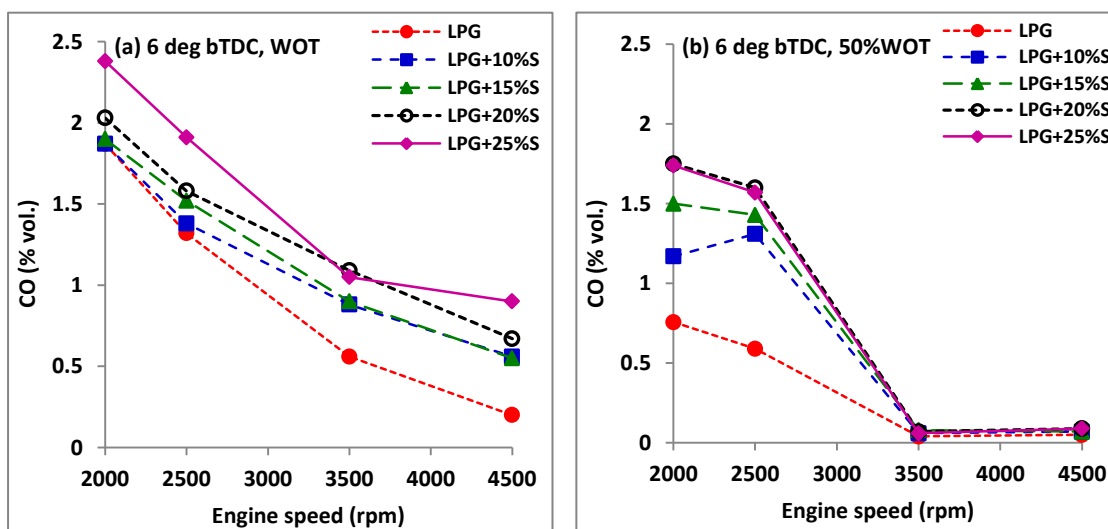


Fig. 5.90 CO with speed for LPG along with steam at 6 deg. bTDC, (a) WOT and (b) 50% WOT

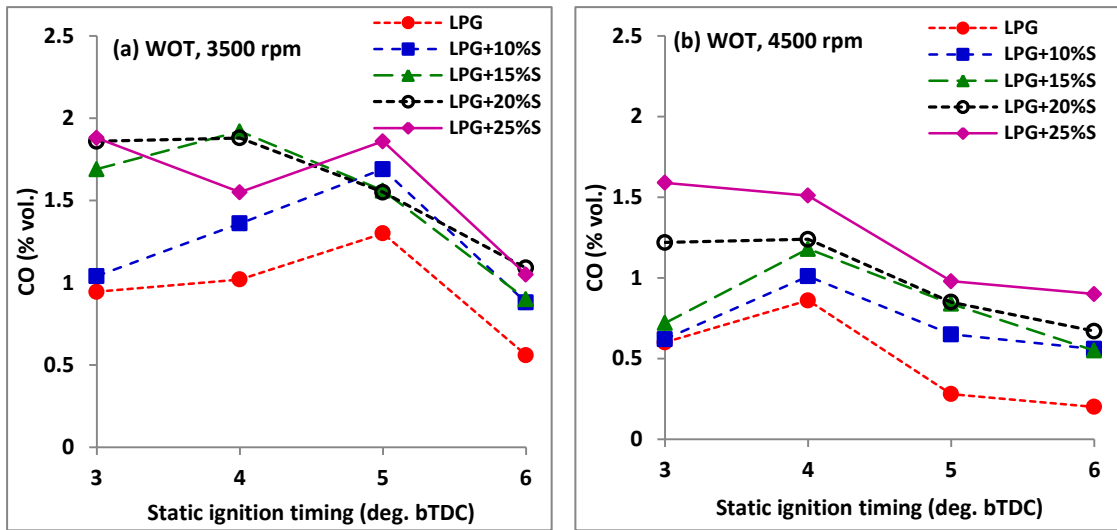


Fig. 5.91 CO emissions at (a) 3500 rpm and (b) 4500 rpm, WOT for LPG along with steam at various static ignition timings

At 50% WOT condition; CO emission is less for LPG without steam induction at lower speeds compared with different percentage of steam and increases with percentage of steam. This is because of induction of steam will decrease the peak combustion pressure and temperature so complete combustion will not take place, hence CO emission will increase. But as speed increases the CO emission will decrease with increase in percentage of steam and reaches LPG with no steam condition. This is because of air-fuel mixture reaches stoichiometric region, so more air will get for the combustion process hence complete combustion will take place. At WOT, at lower speed same trend as that of half throttle. But at higher speed CO emission increased from 0.2% to 0.9% for LPG with no steam to LPG with 25% of steam. This is because the burning period at wide open throttle is decreased at higher speed so complete combustion not occurs. Figure 5.91 shows the WOT variation of CO emissions at various static ignition timings at 3500 rpm and 4500 rpm for different steam to LPG mass ratios. Advancing the static timing improves combustion and thus reduces CO emissions. About 15% steam induction seems to be beneficial.

#### 5.4.9 Hydrocarbon (HC)

Figures 5.92 (a) & (b) and 5.93 (a) & (b) depicts the variation of HC emissions with engine speed for different steam to LPG mass ratio at 5 and 6 deg. bTDC at WOT and

50% WOT respectively. At both throttle opening positions as the percentage of steam increased HC emission is increased compared to LPG operation without steam induction. This is because steam induction will decrease the burning rate of air-fuel mixture. The lower the mixture temperature, combustion chamber deposits, and longer burning period could have contributed to higher emissions from the engine.

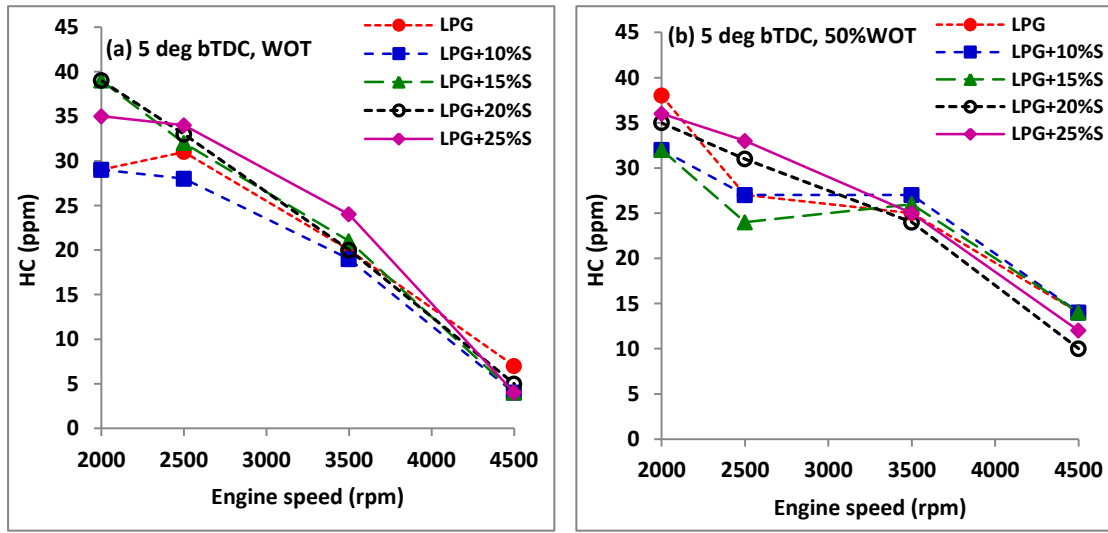


Fig. 5.92 HC with speed for LPG along with steam at 5 deg. bTDC, (a) WOT and (b) 50% WOT

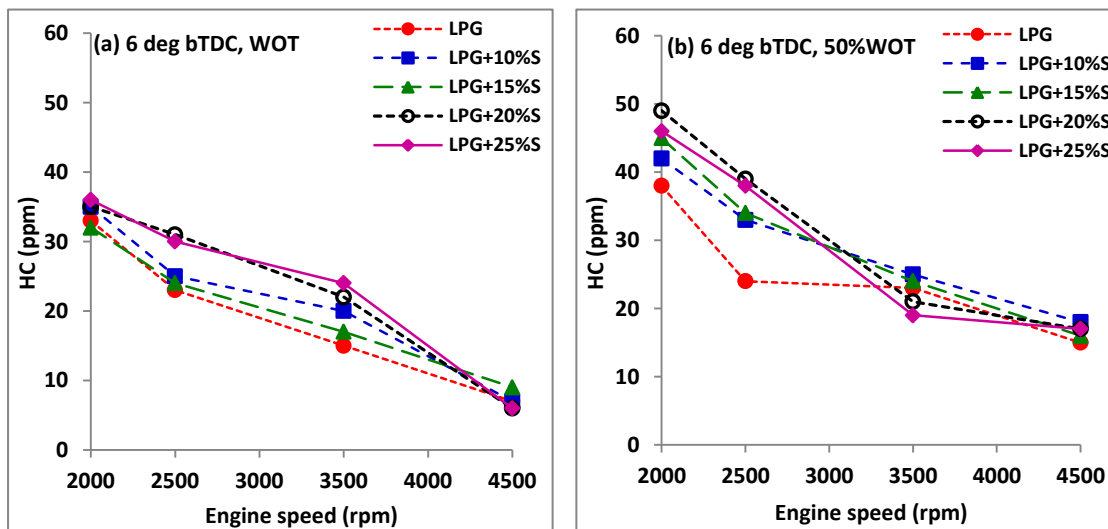


Fig. 5.93 HC with speed for LPG along with steam at 6 deg. bTDC, (a) WOT and (b) 50% WOT

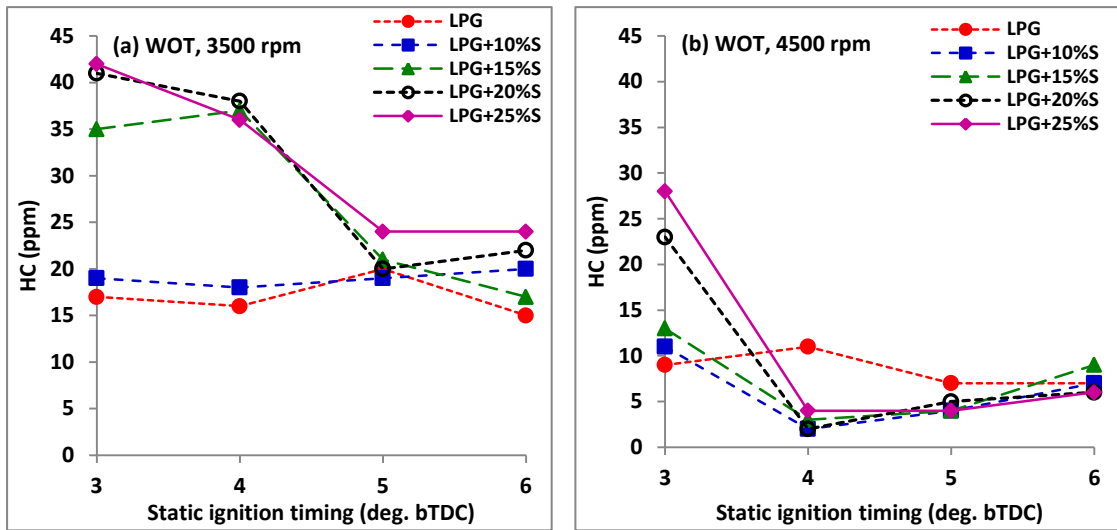


Fig. 5.94 HC at (a) 3500 rpm and (b) 4500 rpm, WOT for LPG along with steam at various static ignition timings.

At 6 deg. bTDC, WOT and 3500 rpm, HC has increased from 15 to 24 ppm with 25% steam induction when compared to LPG without steam induction, whereas at 4500 rpm HC increase is marginal. At 50% WOT condition the HC has increased with 10 and 15% steam induction, whereas it has reduced after this steam induction rate at 3500 rpm. Figures 5.94 (a) & (b) show the WOT variation of HC emissions at various static ignition timings at 3500 rpm and 4500 rpm for different steam to LPG mass ratios. Advancing the static timing improves combustion and thus reduces HC emissions.

#### 5.4.10 Oxides of nitrogen (NO<sub>x</sub>)

Water induction acts as a diluent which will help to control the peak temperature during combustion. The vaporization of water will help to reduce the charge temperature. In addition, the vaporized water will reduce the concentration of both oxygen and nitrogen. It will also alter the specific heats of the charge. Diluents with high specific heat capacity and latent heat of vaporization are always preferred so that a small amount will be enough. The reduced temperature will lower the rate of heat release and thus help to suppress the knocking tendency. Figures 5.95 (a)-(d) show the trends of NO<sub>x</sub> emissions with engine speed at WOT for different steam to fuel mass ratios at 5, 6, 4 and 3 deg. bTDC static ignition timings respectively. Figures 5.96 (a)-(d)

depict the trends at 50% WOT condition for the above mentioned static ignition timings. At wide open throttle condition the trends indicate that the steam induction has resulted in drastic reduction in  $\text{NO}_x$  emissions at all the engine speeds. When steam is injected at steam to fuel mass ratio of 10%, the initial drop is in the range of 20-25% when compared to the emissions without steam induction. As mentioned earlier, the presence of steam makes the cycle peak temperature to come down and lowers  $\text{NO}$  emissions significantly.

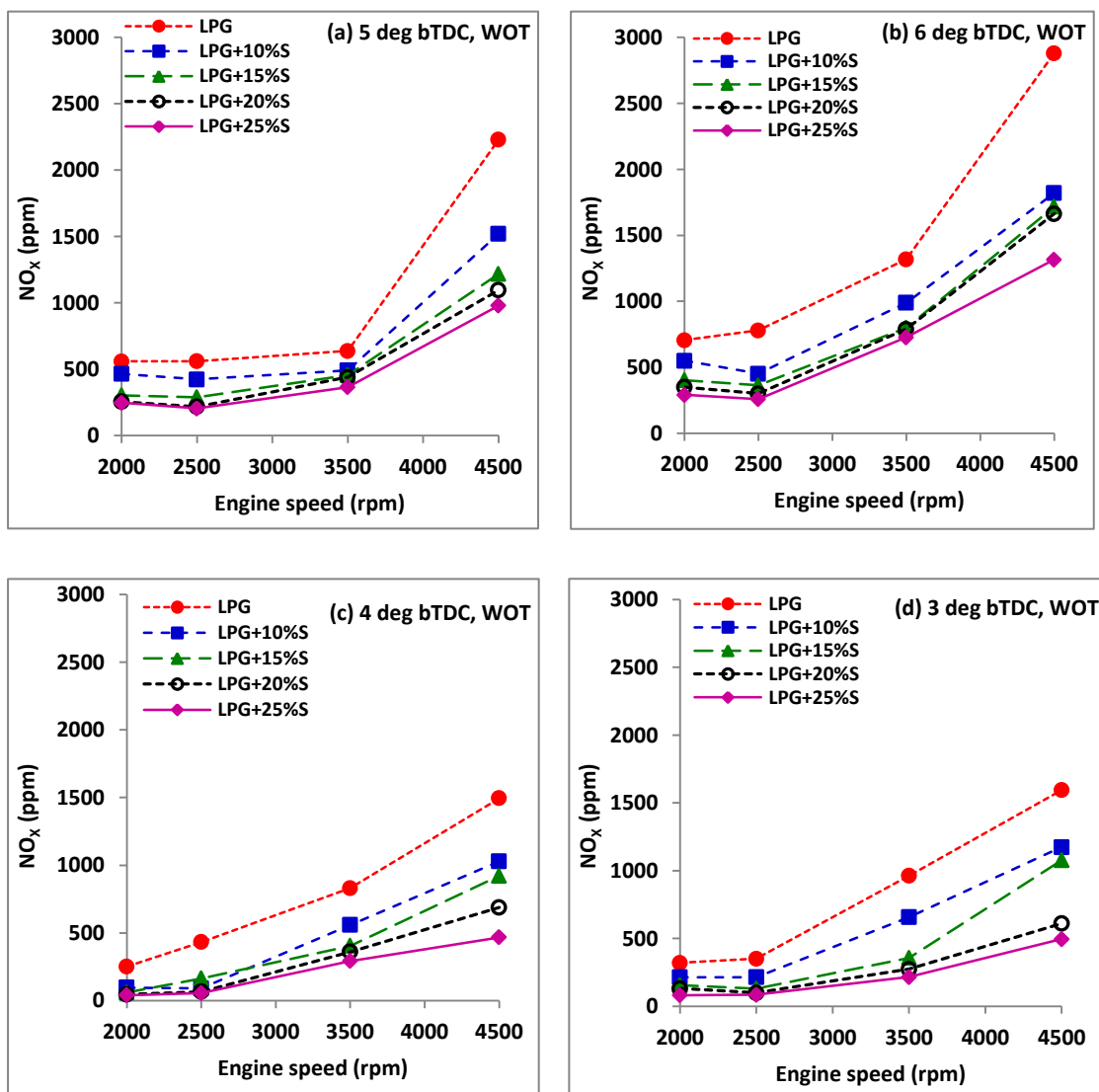


Fig. 5.95  $\text{NO}_x$  with engine speed at WOT and different static ignition timings for LPG along with steam



As the ignition timing is advanced this drop in  $\text{NO}_x$  amount increases. The 50%WOT results are in the same line as that of WOT. Figures 5.97 (a) and (b) show the percentage  $\text{NO}_x$  reduction at 3500 rpm for various steam to fuel mass ratios at WOT and 50%WOT conditions respectively. At WOT condition at 6 deg. bTDC timing, steam to fuel mass ratio of 10% reduces  $\text{NO}_x$  by 25%, while further induction of steam steadily reduce the emissions and when steam to fuel mass ratio of 25% the reduction reaches around 45%.

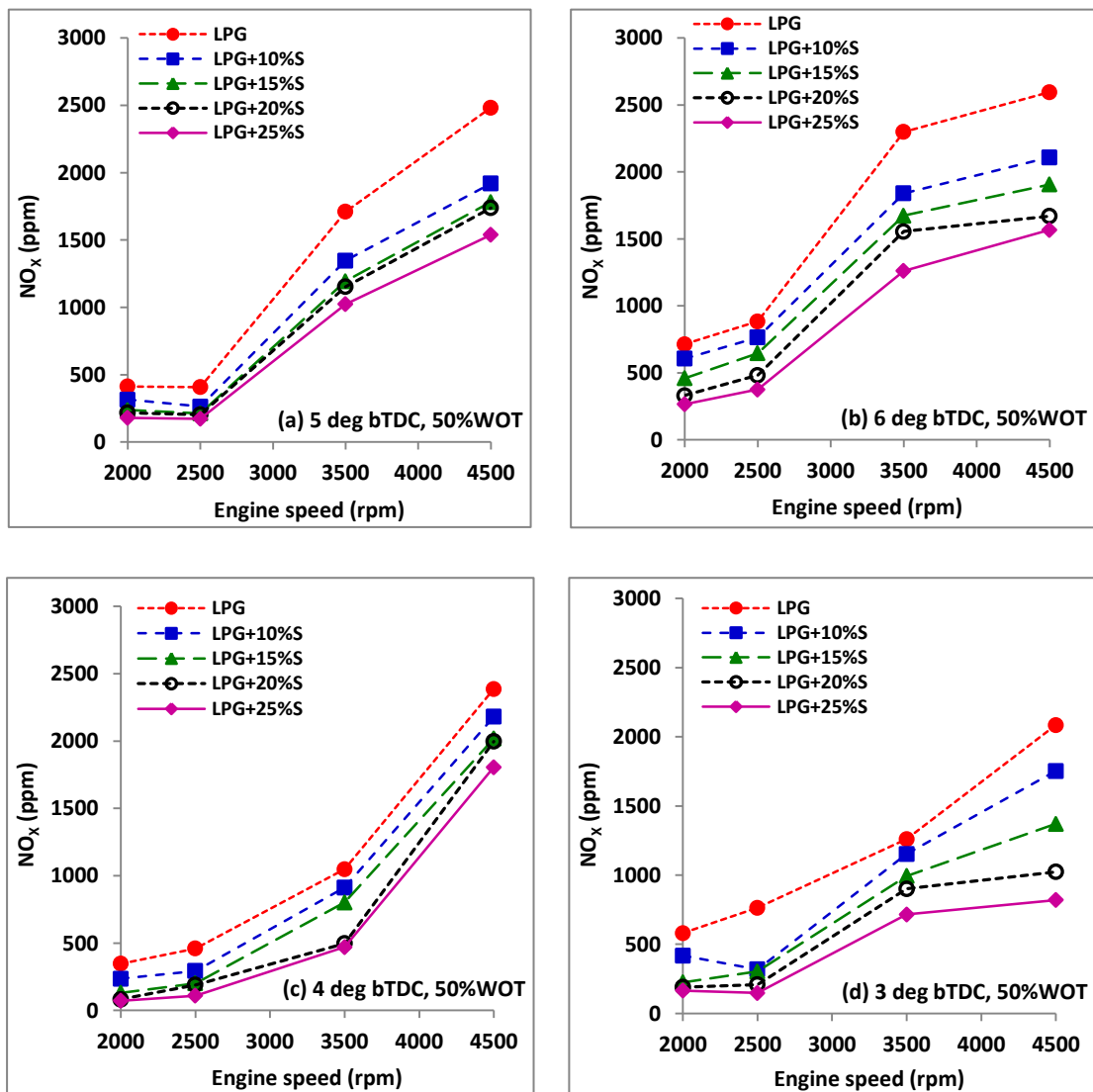


Fig. 5.96  $\text{NO}_x$  with engine speed at 50%WOT and different static ignition timings for LPG along with steam

At 4 and 5 deg. bTDC conditions this reductions are slightly higher reaching up to 58%. Similar drop in NO<sub>x</sub> was observed at 50% WOT condition as well. There again at 6 deg. bTDC timing the reduction was from 20 to 45% with increase in steam to fuel mass ratio from 10 to 25%. Hence it can be observed that peak NO<sub>x</sub> emissions can be brought under control with the use of LPG by steam induction. The reduction can be in the range of 20 to 45% for the optimized static ignition timing of 6 deg. bTDC. Further it was observed that at both the throttle opening conditions tested, the steam near the induction point will be superheated and thus ensures no steam droplet is sticking to the wall and therefore higher proportions of steam to fuel mass can be used. At lower engine speeds the steam was just above saturation temperature and as it is injected to air stream it may condense back to water, which is not desirable. Hence about 10% steam to fuel mass ratio can be used at lower engine speeds where there is a substantial reduction in NO<sub>x</sub> up to 25%. At higher engine speeds the steam to fuel ratio of 25% can be used to get about 45-50% reduction in NO<sub>x</sub>.

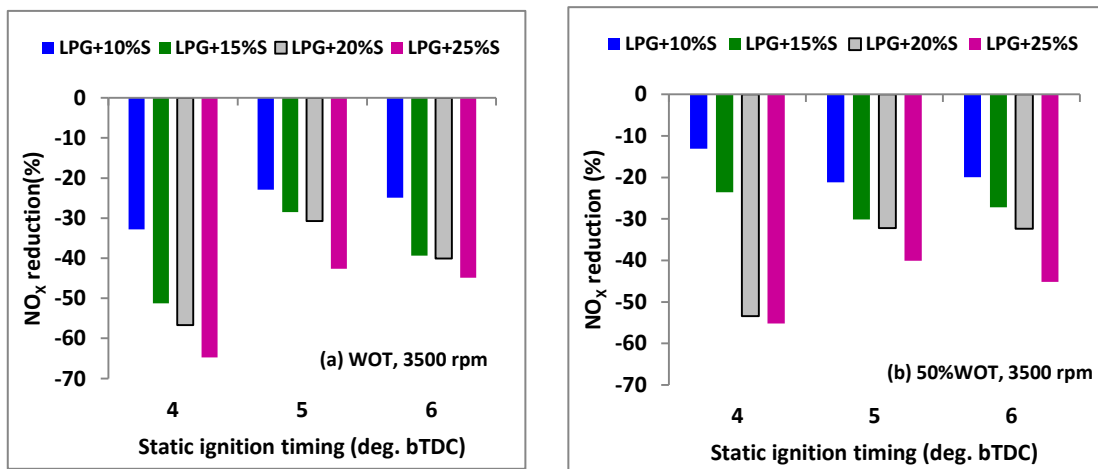


Fig. 5.97 Percentage NO<sub>x</sub> reduction at 3500 rpm at 6 deg. bTDC, (a) WOT and (b) 50% WOT with steam induction along with LPG

#### 5.4.11 Exhaust gas temperature (EGT)

The exhaust gas temperature trends with steam induction rates at WOT for different static ignition timings are shown in fig. 5.98. The induction of steam has resulted in reduction in exhaust gas temperature for all ignition timings. As the percentage of steam increased the EGT has further reduced. These trends explain the reason for NO<sub>x</sub> reduction with steam induction. The EGT reduction is due to lower cycle

temperatures which are result of steam addition. This lower cycle temperature in effect reduces the emissions of  $\text{NO}_x$ .

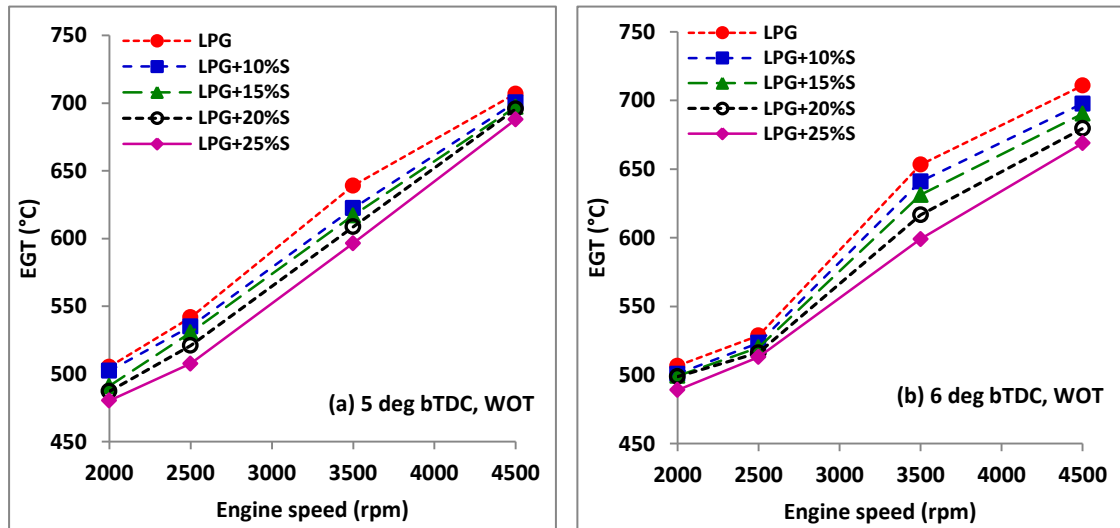


Fig. 5.98 Exhaust gas temperature with engine speed for LPG along with steam at WOT at (a) 5 deg. and (b) 6 deg. static ignition timings

#### 5.4.12 Carbon dioxide ( $\text{CO}_2$ )

Figures 5.99 (a) and (b) depicts the variation of  $\text{CO}_2$  emissions with engine speed for different steam to LPG mass ratio at 6 deg. bTDC at WOT and 50%WOT respectively.

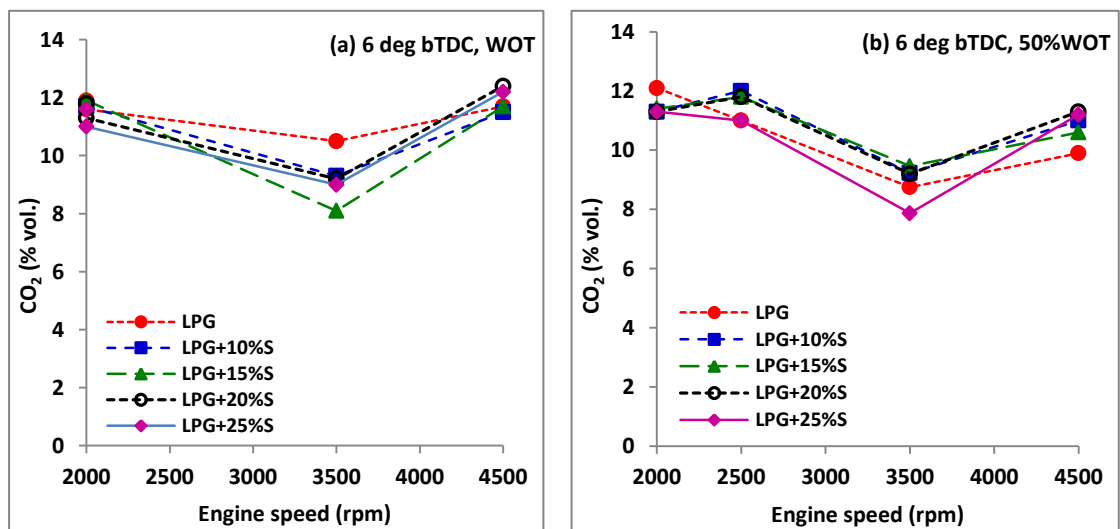


Fig. 5.99  $\text{CO}_2$  emissions with speed for LPG along with steam at (a) WOT and (b) 50%WOT at 6 deg. bTDC

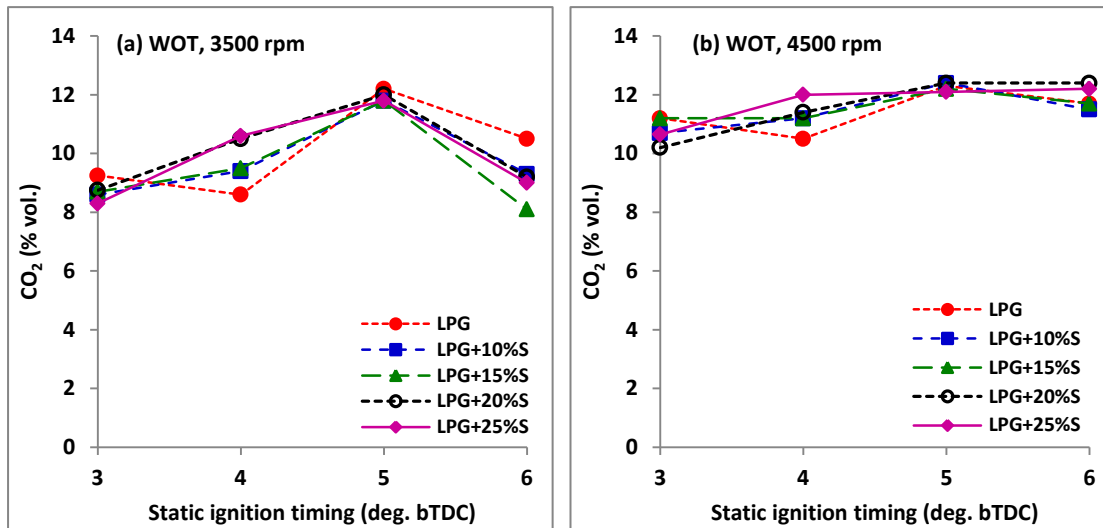


Fig. 5.100 CO<sub>2</sub> emissions at (a) 3500 rpm and (b) 4500 rpm, WOT for LPG along with steam at various static ignition timings

Induction of steam reduces the CO<sub>2</sub> concentration marginally. The effect of static ignition is shown in figure 5.100 which indicates that at WOT condition advancing the static timing reduces CO<sub>2</sub> emissions.

From the experiments with LPG along with steam induction at varying rates, it has been found that steam induction reduces the engine performance but has succeeded in reducing the NO<sub>x</sub> emissions substantially.

- LPG with steam induction has marginally reduced the brake thermal efficiency. At WOT & 3500 rpm, with 15% steam the torque decreased by 3% while BTE has decreased by 3.19% when compared to LPG alone at 6 deg. bTDC. The COV of IMEP has increased by 6.15% at the above conditions.
- It has been found that NO<sub>x</sub> emissions have reduced significantly by 20 - 45% over the entire operating speed range with the induction of steam with a reduction of 40% at WOT, 3500 rpm for LPG with 15% steam induction compared to LPG alone at 6 deg. bTDC.

Addition of steam in proportions more than 15 %, the benefit of NO<sub>x</sub> reduction is marginal. Hence LPG with 15% steam at 6 deg. bTDC is better choice compared to LPG from the point of view of improved engine performance and reduced exhaust emissions.

## 5.5 COMPARATIVE STUDIES WITH LPG-STEAM AND ETHANOL ENRICHED GASOLINE

The ethanol enriched gasoline blend of E20 is selected for comparison based on engine performance combustion and emissions. Steam induction beyond 15% has only marginal benefits in terms of NO<sub>x</sub> reductions. Hence LPG along with 15% steam induction at 6 deg. bTDC is selected and compared with E20.

### 5.5.1 Brake thermal efficiency (BTE)

Figures 5.101 and 5.102 shows the trends of the brake thermal efficiencies of ethanol enriched gasoline and LPG along with steam induction at 6 deg. bTDC. It shows that steam induction has resulted in a marginal decrease in efficiency compared to ethanol enriched gasoline blend. At WOT and 3500 rpm, the reduction is by 3.5%. But this result is better than that for pure gasoline. Overall by the thermal efficiency point of view, E20 is superior to all other fuels.

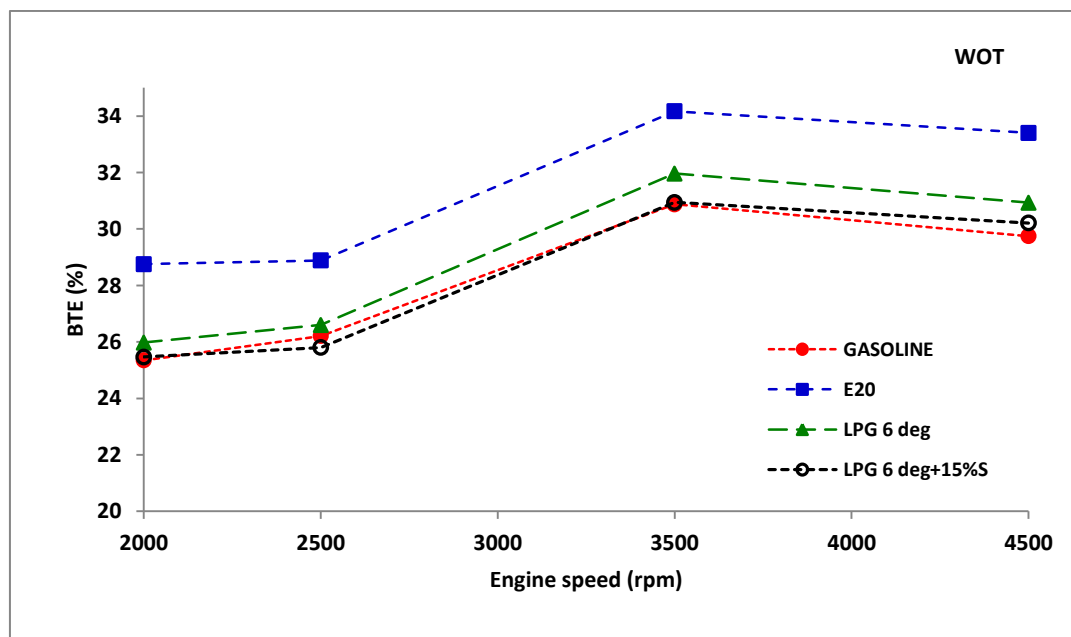


Fig. 5.101 BTE for various fuels at WOT

At 50%WOT condition and 3500 rpm, LPG and LPG along with steam induction has the lowest BTE compared to E20 and gasoline. But the loss in BTE by steam induction is negligible. At speeds higher than 3500 rpm the BTE changes are marginal. Hence at part load, the use of LPG along with steam is preferable.

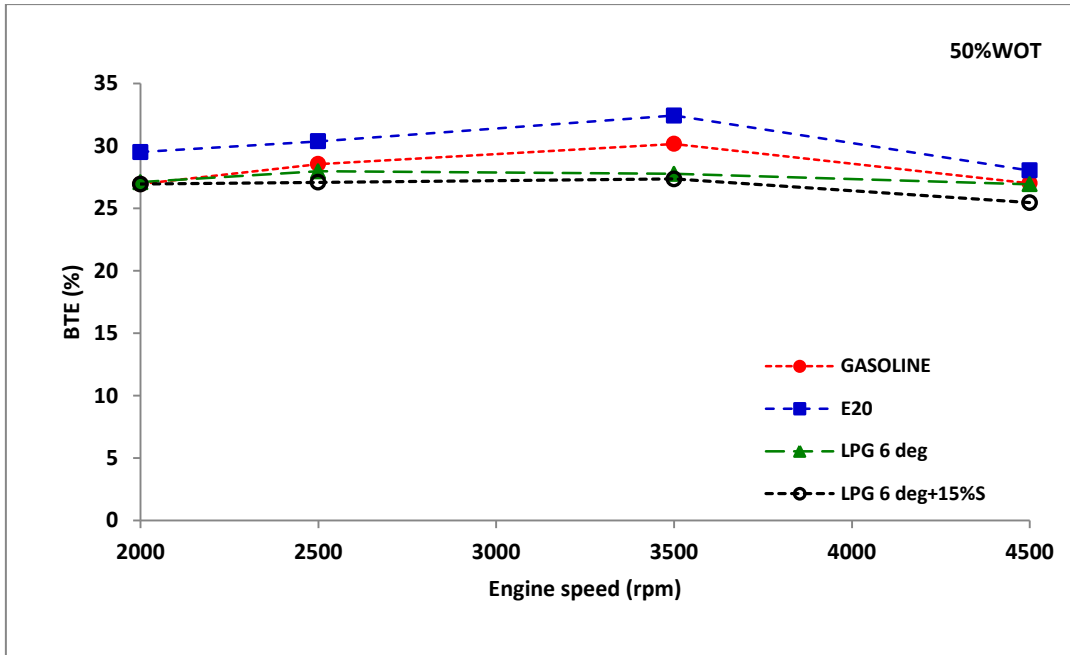


Fig. 5.102 BTE for various fuels at 50% WOT

### 5.5.2 COV of IMEP

The COV of IMEP trends at WOT and 50% WOT conditions are shown in figures 5.103 and 5.104 respectively. At WOT the induction of steam has resulted in a shoot up in COV at 3500 rpm. In other operating speeds the increase is marginal. Similar trends are observed at 50% WOT condition also.

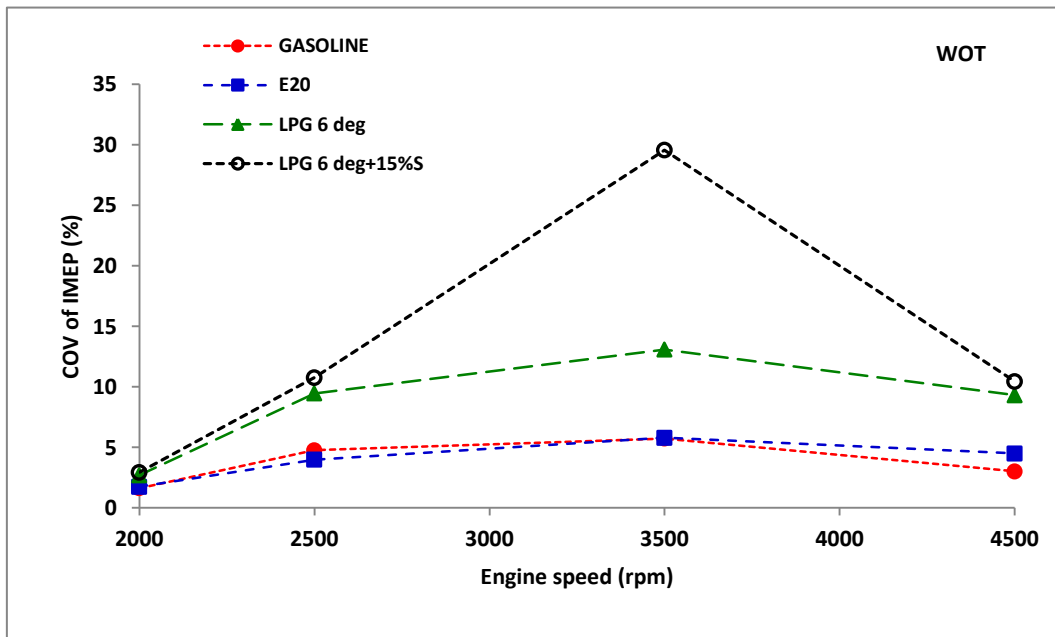


Fig. 5.103 COV of IMEP for various fuels at WOT

The ethanol enriched blend is resulting in smooth combustion and the COV is marginally varying when compared to gasoline. The instability in combustion as indicated by COV of IMEP increases with steam induction along with LPG. At 3500 rpm and WOT condition, LPG+15% steam has a COV of 30% compared to 6% for E20.

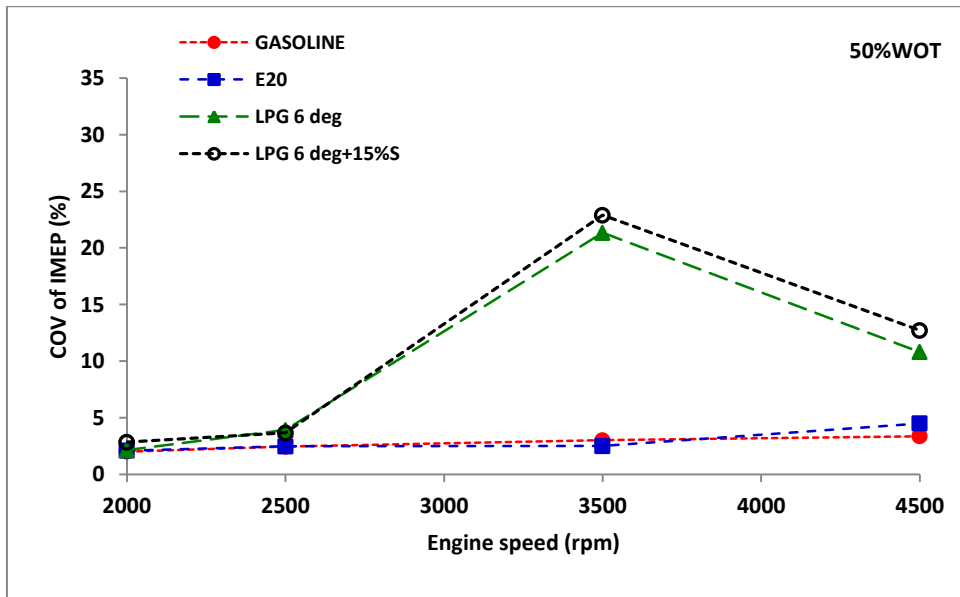


Fig. 5.104 COV of IMEP for various fuels at 50% WOT

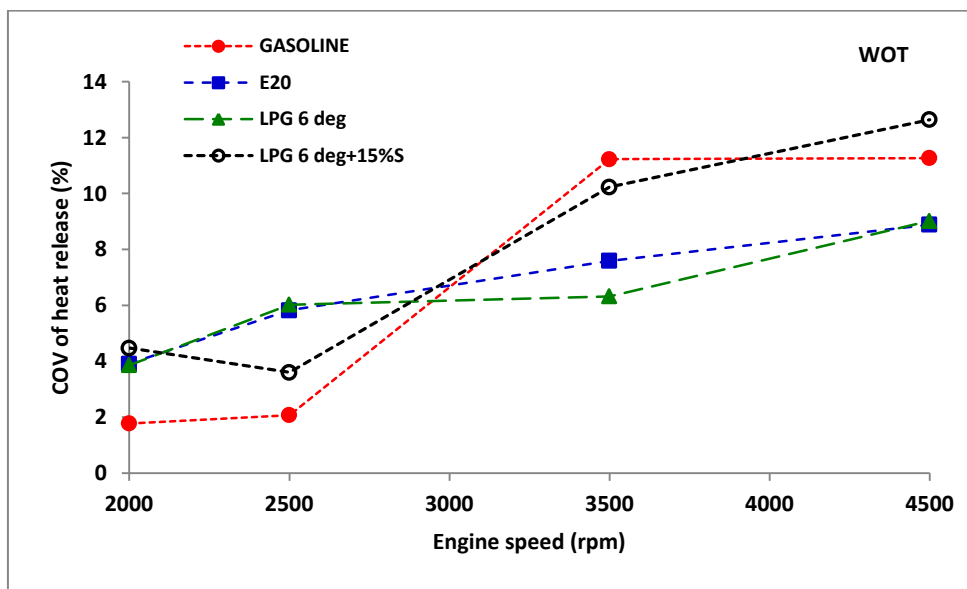


Fig. 5.105 COV of heat release per cycle for various fuels at WOT

### 5.5.3 COV of heat release

The COV of heat release trends at WOT and 50%WOT conditions are shown in figures 5.105 and 5.106 respectively. At WOT the induction of steam has resulted in reduction of COV at lower speeds, where as it has increased at higher engine speeds. At 3500 rpm, LPG with steam and gasoline are having COV of 10 and 11%, where as E20 and LPG alone are having COV of 7.5 and 6.5% respectively.

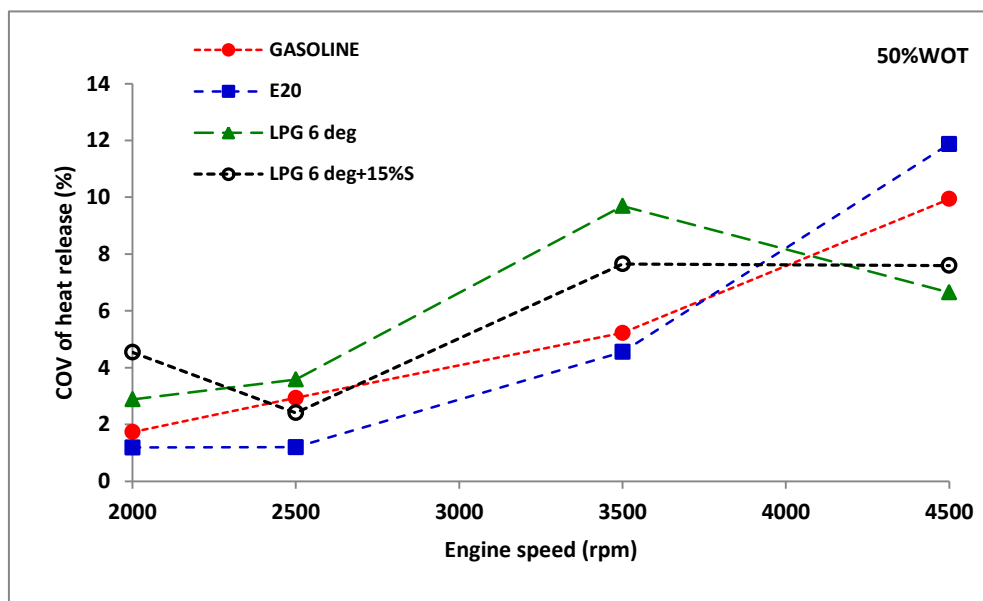


Fig. 5.106 COV of heat release per cycle for various fuels at 50%WOT

At 50%WOT the LPG fuels are resulting in higher COV till speeds of 3500 rpm. Later they are having COV less than that for E20 and gasoline.

### 5.5.4 Carbon monoxide (CO)

The CO emissions for various fuels are shown in figures 5.107 and 5.108 respectively for WOT and 50%WOT conditions. Comparatively LPG fuels are showing better CO reduction characteristics. At WOT and 3500 rpm the CO reduction for LPG+15% steam compared to E20 is from 1.88 to 0.9% by volume. Similar trends can be observed at 50%WOT condition also.



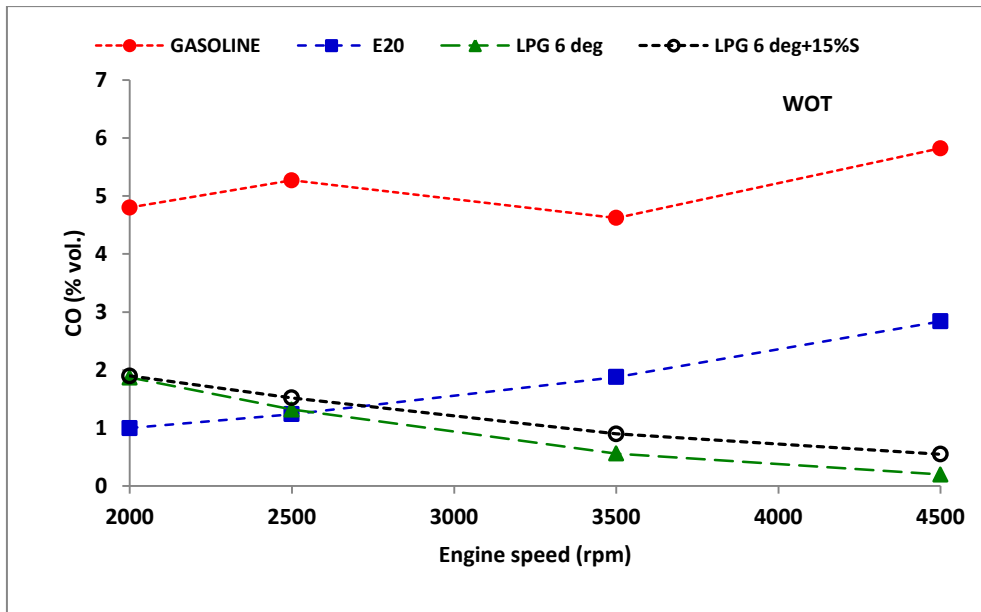


Fig. 5.107 CO for various fuels at WOT

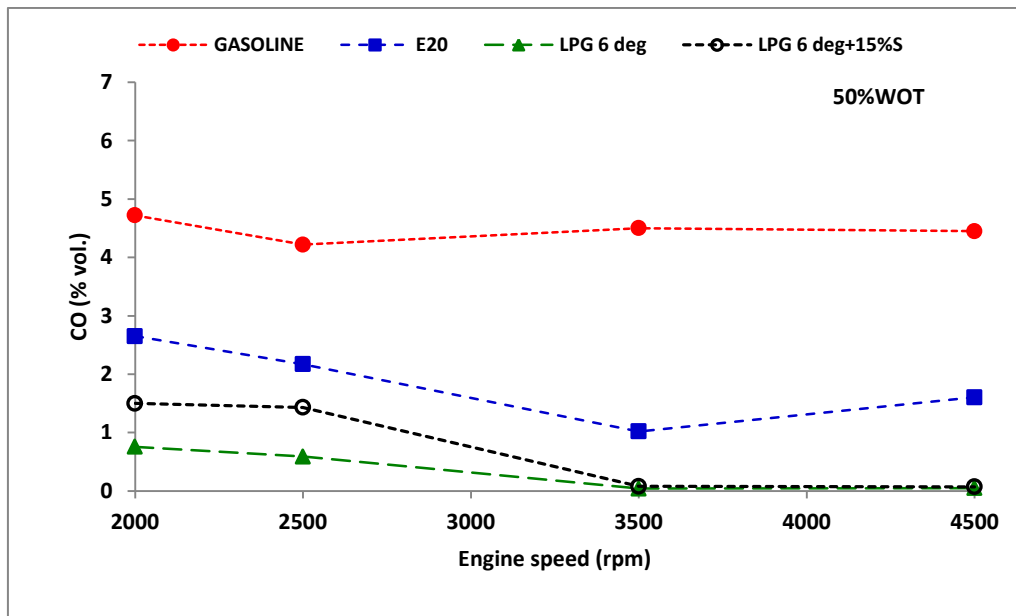


Fig. 5.108 CO for various fuels at 50%WOT

### 5.5.5 Hydrocarbon (HC)

The HC emissions at WOT and 50%WOT conditions are shown in figures 5.109 and 5.110 respectively. LPG fuels are resulting in ultra low HC emissions due to better combustion. For E20 and gasoline the HC emissions reduce gradually with speed, whereas for LPG fuels it is almost constant. Thus CO and HC emission

characteristics with LPG and LPG+15% steam are strongly advocating their use in SI engines.

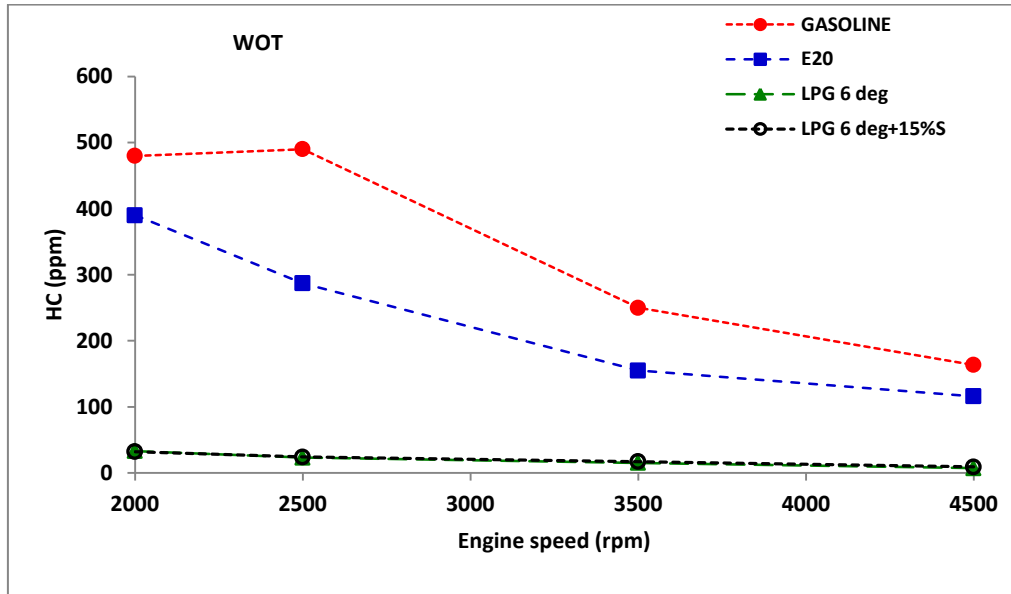


Fig. 5.109 HC for various fuels at WOT

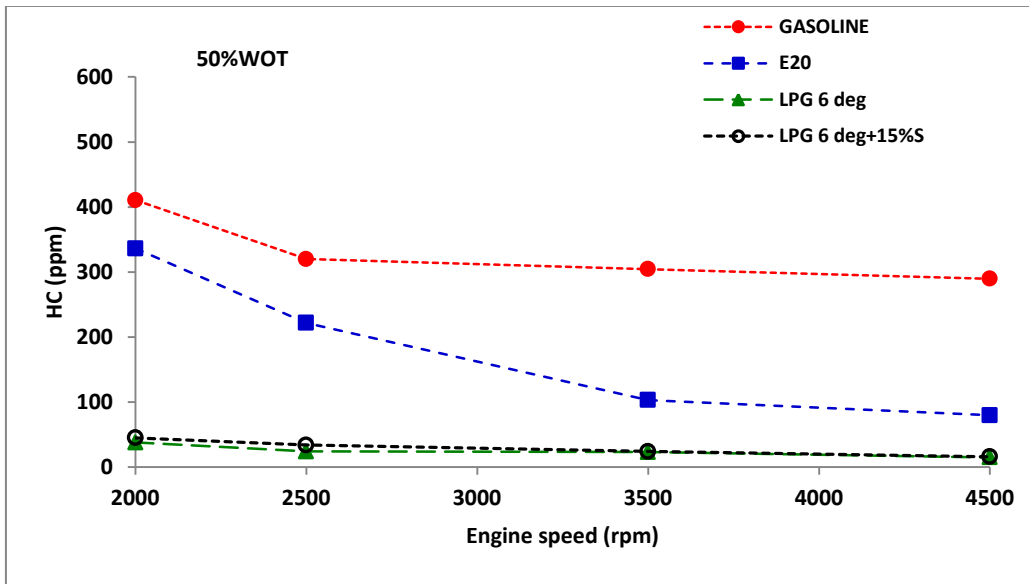


Fig. 5.110 HC for various fuels at 50%WOT

### 5.5.6 Oxides of nitrogen (NO<sub>x</sub>)

Figures 5.111 and 5.112 respectively show the trends of NO<sub>x</sub> at WOT and 50%WOT conditions for the various fuels. Steam induction has resulted in NO<sub>x</sub> values less than the ethanol enriched gasoline values up to 3500 rpm. At 3500 rpm, the reduction is

by 200 ppm. When compared to gasoline, LPG+15% steam is resulting in an increase of 150 ppm at same operating condition. At 50%WOT condition; the addition of steam has brought down the NO<sub>x</sub> emissions to about 125 ppm above that for E20.

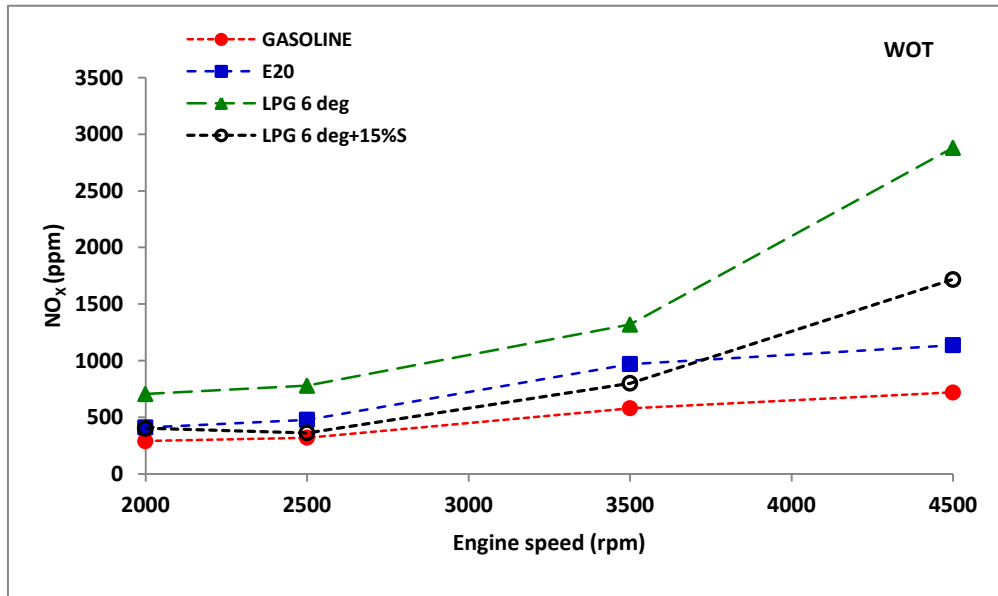


Fig. 5.111 NO<sub>x</sub> for various fuels at WOT

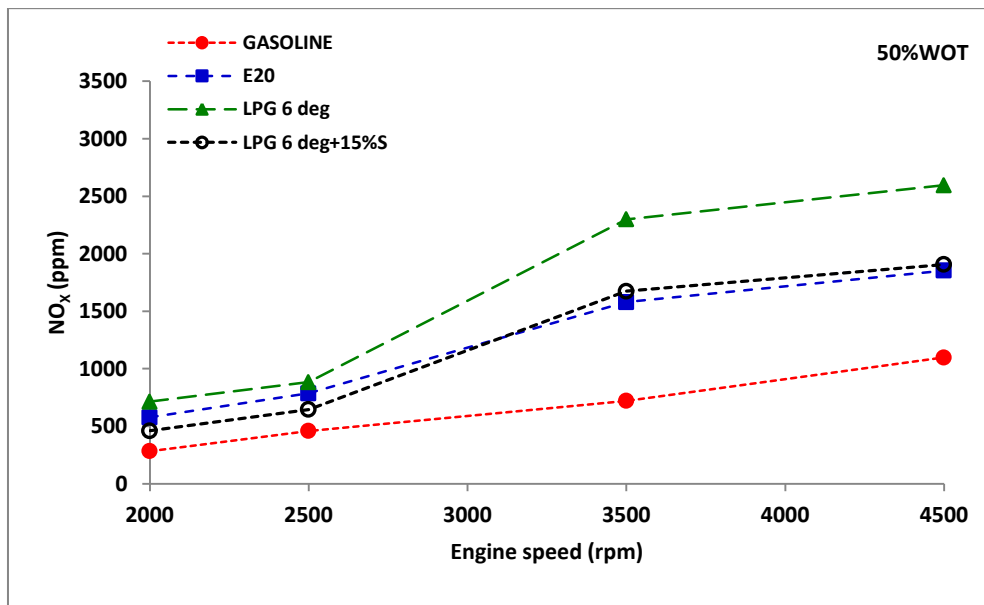


Fig. 5.112 NO<sub>x</sub> for various fuels at 50%WOT

This is a good result considering the near future of LPG being used extensively. However both LPG and E20 have higher NO<sub>x</sub> emissions compared to gasoline operation.

Tables 5.1, 5.2 and 5.3 below summarizes the major results of performance, combustion and emission studies with ethanol enriched gasoline blends, LPG at various static ignition timings and LPG along with steam induction respectively.

Table 5.1: Summary of performance, combustion and emission studies with ethanol enriched gasoline blends (at 3500 rpm)

	<b>WOT</b>	<b>50%WOT</b>
<b>Torque</b>	Increases with blends. E15, E20 gave better torque.	E10 gives comparable torque to gasoline.
<b>Brake thermal efficiency</b>	E20 blend gives the maximum efficiency. Increase is by 10.67 % and 8% for E20 and E15.	E20 has the highest efficiency. Increase is by 7.5 % & 2.8% for E20 and E15.
<b>BSEC</b>	Reduction is by 10.3 % & 8.1% for E20 and E15.	Reduction is by 7 % & 2.7% for E20 and E15.
<b>Cylinder pressure</b>	Above E10 increases the peak pressure.	Above E10 increases the peak pressure.
<b>COV of IMEP</b>	5.8% with E20, 2.4% with E15 compared to 5.7% with gasoline.	2.5% with E20, 2.9% with E15 compared to 3% with gasoline.
<b>COV of Heat release</b>	7.6% with E20, 10.4% with E15 compared to 11.2% with gasoline.	4.5% with E20, 5.7% with E15 compared to 5.2% with gasoline.
<b>CO</b>	Reduction is by 59.3% and 33.1% for E20 and E15.	Reduction is by 77.3% and 71.3% for E20 and E15.
<b>HC</b>	Reduction is by 46.4% and 23.9% for E20 and E15.	Reduction is by 66.2% and 63% for E20 and E15.
<b>NO<sub>x</sub></b>	Increase is by 67.2% and 39.7% for E20 and E15.	Increase is by 119.3% and 101.9% for E20 and E15.

Table 5.2: Summary of performance, combustion and emission studies with LPG at various static ignition timings (at 3500 rpm)

	<b>WOT</b>	<b>50%WOT</b>
<b>Torque</b>	67.3 Nm at 6 deg bTDC with LPG, 65.3 Nm at 5 deg.bTDC with LPG while 66.8 Nm at 5 deg.bTDC with gasoline.	56.3 Nm at 6 deg bTDC with LPG, 57.1 Nm at 5 deg.bTDC with LPG while 58.1 Nm at 5 deg.bTDC with gasoline.
<b>Brake thermal efficiency</b>	With LPG 3.5% and 1.7% increase at 6 & 5 deg. bTDC compared to gasoline at 5 deg. bTDC.	With LPG 2.98% and 2.3% decrease at 6 & 5 deg. bTDC compared to gasoline at 5 deg. bTDC.
<b>COV of IMEP</b>	With LPG 13.1% and 12.2% at 6 & 5 deg. bTDC compared to 5.7% with gasoline at 5 deg. bTDC.	With LPG 21.3% and 3.1% at 6 & 5 deg. bTDC compared to 3% with gasoline at 5 deg. bTDC.
<b>COV of Heat release</b>	With LPG 6.3% and 6.5% compared to 11.2% with gasoline at 5 deg. bTDC.	With LPG 9.7% and 5.5% compared to 5.2% with gasoline at 5 deg. bTDC.
<b>CO</b>	With LPG 87.87% and 71.86% reduction at 6 & 5 deg. bTDC compared to gasoline at 5 deg. bTDC.	99% and 95% reduction at 6 & 5 deg. bTDC compared to gasoline at 5 deg. bTDC.
<b>HC</b>	94% and 92% reduction at 6 & 5 deg. bTDC compared to gasoline at 5 deg. bTDC.	92.4% and 91.78% reduction at 6 & 5 deg. bTDC compared to gasoline at 5 deg. bTDC.
<b>NO<sub>x</sub></b>	127.4% and 10% increase at 6 & 5 deg. bTDC compared to gasoline at 5 deg. bTDC.	219.3% and 137.5% increase at 6 & 5 deg. bTDC compared to gasoline at 5 deg. bTDC.

Table 5.3: Summary of performance, combustion and emission studies of LPG along with steam induction (At 6 deg. bTDC, 3500 rpm)

	<b>WOT</b>	<b>50%WOT</b>
<b>Torque</b>	65.33 Nm and 63.42 Nm with 15% & 25% steam induction with LPG compared to 67.26 Nm for LPG.	52.3 Nm and 52.2 Nm with 15% & 25% steam induction with LPG compared to 53.3 Nm for LPG.
<b>Brake thermal efficiency</b>	3.19% and 6.13% reduction with 15% & 25% steam induction with LPG.	1.48% and 2.59% reduction with 15% & 25% steam induction with LPG.
<b>COV of IMEP</b>	29.56% and 21.82% with 15% & 25% steam induction with LPG compared to 13.08% for LPG.	22.88% and 26.81% with 15% & 25% steam induction with LPG compared to 21.33% for LPG.
<b>COV of Heat release</b>	10.22% and 10.68% with 15% & 25% steam induction with LPG compared to 6.32% for LPG.	7.65% and 6.43% with 15% & 25% steam induction with LPG compared to 9.69% for LPG.
<b>CO</b>	60.71% and 87.5% increase with 15% & 25% steam induction with LPG.	100% and 50% increase with 15% & 25% steam induction with LPG.
<b>HC</b>	13.335 and 60% increase with 15% & 25% steam induction with LPG.	4.3% and -17.3% increase with 15% & 25% steam induction with LPG.
<b>NO<sub>x</sub></b>	39.34% and 44.88% reduction with 15% & 25% steam induction with LPG.	27.18% and 45.15% reduction with 15% & 25% steam induction with LPG.

## 5.6 CONCLUSION

It can be concluded that use of ethanol enriched gasoline of E20 is superior alternative for unmodified multi-cylinder SI engine. The use of LPG is better suited for the use in SI engines with steam induction rate of 15% by mass as a means to reduce NO<sub>x</sub> emissions and to get comparable engine performance at 6 deg. bTDC advanced static ignition timings.

## CHAPTER 6

### CONCLUSIONS AND SCOPE FOR FUTURE WORK

#### 6.1 CONCLUSIONS

The present work was focused on the study of performance and emission characteristics of a four cylinder multipoint port fuel injection gasoline engine modified to run with LPG injection along with steam induction. The engine was modified to operate with injection of LPG by installing four gas injectors and separate gas ECU. Experiments were also carried out with different ethanol enriched gasoline blends of E5, E10, E15 and E20 to determine the baseline blend for comparative study. Experiments with LPG were carried out at various operating conditions of speed, throttle positions and static ignition timings. Various performance, combustion and emission characteristics were studied. A NO<sub>x</sub> reduction technique of steam induction along with LPG injection was developed. Steam flow rates of 10, 15, 20 and 25% by mass of LPG were used along with LPG.

The findings of the experimental work suggest that higher thermal efficiency and therefore improved fuel economy can be obtained from SI engines running on LPG as against gasoline. The results of the study at wide open throttle opening conditions indicate that there is an increase in the brake thermal efficiency with LPG use in the engine at higher operating speeds when compared to gasoline at the factory set static ignition timing of 5 deg. bTDC. Also the exhaust emissions CO and HC have reduced considerably. But the NO<sub>x</sub> emission has increased considerably at elevated engine speeds with LPG fuel when compared to gasoline fuel operation. The results of LPG fuel operation at various static ignition timings indicate that advancing the timing from 5 deg. bTDC to 6 deg. bTDC has resulted in increased brake thermal efficiency, and reduced emissions of CO and HC, compared to retarding the static ignition timing to 4 deg. bTDC and 3 deg. bTDC. However advanced static ignition timing has an adverse effect on NO<sub>x</sub> emissions as it further increases. The use of LPG along with steam induction as means to reduce NO<sub>x</sub> emissions has been successfully tested. The engine performance has only marginally compromised with the steam induction. But a significant reduction up to 45% in NO<sub>x</sub> emissions has been achieved.

The major findings of the experimental research work can be summarized as follows:

- Results have shown that among the various ethanol enriched gasoline fuel blend E20 was the most suitable one from the engine performance and CO & HC emissions points of view. Hence it can be taken as optimized ethanol enriched gasoline at pre-set static ignition timing of 5 deg. bTDC.
- The engine performance has improved with the addition of ethanol, and for E20 at WOT & 3500 rpm, torque increases by 2% and BTE increases by 10.67% when compared to gasoline.
- All the ethanol enriched gasoline fuels have lower COV of IMEP values compared to gasoline fuel operation at WOT with E20 showing an average reduction by 2% over the entire speed range.
- Significant reductions in the CO & HC emissions were achieved while the NO<sub>x</sub> emissions have shown an increasing trend with ethanol enriched gasoline fuels. With E20 at WOT & 3500 rpm value of CO has reduced by 59%, HC reduced by 46% and NO<sub>x</sub> increased by 67%.
- The findings of the experiments with LPG indicate that improved engine performance can be obtained from SI engines running on LPG when compared to gasoline at the pre set static ignition timing of 5 deg. bTDC. Better performance with LPG has been achieved when ignition timing was advanced to 6 deg. bTDC with 3.11% increase in torque at WOT & 3500 rpm compared to LPG combustion at 5 deg. bTDC.
- Advancing the static ignition timing to 6 deg. bTDC has resulted in reduced CO and HC emissions. The CO emissions has reduced by 88% and HC has reduced by 94% compared to gasoline at WOT and 3500 rpm. But the NO<sub>x</sub> emissions has increased by 2 times compared to LPG combustion at 5 deg. bTDC, WOT & 3500 rpm.
- LPG with steam induction has marginally reduced the thermal efficiency due to the dilution of the charge. At WOT & 3500 rpm, the torque decreased by 3% while BTE has decreased by 1.03% when compared to LPG alone at 6 deg. bTDC. The COV of IMEP has increased by 6.15% at the above conditions.



- It has been found that NO<sub>x</sub> emissions have reduced significantly by 20 - 45% over the entire operating speed range with the induction of steam with a reduction of 40% at WOT, 3500 rpm for LPG with 15% steam induction compared to LPG alone at 6 deg. bTDC. No considerable changes in CO and HC emissions were observed.
- Addition of steam in proportions more than 15 %, the benefit of NO<sub>x</sub> reduction is marginal. Hence LPG with 15% steam at 6 deg. bTDC is better choice compared to LPG alone.
- However, compared to ethanol enriched gasoline at 5 deg. bTDC for LPG with 15% steam at 6 deg. bTDC, the thermal efficiency has reduced by 3.23%, COV of IMEP has increased by 15% while the NO<sub>x</sub> emissions has reduced by 17% at WOT and 3500 rpm.

It can be concluded that use of ethanol enriched gasoline of E20 is superior alternative for unmodified multi-cylinder SI engine. The results showed that when running with LPG along with steam induction, it worked as a cooling means for the fuel-air charge and slowing the burning rates, resulting in reduction of the peak combustion temperature. It is found that NO<sub>x</sub> emissions have reduced significantly by 20 - 45% over the entire operating range when compared to baseline LPG. No considerable changes in CO and HC emissions were observed. Hence use of LPG with advanced ignition timing of 6 deg. bTDC with steam induction up to 25% steam to LPG mass ratio at higher engine speeds and up to 10% steam to LPG mass ratio at lower engine speeds can be used. When comparing the performance and emissions of ethanol enriched gasoline and LPG with steam induction, it is noted that, comparatively E20 blends performs better than LPG alone. With steam, the performance with LPG deteriorates. Emissions of CO are reduced with LPG when compared to E20. But a slight increment is noted when steam is inducted. NO<sub>x</sub> emissions are higher for both E20 and LPG when compared to gasoline. However, with the induction of steam, LPG NO<sub>x</sub> can be substantially brought down, but still it is slightly higher when compared to E20.

Test results of ethanol enriched gasoline blends in the car engine indicate that the engine can perform better with ethanol blending, with reduction in exhaust emissions

of CO and HC, with exception of NO<sub>x</sub> increase. Blending up to 20% of ethanol has been tested in a conventional 4 cylinder MPFI engine. Use of LPG injection in the existing MPFI gasoline engine has been tested successfully. Use of steam induction to reduce the NO<sub>x</sub> emissions has been successfully tested. For producing steam the innovative technique of waste gas heat exchanger has been used. A copper tube coiled around the engine exhaust pipe serves as the heat exchanger.

From the experimental investigations it can be concluded that use of ethanol enriched blends in unmodified engine is still a superior alternate for the use of gasoline or LPG as a sole fuel. However with the current option of LPG as alternative fuel to SI engines, it can be used along with steam induction as a means to considerably reduce NO<sub>x</sub> emissions, with marginal reduction in engine performance.

Table 6.1 summarizes the experimentally optimized operating range of major parameters based on the results obtained.

Table 6.1: Experimentally optimized operating range of major parameters

		<b>Ethanol enriched gasoline</b>	<b>LPG</b>	<b>LPG with steam</b>
<b>Engine speed</b>	Performance	3500-4500 rpm	3500-4500 rpm	3500-4500 rpm
	Combustion	<3500 rpm	<3500 rpm	<3500 rpm
	Emissions	>3500 rpm (HC) <3500 rpm (NO <sub>x</sub> )	>3500 rpm <3500 rpm (NO <sub>x</sub> )	>3500 rpm <3500 rpm (NO <sub>x</sub> )
<b>Throttle valve opening</b>	Performance	>50% WOT	100% WOT	100% WOT
	Combustion	50%-75% WOT	100% WOT	100% WOT
	Emissions	75%-100% WOT	100% WOT	100% WOT
<b>Static ignition timing (CA bTDC)</b>	Performance	-	6 deg. bTDC	6 deg. bTDC
	Combustion	-	5 deg. bTDC	5/6 deg. bTDC
	Emissions	-	6 deg. bTDC (CO/HC) 4 deg. bTDC (NO <sub>x</sub> )	6 deg. bTDC (CO/HC) 4/5 deg. bTDC (NO <sub>x</sub> )
<b>Ethanol enriched gasoline blend ratio</b>	Performance	E15-E20	-	-
	Combustion	E15	-	-
	Emissions	E15-E20 E5-E10 (NO <sub>x</sub> )	-	-
<b>Steam induction rate (% mass)</b>	Performance	-	-	10-15%
	Combustion	-	-	10%
	Emissions	-	-	10-15% (CO/HC) 20-25% (NO <sub>x</sub> )

## 6.2 SCOPE FOR FUTURE WORK

The experimental investigation carried out in this research throws light over many possibilities of future studies. These include fuel modification, fuelling strategy, comparative studies with other NO<sub>x</sub> reduction methods etc. Some of the future works which can be taken up are listed below:

1. Dual fuel operation of gasoline and LPG can be studied and the results can be compared with use of LPG alone.
2. Direct injection of water in to combustion chamber can be devised and the results can be compared.
3. Other NO<sub>x</sub> reduction techniques like EGR, SCR can be used and compared with the steam induction technique when the engine is running on LPG.
4. Liquid LPG (LiLPG) injection can be done instead of using vaporizer, and the results can be compared.
5. Combustion studies with more than 500 combustion cycles can be done.
6. With the installation of a programmable ECU, the engine can be run with different equivalence ratios at a given operating condition so that the lean burn limit of LPG can be studied. With the help of programmable ECU, the pulse width of LPG injection can be modified.
7. Engine studies can be conducted in the modified setup using CNG as another alternate gaseous fuel, since the existing gas injection system can be used for injecting CNG also.
8. Since ethanol blending also results in higher NO<sub>x</sub> emissions, some kind of NO<sub>x</sub> reduction technique can be used.
9. Computer simulation studies of LPG combustion and NO<sub>x</sub> reduction by steam induction can be done.

## REFERENCES

1. Abd-Alla, G. H., (2002), "Using exhaust gas recirculation in internal combustion engines: A review", *Energy Conversion and Management*, 43, pp.1027–1042.
2. Abdel-Rahman, A. A. and Osman, M. M., (1998), "Experimental investigation on varying the compression ratio of SI engine working under different ethanol-gasoline fuel blends", *International Journal of Energy Research*, Volume 21, Issue 1, pp. 31–40.
3. Adnan, R., Masjuki, H. H. and Mahlia, T. M. I., (2012), "Performance and emission analysis of hydrogen fueled compression ignition engine with variable water injection timing", *Energy*, 43, pp. 416-426.
4. Agarwal, A. K., (2007), "Biofuels (alcohols and biodiesel) applications as fuels for internal combustion engines", *Progress in Energy and Combustion Science*, 33, pp. 233–271.
5. Agarwal, D., Singh, S. K. and Agarwal, A. K., (2011), "Effect of Exhaust Gas Recirculation (EGR) on performance, emissions, deposits and durability of a constant speed compression ignition engine", *Applied Energy*, 88, pp. 2900–2907.
6. Agrawal, A. K., Singh, S. K., Sinha, S. and Shukla, M. K., (2004), "Effect of EGR on the exhaust gas temperature and exhaust opacity in compression ignition engines", *Sadhana*, Vol. 29, Part 3, pp. 275–284.
7. Al-Farayedhi, A. A., Al-Dawood, A. M. and Gandhidasan, P., (2004), "Experimental investigation of SI engine performance using oxygenated fuel", *Journal of Engineering for Gas Turbines and Power*, Transactions of the ASME, Vol. 126, pp. 178-191.
8. Al-Hasan, M., (2003), "Effect of ethanol–unleaded gasoline blends on engine performance and exhaust emission", *Energy Conversion and Management*, 44, pp. 1547–1561.
9. Asad Naeem Shah, Yun-Shan Ge, Lei Jiang and Zhi-Hua Liu, (2009), "Performance evaluation of a urea-water selective catalytic reduction (SCR) for

- controlling the exhaust emissions from a diesel engine”, *Turkish J. Eng. Env. Sci*, 33, pp. 259 – 271.
10. Badar, O., Alsayed, N. and Manaf, M., (1998), “A parametric study on the lean misfiring and knocking limits of gas fuelled spark ignition engine”, *Applied Thermal Engineering*, Vol. 18, No. 7, pp. 579-594.
  11. Bae, C., Koo, J. and Cho, Y., (2001), “Exhaust gas recirculation in a spark-ignition LPG engine”, *Proceedings of the Third Asia-Pacific Conference on Combustion*, Seoul, Korea, No. A134.
  12. Bayraktar, H. and Durgun, O., (2005), “Investigating the effects of LPG on spark ignition engine combustion and performance”, *Energy Conversion and Management*, 46, pp. 2317–2333.
  13. Bayraktar, H., (2005), “Experimental and theoretical investigation of using gasoline–ethanol blends in spark-ignition engines”, *Renewable Energy*, 30, pp. 1733–1747.
  14. Beroun, Stanisiav, Martins, and Jorge, (2001), “The development of gas (CNG, LPG, H<sub>2</sub>) engines for buses and trucks and their emission and cycle variability characteristics”, *SAE Paper*, 2001-01-0144.
  15. Bielaczyc, P., Szczotka, A. and Brodzinski, H., (2001), “Analysis of the exhaust emissions from vehicles fuelled with petrol or LPG and CNG alternatively”, *Journal of Kones. Combustion Engines*, Vol. 8, No. 1-2, pp. 363-369.
  16. Blazek, J., (2004), “The combustion process analysis by means of in-cylinder pressure measurement”, *Proceedings of the International Scientific Meeting Motor Vehicles & Engines*, Kragujevac, Czech Republic, No. YU04019.
  17. Brown, B. R., (2001), “Combustion data acquisition and analysis”, *M.Engg. Project Report*, No. 00TTD010, Department of Aeronautical and Automotive Engineering, Loughborough University.
  18. Brusstar, M., Stuhldreher, M., Swain, D. and Pidgeon, W., (2002), “High efficiency and low emissions from a port-injected engine with neat alcohol fuels”, *SAE paper*, 2002-01-2743.
  19. Catania, A. E., Misul, D., Mittica, A. and Spessa, E., (2001), “A refined two-zone heat release model for combustion analysis in SI engines”, *Proc. of the fifth*

- international symposium on diagnostics and modeling of combustion in internal combustion engines (COMODIA 2001)*, Nagoya, pp. 290-299.
20. Caton, J. A., McDermott, M. and Chone, R., (1997), "Development of a dedicated LPG-fueled spark-ignition engine and vehicle for the 1996 propane vehicle challenge", *SAE Paper*, 972692.
  21. Celik, M. B., (2008), "Experimental determination of suitable ethanol–gasoline blend rate at high compression ratio for gasoline engine", *Applied Thermal Engineering*, 28, pp. 396–404.
  22. Ceviz, M. A. and Yuksel, F., (2005), "Effects of ethanol–unleaded gasoline blends on cyclic variability and emissions in an SI engine", *Applied Thermal Engineering*, 25, pp. 917–925.
  23. Ceviz, M.A. and Yuksel, F., (2006), "Cyclic variations on LPG and gasoline-fuelled lean burn SI engine", *Renewable Energy*, 31, pp. 1950–1960.
  24. Cheng, W. K., Hamrin, D. and Heywood, J. B., (1993), "An overview of hydrocarbon emissions mechanisms in spark-ignition engine", *SAE Paper*, 932708.
  25. Dagaut, P. and Ali, K. H., (2003), "Kinetics of oxidation of a LPG blend mixture in a JSR: experimental and modeling study", *Fuel*, vol. 82, pp. 475–480.
  26. Das, S. K., (2011), "Energy statistics 2011", *Central statistics office, Ministry of statistics and programme implementation*, Government of India, New Delhi, Eighteenth Issue, [www.mospi.gov.in](http://www.mospi.gov.in).
  27. Einewall, P. and Johansson, B., (2000), "cylinder to cylinder and cycle to cycle variations in a six cylinder lean burn natural gas engine", *SAE Paper*, 2000-01-1941.
  28. Eriksson, L. and Andersson, I., (2002), "An analytic model for cylinder pressure in a four stroke SI engine", *SAE paper*, 2002-01-0371.
  29. Eyidogan, M., Ozsezen, A. N., Canakci, M. and Turkcan, A., (2010), "Impact of alcohol–gasoline fuel blends on the performance and combustion characteristics of an SI engine", *Fuel*, 89, pp. 2713–2720.
  30. Fontana, G. and Galloni, E., (2010), "Experimental analysis of a spark-ignition engine using exhaust gas recycle at WOT operation", *Applied Energy*, Volume 87, Issue 7, pp. 2187-2193

31. Franz, B. and Roth, P., (2000), "Injection of a H<sub>2</sub>O<sub>2</sub>/water solution into the combustion chamber of a direct injection diesel engine and its effect on soot removal", *Proceedings of the Combustion Institute*, 28, pp. 1219-1225.
32. Furuhashi, T., Kawata, T., Mizukoshi, N. and Arai, M., (2010), "Effect of steam addition pathways on NO reduction characteristics in a can-type spray combustor", *Fuel*, 89, pp. 3119-3126.
33. Gadallah, A. H., Elshenawy, E. A., Elzahaby, A. M., El-Salmawy, F. A. and Bawady, A. H., (2009), "Effect of direct water injection on performance and emissions of a hydrogen fuelled direct injection engine" *Proceedings of the International Conference EVER09*, Monaco, Paper No. 178.
34. Gatowski, J. A., Balles, E. N.K., Chun, M., Nelson, F. E., Ekchian, J. A. and Heywood, J. B., (1984), "Heat release analysis of engine pressure data", *SAE paper*, 841359, 5.961-5.997.
35. Ghojel, J. and Honnery, D., (2005), "Heat release model for the combustion of diesel oil emulsions in DI diesel engines", *Applied Thermal Engineering*, 25, pp. 2072–2085.
36. Goering, C. E., (1998), "Engine heat release via spread sheet", *Transactions of the ASAE*, Vol. 41(5), pp. 1249-1253.
37. Goto, S., Lee, D., Harayama, N., Honjo, F., Ueno, H., Honma, H., Wakao, Y. and Mori, M., (2000), "Development of LPG SI and CI engines for heavy duty vehicles", *Proceedings of the Seoul 2000 FISITA World Automotive Congress*, Seoul, Korea, No. F2000A171.
38. Gumus, M., (2011), "Effects of volumetric efficiency on the performance and emissions characteristics of a dual fueled (gasoline and LPG) spark ignition engine", *Fuel Processing Technology*, 92, pp. 1862–1867.
39. Han, S. B., (2000), "Cycle-to-cycle variations under cylinder-pressure-based combustion analysis in spark ignition engines", *KSME International Journal*, Vol. 14, No. 10, pp. 1151-1158.
40. Heywood, J. B., (1988), "Internal combustion engines fundamentals", *McGraw Hill Book Company*, New York.



41. Hoekstra, R. L., Blarigan, P. V. and Mulligan, N., (1996), "NO<sub>x</sub> emissions and efficiency of hydrogen, natural gas, and hydrogen/ natural gas blended fuels", *SAE Paper*, 961103.
42. Hsieh, W., Chen, R., Wu, T. and Lin, T., (2002), "Engine performance and pollutant emission of an SI engine using ethanol–gasoline blended fuels", *Atmospheric Environment*, Volume 36, Issue 3, pp. 403-410.
43. Huang, Z., Miao, H., Zhou, L. and Jiang, D., (2000), "Combustion characteristics and hydrocarbon emissions of a spark ignition engine fuelled with gasoline-oxygenate blends", *Proc. IMechE, Part D: Journal of Automobile Engineering*, Volume 214, Number 3, pp. 341-346.
44. IMPCO Technologies, (1998), "Additional development of a dedicated liquefied petroleum gas (LPG) ultra low emissions vehicle (ULEV)", *National Renewable Energy Laboratory report*, NREL/SR-540-25155.
45. Ishli, K., Sasaki, T., Urata, Y. and Ohno, T., (1997), "Investigation of cyclic variation of IMEP under lean burn operation in spark-ignition engine", *SAE Paper*, 972830.
46. Jeuland, N., Montagne, X. and Gautrot, X., (2004), "Potentiality of Ethanol as a Fuel for Dedicated Engine", *Oil & Gas Science and Technology – Rev. IFP*, Vol. 59, No. 6, pp. 559-570.
47. Johnson, E., (2003), "LPG: a secure, cleaner transport fuel? A policy recommendation for Europe", *Energy Policy*, vol. 31, pp. 1573–1577.
48. Jothi, N. K. M., Nagarajan, G. and Renganarayanan, S., (2008), "LPG fueled diesel engine using diethyl ether with exhaust gas recirculation". *International Journal of Thermal Sciences*, 47, pp. 450–457.
49. Kadam, K. L., (2002), "Environmental benefits on a life cycle basis of using bagasse-derived ethanol as a gasoline oxygenate in India", *Energy Policy*, 30, pp. 371–384.
50. Kalaghatgi, G. T., (1987), "Spark ignition, early flame development and cyclic variation in I.C. engines", *SAE Paper*, 870163.
51. Kaminski, T., Wendeker, M., Urbanowicz, K. and Litak, G., (2004), "Combustion process in a spark ignition engine: dynamics and noise level estimation", *Chaos*, 14, pp. 461-466.

52. Khatri, D. S., Singh, V., Pal, N. K., Maheshwari, M., Singh, S., Chug, S., Singh, R. and Bhat, A., (2009), "HCNG evaluation using a sequential gas injection system for a passenger car". *SAE Paper*, 2009-26-30.
53. Kim, C. and Bae, C., (1999), "Hydrocarbon emissions from a gas fueled SI engine under lean burn conditions", *SAE paper*, 1999-01-3512.
54. Knapp, K. T., Stump, F. D. and Tejada, S. B., (1998), "The effect of ethanol fuel on the emissions of vehicles over a wide range of temperatures", *J. Air & Waste Manage. Assoc.*, Vol. 48, pp. 646-653.
55. Kowalewicz, A., (2000), "Lean-Burn Engine – Potential Analysis", *Proceedings of the Seoul 2000 FISITA World Automotive Congress*, Seoul, Korea, No. F2000A141.
56. Kowalewicz, A., (2001), "Lean-burn engine-potential analysis", *International Journal of Automotive Technology*, Vol. 2, No. 4, pp. 147-155.
57. Kumar, A., Khatri, D. S. and Babu, M. K. G., (2009), "An investigation of potential and challenges with higher ethanol-gasoline blend on a single cylinder spark ignition research engine", *SAE paper*, 2009 - 01 – 0137.
58. Kuo, P. S., (1996), "Cylinder pressure in a spark-ignition engine: a computational model", *J. Undergrad. Sci. Engineering Sciences*, 3: (Fall 1996), pp. 141-145.
59. Lanzafame, R., (1999), "Water injection effects in a single-cylinder CFR engine", *SAE paper*, 1999-01-0568.
60. Larbi, N. and Bessrou, J., (2010), "Measurement and simulation of pollutant emissions from marine diesel combustion engine and their reduction by water injection", *Advances in Engineering Software*, 41, pp. 698-906.
61. Lee, K. and Ryu, J., (2005), "An experimental study of the flame propagation and combustion characteristics of LPG fuel", *Fuel*, 84, pp.1116-1127.
62. Lee, K. W. and Kim, K., (2001), "Influence of initial combustion in SI engine on following combustion stage and cycle-by-cycle variations in combustion process", *International Journal of Automotive Technology*, Vol. 2, No. 1, pp. 25-31 .
63. Lee, S., Oh, S. and Choi, Y., (2009), "Performance and emission characteristics of an SI engine operated with DME blended LPG fuel", *Fuel*, 88, pp. 1009–1015.

64. Litak, G., Kaminski, T., Czarnigowski, J., Sen, A. K. and Wendeker, M., (2009), “Combustion process in a spark ignition engine: analysis of cyclic peak pressure and peak pressure angle oscillations”, *Meccanica*, 44: 1–11.
65. Litak, G., Wendeker, M., Krupa, M. and Czarnigowski, J., (2004), “A numerical study of a simple stochastic/deterministic model of cycle-to-cycle combustion fluctuations in spark ignition engines”, 23 May 2004, <http://www.arxiv.org/abs/nlin/0405054v1>.
66. Loganathan, M. and Ramesh, A., (2007), “Study on manifold injection of LPG in two stroke SI engine”, *Journal of the Energy Institute*, Vol. 80, No. 3, pp. 168-174.
67. Mafra, M. R., Fassani, F. L., Zanoelo, E. F. and Bizzo, W. A., (2010), “Influence of swirl number and fuel equivalence ratio on NO emission in an experimental LPG-fired chamber”, *Applied Thermal Engineering*, 30, pp. 928-934.
68. Maiboom, A. and Tauzia, X., (2011), “NO<sub>x</sub> and PM emissions reduction on an automotive HSDI Diesel engine with water-in-diesel emulsion and EGR: An experimental study”, *Fuel*, 90, pp. 3179–3192.
69. Masi, M. and Gobato, P., (2012), “Measure of the volumetric efficiency and evaporator device performance for a liquefied petroleum gas spark ignition engine”, *Energy Conversion and Management*, 60, pp.18–27.
70. Mendera, K. Z., (2004), “Thermodynamic analysis of spark ignition engine pressure data”, *Journal of KONES Internal Combustion Engines*, Vol. 11, No.3-4, pp. 45-52.
71. Moffat, R. J., (1982), “Contributions to the theory of single-sample uncertainty analysis”, *Transactions of the ASME- Journal of Fluids Engineering*, Vol. 104, pp. 250-258.
72. Murillo, S., Miguez, J. L., Porteiro, J., Gonzalez, L. M. L., Granada, E. and Moran, J. C., (2005), “LPG: Pollutant emission and performance enhancement for spark-ignition four strokes outboard engines”, *Applied Thermal Engineering*, 25, pp. 1882–1893.
73. Mustafa, K. F. and Briggs, H. W. G., (2008), “Effect of variation in liquefied petroleum gas (LPG) proportions in spark ignition engine emissions”, *Proceedings of the International Conference on Environment-08*.

74. Myung, C. L., Choi, K., Kim, J., Lim, Y., Lee, J. and Park, S., (2012), “Comparative study of regulated and unregulated toxic emissions characteristics from a spark ignition direct injection light-duty vehicle fueled with gasoline and liquid phase LPG (liquefied petroleum gas)”, *Energy*, vol. 44, issue 1, pp. 189–196.
75. Najafi, G., Ghobadian, B., Tavakoli, T., Buttsworth, D. R., Yusaf, T. F. and Faizollahnejad, M., (2009), “Performance and exhaust emissions of a gasoline engine with ethanol blended gasoline fuels using artificial neural network”, *Applied Energy*, 86, pp. 630–639.
76. Nguyen, Q. A. and Wu, Y. Y., (2009), “Experimental investigations of using water-gasoline emulsions as a NO<sub>x</sub> treatment and its effects on performance and emissions of lean-burn spark-ignition engine”, *Proceedings of the International Conference on Power Engineering-09 (ICOPE-09)*, Kobe, Japan.
77. Niven, R. K., (2005), “Ethanol in gasoline: environmental impacts and sustainability review article”, *Renewable and Sustainable Energy Reviews*, 9, pp. 535–555.
78. Oh, S., Kim, S., Bae, C., Kim, C. and Kang, K., (2002), “Flame propagation characteristics in a heavy duty LPG engine with liquid phase port injection”, *SAE paper*, 2002-01-1736.
79. Ozcan, H. and Soylemez, M. S., (2005), “Thermal balance of LPG fuelled, four stroke SI engine with water addition”, *Energy conversion and Management*, 47, pp. 570-581.
80. Ozcan, H. and Soylemez, M. S., (2005a), “Experimental investigation of the effects of water addition on the exhaust emissions of a naturally aspirated, liquefied-petroleum-gas-fueled engine”, *Energy and Fuels*, 19, pp. 1468-1472.
81. Ozdor, N., Dulger, M. and Sher, E., (1994), “Cyclic variability in spark ignition engines-a literature survey”, *SAE Paper*, 940987.
82. Ozsezen, A. N. and Canakci, M., (2011), “Performance and combustion characteristics of alcohol gasoline blends at wide-open throttle”, *Energy*, 36, pp. 2747-2752.

83. Pohit, S., Biswas, P. K., Kumar, R., Jha, J., (2009), "International experiences of ethanol as transport fuel: Policy implications for India", *Energy Policy*, vol. 37, pp. 4540–4548.
84. Prasath, B. R., Porai, P. T. and Shabir, M. F., (2010), "Two-zone modeling of diesel / biodiesel blended fuel operated ceramic coated direct injection diesel engine", *International Journal of Energy and Environment*, Volume 1, Issue 6, pp. 1039-1056.
85. Price, P., Guo, S. and Hirschmann, M., (2004), "Performance of an evaporator for a LPG powered vehicle", *Applied Thermal Engineering*, vol. 24, pp. 1179–1194.
86. Pundir, B. P., Zvonow, V. A. and Gupta, C. P., (1981), "Effect of charge non-homogeneity on cycle-by-cycle variations in combustion in SI engines", *SAE Paper*, 810774.
87. Rajan, S. and Sanjeev, F. F., (1983), "Water-ethanol gasoline blends as spark ignition engine fuels", *Fuel*, Vol 62, pp. 117-121.
88. Ramachandran, S., (2009), "Rapid thermodynamic simulation model of an internal combustion engine on alternate fuels", *Proceedings of the International Multi Conference of Engineers and Computer Scientists 2009*, Hong Kong, Vol. II.
89. Ray, S., Miglani, S., Goldar, A., (2011), "Ethanol blending policy in India: Demand and supply issues", *ICRIER policy series* (Indian Council for Research on International Economic Relations), No.9, Dec, 2011.
90. Sadiq Al-Baghdadi, M. A. R., (2001), "The safe operation zone of the spark ignition engine working with dual renewable supplemented fuels (hydrogen+ethyl alcohol)", *Renewable Energy*, 22, pp. 579–583.
91. Saraf, R. R., Thipse, S. S. and Saxena, P. K., (2009), "Comparative emission analysis of gasoline/LPG automotive bifuel engine", *International Journal of Environmental Science and Engineering*, 1:4, pp. 198-201.
92. Saravanan N. and Nagarajan G. (2009), "An insight on hydrogen fuel injection techniques with SCR system for NO<sub>x</sub> reduction in a hydrogen–diesel dual fuel engine", *International Journal of hydrogen energy*, 34(2009), pp. 9019–9032.

93. Sessaiah, N., (2010), "Efficiency and exhaust gas analysis of variable compression ratio spark ignition engine fuelled with alternative fuels", *International Journal of Energy and Environment*, Volume 1, Issue 5, pp.861-870.
94. Shehata, M. S., (2010), "Cylinder pressure, performance parameters, heat release, specific heats ratio and duration of combustion for spark ignition engine", *Energy*, 35, pp.4710-4725.
95. Shenghua, L., Clemente, E. R. C., Tiegang, H. and Yanjv, W., (2007), "Study of spark ignition engine fueled with methanol/gasoline fuel blends", *Applied Thermal Engineering*, 27, pp. 1904–1910.
96. Shiao, Y. and Moskwa, J. J., (1995), "Cylinder pressure and combustion heat release estimation for SI engine diagnostics using nonlinear sliding observers", *IEEE transactions on control systems technology*, Vol. 3, No. I, pp. 70-78.
97. Srinivasan, C. A. and Saravanan, C. G., (2010), "Study of combustion characteristics of an SI engine fuelled with ethanol and oxygenated fuel additives", *Journal of Sustainable Energy & Environment*, 1, pp. 85-91.
98. Subramanian, K. A., (2011), "A comparison of water–diesel emulsion and timed injection of water into the intake manifold of a diesel engine for simultaneous control of NO and smoke emissions", *Energy Conversion and Management*, 52, pp. 849–857.
99. Subramanian, V., Mallikarjuna, J. M., Ramesh, A., (2007), "Effect of water injection and spark timing on the nitric oxide emission and combustion parameters of a hydrogen fuelled spark ignition engine", *International Journal of Hydrogen Energy*, 32, pp.1159-1173.
100. Tauzia, X., Maiboom, A. and Shah, S. R., (2010), "Experimental study of inlet manifold water injection on combustion and emissions of an automotive direct injection diesel engine", *Energy*, 35, pp. 3628-3639.
101. Tazerout, M., Le Corre, O. and Ramesh, A., (2000), "A new method to determine the start and end of combustion in an internal combustion engine using entropy changes", *Int.J. Applied Thermodynamics*, Vol.3, (No.2), pp. 49-55.
102. Tesfa, B., Mishra, R., Gu, F. and Ball, A. D., (2012), "Water injection effects on the performance and emission characteristics of a CI engine operating with biodiesel", *Renewable Energy*, 37, pp. 333-344.

103. Topgul, T., Yucesu, H. S., Cinar, C. and Koca, A., (2006), "The effects of ethanol–unleaded gasoline blends and ignition timing on engine performance and exhaust emissions", *Renewable Energy*, 31, pp. 2534–2542.
104. Vianna, J. N. S., Reis, A. V., Oliveira, A. B. S., Fraga, A. G. and De Sousa, M. T., (2005), "Reduction of pollutants emissions on SI engines - accomplishments with efficiency increase", *J. of the Braz. Soc. of Mech. Sci. & Eng.*, Vol. XXVII, No. 3, pp. 217-222.
105. Villarroel, M., (2004), "The effects of cycle-to-cycle variations on nitric oxide (NO) emissions for a spark-ignition engine: numerical results", *Master of Science thesis*, Texas A&M University.
106. Whitelaw, J. H. and Xu, H. M., (1995), "Cyclic variations in lean-burn spark ignition engine without and with swirl", *SAE Paper*, 950683.
107. Woo, Y. and Bae, C., (2007), "Stratified exhaust gas recirculation under lean operation of a liquefied petroleum gas spark ignition engine with liquid phase injection", *Proc. IMechE, Part D: J. Automobile Engineering*, Vol. 221.
108. Woo, Y., Yeom, K., Bae, C., Oh, S. and Kang, K., (2004), "Effects of stratified EGR on the performance of a liquid phase LPG injection engine", *SAE paper*, 2004-01-0982.
109. Yamamoto, H. and Misumi, M., (1987), "Analysis of cyclic combustion variation in a Lean operating SI engine", *SAE Paper*, 870547.
110. Yamin, J. A. and Badran, O.O., (2001), "Analytical study to minimise the heat losses from a propane powered 4-stroke spark ignition engine", *Renewable Energy*, 27, pp. 463–478.
111. Young, M. B., (1982), "Cyclic dispersion in the homogeneous-charge spark-ignition engine-a literature survey", *SAE Paper*, 810026.
112. Yousufuddin, S. and Mehdi, S. N., (2008), "Performance and emission characteristics of LPG-fuelled variable compression ratio SI engine", *Turkish J. Eng. Env. Sci.*, 32, pp. 7 – 12.
113. Yuksel, F. and Yuksel, B., (2004), "The use of ethanol–gasoline blend as a fuel in an SI engine", *Renewable Energy*, 29, pp. 1181–1191.

114. Zervas, E., (2004), “Correlations between cycle-to-cycle variations and combustion parameters of a spark ignition engine”, *Applied Thermal Engineering*, 24, pp. 2073–2081.
115. Zhaoda, Y., Chongguang, Z., Yunhua, C., Shichuan, S., Xizhen, W., li, L. and Lvren, J., (2002), “The control technology for emissions of LPG engine”, *Proceedings of the conference on Better Air Quality in Asian and Pacific Rim Cities*, Hong Kong SAR, No.PS-17.
116. Zhou, A. and Thomson, E., (2009), “The development of biofuels in Asia”, *Applied Energy*, vol. 86, pp. S11–S20.



## APPENDIX I

### SPECIFICATIONS OF THE EXPERIMENTAL SETUP

Engine	Make: Maruti , Model: Zen MPFI, Type: 4 Cylinder, 4S, Petrol (MPFI), water cooled, Power: 44.8 (60 BHP) kW @ 6000 rpm, Torque: 78.5 Nm (8 kgm) @ 4500rpm, stroke: 61mm,bore: 72mm, 993 cc, CR 9.4:1, 4-valves per cylinder, SOHC
Dynamometer	Make: Saj test plant Pvt. Ltd., Model: AG80, Type: eddy current, water cooled, with loading unit
Dynamometer Loading unit	Make: Cuadra, Model AX-153, Type :variable speed, Supply 230V AC.
Propeller shaft	Make: Hindustan Hardy Spicer, Model: 1260, Type: A, with universal joints
Air Box	M S fabricated with orifice meter and manometer
Fuel tank	Capacity 15 lit with glass fuel metering column
Manometer	Make: Apex, Model: MX-104, Range 100-0-100 mm,Type U tube
Fuel measuring unit	Make Apex, Glass, Model:FF0.090
Piezo sensor	Make: PCB Piezotronics, Model: HSM111A22, Range:5000 psi, Diaphragm stainless steel type & hermetic sealed
Calorimeter	Type: Pipe in pipe
Crank angle sensor	Make Kubler-Germany, Model- 8.3700.1321.0360 , Dia: 37mm , Shaft Size: Size 6mmxLength 12.5mm, Supply Voltage 5-30V DC
Engine indicator	Make-Cuadra, Model AX-104, Type Duel channel
Engine interface	Make-Cuadra, Model AX-408, No of channels 8.
Temperature	Type: RTD, PT100 and Thermocouple, Type K

sensor	
Load sensor	Make: Sensotronics Sanmar Ltd., Model: 60001, Type S beam, Universal, Capacity 0-50 kg, Load cell type: strain gauge,
Fuel flow transmitter	Make: Yokogawa, Model: EJA110-EMS-5A-92NN, Calibration range 0-500 mm H <sub>2</sub> O, Output linear DP transmitter,
Rotameter	Make: Eureka, Engine cooling 100-1000 lph; Calorimeter 25-250lph
Pump	Type Monoblock
Add on card	Make: Dynalog, Model - PCI1050, Resolution 12 bit, 8/16 input, Mounting PCI slot
Software	EngineSoft - Engine performance analysis software
Overall dimensions	W 2000 x D 2750 x H 1750 mm

## APPENDIX II

### SPECIFICATIONS OF GAS ECU

Model: Sequential gas injection controller of IV generation OSCAR-N OBD CAN of Europe Gas

Sl. No.	Parameters	Specifications
1	Processor	16bit / 50MHz
2	Voltage Supply	12 volt DC
3	Input Signals	Gas Temperature
		Gas pressure
		Petrol Injection Time
		O <sub>2</sub> - sensor
4	Output Signals	Gas injectors

**APPENDIX III**  
**SPECIFICATIONS OF THE EXHAUST GAS ANALYZER**

Make: AVL Digas 444

<b>Measured values</b>	<b>Measurement range</b>	<b>Resolution</b>
<b>CO</b>	0 ... 10 % Vol.	0.01 % Vol.
<b>HC</b>	0 ... 20,000 ppm	10 ppm
<b>CO<sub>2</sub></b>	0 ... 20 % Vol.	0.1 % Vol.
<b>O<sub>2</sub></b>	0 ... 22 % Vol.	0.01 % Vol.
<b>NO</b>	0 ... 5,000 ppm	1 ppm
<b>Lambda</b>	0 ... 9.999 calculated	0.001

# LIST OF PUBLICATIONS BASED ON Ph.D RESEARCH WORK

## International Refereed Journal Papers

1. **Shankar K. S**, Mohanan P, (2011), “MPFI Gasoline Engine Combustion, Performance and Emission Characteristics with LPG injection”, *Int. J. Energy & Environment*, Volume 2, Issue 4, pp.761-770.
2. **Shankar K. S**, Mohanan P (2010), “The effect of LPG injection on Combustion, Performance and Emission Characteristics of a MPFI Engine”, *Journal of Middle European Construction and Design of CArs (MECCA)*, No. 3+4, 2010, Vol. VIII, pp.40-48.

## International Conference Papers

1. **Shankar K. S**, Mohanan P (May 2013), “Performance and Emission Studies of a LPG Fueled Spark Ignition Engine with Steam Induction”, *Proceedings of 9<sup>th</sup> Asia-Pacific Conference on Combustion*, Gyeongju Hilton, Gyeongju, Korea, 19-22 May 2013, Session 38.
2. **Shankar K. S**, Mohanan P (Feb. 2013), “Combustion and emission studies of a LPG fueled spark ignition engine with steam induction”, *Proceedings of the International Conference on Alternative Fuels for I. C. Engines*, MNIT, Jaipur, India, 6-8 February, 2013, pp.86-91.
3. **Shankar K. S**, Vishal A. S, Mohanan P (Dec. 2010), “MPFI Gasoline Engine Performance and Emission Characteristics with LPG Injection”, *Proceedings of the 8<sup>th</sup> Asia Pacific Conference on Combustion (8<sup>th</sup> ASPACC)*, Hyderabad, India, Sl. No. 213, p. 340; (pp.1390-1397 in CD)
4. **Shankar K. S**, Mohanan P (May 2010), “Effect of operating variables on the cycle-by-cycle combustion variations and emissions of a multi-cylinder S. I. Engine fueled with blends of gasoline with ethanol”, *Proceedings of the International Conference on Frontiers in Mechanical Engineering ( FIME 2010)*, National Institute of Technology Karnataka, Surathkal, Karnataka, India, TH-128, pp. 136-145.

### **National Conference Papers**

1. **Shankar K. S**, Vighnesha Nayak, Mohanan P (Dec. 2011), “Performance and Emission Characteristics of a MPFI Engine with E15, E20 and LPG Injection”, *Proceedings of the 22<sup>nd</sup> National Conference on IC Engines and Combustion (22<sup>nd</sup> NCICEC)* NIT-Calicut, Kerala, India, 10th -13th December, 2011, Paper No: 1-030, pp. 109-115.
2. Vighnesha Nayak, **Shankar K. S**, Suresh Kumar Y , Mohanan P (Dec. 2011), “Performance analysis and emission characteristics of LPG injected MPFI four cylinder petrol engine using steam induction”, *Proceedings of the 22<sup>nd</sup> National Conference on IC Engines and Combustion (22<sup>nd</sup> NCICEC)* NIT-Calicut, Kerala, India, 10th -13th December, 2011, Paper No: 1-029, pp. 157-162.
3. **Shankar K. S**, Vighnesha Nayak, George Varghese, Mohanan P (May 2011), “MPFI Gasoline Engine Performance and Emission Characteristics with Ethanol-Gasoline Blends and LPG Injection”, *Proceedings of the National Conference on Recent Trends in Alternate Sources of Energy and Pollution Control (RASE)*,KVG College of Engg., Sullia Karnataka, 13th & 14th May 2011.
4. **Shankar K. S**, Haridas Rathod, Mohanan P (Dec. 2009), “Cycle-by-cycle combustion variations of a multi-cylinder S.I. engine fueled with blends of gasoline with ethanol”, *Proceedings of the XXI National Conference on Internal Combustion Engines and Combustion (20<sup>th</sup> NCICEC)*, BIET, Davangere, Karnataka, India, pp. 137-142. **(Best paper awarded)**

## **BIO-DATA**

**SHANKAR K. S**

Assistant Professor

Department of Mechanical Engineering

P. A College of Engineering, Mangalore.-574153, Karnataka, India

E-mail: shanksks@gmail.com

Cell: +91 9480169929

- Post Graduate (2004) M. Tech. in Heat Power Engineering from National Institute of Technology Karnataka (NITK), Surathkal.
- Graduate in Mechanical Engineering (1999) from Mangalore University with first class with distinction and 4<sup>th</sup> rank.
- Areas of research: I. C Engines, Combustion, Alternate fuels.
- Published two Papers in International Refereed Journals and presented 08 papers at International Conferences & 09 papers at National conferences.
- 12 years of teaching experience.
- Life member of ISTE and Combustion Institute- Indian Section.